FAKULTA
APLIKOVANÝCH VĚD
ZÁPADOČESKÉ
UNIVERZITY
V PLZNI

Dynamické systémy na grafech

RNDr. Vladimír Švígler

disertační práce
k získání titulu **doktor** (**Ph.D.**)
v oboru **Aplikovaná matematika**

Školitel: doc. RNDr. Petr Stehlík, Ph.D.

Katedra matematiky

Plzeň 2021

FAKULTA
APLIKOVANÝCH VĚD
ZÁPADOČESKÉ
UNIVERZITY
V PLZNI

Dynamical Systems on Graphs

Vladimír Švígler

dissertation thesis
for taking the academic degree **Doctor of Philosophy** (**Ph.D.**)
in specialization **Applied Mathematics**

Supervisor: Petr Stehlík

Department of Mathematics

Pilsen 2021

Deklarace

Prohlašuji, že jsem tuto práci zpracoval samostatně. Je založena na vědeckých výsledcích, jejichž jsem autorem nebo spoluautorem, a na zdrojích, které jsou citovány a uvedeny v seznamu literatury.

V Plzni .....

.....
Vladimír Švígler

Declaration

I declare that the presented thesis is my original work. It is based on the scientific results which I have authored or co-authored and on cited sources which are contained in the list of references.

In Pilsen .....

.....
Vladimír Švígler

Abstrakt

Záměrem této práce je shrnout naše nedávné výsledky týkající se konkrétních fenoménů vyskytujících se v dynamických systémech na grafech. Soustředíme se na dynamické systémy s diskrétní a spojitou prostorovou strukturou a časem. Velký důraz klademe na jevy, které se projevují výhradně u systémů s diskrétní prostorovou strukturou narozdíl od jejich spojitých protějšků. Toto srovnání uvažujeme z pohledu možných aplikací v numerické analýze a modelování systémů, u nichž homogenizace prostoru vede k významné redukci chování. Dvěma hlavními tématy jsou evoluční hry na grafech a reakčně-difúzní rovnice.

Evoluční hra na grafu je model, jenž popisuje interakce hráčů uspořádaných v nějaké dané prostorové struktuře. Každý hráč má přiřazenu strategii (spolupráce nebo nespolupráce), která je aktualizována v souladu s pravidly hry. Tento model je příkladem systému s diskrétní časovou strukturou a stavovým prostorem. Zkoumáme souvislost mezi strukturou podkladového grafu a existencí pevných bodů systému. Také ukážeme, že evoluční hra na grafu může obsahovat periodické orbity libovoné délky.

Reakčně-difúzní rovnice tradičně popisují časový vývoj systémů modelujících chemické, fyzikální, biologické a další děje. Zde se zaměřujeme hlavně na periodická stacionární řešení a cestující vlny v bistabilních reakčně-difúzních rovnicích na mřížce. Mřížkové diferenciální rovnice mohou být chápány buď jako důsledek diskretizace parciálních reakčně-difúzních rovnic na reálné ose pomocí metody konečných diferencí, ale mají své opodstatnění i jako samostatné modely. Za základním model uvažujeme Nagumovu rovnici na mřížce, tj. rovnici, jejíž reakční člen je kubický polynom. Mnoho výsledků je ale platných i pro obecné bistabilní rovnice na mřížkách. Bistabilní rovnice na mřížce má na rozdíl od odpovídající parciální diferenciální rovnice nekonečné množství prostorově heterogenních stacionárních řešení. Toto chování se občas nazývá "prostorový chaos", protože počet řešení je dispropocionálně vyšší než počet uzlů (počet rovnic). V této práci ukážeme, jak lze zavést značící schéma pro periodická stacionární řešení a jak určit jejich přesný počet, pokud budeme uvažovat symetrie rovnice. Naše zkoumání cestujících vln započneme "selháním propagace", tj. situací, při které monotonní vlna necestuje. To obvykle nastává u mřížkové rovnice s malou intenzitou difúze. Obecně se uvažuje, že bohatá struktura stacionárních řešení zabraňuje monotonním vlnám v cestování. Část týkající se cestujících vln uzavřeme představením tzv. "vícebarevných vln"; nemonotonních vln spojujících dvě periodická stacionární řešení rovnice na mřížce. Tyto vlny mohou cestovat i pro kombinace parametrů, kdy monotonní vlny projevují "selhání propagace". Dále je můžeme spojovat do složitějších struktur a studovat jejich srážky. V neposlední řadě pozorujeme nemonotonní závislost rychlosti vlny na intenzitě difúze, což je kvalitativní rozdíl v chování oproti vlnám v Nagumově parciální diferenciální rovnici.

Abstract

The goal of this thesis is to summarize our recent results regarding the spatial patterns, periodic orbits and travelling waves of dynamical systems on graphs. We focus on dynamical systems with both discrete and continuous temporal structure and a state space. A strong interest lies in observing phenomena which are unique to dynamical systems with a discrete spatial structure in comparison to their better known counterparts with a continuous spatial domain. This comparison is considered with respect to possible applications in the numerical analysis and modelling of systems whose spatial homogenization leads to a significant reduction of behaviour richness. The two main topics are evolutionary games on graphs and reaction-diffusion equations.

Evolutionary game on a graph is a model which describes interactions of players which are organized in a given spatial structure. Each player is assigned a strategy (cooperation or defection in our setting) that is updated in accordance with game rules. This model is an example of a system with a discrete temporal structure and a discrete state space. We examine the connection of the underlying graph structure to the inherent existence of steady states. We also provide proof of existence of arbitrarily long periodic orbits of evolutionary games on a graph.

Reaction-diffusion equations usually describe evolution of systems related to chemistry, physics, biology and other fields. The main interest of this part lies in examination of periodic steady states and travelling waves in bistable lattice reaction-diffusion equations (LDE). Roughly speaking, lattice differential equation can be understood as a spatial finite difference discretization of reaction diffusion equation on a real line but has its practical context as a standalone model. The focal model is the Nagumo LDE whose reaction term is driven by a nonlinear cubic function; many results are however applicable to general bistable case. A bistable LDE can possess an infinite number of steady states contrary to its continuous counterpart. This behaviour is sometimes described as spatial chaos since the number of solutions is disproportionally large in comparison to the number of the LDE vertices. We provide results which help to categorize and count the solutions with respect to various symmetries present in the equation. We start our inspection of travelling waves with propagation failure; a situation when the monotonous wave is standing. It usually happens in the LDE in regime with small diffusion intensity. Arguably, the rich structure of stable steady states prevents the waves from travelling in this setting. The study of travelling waves is concluded by introduction of results concerning multichromatic waves which are non-monotonous waves connecting two periodic stable steady states of LDE. Such waves exhibit rich behaviour such as ability to travel in the pinning region, possibility to connect multiple waves to product intricate wave collisions and non-monotonous dependence of the wave speed on the diffusion intensity which is inherent to Nagumo partial differential equation.

要旨

本論文の目的は，グラフ上の力学系の分野において，ある現象と今後の発展の可能性を考察することである．本研究では，離散的・連続的な時間構造と状態空間を持つ力学系に焦点を当てており，特に離散的な空間構造を持つ力学系に特有の現象を，連続的な空間領域を持つ力学系と比較して観察することに強い関心を向けている．この比較は，空間的均質化が振舞の豊かさの大幅な減少をもたらす系の数値解析やモデリングにおける応用の可能性を考慮したものである．2つの主な話題は，グラフ上の進化ゲームと反応拡散方程式である．

グラフ上の進化ゲームとは，与えられた空間構造に編成されたプレイヤーの相互作用を記述するモデルのことである．各プレイヤーにはゲームルールに従って更新される戦略（協調または裏切り）が割り当てられる．このモデルは，離散的な時間構造と離散的な状態空間を持つシステムの一例である．本研究では，このモデルの基礎グラフの構造と定常状態の存在性との関係を考察する．また，グラフ上に任意長の周期的な進化ゲームの軌道が存在することを証明する．

反応拡散方程式は通常，化学，物理学，生物学などの分野に関連する系の進化を記述するものである．ここでは，双安定格子反応拡散方程式 (LDE: lattice reaction-diffusion equation) における周期定常状態と周期進行波を調べることに主眼を置いている．概略を言えば，格子微分方程式は，実数上の反応拡散方程式を空間的有限差分に関する離散化として理解できるが，実用的にはスタンドアロンモデルとしての意味合いがある．焦点となるモデルは，反応項が非線形三次関数で駆動される Nagumo LDE であるが，多くの結果は一般的な双安定である場合にも適用可能である．双安定 LDE は，連続的なものとは逆に，無数の定常状態を持ちうる．この振舞は，LDE の頂点数と比較して解の数が過度に大きいため，空間カオスと表現されることもある．本研究では，方程式に存在する様々な対称性に関して解を分類し，それらを数えるのに役立つ成果を提供する．まず，伝播阻害を伴う進行波の検証，すなわち単調な進行波が形成される状態から開始する．このことは LDE において通常，拡散強度が小さい領域で起こる．おそらく，安定した定常状態の構造が豊富であるために，このような設定では波が伝播しないのではないかと考えられる．この進行波に関する研究は，LDE の 2 つの周期安定定常状態を結ぶ非単調波である多色波に関する結果を導入することで結論づけられる．このような波は，ピンニング領域を進行する能力，複数の波を連結して複雑な波の衝突を生成する可能性，Nagumo 偏微分方程式に固有の拡散強度に対する波の速度の非単調従属性などの豊かな振舞を示すものである．

Acknowledgement

I would like to express my gratitude to Petr Stehlík for his constant support and positive attitude, to Jonáš Volek for reading this thesis and providing useful insights throughout the doctoral study and to Takamasa Yashima for the translation of the abstract. None of this would be possible without my family.

In Pilsen .....

.....
Vladimír Švígler

Contents

Chapter 1

Introduction

A dynamical system is a system whose state is time-dependent. Modelling the real-world phenomena via dynamical systems is common in physics (e.g., pendulum movement, fluid flow [13], object temperature change via the heat equation), chemistry (e.g., concentration and temperature of chemical substances during a reaction [27]), biology (e.g., abundance of organisms, number of individuals with certain morphological or behavioural trait [52]), sociology (e.g., age structure of a population, distribution of the supporter of political parties [25, 53]) and other sciences. The description of each dynamical system includes:

- a *spatial structure* in which the process takes place (e.g., a pipe in which a fluid flows, a Petri dish in which a chemical reaction takes place, a certain part of a natural reservation in which the animal presence is being observed, a country in which the political preferences are studied),
- a *temporal structure* which is used to determine the state of the system; a usual choice is either a continuous time when it makes sense to investigate the state of the system constantly (usually in mechanical and chemical systems) or a discrete time when it makes sense to investigate the system at isolated moments (e.g., regular observations of an age structure of a population),
- a *state space* which is the set of all possible states of the system (e.g., all possible angles and angular velocities of a pendulum, all theoretically possible concentrations of reactants, all numbers representing the size of animal population).

Similarly to the temporal structure, the spatial structure and the state space can differ qualitatively depending on specific applications. Using the previous examples of the spatial structures, the interior of a pipe or a Petri dish forms a continuous nontrivial object in a three-dimensional space. On the other hand, it makes sense to examine political preferences only in habited places such as cities, towns and villages. Naturally, their locations form a set of isolated points on a geographical map. In the same spirit, the state space of temperatures of a chemical reaction forms a continuous scale of possible temperatures but the animal count is an integer by its nature.

We focus on dynamical systems with both continuous and discrete temporal structures and state spaces in our research. However, the main interest lies in comparison of the behaviour of systems with various spatial structures. There are two main reasons for this approach. The spatial structure of some dynamical systems may appear qualitatively different under various scales of observation. For example, a medium such as sandstone may seem homogeneous but one can see that it is actually porous under a proper magnification; it is composed of cemented grains with not negligible spaces in between the grains. The other motivation is more of a technical nature. In dynamical systems described by partial differential equations the spatial domain is assumed to be continuous. It is however impossible to obtain an exact solution of many of equations. Such equations are solved numerically, i.e., a proper discretization of the spatial (and temporal) domain is found and numerical solvers are applied to obtain a solution. In fact, many numerical solvers are treating a spatially (and temporally) discrete counterpart of the original problem. It has been shown that these complementary dynamical systems can exhibit qualitatively different and usually richer behaviour.

The conflict in behaviour of continuous and discrete system can be distinctly demonstrated on the logistic equation and the logistic map. The logistic equation

$$x' = rx(1 - x)$$

is a model which describes growth of a hypothetical population with the environment carrying capacity [68] and can be solved explicitly in the form of a sigmoid function. The sign of the Malthusian parameter r decides whether the population saturates the capacity or becomes extinct. After replacing the derivative in logistic

function with the forward difference $\frac{\mathrm{d}x}{\mathrm{d}t} \sim (x_{t+h} - x_t)/h$ and rescaling one can obtain the logistic map

$$x_{t+h} = r x_t (1 - x_t)$$

whose behaviour depending on the parameter r is much more intricate such as existence of cycles of arbitrary length and eventually chaotic behaviour [42, 60] which has no actual counterpart in the continuous case. Despite some qualitative differences, there were attempts to unify differential and difference calculus [4, 24]; this approach also obtained its share of criticism [22].

The discrete models, they are also used in the numerical treatment of differential equations. The logistic map is in fact the iterative scheme of the Euler method and the theoretical results indicate, that unsuitable choice of the time step may result not only in inaccurate result but even in completely different behaviour. Another example is the pinning phenomenon. The Nagumo partial differential equation

$$u_t(x,t) = d\, u_{xx}(x,t) + u(x,t)\big(u(x,t) - a\big)\big(1 - u(x,t)\big), \quad a \in (0,1)$$

acting as a prototype model describing propagation of a signal in discrete media possesses travelling wave solutions with non-zero speed provided $a \neq 1/2$, [20]. The Nagumo lattice differential equation on the other hand

$$u_i'(t) = d\left(u_{i-1}(t) - 2u_i(t) + u_{i+1}(t)\right) + u_i(t)\big(u_i(t) - a\big)\big(1 - u_i(t)\big), \quad a \in (0,1)$$

has a set of parameter tuples (a, d) with nontrivial volume such that the travelling waves solutions have zero speed; we say that they are pinned [35, 72]. This phenomenon is also present in other systems [6, 26] and exhibits when other than the second-difference spatial discretization is used [34], although it may be prevented. The last example of a discrete system partially motivated by continuous problems introduced here are the cellular neural networks [5, 16], which can be used as analog numerical partial differential equation solvers; the influence of the discrete spatial structure is crucial to analyze in their treatment.

The presented ideas lead us naturally to dynamical systems on graphs (sometimes called networks in applications). A graph consists of two sets: the set of vertices which are the points of interest and the set of edges which encode the relations between the vertices (e.g., scientists are depicted by vertices and if any two of them collaborated on a paper, there is an edge between them). See Figure 1.1 for examples of graphs. The reason for the use of such models and their investigation is multifold:

- The graph structure represents a coupling of different parts of the system (e.g., coupling in a physical or chemical system [12, 16, 39] or interaction channels between individuals in biological systems [37, 66]).
- The graph represents the state changes of another dynamical system (e.g., age-structured models [65]).
- In numerical analysis, the spatial discretization of a problem described by a partial differential equation leads to a formulation of a dynamical system whose spatial structure is discrete and can be represented by a graph (e.g., finite difference scheme [40]).

The above described systems lead to a structure description by regular lattices, i.e., infinite graphs with regular and simple structure. A distribution of active transmission sites along a myelinated axon is modelled by a one-dimensional lattice (a simple path of connected vertices, Figure 1.1a) [3]. A discretization of a spatial domain of a problem described by a partial differential equation leads to a multidimensional grid with vertices placed in the intersections, Figure 1.1b, [40]. Lately, the regular structure has been found unsuitable for an exhaustive description of certain systems [37, 66]. Considering the underlying structure being a general graph seems to be able to fill this gap. The graph can capture the irregular structure of certain theoretical and/or real-life systems such as interactions between individuals in a society, road network of a country or a discretization of an irregular domain, Figure 1.1c.

The research focus in this field forks into various specializations. Problems motivated by applications (e.g., behaviour of neural networks, evolution of spatially heterogeneous biological and/or ecological communities, synchronization) are studied as well as problems of additional theoretical significance (e.g., travelling wave solutions, bifurcations).

In this thesis, we pursue two main research directions - evolutionary games on graphs and reaction-diffusion systems on graphs. The spatial structure of the systems is discrete. However, the temporal structure and the state space structure differs; evolutionary games on graphs are considered to have a discrete set of states and discrete time steps whereas the reaction-diffusion systems are modelled by differential equation systems and thus have continuous time and a continuous state space. Common interest lies in the study of nonhomogeneous (coexistence) steady states which are sometimes called patterns; a notion without any proper counterpart in spatially continuous systems. The nonhomogeneous steady states are usually sensitive to parameter settings and require certain balance to be present in the system.

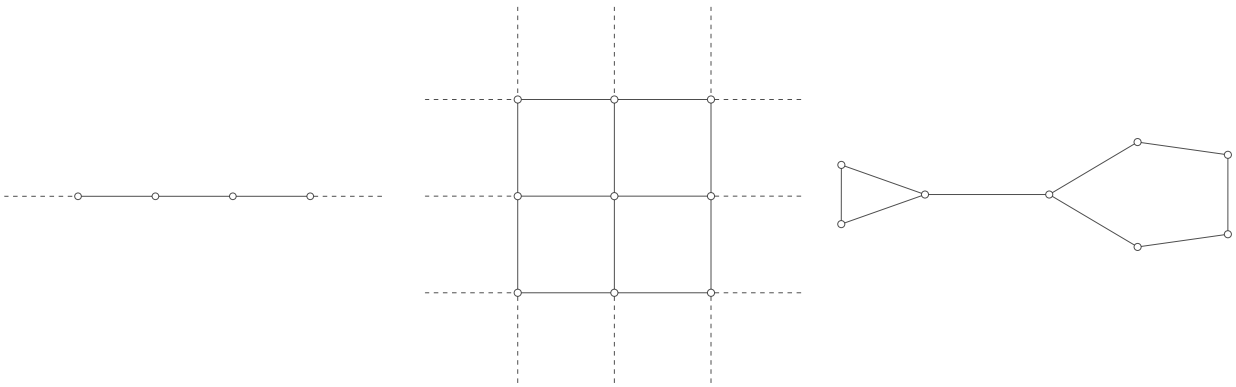

a: One-dimensional lattice. b: Two-dimensional lattice. c: A general graph.

Figure 1.1: Examples of types of graphs.

The evolutionary games on graphs (a game-theoretical model for describing the spread of cooperative and defective behaviour) are examined in §2. We turn our attention to the existence of steady states and periodic orbits and their properties with respect to various settings including the graph (spatial) structure. The main object of interest in §3 is the Nagumo lattice differential equation. We namely focus on spatially heterogeneous periodic stationary solutions and their regions of existence in the parameter space. Further, special wave-type solutions which can be perceived as waves connecting two periodic stationary solutions out of which at least one is a heterogeneous one; the so-called *multichromatic waves*.

Chapter 2

Evolutionary games on graphs

Many similar definitions of the *game theory* exist in literature. Here, we can settle with the definition of Murray [53] that "game theory can be defined as the study of mathematical models of conflict and cooperation between intelligent rational decision-makers". These decision makers are usually called *players*. This definition indicates the crucial difference between classical optimization and decision making in the virtue of the game theory. In classical optimization, one looks for an optimal solution with respect to certain given conditions. On the other hand, the problem definition in game theory contains other players and each decision must be made with respect to the possible reactions of the other players. For the comprehensive overview of the history of game theory we refer to, e.g., [9, 25, 53].

In this chapter, we focus on the so called *social dilemmas*, e.g., the games in which each individual profits from cooperative behaviour of other players. One of the great foci of the social dilemmas is to figure out the mechanism of cooperation emergence and preservation. We refer to a summarizing paper by Martin A. Nowak [57] as a starting point.

The chapter is organized as follows. We start in §2.1 with general introduction of basic game-theoretical concepts and their relation to dynamical systems. The examined model is rigorously defined in §2.2. We follow with results describing the interplay of graph structure and existence of fixed points of evolutionary games on a graph in §2.3. The chapter is concluded by an exposition of claims proving the existence of periodic orbits of arbitrary length in §2.4 and a short summary if open questions and possible further research directions in §2.5.

2.1 Preliminaries

2.1.1 Matrix games

We explain the concept of matrix games in a quite narrow interpretation consisting of two equivalent players (both of them are humans who possess an equivalent social status or animals of the same species) and both of them are placed in the situation in which they have to choose whether to cooperate (C or 0) or to defect (D or 1). The set of possible strategies is denoted by $S = \{0, 1\}$. For more general treatment on this topic (multiple players, multiple strategies or unequal payoffs of players) we refer to [25].

Let us have two players who have to simultaneously choose whether to cooperate or to defect at a given moment. Let us note that both players make decision at the same time; the numbering of the players is introduced purely for clarity of the game description. Naturally, there are four possible outcomes and the whole game can be described by the utility matrix

$$\begin{array}{c|cc} & C & D \\ \hline C & a & b \\ D & c & d \end{array}. \tag{2.1}$$

The matrix (2.1) reads as follows. If both players choose to cooperate or to defect their mutual payoff will be a or d, respectively. If the first player chooses to cooperate and the second one to defect, their respective payoffs are b and c. If the first player chooses to defect and the second one to cooperate their respective payoffs are c and b.

In order to restrict ourselves to the case of social dilemma games, we pose certain conditions on the parameter quadruple (a, b, c, d):

(M1) For the sake of brevity, we assume that no two parameters are equal.

(M2) It is always better if both players cooperate than if they both defect, i.e., $a > d$.

(M3) If only one cooperates, it is more advantageous to be the defector, i.e., $c > b$.

(M4) No matter what strategy a player chooses, it is always better for him/her if his/her opponent cooperates, i.e., $a > b$ and $c > d$.

(M5) a, c are positive, i.e., there is a positive reward for cooperation of the opponent.

This allows us to define the following.

Definition 2.1.1. The set of all parameter quadruples $(a, b, c, d) \in \mathbb{R}^4$ satisfying conditions (M1)–(M5) is called the *set of admissible parameters* and denoted by $\mathcal{P}$.

Note, that the condition (M1) is not particularly important for the idea of social dilemma games modelling. It is the part of the *generic payoffs assumption* which states, that for the sake of clarity, we ignore the sets of measure zero in the parameter space (the space $\mathbb{R}^4$ in our case). We refer to [9] for further discussion. The conditions (M2)–(M5) can be compactly written as

$$\min\{a, c\} > \max\{b, d, 0\}.$$

The set $\mathcal{P}$ can be naturally decomposed into four classes each of which induces qualitatively different game behaviour:

$$\begin{aligned} \mathcal{P}_{\mathrm{PD}} &= \big\{(a,b,c,d) \in \mathcal{P} :\ c > a > d > b\big\}, \\ \mathcal{P}_{\mathrm{HD}} &= \big\{(a,b,c,d) \in \mathcal{P} :\ c > a > b > d\big\}, \\ \mathcal{P}_{\mathrm{SH}} &= \big\{(a,b,c,d) \in \mathcal{P} :\ a > c > d > b\big\}, \\ \mathcal{P}_{\mathrm{FC}} &= \big\{(a,b,c,d) \in \mathcal{P} :\ a > c > b > d\big\}. \end{aligned} \tag{2.2}$$

In connection to the sets $\mathcal{P}_{\mathrm{PD}}, \mathcal{P}_{\mathrm{HD}}, \mathcal{P}_{\mathrm{SH}}, \mathcal{P}_{\mathrm{FC}}$ we speak about four scenarios called *Prisoner's Dilemma* (PD) scenario, *Hawk and Dove* (HD) scenario, *Stag Hunt* (SH) scenario and *Full Cooperation* (FC) scenario. See [66] for a deeper analysis and the origin of the scenario names.

To be able to analyse the game given by the matrix (2.1) deeper we introduce the concept of the *mixed strategy*. The first player chooses to cooperate with probability $p \in [0, 1]$ (and to defect with probability $1 - p$). Analogously, the second player chooses to cooperate with probability q. If $p \in (0, 1)$ we say that the first player plays a mixed strategy. If $p \in \{0, 1\}$ then we say that the first player plays a *pure strategy*. The respective expected payoffs of the players playing strategies p, q (possibly pure ones) are denoted $\pi_1(p, q)$, $\pi_2(p, q)$. Based on the probability of the possible outcomes, we can straightforwardly derive

$$\pi_1(p, q) = pqa + p\,(1 - q)\,b + (1 - p)\,qc + (1 - p)(1 - q)\,d, \tag{2.3}$$

$$\pi_2(p, q) = pqa + (1 - p)\,qb + p\,(1 - q)\,c + (1 - p)(1 - q)d. \tag{2.4}$$

We can now introduce the concept of the *Nash equilibrium*. Roughly speaking, the strategy pair (p^*, q^*) is the Nash equilibrium if none of the players can single-handedly increase his/her payoff by the strategy change. This concept was developed by John F. Nash, see [56].

Definition 2.1.2. [9, Definition 3.3., p. 36] In a two-player game where players are allowed to play mixed strategies, a strategy pair (p^*, q^*) forms a Nash equilibrium if

$$\begin{aligned} \pi_1(p^*, q^*) &\geq \pi_1(p, q^*) \qquad \text{for all} \qquad p \neq p^*, \\ \pi_2(p^*, q^*) &\geq \pi_2(p^*, q) \qquad \text{for all} \qquad q \neq q^*, \end{aligned}$$

where $\pi_i(p, q)$ denotes the payoff of the i-th player if the first player uses strategy p while the second one uses q.

The search for Nash equilibria is done through the analysis of the *best response*, i.e., what is the optimal p for the first player provided the second player plays some q. Let us rearrange the expressions (2.3) and (2.4)

$$\pi_1(p, q) = p\left[q\,(a - b - c + d) + b - d\right] + q\,(c - d) + d, \tag{2.5}$$

$$\pi_2(p, q) = q\left[p\,(a - b - c + d) + b - d\right] + p\,(c - d) + d, \tag{2.6}$$

and define

$$\psi(r) = r\,(a - b - c + d) + b - d.$$

Note that $\psi(r^*) = 0$ if $r^* = (d - b)/(a - b - c - d)$ but $r^* \in [0, 1]$ is not assured. We will now discuss the four scenarios (FC, HD, SH, PD) separately. All the results are depicted in Figure 2.1. See Table 2.1 on p. 10 for an overall summary.

FC: The function $\psi(r)$ is positive for all $r \in [0,1]$. Thus, it is always advantageous to cooperate ($p = q = 1$) regardless of the opponent's strategy and the only Nash equilibrium is $(1,1)$.

HD: It can be shown that $r^* \in (0,1)$; $\psi(r)$ is positive for $r \in [0, r^*)$ and negative for $r \in (r^*, 1]$ since $c > a > b > d$. Thus, if $p = r^*$, the second player can not gain a higher payoff by the change of his/her strategy (π_2 is now independent of q) and vice versa. The best response of the second player to $p = 1$ is $q = 0$ and the best response of the first player to $q = 0$ is $p = 1$. The same idea can be used for the case $p = 0$, $q = 1$. The Nash equilibria are $(0,1)$, (r^*, r^*), $(1,0)$.

SH: Similarly to the HD scenario, $r^* \in (0,1)$ holds. But, $\psi(r)$ is negative for $r \in [0, r^*)$ and positive for $r \in (r^*, 1]$ since $a > c > d > b$. By an analogous argumentation as in the HD case, the Nash equilibria $(0,0), (r^*, r^*), (1,1)$ can be obtained.

PD: The function $\psi(r)$ is negative for all $r \in [0,1]$. Thus, it is always advantageous to defect ($p = q = 0$) regardless of the opponent's strategy and the only Nash equilibrium is $(0,0)$.

2.1.2 Replicator dynamics

The replicator dynamics describe the evolution of different individual types ratio in a population. Here, we show the close connection of the replicator dynamics to the Malthusian growth model and perform a stability analysis of the model. The leading principle in the derivation of the replicator model is that the population is big, well mixed (spatial homogenity assumption) and individuals encounter each other with an even probability.

It was stated by Thomas R. Malthus in An Essay on the Principle of Population [47], that without any outer restriction, the size of the human population increases geometrically. This was later generalized to describe the growth of any natural population. This postulate can be modelled by the ordinary differential equation (ODE)

$$n' = (\beta - \delta)\, n, \tag{2.7}$$

which has the solution

$$n(t) = n_0\, e^{(\beta-\delta)\, t},$$

where n_0 is the initial population size, n is the total population size, $\beta, \delta > 0$ are the per-capita birth and death rates, respectively (i.e., the population size at time $t+1$ is the population size at time t multiplied by the factor $\exp(\beta - \delta)$. The ODE (2.7) is also called the *Malthusian growth model*. A simple analysis of the equation (2.7) yields that

- $n(t) \to 0$ as $t \to +\infty$ for $\beta - \delta < 0$,
- $n(t) \to +\infty$ as $t \to +\infty$ for $\beta - \delta > 0$,
- $n(t) \equiv n_0$ for $\beta - \delta = 0$.

The dynamics of one population with individuals showing different behaviour (e.g., cooperative (n_1) and defective (n_2)) can be now modelled by an ODE system which is a slight modification of the Malthusian growth model (2.7)

$$\begin{aligned} n_1' &= \big(\beta - \delta + \tilde{\pi}_1(n_1, n_2)\big)\, n_1, \\ n_2' &= \big(\beta - \delta + \tilde{\pi}_2(n_1, n_2)\big)\, n_2, \end{aligned} \tag{2.8}$$

where $\beta > 0$ is the per-capita birth rate of individuals, $\delta > 0$ is the per-capita death rate of individuals and $\pi_i : \mathbb{R}^+ \times \mathbb{R}^+ \to \mathbb{R}$ is the utility of individuals of the i-th type provided there are n_1 individuals of the first type and n_2 individuals of the second type. We assume that the utilities π_i are given by the outcomes of the matrix games (2.1) played by individuals in a well mixed population. Assuming $n_1, n_2 \gg 1$, we have

$$\tilde{\pi}_1(n_1, n_2) \approx a\, \frac{n_1}{n_1 + n_2} + b\, \frac{n_2}{n_1 + n_2}, \tag{2.9}$$

$$\tilde{\pi}_2(n_1, n_2) \approx c\, \frac{n_1}{n_1 + n_2} + d\, \frac{n_2}{n_1 + n_2}, \tag{2.10}$$

since the encounters are considered to be random and proportional to the individual types frequencies[1]. Let us denote $n = n_1 + n_2$ and $x_i = n_i/n$ for $i = 1, 2$. Note that $x_1 + x_2 = 1$ holds from definition. This allows us to

[1] Sufficiently great n_1 and n_2 allow us to neglect the impossibility of an individual playing with him/herself. Otherwise, the expressions (2.9), (2.10) would take cumbersome form which would be difficult to handle properly.

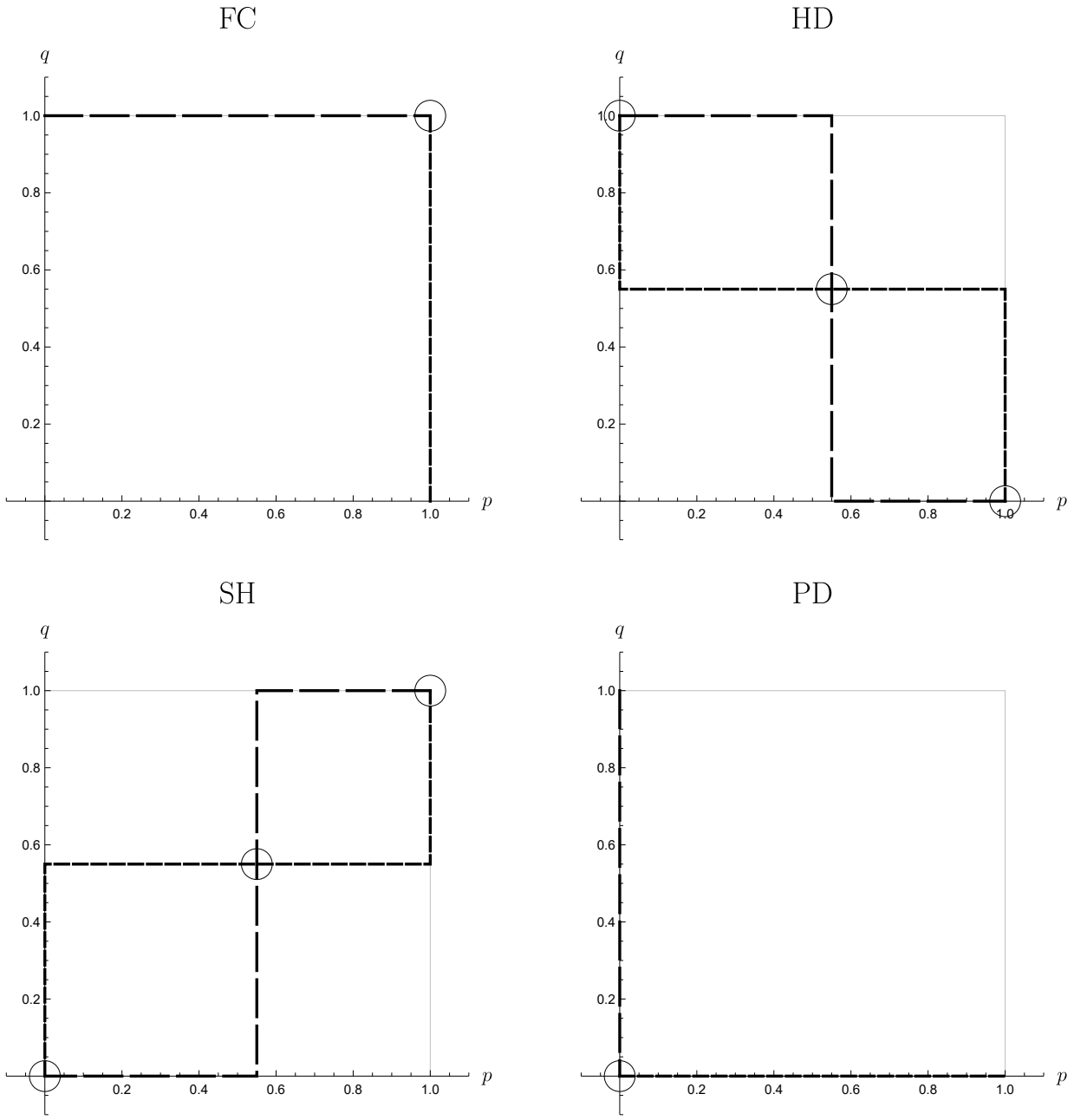

Figure 2.1: Best response diagrams for the matrix game (2.1). The best response of the first player is depicted by the short-dashed line and can be viewed as a multivalued function $p(q)$. The best response of the second player is depicted by the long-dashed line and can be viewed as a multivalued function $q(p)$. The diagrams are depicted for generic FC and PD scenarios. The parameters for the HD scenario were: $a = 1, b = 0.55, c = 1.45, d = 0$ and thus $r^* = 0.55$. The parameters for the SH scenario were: $a = 1, b = -0.275, c = 0.775, d = 0$ and thus $r^* = 0.55$. See the end of §2.1.1 for further details.

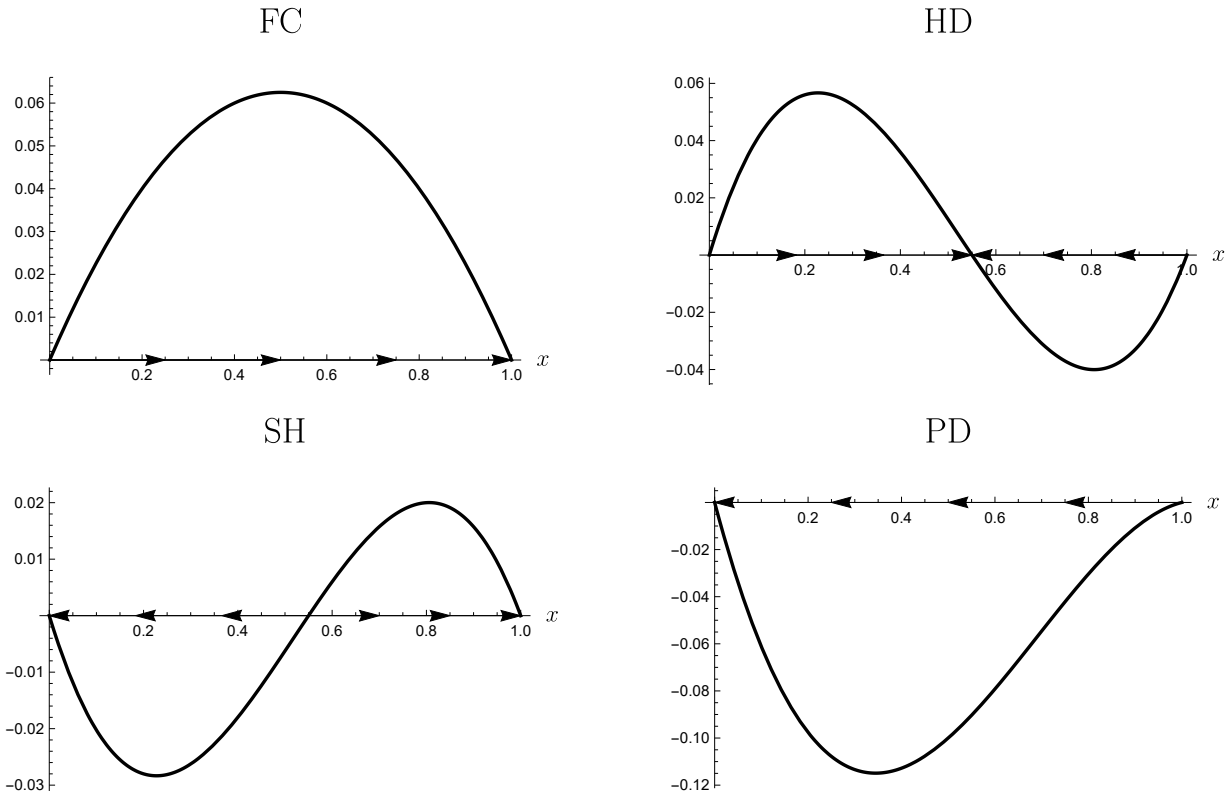

Figure 2.2: The examples of the right-hand sides of (2.15) for all scenarios. The arrows indicate the one-dimensional phase portrait of the system and thus the fixed points' stability. The functions were depicted with parameters a, d set to $a = 1, d = 0$. The parameters b, c varied in the following way: FC: $b = 0.25, c = 0.75$, HD: $b = 0.55, c = 1.45$, SH: $b = -0.275, c = 0.775$, PD: $b = -0.75, c = 1.05$. Note, that the parameters for HD and SH scenarios are the same as in Figure 2.1 and the equilibria and the fixed point values correspond ($r^* = x^* = 0.55$).

define $x = x_1$ and substitute $x_2 = 1 - x$. The utility functions (2.9), (2.10) can be now equivalently reformulated as

$$\pi_1(x) = ax + b\,(1 - x), \tag{2.11}$$

$$\pi_2(x) = cx + d\,(1 - x). \tag{2.12}$$

To observe the dynamics of x, the elementary calculus gives

$$x' = \left(\frac{n_1}{n}\right)' = \big[\pi_1(x) - \overline{\pi}(x)\big]\, x, \tag{2.13}$$

where

$$\overline{\pi}(x) = x\,\pi_1(x) + (1 - x)\,\pi_2(x) \tag{2.14}$$

is the population mean utility provided there is a ratio x of type 1 individuals.

The existence of the equation (2.13) fixed points and their stability are directly dependent on the game theoretical parameter quadruple $(a, b, c, d) \in \mathcal{P}$ ordering. First, let use rewrite (2.13) as

$$x' = x\,(1 - x)\big((a - b - c + d)\,x + b - d\big). \tag{2.15}$$

Each of the four scenarios has at least two fixed points under the replicator dynamics ($x = 0$ and $x = 1$). There is also a third fixed point for HD and SH scenarios, i.e., $x^* = (d - b)/(a - b - c + d)$. Analysing the sign of the expression on the right-hand side of (2.15) one can decide on the stability of the fixed points, see Figure 2.2. The stability results of this section and §2.1.1 are summarized in Table 2.1. Information on further connections of the replicator dynamics fixed points, equilibria and the matrix games' stable strategies can be found in [9, 25].

Let us note that the form of (2.15) allows us to introduce linear parameter substitution

$$\tilde{y} = \frac{y - d}{a - d}, \quad \text{where} \quad y = a, b, c, d. \tag{2.16}$$

Scenario	Parameters	Nash equilibria	Fixed points	Stable fixed points
FC	$a > c > b > d$	$\{(1,1)\}$	$\{0,1\}$	$\{1\}$
HD	$c > a > b > d$	$\{(0,1),(x^*,x^*),(1,0)\}$	$\{0,x^*,1\}$	$\{x^*\}$
SH	$a > c > d > b$	$\{(0,0),(x^*,x^*),(1,1)\}$	$\{0,x^*,1\}$	$\{0,1\}$
PD	$c > a > d > b$	$\{(0,0)\}$	$\{0,1\}$	$\{0\}$

Table 2.1: Summary of the matrix games' Nash equilibria and the replicator dynamics fixed points for each of the four scenarios in (2.2).

Without loss of generality, we can thus assume $a = 1$ and $d = 0$ and the system (2.15) preserves qualitative properties of its equilibria. This substitution enables us to depict the parameter regions in plane, see Figure 2.3.

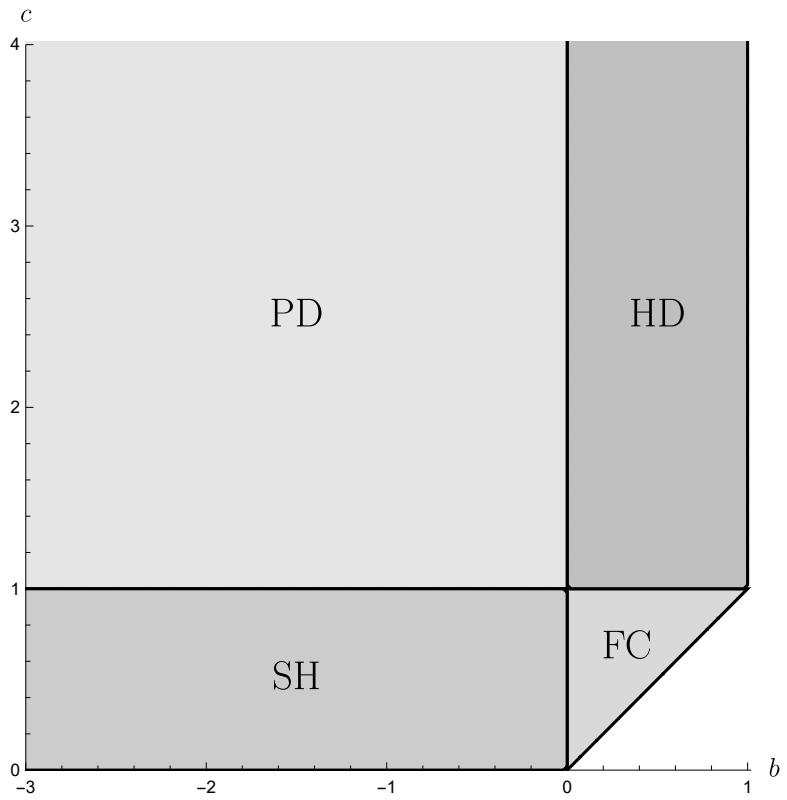

Figure 2.3: Admissible parameter regions $\mathcal{P}_{\mathrm{FC}}$, $\mathcal{P}_{\mathrm{HD}}$, $\mathcal{P}_{\mathrm{SH}}$, $\mathcal{P}_{\mathrm{PD}}$ with $a = 1$ and $d = 0$ fixed. Note, that the whole region $\mathcal{P}$ is unbounded for $c \to +\infty$ and $b \to -\infty$.

2.2 Model formulation

The focal dynamical system of this chapter describes the spread of cooperation and defection with a discrete time setting. Contrary to the replicator dynamics, we do not assume a large population size and we furthermore assume spatial nonhomogenity. The framework presented here is a purely deterministic one with a small exception. For a general framework of the evoutionary games on graphs see [17, 18].

We consider undirected connected graphs $\mathcal{G}$ as the spatial structure of our game with the vertices V being players. The interactions between vertices are defined by a set of edges E (no edge means no direct interaction). The m-neighborhood of the vertex i (the set of all vertices having distance to i exactly m) is denoted by $N_m(i)$. We also define

$$N_{\leq m}(i) = \bigcup_{n=1}^{m} N_n(i) \cup \{i\}.$$

The evolutionary game on a graph can be formally defined as follows.

Definition 2.2.1. The *evolutionary game on a graph* is a quintuple $(\mathcal{G}, \mathbf{p}, \pi, \mathcal{T}, \varphi)$, where

1. $\mathcal{G} = (V, E)$ is a connected graph,
2. $\mathbf{p} = (a, b, c, d) \in \mathcal{P}$ are game-theoretical parameters,
3. $\pi : S^V \to \mathbb{R}^V$ is a utility function,
4. $\mathcal{T} : \mathbb{N}_0 \to 2^V$ is an update order,
5. $\varphi : (\mathbb{N}_0)^2_{\geq} \times S^V \to S^V$ is a dynamical system.

The set $(\mathbb{N}_0)^2_{\geq}$ is the set of all ordered pairs $(t, s) \in \mathbb{N}_0^2$ such that $t \geq s$. The strategy vector (the state of the system) is denoted by $X = (X_1, \ldots, X_{|V|}) \in S^V$. For a strategy vector $X \in S^V$, the strategy of the vertex i is X_i. The utility of the player i is denoted by $\pi_i(X)$.

The utility function is supposed to capture payoffs of the players from the matrix games played with his/her neighbours. The first natural choice is the *aggregate utility function* which sums the utilities

$$\pi_i^A(X) = a \sum_{j \in N_1(i)} X_i X_j + b \sum_{j \in N_1(i)} X_i(1 - X_j) + c \sum_{j \in N_1(i)} (1 - X_i) X_j + d \sum_{j \in N_1(i)} (1 - X_i)(1 - X_j). \tag{2.17}$$

An another possible choice is to consider the *mean utility function* which averages the aggregate utility function over the number of the players' neighbours

$$\pi_i^M(X) = \frac{\pi_i^A(X)}{|N_1(i)|}. \tag{2.18}$$

The mean utility function has a convenient property of preserving the order of the utilities under the parameter transformation (2.16). The transformed mean utility function $\tilde{\pi}_i^M$ is given by positive linear transformation of the original mean utility function π_i^M. Indeed,

$$\tilde{\pi}_i^M(X) = \frac{\tilde{\pi}_i^A(X)}{|N_1(i)|} = \frac{1}{|N_1(i)|} \left(\frac{\pi_i^A(X)}{a - d} - \frac{d}{a - d} |N_1(i)| \right) = \frac{1}{a - d} \pi_i^M(X) - \frac{d}{a - d}$$

holds since

$$|N_1(i)| = \sum_{j \in N_1(i)} X_i X_j + \sum_{j \in N_1(i)} X_i(1 - X_j) + \sum_{j \in N_1(i)} (1 - X_i) X_j + \sum_{j \in N_1(i)} (1 - X_i)(1 - X_j).$$

We can thus, without loss of generality, assume $a = 1, d = 0$ as in the case of replicator dynamics. Note that $|N_1(i)|$ is constant on regular graphs and both utilities π^M and π^A are the same. However, on irregular graphs this is no longer true and one could argue which utility is more realistic.

The update order $\mathcal{T}$ is a function which determines candidate vertices to be updated in the immediate time step. It can possess various properties. The update order $\mathcal{T}$ is called:

- *non-omitting*, if for each vertex $i \in V$ and each $t_0 \in \mathbb{N}_0$, there exists $t > t_0$ such that $i \in \mathcal{T}(t)$; otherwise $\mathcal{T}$ is called *omitting*,
- *periodic*, if there exists $T \in N$ such that $\mathcal{T}(t + T) = \mathcal{T}(t)$ for each $t \in \mathbb{N}_0$,
- *synchronous*, if $\mathcal{T}(t) = V$ for each $t \in \mathbb{N}_0$; otherwise $\mathcal{T}$ is called *asynchronous*,
- *sequential*, if vertices can be ordered so that $\mathcal{T}(t) = \{(t + 1) (\mathrm{mod}\ |V|)\}$.

The dynamical system φ is in general required to satisfy the two-parameter semiflow property

$$\varphi(t, t; X) = X, \qquad \varphi\big(t, r; \varphi(r, s; X)\big) = \varphi(t, s; X)$$

for all $X \in S^V$ and $r, s, t \in \mathbb{N}_0$ such that $t \geq r \geq s$. In this thesis, we consider the *deterministic imitation dynamics* only. The idea is that each player imitates the strategy of his/her strongest neighbour (including him/herself)

$$\varphi_i(t + 1, t, X) = \begin{cases} X_{\max} & i \in \mathcal{T}(t),\ |A_i(X)| = 1 \text{ and } A_i(X) = \{X_{\max}\}, \\ X_i & \text{otherwise,} \end{cases}$$

where

$$A_i(x) = \big\{ X_k \,|\, k \in \operatorname{argmax}\big\{ \pi_j(X) \,|\, j \in N_{\leq 1}(i) \big\} \big\},$$
$$\varphi_i = \mathrm{proj}_i \circ \varphi : S^V \to S.$$

When some player i has the strongest cooperating and the strongest defecting neighbour simultaneously it preserves its strategy. We refer to [17] for further discussion on other related dynamical systems.

It has been shown in [63], that considering a version of stochastic update order and taking the limit for the time step $\Delta t \to 0$ and $|V| \to +\infty$ on a complete graph, the trajectory of the system uniformly approaches the trajectory of the corresponding replicator dynamics. However, the trajectory of evolutionary game on graph can show qualitatively different behaviour to the one of replicator dynamics (e.g., cooperation can prevail and spread even for the PD scenario, see §2.3 and §2.4) considering and arbitrary graph.

The origins of the evolutionary game on a graph idea can be tracked to [58]. Note that the model presented here can be understood as a subclass of cellular automata on a graph [48]. See [19] or Appendix C for further references on models related to the evolutionary games on a graph.

2.3 Fixed points

The results of this section were mainly published in the paper [18] (included in Appendix B).

Table 2.1 summarized the equilibria and fixed points of matrix games and replicator dynamics. The structure of equilibrium points was qualitatively different for each of the four scenarios. We show that the fixed point sets of the evolutionary games on graphs have much richer structure. This also indicates that the structure of the population might be an important factor in the emergence and the preservation of cooperation.

Let us start with a formal definition of a *fixed point*. Note that every strategically homogeneous state (everyone cooperates or everyone defects) is a fixed point under deterministic imitation dynamics. Thus, there is a need to define a *coexistence fixed point*.

Definition 2.3.1. Given an evolutionary game $\mathcal{E} = (\mathcal{G}, \mathbf{p}, \pi, \mathcal{T}, \varphi)$ on a graph, the state $X = (X_1, \dots, X_{|V|}) \in S^V$ is a fixed point of $\mathcal{E}$ if $\varphi(t+1, t; X) = X$ for all $t \in \mathbb{N}$.

Further, if $0 < \sum_{i \in V} X_i < |V|$, then the state X is called a coexistence fixed point.

Note, that if a certain strategy vector $X \in S^V$ is a fixed point under certain non-omitting update order $\mathcal{T}$ then it is a fixed point under any arbitrary update order.

The behaviour of evolutionary games on graphs fixed points with the underlying graph belonging to a particular class (complete graph, wheel graph) was examined in [17]. Certain notion of stability and attractivity was also discussed therein. Unfortunately, any known concept of stability does not seem to correspond with any expected and intuitive behaviour.

The next theorem shows that given any parameter quadruple $\mathbf{p} = (a, b, c, d)$ there is always an underlying graph such that its evolutionary game on a graph has a coexistence fixed point. In other words, the structure of the population enabling a balanced state can be found for any given game rules (game-theoretical parameters).

Theorem 2.3.2. *[18, Theorem 4.1., Theorem 6.1] Let π be either mean or aggregate utility function. For each $\mathbf{p} = (a, b, c, d)$ there exists a connected graph $\mathcal{G}$ such that for any update order $\mathcal{T}$ the evolutionary game on a graph $(\mathcal{G}, \mathbf{p}, \pi, \mathcal{T}, \varphi)$ has a coexistence fixed point.*

The proofs of both parts of Theorem 2.3.2 are carried out in [18]; we just discuss their ideas here. Hopefully, we are able to demonstrate that the mechanism of cooperation preservation is not in contradiction with a common sense.

Note that vertex strategy cannot change if the vertex is surrounded by vertices playing the same strategy. It is thus reasonable to define clusters of cooperators and clusters of defectors and their inner and boundary vertices. The inner (IC) and boundary (BC) cooperators are defined

$$V_{IC} = \big\{ i \in V \mid X_i = 1 \text{ and } X_j = 1 \text{ for all } j \in N_1(i) \big\},$$
$$V_{BC} = \big\{ i \in V \mid X_i = 1 \text{ and there exists } j \in N_1(i) \text{ with } X_j = 0 \big\}.$$

Boundary (BD) and inner (ID) defectors are defined analogously.

Sketch of the proof of Theorem 2.3.2. Let us consider the case with mean utility function π^M first. Given parameter quadruple $\mathbf{p} = (a, b, c, d)$ we construct a graph (dependent on $\mathbf{p}$) as in Figure 2.4.

The subgraph consisting of boundary cooperators (BC) and boundary defectors (BD) forms a complete bipartite graph. All boundary cooperators have the same number of inner cooperators (IC) attached. Similarly, all boundary defectors have the same number of inner defectors (ID) attached. The trick is to balance the number of all four types of vertices (IC, BC, BD, ID) with respect to the given parameter quadruple $\mathbf{p}$ such that the inequality

$$\pi^M_{\mathrm{IC}} > \pi^M_{\mathrm{BD}} > \pi^M_{\mathrm{BC}}$$

holds.

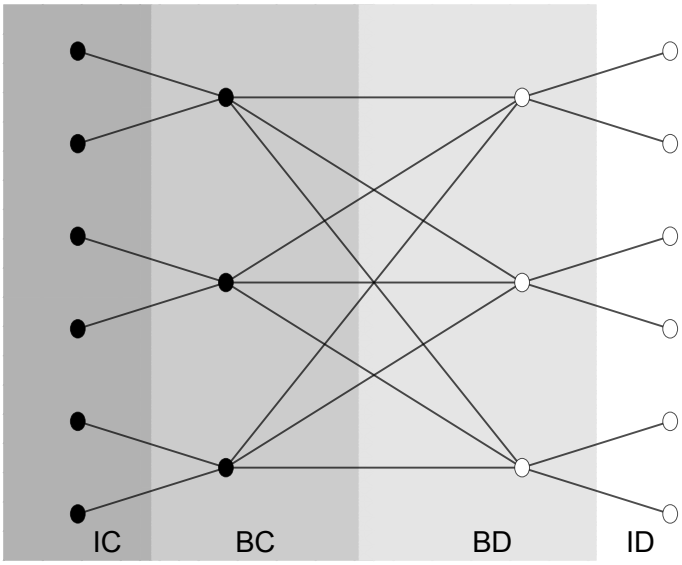

Figure 2.4: Construction of a graph with a coexistence equilibrium for any given parameters, see Theorem 2.3.2. Black vertices represent cooperators, white vertices defectors. Source: [18].

It can be shown that this balance is always possible. The boundary defectors then have the highest utility in their neighbourhood and do not change their strategy. Boundary cooperators have lower utility than boundary defectors but the strong inner cooperators prevent them from the strategy change. As mentioned above, the inner cooperators and the inner defectors cannot change their strategy under the deterministic imitation dynamics.

Considering the aggregate utility function π^A we just add a certain number of cooperating vertices to the inner cooperators. This enables us to create the same type of balance as discussed above to obtain

$$\pi^A_{\mathrm{IC}} > \pi^A_{\mathrm{BD}} > \pi^A_{\mathrm{BC}}$$

which concludes this sketch of the proof. □

Speaking in the terms of cooperation preservation, the idea is that the boundary cooperators need not have to have the highest utility to prevail. The important fact is that they have a strong cooperating neighbour whose utility is not lowered by any defecting neighbour.

A result from [18] complementary to Theorem 2.3.2 is that given any connected graph the parameters $\mathbf{p} = (a, b, c, d)$ can be chosen such that the resulting evolutionary game on a graph has a coexistence fixed point.

Theorem 2.3.3. *[18, Theorem 4.2., Theorem 6.2.] Let π be either mean or aggregate utility function. For each connected graph $\mathcal{G}$ there exists a parameter vector $\mathbf{p} = (a, b, c, d)$ such that for any update order $\mathcal{T}$ the evolutionary game on a graph $(\mathcal{G}, \mathbf{p}, \pi, \mathcal{T}, \varphi)$ has a coexistence fixed point.*

Sketch of the proof of Theorem 2.3.3. Let us consider the case with the mean utility function π^M first. Assume that the graph $\mathcal{G}$ is complete. It is then straightforward to pick an arbitrary coexistence state and suitable parameters such that $\pi_i = \pi_j$ for all $i, j \in V(\mathcal{G})$ [2]. Let us assume that the graph $\mathcal{G}$ is not complete. There is surely a vertex which is not connected to all the other vertices in $\mathcal{G}$. Denoting this vertex i, we construct a coexistence state as in Figure 2.5.

The parameters $\mathbf{p} = (a, b, c, d)$ can be now chosen dependent on the vertex maximal degree such that

$$\pi^M_i > \pi^M_{\mathrm{BD}} > \pi^M_{\mathrm{BC}}. \tag{2.19}$$

The approach is identical if the aggregate utility function π^A is considered. □

2.4 Periodic orbits

The results of this section were mainly published in paper [19] (included in Appendix C).

Another of the coexistence phenomena observed in dynamical systems is the periodic behaviour. Let us start with a formal definition of a *periodic orbit* of the evolutionary games on graphs.

[2] Note that given a complete graph $\mathcal{K}_n$ and a coexistence state the suitable parameter vector $\mathbf{p} = (a, b, c, d)$ forms a set of measure zero in the space $\mathbb{R}^4$. It is arguable whether this can be considered as the violation of the generic payoffs assumption. On the other hand, the class of complete graphs can be considered a very small one in the class of all graphs.

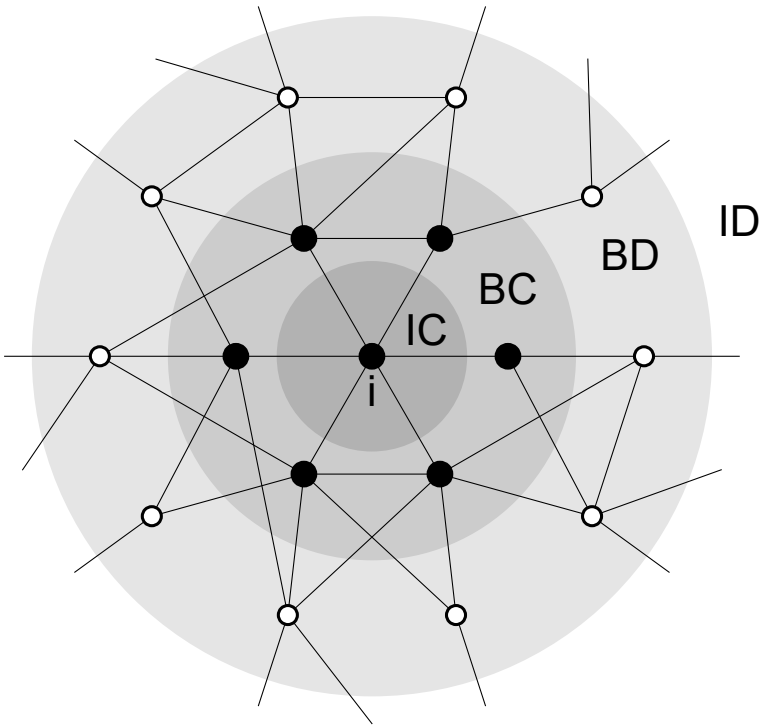

Figure 2.5: Construction of a coexistence equilibrium on an arbitrary graph, see Theorem 2.3.3. Source: [18].

Definition 2.4.1. Given an evolutionary game $\mathcal{E} = (\mathcal{G}, \mathbf{p}, \pi, \mathcal{T}, \varphi)$ on a graph and an initial state X_0, the sequence of strategy vectors $\mathcal{X} = \big(X(0), X(1), \dots\big) \in \big[S^V\big]^{\mathbb{N}_0}$ is called the *trajectory* of $\mathcal{E} = (\mathcal{G}, \mathbf{p}, \pi, \mathcal{T}, \varphi)$ with initial state X_0 if for all $t \in \mathbb{N}_0$ we have

$$X(0) = X_0,$$
$$X(t+1) = \varphi\big(t+1, t; X(t)\big).$$

The trajectory is called *periodic with period* $p \in \mathbb{N}$ if $X(t+p) = X(t)$ for $t \in \mathbb{N}_0$.

The behaviour of periodic orbits of the evolutionary games on graphs with the underlying graph belonging to a certain class (complete graph, wheel graph) was again examined in [17].

The main question of [19] was whether there exists a graph such that the evolutionary game on graph has a periodic orbit of arbitrary length.

Question 2.4.2. *[19, Question 1] Given admissible parameters $\mathbf{p} = (a, b, c, d) \in \mathcal{P}$, a utility function π, an update order $\mathcal{T}$, dynamics φ and a number $p \in \mathbb{N}$, does there exist a connected graph $\mathcal{G}$ and an initial state X_0 such that $\mathcal{X}$ is a periodic trajectory of the evolutionary game $\mathcal{E} = (\mathcal{G}, \mathbf{p}, \pi, \mathcal{T}, \varphi)$ on a graph with minimal period p?*

This question was answered positively for the mean utility function π^M, the synchronous update order $\mathcal{T}$ and the deterministic imitation dynamics φ. Further, certain restriction on the underlying graph $\mathcal{G}$ were posed. This is investigated later. The general answer to Question 2.4.2 is formally summarized in the following theorem.

Theorem 2.4.3. *[19, Theorem 3.1] Let $\mathbf{p} = (a, b, c, d) \in \mathcal{P}$ be admissible parameters, π the mean utility function, $\mathcal{T}$ the synchronous update order, φ the deterministic imitation dynamics and $p \in \mathbb{N}$. Then there exists a graph $\mathcal{G}$ and an initial state X_0 such that $\mathcal{X} = \big(X(0), X(1), \dots\big)$ is a periodic trajectory of minimal length p of the evolutionary game $\mathcal{E} = (\mathcal{G}, \mathbf{p}, \pi, \mathcal{T}, \varphi)$ on a graph with initial state X_0.*

As in the fixed point case, the proof of Theorem 2.4.3 will be just sketched. The proof relies on a construction of an underlying graph and an initial condition based on the given parameters $\mathbf{p} = (a, b, c, d)$ and the subsequent analysis of the dynamics. Two different constructions will be separately presented for the cases $a > c$ and $c > a$.

Sketch of the proof of Theorem 2.4.3. Let us suppose that $a > c$. The construction of our graph depends on p and three parameters $q, r, s \in \mathbb{N}$. See Figure 2.6 for an illustration of the graph structure. Let $\mathcal{S}$ be a bipartite graph with classes S_1 and S_2 each having s vertices. Add a vertex $h_{\mathcal{S}}$ incident with all vertices in S_1 and a vertex $f_{\mathcal{S}}$ incident with exactly one vertex in S_2.

Now take $2p-1$ copies of the complete graph with q vertices, denoted by $\mathcal{K}_{-(p-1)},\dots,\mathcal{K}_{p-1}$, and chain them together to form a ladder-like structure. Add one vertex g connected to all vertices in $\mathcal{K}_0$. Denote the vertices in $\mathcal{K}_n$ by $\{k_{n,\ell} \mid \ell = 1,\dots,q\}$ for $n = -(p-1),\dots,p-1$ such that $k_{n,\ell}$ and $k_{n+1,\ell}$ are connected by an edge for $n = -(p-1),\dots,p-2$ and $\ell = 1,\dots,q$. Add $q\cdot r$ many copies of $\mathcal{S}$ and denote them by $\mathcal{S}_{\ell,m}$ for $\ell = 1,\dots,q$ and $m = 1,\dots,r$. Connect $f_{\mathcal{S}_{\ell,m}}$ to all vertices in $\{k_{n,\ell} \mid n = -(p-1),\dots,p-1\}$ for $m = 1,\dots,r$ and $\ell = 1,\dots,q$ and to one vertex in $\mathcal{S}_{\ell,m}$. Next, connect a vertex $h_{\mathcal{S}_{\ell,m}}$ to each of the vertices in the opposite partition of $\mathcal{S}_{\ell,m}$. We denote the graph thus obtained $\mathcal{G}$.

Set $H = \{h_{\mathcal{S}_{\ell,m}} \mid \ell = 1,\dots,q,\ m = 1,\dots,r\}$. Let I be the set of all neighbours of the vertices in H, let J be the set of all neighbours of vertices in I which are not already in H, and set $F = \{f_{\mathcal{S}_{\ell,m}} \mid \ell = 1,\dots,q,\ m = 1,\dots,r\}$. Finally set $K_n = \{k_{n,\ell} \mid \ell = 1,\dots,q\} \cup \{k_{-n,\ell} \mid \ell = 1,\dots,q\}$ for $n = 0,\dots,p-1$ and $K = \bigcup_{n=0}^{p-1} K_n$.

Let X_0 be the state in which all vertices in $H \cup I \cup K_0 \cup \{g\}$ are cooperating and all other vertices are defecting, that is,

$$(X_0)_i = \begin{cases} 1, & i \in I \cup H \cup K_0 \cup \{g\}, \\ 0, & i \in F \cup J \cup \bigcup_{n=1}^{p-1} K_n. \end{cases}$$

Let $\mathcal{X} = \big(X(0), X(1), \dots\big)$ be the trajectory of the evolutionary game with parameters (a,b,c,d), the syn-

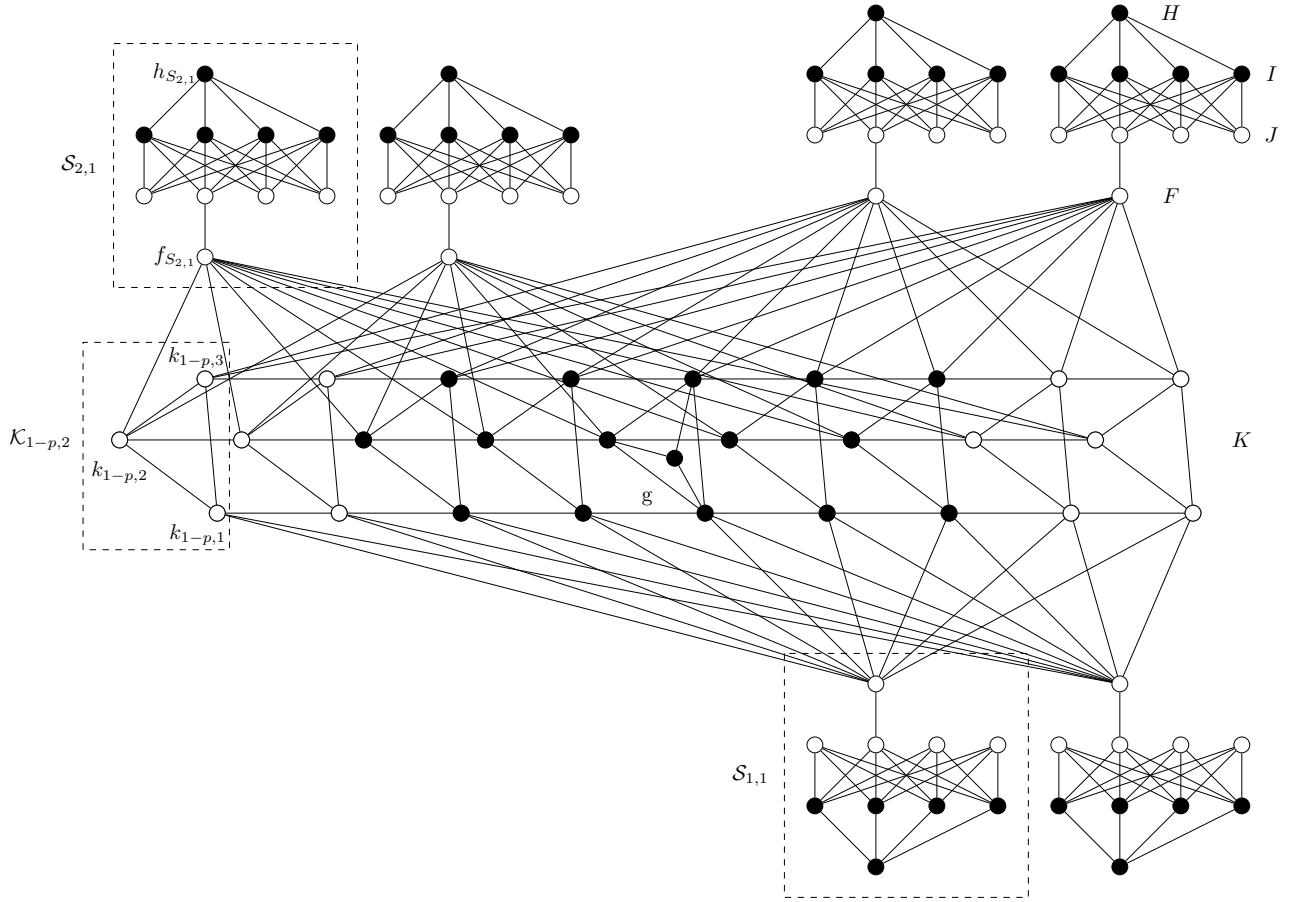

Figure 2.6: Example of the graph $\mathcal{G}$ in the proof of Theorem 2.4.3 for $a > c$ with the parameters $p = 5, q = 3, r = 2$ and $s = 4$. The cooperators are depicted by full circles. Source: [19].

chronous update order, the mean utility function and the deterministic imitation dynamics on the graph $\mathcal{G}$ constructed above with initial state X_0. Let $\pi_i(t) = \pi\big(X_i(t)\big)$ be the utility of the vertex i at time t. It can be shown that for suitable parameters q, r, s the dynamics with initial value X_0 is the following. All vertices not in K do not change their strategy and cooperation spreads along the ladder for p time steps. After p time steps, we reach again the initial state X_0 since all vertices in $K \setminus K_0$ switch back to defection. More precisely, for $t = 1,\dots,p-1$ we have

$$X_i(t) = \begin{cases} X_i(0), & i \in F \cup H \cup I \cup J \cup K_0 \cup \{g\}, \\ 1, & i \in \bigcup_{n=0}^{t} K_n, \\ 0, & i \in \bigcup_{n=t+1}^{p-1} K_n \end{cases}$$

and $X(p) = X(0)$.

The proof in [19] shows that there always exist parameters q, r, s such that the dynamics of the game are as described above provided $a > c$. This discussion is rather technical and not included.

Let us suppose that $c > a$. Let us define a graph $\mathcal{G}$ depending on p and four parameters $o, q, r, s \in \mathbb{N}$ as depicted in Figure 2.7. We start with p complete graphs $\mathcal{K}_1, \dots, \mathcal{K}_p$ on o vertices. Again, the subgraphs $\mathcal{K}_n$ for $n = 1, \dots, p$ are connected in series to form a ladder-like structure. There is a subgraph $\mathcal{K}_{p+1}$ which is a complement of a complete graph on o vertices (isolated vertices) connected to the ladder in the same manner. The vertices of $\mathcal{K}_n$ are denoted by $k_{n,m}$ for $n = 1, \dots, p+1$ and $m = 1, \dots, o$, forming the sets K_n. Every vertex in the interior of the ladder (the vertices in K_2 to K_p) is connected to the vertex g_R. Additionally, the vertex g_R has $q + 1$ other neighbours. It has q neighbouring vertices of degree one forming the set H and a neighbour which we call g_D. The vertex g_D has r neighbouring vertices of degree one forming the set I and s neighbouring vertices of degree two forming the set J. Each vertex in J is connected to the vertex g_C.

Let X_0 be the initial state defined by

$$(X_0)_i = \begin{cases} 1, & i \in K_1 \cup J \cup \{g_C\}, \\ 0, & i \in \bigcup_{n=2}^{p+1} K_n \cup H \cup I \cup \{g_D, g_R\}. \end{cases}$$

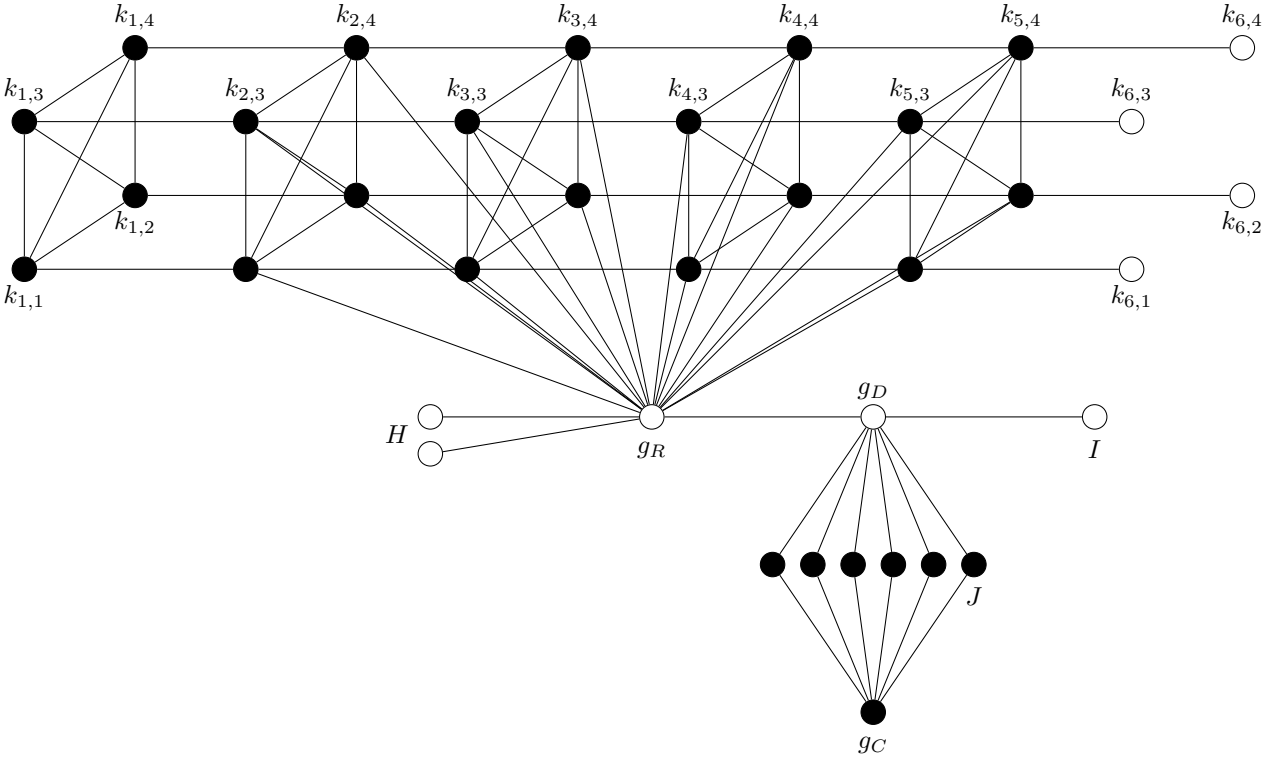

Figure 2.7: Example of the graph $\mathcal{G}$ in the proof of Theorem 2.4.3 for $c > a$ with parameters $p = 5, o = 4, s = 6, r = 1$, $q = 2$ with strategy vector $X(4)$. Cooperators are depicted by full circles. Source: [19].

Let $\mathcal{X} = \big(X(0), X(1), \dots\big)$ be trajectory of the evolutionary game with parameters (a, b, c, d), the synchronous update order, the mean utility and the deterministic imitation dynamics on the graph $\mathcal{G}$ constructed above with initial state X_0. It can be shown that for suitable parameters o, q, r, s the dynamics with the initial value X_0 is the following. The cooperation spreads along the ladder $\mathcal{K}_n$ to $\mathcal{K}_p$ and at time $t = p-1$ the strategy of all vertices of $\mathcal{K}_2$ to $\mathcal{K}_p$ is reset to defection. Formally,

$$X_i(t) = \begin{cases} 1, & i \in \bigcup_{n=1}^{t+1} K_n, \\ X_i(t-1), & \text{otherwise} \end{cases}$$

holds for $t = 1, \dots, p-1$ and $X(t+p) = X(t)$ for $t \in \mathbb{N}_0$. See Figure 2.7 for illustration.

The proof in [19] shows that there always exist parameters o, p, q, r, s such that the dynamics of the game are as described above, provided $c > a$. This discussion is rather technical and not included here. □

All the previous constructions relied heavily on the cycles present in the underlying graph. The reset to the initial states was ensured by one or more defecting vertices connected to all vertices changing their strategy.

Interestingly, the evolutionary games on graphs can show a periodic behaviour even when the underlying graph is a tree. This needs a completely different approach to the dynamics. The idea is summarized in the following theorem. Note that we restrict ourselves to the HD scenario only which has a mixed Nash equilibrium in the matrix game and a stable non-trivial equilibrium in replicator dynamics.

Theorem 2.4.4. *[19, Theorem 4.1] Let $\mathbf{p} = (a, b, c, d) \in \mathcal{P}$ be admissible parameters satisfying the conditions of the HD scenario, $c > a > b > d$, π the mean utility function, $\mathcal{T}$ the synchronous update order, φ the deterministic imitation dynamics and $p_0 \in \mathbb{N}$. There exists an acyclic graph $\mathcal{G}$, a number $p \in \mathbb{N}_0$ such that $p \geq p_0$ and an initial state X_0 such that $\mathcal{X} = \big(X(0), X(1), \dots\big)$ is a periodic trajectory of minimal length p of the evolutionary game $\mathcal{E} = (\mathcal{G}, \mathbf{p}, \pi, \mathcal{T}, \varphi)$ on a graph with initial state X_0.*

Sketch of the proof of Theorem 2.4.4. Let us define a graph $\mathcal{G}$ whose structure is dependent on two parameters $q, r \in \mathbb{N}$. The graph $\mathcal{G}$ is a rooted r-nary tree such that:

- the root h_0 has only one child h_1,
- every vertex at the level 1 to $q-2$ has exactly r children,
- exactly r^2 vertices at the level $q-1$ with pairwise different predecessors at the third level are leaves,
- every other vertex at the level $q-1$ has r children which are leaves.

See Figure 2.8 for illustration.

For the sake of simplicity, we only focus on one branch of the tree $\mathcal{G}$ rooted in a fixed vertex h_3 at the level three. The vertices in the other branches follow the same dynamics by symmetry reasons (the initial state and the graph $\mathcal{G}$ are invariant with respect to an automorphism exchanging the whole branches rooted at level 3). The descendant of h_1 at the level $q-1$ in the fixed branch which is a leaf is denoted by h_{q-1}. The vertices in a path from h_1 to h_{q-1} are be denoted by $h_1, h_2, \dots, h_{q-1}$ in an increasing manner. The vertices in $H = \{h_1, \dots, h_{q-1}\}$ are called the *special vertices*. The set of all descendants of h_m for $m = 3, \dots, q-2$ which are not in H will be denoted by I_m. Vertices in $I = \bigcup_{m=3}^{q-2} I_m$ are called the *ordinary vertices*. Let the initial condition X_0 be such that every vertex in levels $0, \dots, q-2$ is cooperating and every other vertex is defecting, that is

$$(X_0)_i = \begin{cases} 1, & i \in N_{\leq q-2}(h_0), \\ 0, & \text{otherwise.} \end{cases}$$

See Figure 2.8 for illustration of the graph construction and the initial condition X_0.

A complete description of the system dynamics is rather technical. The key ingredient to understanding the dynamics are two local situations. There exists the value of q such that

(T1) a cooperating inner vertex with one cooperating neighbour switches all other neighbouring defectors to cooperation while preserving its strategy, see Figure 2.9a,

(T2) a defecting inner vertex with one defecting neighbour switches all other neighbouring cooperators to defection while preserving its strategy, see Figure 2.9b.

The main idea of the dynamics is that the special vertices H gradually switch from cooperation to defection. This is induced by the behaviour (T1). When the only cooperating special vertices are h_0 and h_1, the cooperation starts to spread towards the leaves. This is induced by the behaviour (T2). The dynamics of other (non-special) vertices can also be explained by (T1) and (T2). For better illustration, see the figure sequence in the closing pages of the paper [19] (included in Appendix C). □

2.5 Open questions and further directions

We provide a structured overview of possible further directions and open questions in this final section.

Stability and attractivity: A natural and surprisingly nontrivial question concerns the stability of the equilibria of evolutionary games on graphs. In [18, Definition 7] the stability via a perturbation of a single vertex in a state was defined and results for complete and k-regular graphs were provided therein. It however seems that this concept is very difficult to study on general graphs. Is there a sophisticated way to analyse the stability of the equilibria in this sense? Alternatively, is there a better concept of stability/attractivity for evolutionary games on graphs? The stability can be moreover regarded with respect to the existence of edges, i.e., is the current state stable with respect to a small structure change?

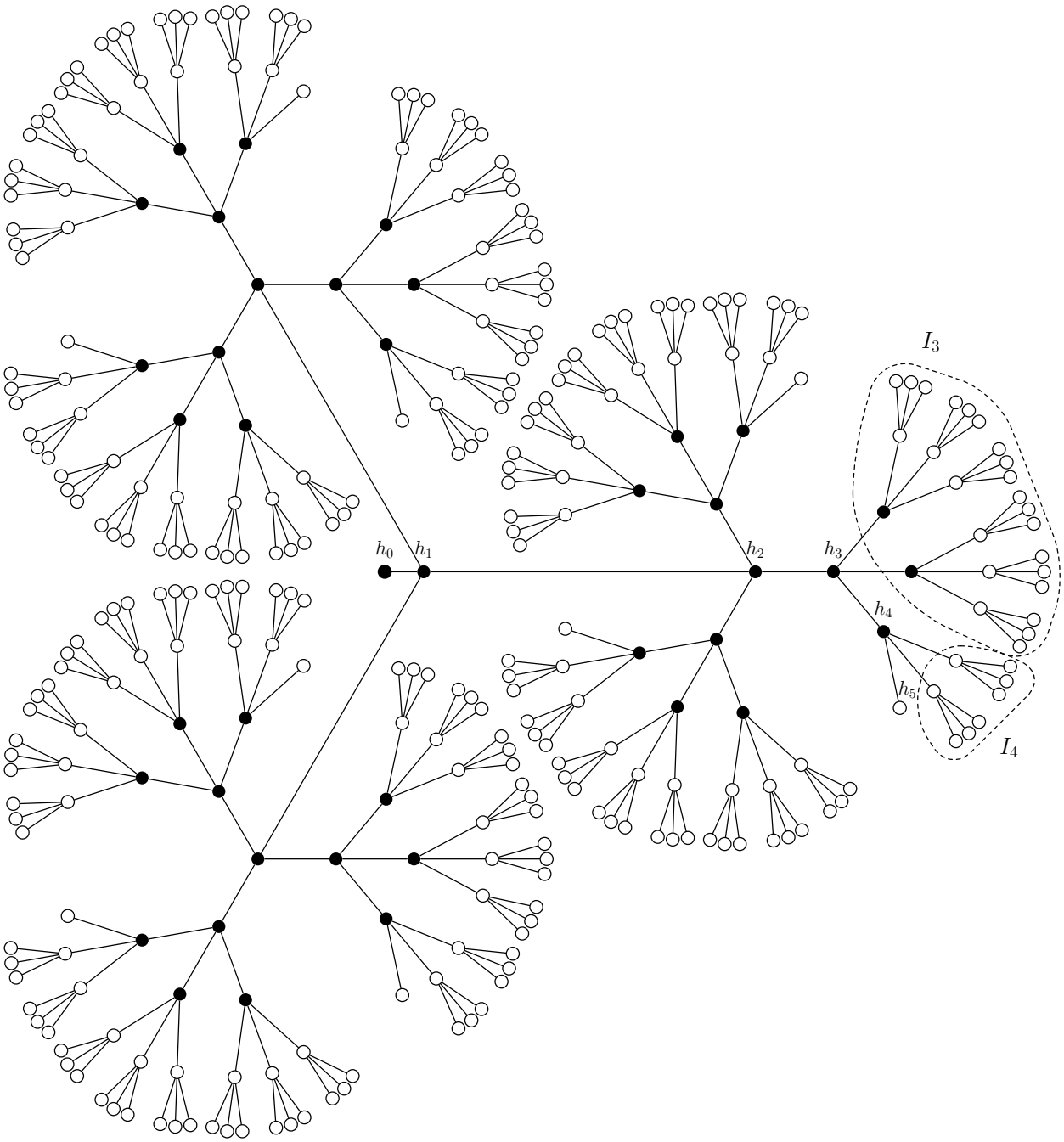

Figure 2.8: Example of the graph constructed in the proof of Theorem 2.4.4 with an initial condition. The cooperators are depicted by filled black circles, defectors by white circles. The parameters are $r = 3$, $q = 6$. Source: [19].

Attractive states examination: Construct efficient methods for finding all attractors for a given graph and admissible parameters $(a, b, c, d) \in \mathcal{P}$.

Different dynamics: Examine behaviour of the evolutionary games on a graph under dynamics different to the deterministic imitation dynamics. Namely, the *deterministic death-birth* dynamics, in which only the vertices with the globally lowest utility adopt the state of its neighbour with highest utility or deterministic *birth-death dynamics* in which only vertices in the neighbourhood of vertices with the globally highest utility are updated.

Examination of particular classes of graphs: Behaviour of simple classes of graphs (cycle graphs, path graphs, planar graphs, etc.) can be examined analytically in the same manner as complete graphs in [17].

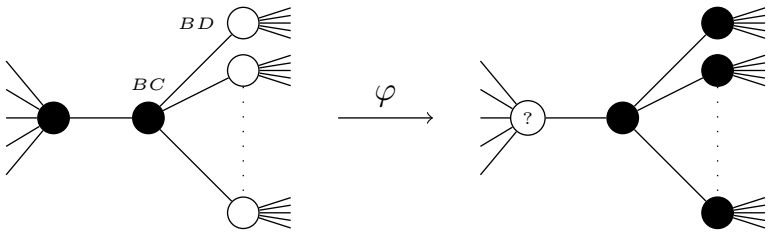

a: Illustration of claim (T1).

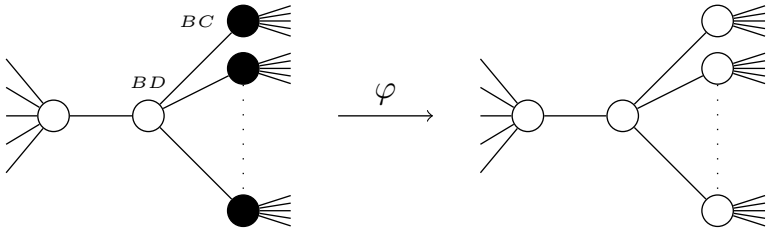

b: Illustration of claim (T2).

Figure 2.9: Examples of the local behaviour of the evolutionary game on a graph in the proof of Theorem 2.4.4. Note that the orientation of the pictures may be sligthly misleading since cooperating and defecting neighbours do not need to be on the same level of the tree (e.g., the local behaviour claim (T2) is still valid if the central defector have one defecting offspring and all the other neighbours cooperating.) Source: [19].

Graph Limits: The asymptotic properties of the evolutionary games on a graph were examined in [63]. It has been shown that the replicator dynamics can be considered as a limit of evolutionary game on a graph with $\mathcal{G} = \mathcal{K}_n$ being complete as $n \to \infty$. This limiting behaviour can be analysed for the evolutionary games on graphs with noncomplete underlying graphs, e.g., bipartite graphs, cycle graphs, etc. (generally any graph type which admits a graph limit in a feasible way).

Chapter 3

Travelling waves in the Nagumo lattice differential equation

Note to notation

Let us shortly elaborate on the notation of the derivatives in the forthcoming text. We express the derivative of the function in one variable by the prime mark (the Lagrange's notation), i.e., $g'(x)$. We mostly denote the partial derivative via the lower index, i.e., $f_u(u;a)$ but in specific cases we may resort to the use of the Leibnitz's notation, i.e., $\frac{\partial}{\partial u}f(u;a)$, to avoid confusion with the used indexing. The derivatives of multivariate transformations are expressed via the Euler's notation, i.e., $D_1u(x,t)$ where the number denotes the position of the variable with respect to which we calculate the derivative. For example, for $x=(x_1,x_2,\dots,x_n)\in\mathbb{R}^n$ and $u=(u_1,u_2,\dots,u_n):\mathbb{R}^n\times\mathbb{R}\to\mathbb{R}^n$ we have

$$D_1u(x,t)=\begin{pmatrix}\frac{\partial}{\partial x_1}u_1(x,t) & \frac{\partial}{\partial x_2}u_1(x,t) & \dots & \frac{\partial}{\partial x_n}u_1(x,t)\\ \frac{\partial}{\partial x_1}u_2(x,t) & \frac{\partial}{\partial x_2}u_2(x,t) & \dots & \frac{\partial}{\partial x_n}u_2(x,t)\\ \vdots & \vdots & \ddots & \vdots\\ \frac{\partial}{\partial x_1}u_n(x,t) & \dots & \dots & \frac{\partial}{\partial x_n}u_n(x,t)\end{pmatrix}$$

and

$$D_2u(x,t)=u_t(x,t).$$

The second part of this thesis is devoted to the investigation of periodic stationary solutions and travelling waves in the Nagumo lattice differential equation, which is the model with the discrete spatial structure, the continuous temporal structure and the continuous state space

$$u_i'(t)=d\big(u_{i-1}(t)-2u_i(t)+u_{i+1}(t)\big)+f\big(u_i(t);a\big),\tag{3.1}$$

where $i\in\mathbb{Z}, t>0$ and $d>0$. The nonlinear term is given by

$$f(s)=f(s;a)=s(1-s)(s-a),\quad a\in(0,1).\tag{3.2}$$

The spatial structure of the equation (3.1) can be expressed as a one-dimensional path, see Figure 1.1a. Let us start with a brief and general introduction to reaction-diffusion equations with homogeneous spatial structure (partial differential equations, PDE) and non-homogenous spatial structure (graph differential equations and lattice differential equations) to be able to present some of the properties of the equation (3.1) in a proper context. This treatise on reaction-diffusion equations does not aspire to be complete but focuses on specific parts of this wide topic.

Reaction-diffusion differential equations The reaction-diffusion partial differential equation is usually considered to be in the form

$$u_t(x,t)=d\,\Delta u(x,t)+f\big(t,x,u(x,t)\big),\tag{3.3}$$

where $n \geq 2$, $x = (x_1, x_2, \ldots, x_n) \in \Omega \subset \mathbb{R}^n$, Ω being an open subset of $\mathbb{R}^n$. The value $d \in \mathbb{R}$ expresses the strength of the diffusion, the operator Δ is the Laplacian

$$\Delta u(x,t) = u_{x_1x_1}(x,t) + u_{x_2x_2}(x,t) + \ldots + u_{x_nx_n}(x,t). \tag{3.4}$$

We can specially assume $x \in \mathbb{R}$, one-dimensional spatial variable. The equation (3.3) then formally reduces to

$$u_t(x,t) = d\, u_{xx}(x,t) + f\big(t, x, u(x,t)\big).$$

Here, $d > 0$ and $x \in I \subset \mathbb{R}$ where I is an open interval. The reaction term g is a strictly local function dependent on the values at the exact point $x \in \mathbb{R}^n$ only. In contrary, the diffusion operator Δ is not strictly local since the derivatives in the Laplacian consider not only the values at the point $x \in \mathbb{R}^n$ but also in an infinitesimal neighbourhood[1]. This distinction is clearly recognizable in the further text when we resort to the graph reaction-diffusion equations and the lattice reaction-diffusion equations. The equations of type (3.3) and their systems are used for modelling various processes in chemistry [27], biology [51], population dynamics [52] and other fields. From mathematical point of view, the equation of type (3.4) can possess travelling wave solutions which are stable with respect to a reasonable perturbation [43] and their systems can even exhibit pattern formation [51].

Reaction-diffusion equations on graphs The models of type (3.3) assume that the spatial structure (the set Ω) is connected and continuous. On the other hand, one can assume that there are several patches or locations in which the reaction locally takes place and they are connected via paths where the transport is ensured via diffusion. A simple example is a system of coupled biochemical reactors [38]. The spatial structure is then mathematically described by an undirected graph as in each of the three examples in Figure 1.1. Let $\mathcal{G} = (V, E)$ be an undirected graph, V be the set of vertices which is possibly countable and E be the set of edges. For simplicity, we assume that each vertex $i \in V$ has a finite number of edges attached and this number is globally bounded from above by some finite value. A general reaction-diffusion differential equation on a graph then takes the form

$$u_i'(t) = \sum_{j \in \mathcal{N}(i)} d_{ij} \big(u_j(t) - u_i(t)\big) + f\big(i, u_i(t)\big), \tag{3.5}$$

where $i \in V$, $D = (d_{ij})_{i,j \in V}$ is a possibly infinite matrix with nonnegative[2] entries, $d_{ij} \geq 0$. Let us point out that as in the case of the PDE (3.4), the linear diffusion term in (3.5) is non-local since it processes values from the intermediate neighbourhood of the vertex of interest (the vertex i) but the nonlinear reaction term is strictly local in this sense. The equations of type (3.5) arise in of modelling various phenomena in biology [3], epidemiology [15], population dynamics [61] and other fields (we advise the reader to see the citations therein). Let us also note that we restricted ourselves to the reaction-diffusion equations only and completely neglected other possible dynamics of the differential equations on graphs in this treatise.

Here, we further distinguish two classes of the equations of type (3.5): *the graph reaction-diffusion differential equations* (GDE) and *the lattice reaction-diffusion differential equations* (LDE). Note that the terminology is not fully unified in the literature but by graph differential equations, we consider equations of type (3.5) where the set of the vertices V is finite $|V| < +\infty$. On the other hand, the lattice differential equations are also of the type (3.5) with the countable set of vertices V but an additional (and a fairly strong one) regularity of the edge connections is required, see Figures 1.1a, 1.1b.

Bistable equations The LDE (3.1) is used as a prototype bistable equation arising from the modelling of the nerve impulse propagation through a myelinated axon [3]. The bistable equations have their use in modelling of active transmission lines [54, 55], cardiophysiology [2], nonlinear optics [36], population dynamics [41] and other fields. The idea of this model originates in spatially continuous PDE, the *FitzHugh-Nagumo equation* ([21, 54]) used to describe signal propagation in homogeneous media

$$u_t(x,t) = d\, u_{xx}(x,t) + f\big(u(x,t); a\big) \tag{3.6}$$

with the cubic nonlinearity (3.2). One can also consider a general cubic nonlinearity

$$\begin{aligned} &f_{\text{gen}}(0;a) = f_{\text{gen}}(a;a) = f_{\text{gen}}(1;a) = 0\,, \quad f_{\text{gen}}'(0;a) < 0\,, \quad f_{\text{gen}}'(1;a) < 0, \\ &f_{\text{gen}}(x;a) < 0 \text{ for } x \in (0,a)\,, \quad f_{\text{gen}}(x;a) > 0 \text{ for } x \in (a,1) \end{aligned} \tag{3.7}$$

[1] There is also a wide research field focusing on the so-called nonlocal diffusion operators in the form of kernel integral, e.g., [11]. The operator then depends not only on an infinitesimal neighbourhood of the point of interest but on the values in the neighbourhood with nontrivial area/volume.

[2] In some models, this assumption is relaxed and sometimes the diffusion intensity is even required to be negative [10, 33].

with (3.2) as a special case[3]. The fundamental idea is that the equation

$$u'(t) = f_{\text{gen}}\big(u(t)\big)$$

has two asymptotically stable steady states $u^* \in \{0, 1\}$ and one unstable solution $u^* = a$. The parameter a is also called the *detuning parameter* and it naturally describes the basins of attraction of the two stable stationary solutions. The equation (3.6) exhibit travelling wave behaviour whose properties are discussed later in Section 3.1.1. We only mention that the waves travel for almost all values of the detuning parameter $a \in (0, 1)$.

Nagumo lattice equation The LDE (3.1), as some versions of (3.4), possesses travelling wave solutions and spatially heterogeneous stationary solutions. Any of the structures does not however behave as one should expect from the continuous case. There is a nontrivial region in the parameter (a, d)-space such that the wave solution of the LDE (3.1) does not travel (it is pinned) contrary to a singular case of $a = 1/2$ for the Nagumo PDE. The pinning phenomenon can be partially explained by the existence of countably many asymptotically stable stationary solutions for sufficiently small diffusion rate r which prevent the waves from propagation, [35]. This constitutes one of our major motivations for the study of periodic stationary solutions of the LDE (3.1); the existence regions of the periodic stationary solutions actually seem to mostly occupy the pinning region, [32]. The periodic stationary solutions are also building blocks of the multichromatic waves, the waves which are not monotone and connect two stationary solutions of the LDE (3.1) out of which at least one is spatially heterogeneous, see Figure 3.1. The multichromatic waves' travelling regions are smaller in comparison to the

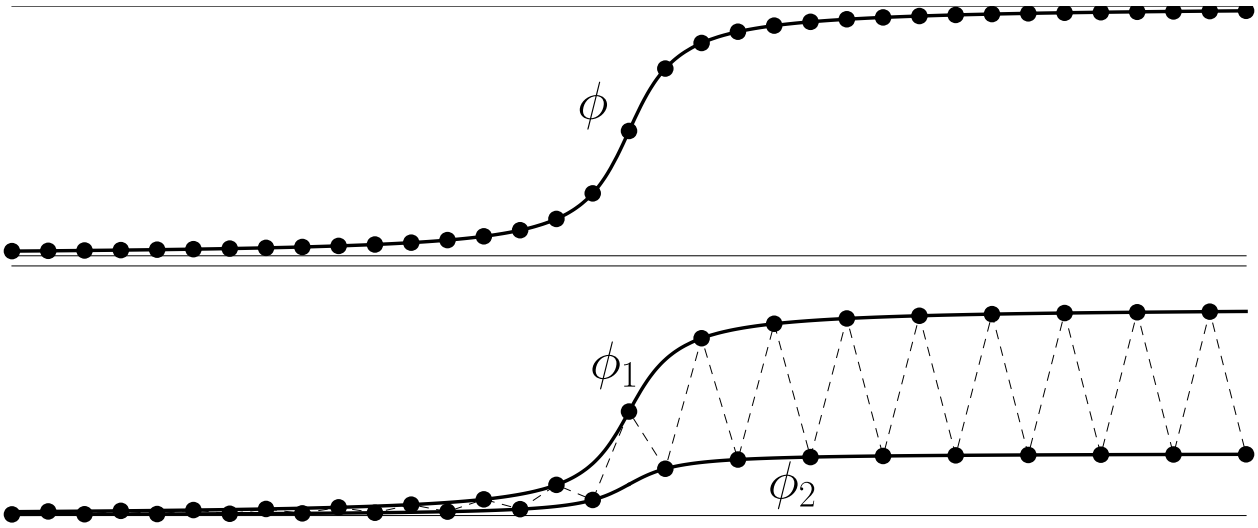

Figure 3.1: Illustrative examples of the monochromatic wave and multichromatic wave (we call this particular wave a birchomatic one). The monochromatic wave (the upper panel) can be interpolated by a monotone profile (3.10). The bichromatic wave can be partially interpolated by two monotone profiles (3.33).

classical monotone (monochromatic) waves but they travel even when the monochromatic waves are pinned, [30, 32]. They can be also composed to produce intricate wave collisions.

The following chapter consists mostly of the summary of results from [30–32, 69] ([31, 32, 69] are included in Appendices D, E, F as co-authored or authored publications). The text is organized as follows. We start with introductory results which mainly concern the comparison of travelling wave behaviour in the Nagumo PDE and the Nagumo LDE in §3.1. The periodic stationary solutions of the LDE (3.1) are examined in §3.2. In §3.2.1, we develop a naming scheme for the solutions. We closely focus on two-, three- and four-periodic solutions in §3.2.2. Subsequently, §3.2.3 is devoted to counting formulas determining the numbers of inequivalent (distinct) periodic stationary solutions and their existence regions. Using the aforementioned results, we provide proof of existence of the multichromatic waves and show numerical experiments further exposing their properties in §3.3.1. The chapter is concluded by discussion of possible extensions and open questions, §3.4.

3.1 Preliminaries and introductory results

We include a brief overview describing known properties of the travelling waves in the (3.1) and its spatially continuous counterpart, the Nagumo PDE. Let us note that the LDE (3.1) is well-posed in the space $\ell^\infty(\mathbb{Z}, \mathbb{R})$, [67].

[3]We usually work with the cubic nonlinear term (3.2). Many results can be also applied to the model with the general nonlinearity (3.9) but the additional regularity of the cubic is essential in some proofs. We shall inform individually whether the cubic or the general bistability is considered.

3.1.1 Travelling waves in the Nagumo PDE

Since the Nagumo LDE (3.1) can arise as a spatial discretization of a continuous PDE, we first summarize the properties of the travelling waves in the equation

$$u_t(x,t) = d\,u_{xx}(x,t) + f\big(u(x,t);a\big), \tag{3.8}$$

where $d, t > 0, x \in \mathbb{R}$ and

$$f(s) = f(s;a) = s(1-s)(s-a), \quad a \in (0,1). \tag{3.9}$$

As stated above, even though the equation (3.1) acts as a standalone model in various fields, the comparison between the continuous and the discrete case is important from the mathematical point of view.

The existence and the stability of the travelling wave solutions in the form

$$u(x,t) = \phi(x-ct)\,, \quad \phi(-\infty) = 0\,, \quad \phi(+\infty) = 1\,, \tag{3.10}$$

for the PDE (3.8) were examined in [20]. Substituting (3.10) into (3.8) leads to a problem

$$-c\,\phi'(\xi) = d\,\phi''(\xi) + f\big(\phi(\xi);a\big)\,, \tag{3.11}$$

with $\xi = x - ct$ which can be understood as a search for an unknown function $\phi : \mathbb{R} \to [0,1]$ and speed $c \in \mathbb{R}$. Considering $\psi = \phi'$, the system equivalent to (3.11) can be formulated

$$\begin{aligned} \psi'(\xi) &= \frac{c}{d}\,\psi(\xi) - \frac{1}{d}\,f\big(\phi(\xi);a\big), \\ \phi'(\xi) &= \psi(\xi). \end{aligned} \tag{3.12}$$

The heteroclinic orbit of the system (3.12) connecting the unstable stationary solution of the saddle type $(0,0)$ and the stable node $(1,0)$ represents the sought solution profile of the form (3.10). An incomplete summary of the results from [20] follows. The problem (3.8) possesses a monotone travelling wave solution ϕ if $a \neq 1/2$ and the direction (the sign of the speed c) is given by the formula[4]

$$\operatorname{sign}(c) = \operatorname{sign}\left(a - \frac{1}{2}\right).$$

If the initial condition u_0 has a "sufficiently similar" shape to ϕ then the solution of the problem (3.8) uniformly approaches the travelling wave solution ϕ with exponential speed.

3.1.2 Pinning in the Nagumo LDE (3.1)

Qualitatively different properties of the travelling wave solutions can be observed for the LDE (3.1). Substituting (3.10) into (3.1) leads to a *functional differential equation of a mixed type* (MFDE)

$$-c\,\phi'(\xi) = d\,\big(\phi(\xi-1) - 2\phi(\xi) + \phi(\xi+1)\big) + f\big(\phi(\xi);a\big) \tag{3.13}$$

with $\xi = x - ct$ where we search for an unknown profile $\phi : \mathbb{R} \to [0,1]$ and a speed $c \in \mathbb{R}$ subject to (3.10).

A rather complex treatise was performed by Mallet-Paret in [46] where an appropriate linear operator was formulated; its spectral properties were examined in the associated paper [45]. Let us note that these papers focus on a wider class of MFDE while the problem (3.13) being a special case. The results show that there exists a solution couple (c,ϕ) for each combination of the parameters $d > 0, a \in (0,1)$. The profile ϕ is moreover monotone.

We now turn our attention to the so-called *pinning* phenomenon. As we commented in the previous paragraph, the wave profiles travel for the PDE (3.3) provided $a \neq 1/2$. This is however not true for the LDE (3.1) which is illustrated by Figure 3.2. In a chronological order, Keener in [35] gave sufficient conditions on the existence of the travelling front solutions of the LDE (3.1) and conditions which cause the propagation failure. If $d > 0$ is sufficiently small, then every doubly infinite sequence $s = (s_i)_{i\in\mathbb{Z}}$, $s_i \in \{0,1\}$ represents one asymptotically stable steady state $u = (u_i)_{i\in\mathbb{Z}}$ of the LDE (3.1) such that $u_i \in [0,a)$ if $s_i = 0$ and $u_i \in (a,1]$ if $s_i = 1$. Moreover, their stability prevents the propagation of the waves of the form (3.10). In the case of

[4] This is also true for a general bistable nonlinearity of type (3.7) with

$$\operatorname{sign}(c) = -\operatorname{sign}\left(\int_0^1 f_{\mathrm{gen}}(s;a)\,\mathrm{d}s\right).$$

the problem with the cubic nonlinearity (3.9), the waves do not propagate if $d < a^2/4$ and $d < (1-a)^2/4$ hold simultaneously.

But, if d is great enough there are travelling wave solutions of the form (3.10) emerging from the Heaviside initial condition which are travelling to left ($c < 0$) for a close enough to 0 and travelling to the right for a close enough to 1. Namely, in the case of the cubic nonlinearity (3.9), the travelling wave solution is travelling to the left if

$$d > \zeta(a) = \frac{2a^2 - a + 2 - 2(a+1)\sqrt{a^2 - 3a + 1}}{25}$$

and to the right if $d > \zeta(1-a)$. The conditions above can ensure the existence of the travelling wave solutions on the subintervals of $a \in (0,1)$ such that $\eta(a) = a^2 - 3a + 1$ ($\eta(1-a)$, respectively) are nonnegative functions for the wave travelling to the left (right, respectively). The numerical experiments however show that the conditions are only sufficient, see Figure 3.2.

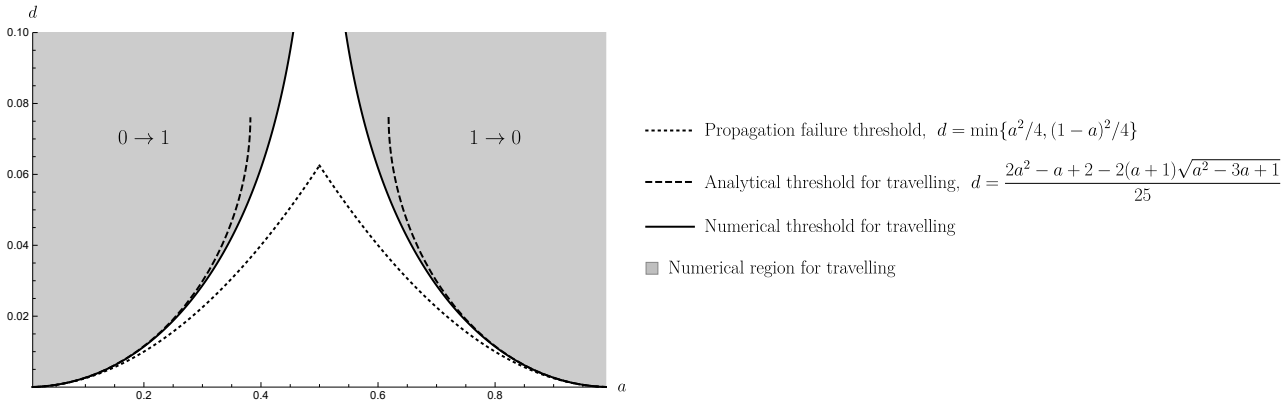

Figure 3.2: Analytical results from [35] including results of numerical experiments. Note that the numerical experiments are in accordance with the claims from [46]. The region description $0 \to 1$ means that the wave travels due to the gradual change of solution values close to 0 to the values close to 1.

Another description of the pinning region in the (a,d)-plane was made by Zinner in [72]. Namely, for fixed $a \in (0,1) \setminus \{1/2\}$ and $d \gg 1$ great enough the speed $c \neq 0$ is nonzero. Considering the parameter play the other way around Mallet-Paret in [46] showed that for fixed $d > 0$ the solutions in the form (3.10) travel to left ($c < 0$) if $a \approx 0$ and travel to right ($c > 0$) if $a \approx 1$.

The results in the works devoted to the crystalographic pinning [26, 44] indicate the existence of two constants $a_-(d), a_+(d) \in (0,1)$ such that $c = 0$ for any $a \in \big(a_-(d), a_+(d)\big)$ which corresponds to the propagation failure result for small d in [35].

As a final remark of this section, we emphasize that the pinning seems to be present in more general class of LDE since, for example, the results from [26, 44, 46] are applicable to the two-dimensional reaction-diffusion LDE

$$u_i'(t) = d\left(u_{i-1,j}(t) + u_{i+1,j}(t) + u_{i,j-1}(t) + u_{i,j+1}(t) - 4u_{i,j}(t)\right) + f\big(u_{i,j}(t); a\big) \tag{3.14}$$

with the general bistable nonlinearity (3.9) and the research is still ongoing [28].

3.2 Periodic stationary solutions of the Nagumo LDE

The section on the periodic solutions of the Nagumo lattice equation plays a twofold role in this thesis as in the analysis of the travelling waves in the LDE (3.1). Firstly, it is heavily indicated, that the region of existence of stable stationary solutions of the LDE (3.1) inhabit primarily (but not exclusively) the pinning region [35], see also Figure 3.3.

Secondly, the periodic stationary solutions are building blocks of the so-called multichromatic waves which can be considered generalizations of the waves of type (3.10) with novel and interesting behaviour. The multichromatic waves shall be discussed later.

Here, we mainly summarize the results from the papers [30–32, 69] (the publications [31, 32, 69] are included in Appendices D, E, F, respectively, as co-authored or authored publications).

For now on, we denote doubly-infinite sequences (mainly the stationary solutions of the LDE (3.1)) by the italic letters, e.g., $u = (u_i)_{i\in\mathbb{Z}} \in \mathbb{R}^{\mathbb{Z}}$, and we use the roman letters for vectors and their elements, e.g., $\mathrm{u} = (\mathrm{u}_1, \mathrm{u}_2, \ldots, \mathrm{u}_n) \in \mathbb{R}^n$ for some $n \in \mathbb{N}$.

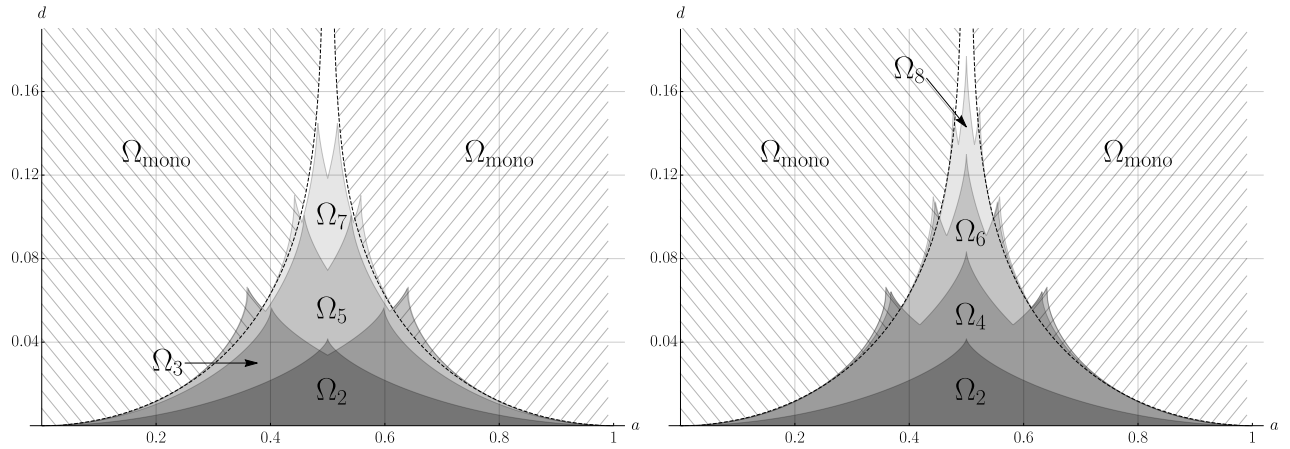

Figure 3.3: The existence regions of periodic stationary solutions of the LDE (3.1). The label Ω_i depicts the region for i-periodic solutions. Ω_{mono} is the travelling region of monochromatic waves, compare to Figure 3.2. Source: [32].

3.2.1 Qualitative properties of the periodic solutions

The stationary solutions of the LDE (3.1) must solve a countable system of parameter-dependent polynomial equations

$$d\big(u_{i-1}(t) - 2u_i(t) + u_{i+1}(t)\big) + f\big(u_i(t); a\big) = 0,$$

where $d > 0$, $a \in (0, 1)$ and $i \in \mathbb{Z}$. If we restrict ourselves to the case of the periodic stationary solutions the problem then includes a finite number of equations only. Indeed, we can define the graph differential equation (GDE) by

$$\begin{cases} \mathrm{u}_1'(t) = & d\big(\mathrm{u}_n(t) - 2\mathrm{u}_1(t) + \mathrm{u}_2(t)\big) + f(\mathrm{u}_1(t); a), \\ \mathrm{u}_2'(t) = & d\big(\mathrm{u}_1(t) - 2\mathrm{u}_2(t) + \mathrm{u}_3(t)\big) + f(\mathrm{u}_2(t); a), \\ & \vdots \\ \mathrm{u}_i'(t) = & d\big(\mathrm{u}_{i-1}(t) - 2\mathrm{u}_i(t) + \mathrm{u}_{i+1}(t)\big) + f(\mathrm{u}_i(t); a), \\ & \vdots \\ \mathrm{u}_n'(t) = & d\big(\mathrm{u}_{n-1}(t) - 2\mathrm{u}_n(t) + \mathrm{u}_1(t)\big) + f(\mathrm{u}_n(t); a) \end{cases} \tag{3.15}$$

on a cycle graph with n vertices. The link between the n-periodic stationary solutions of the LDE (3.1) and the stationary solutions of the GDE (3.15) is stated in the following lemma.

Lemma 3.2.1 ([31, Lemma 1])**.** *Let $n \geq 3$. The vector $\mathrm{u} = (\mathrm{u}_1, \mathrm{u}_2, \ldots, \mathrm{u}_n)$ is a stationary solution of the GDE* (3.15) *if and only if its periodic extension u is an n-periodic stationary solution of the LDE* (3.1)*. Moreover, u is an asymptotically stable solution of the GDE* (3.15) *if and only if u is an asymptotically stable solution of the LDE* (3.1) *with respect to the ℓ^∞-norm.*

Let $\mathrm{u} = (\mathrm{u}_1, \mathrm{u}_2, \ldots, \mathrm{u}_n) \in \mathbb{R}^n$ be a vector, then its periodic extension $u = (u_i)_{i\in\mathbb{Z}} \in \mathbb{R}^{\mathbb{Z}}$ is given by

$$u_i = \mathrm{u}_{1+\mathrm{mod}(i,n)}, \quad i \in \mathbb{Z},$$

where $\mathrm{mod}(i, n)$ is a remainder of the integer division i/n, i.e., $\mathrm{mod}(4, 2) = 0$ and $\mathrm{mod}(3, 2) = 1$.

Remark 3.2.2. The statement of Lemma 3.2.1 can be reformulated for two-periodic solutions of the LDE (3.1). The only technical difference is that the two-periodic stationary states are equivalent to the stationary solutions of the GDE

$$\begin{cases} \mathrm{u}_1'(t) = & 2d\big(\mathrm{u}_2(t) - \mathrm{u}_1(t)\big) + f\big(\mathrm{u}_1(t); a\big), \\ \mathrm{u}_2'(t) = & 2d\big(\mathrm{u}_1(t) - \mathrm{u}_2(t)\big) + f\big(\mathrm{u}_2(t); a\big). \end{cases} \tag{3.16}$$

The doubled diffusion coefficient originates from the fact, that we actually consider the GDE on cycle graph with two vertices which is actually a two-vertex path with a doubled edge. Note that when we reference the GDE (3.15), we implicitly include the equation (3.16) for the case $n = 2$. This enables us to simplify the text significantly.

From now on, we shall assume the initial conditions of the LDE (3.1) and of the GDE (3.15) such that $u_0 \in [0,1]^{\mathbb{Z}}$ and $\mathrm{u}_0 \in [0,1]^n$. Although these conditions might seem restrictive the following lemmas show that they are quite natural.

Lemma 3.2.3. *Let* $\mathrm{u}(0) = \mathrm{u}_0 \in [0,1]^n$*, then there exists a unique solution of the GDE* (3.15)*. Moreover* $\mathrm{u}(t) \in [0,1]^n$*.*

Proof. The proof is a consequence of [64, Theorem 18] and is thus omitted. □

Lemma 3.2.4. *Let* u *be a stationary solution of the GDE* (3.15)*. Then* $\mathrm{u} \in [0,1]^n$*.*

Proof. The proof is a consequence of [62, Lemma 3.1] and is thus ommited. □

Thanks to the statement of Lemma 3.2.1 we can turn our attention to the investigation of the stationary solutions of the GDE (3.15). To enlighten the notation, we introduce the following function $h : \mathbb{R}^n \times [0,1] \times \mathbb{R}_0^+ \to \mathbb{R}^n$ by

$$h(\mathrm{u}; a, d) = \begin{pmatrix} d\,(\mathrm{u}_n - 2\mathrm{u}_1 + \mathrm{u}_2) + f(\mathrm{u}_1; a) \\ d\,(\mathrm{u}_1 - 2\mathrm{u}_2 + \mathrm{u}_3) + f(\mathrm{u}_2; a) \\ \vdots \\ d\,(\mathrm{u}_{n-1} - 2\mathrm{u}_n + \mathrm{u}_1) + f(\mathrm{u}_n; a) \end{pmatrix}. \tag{3.17}$$

The roots $\mathrm{u} \in \mathbb{R}^n$ of $h(\,\cdot\,; a, d)$ are clearly stationary solutions of the GDE (3.15) and also $\mathrm{u} \in [0,1]^n$ holds from Lemma 3.2.4. Each of the roots $\mathrm{u} \in [0,1]^n$ also define a periodic extension $u \in [0,1]^{\mathbb{Z}}$ which is an n-periodic stationary solution of the LDE (3.1) and the correspondence is one-to-one, both from Lemma 3.2.1. This implies that the knowledge of the system (3.17) complete root set is equivalent to the knowledge of the n-periodic stationary solution set of the LDE (3.1) and we can thus fully turn our attention to the system of polynomial equations

$$h(\mathrm{u}; a, d) = 0. \tag{3.18}$$

The system (3.18) consists of n cubic polynomials and thus it is expected to have 3^n solutions (including possibly the complex solutions and multiplicities), [71]. Indeed, the system with zero diffusion

$$h(\mathrm{u}; a, 0) = 0$$

has exactly 3^n solutions in the form $\mathrm{u} \in \{0, a, 1\}^n$. Moreover, we have

$$D_1 h(\mathrm{u}; a, 0) = \operatorname{diag}\big(g_{\mathrm{u}}(\mathrm{u}_1; a), g_{\mathrm{u}}(\mathrm{u}_2; a), \ldots, g_{\mathrm{u}}(\mathrm{u}_n; a)\big),$$

where

$$\begin{aligned} g_{\mathrm{u}}(0; a) &= -a < 0, \\ g_{\mathrm{u}}(a; a) &= a(1-a) > 0, \\ g_{\mathrm{u}}(1; a) &= a - 1 < 0. \end{aligned}$$

The matrix $D_1 h(u; a, 0)$ is thus regular at the solutions of $h(\mathrm{u}; a, 0)$ and the solutions $\mathrm{u} \in \{0, a, 1\}^n$ can be continued with their stability preserved for $d > 0$ sufficiently small via the implicit function theorem. This is the basis of our naming scheme for the solutions of (3.18). We want to label each of the solutions u of (3.18) by a word $\mathrm{w} \in \{\mathfrak{o}, \mathfrak{a}, \mathfrak{1}\}^n$. Note that we do use an alternative letters $\mathfrak{o}, \mathfrak{a}, \mathfrak{1}$ since the parameter $a \in (0,1)$ is allowed to vary. For simplicity, we denote the alphabet $\mathcal{A}_3 = \{\mathfrak{o}, \mathfrak{a}, \mathfrak{1}\}$ and its restricted version $\mathcal{A}_2 = \{\mathfrak{o}, \mathfrak{1}\}$. The constants words, e.g., $\mathfrak{ooo}$, $\mathfrak{aaaa}$, $\mathfrak{11}$ etc. are denoted by a single letter, i.e., $\mathfrak{o}$, $\mathfrak{a}$, $\mathfrak{1}$, respectively. This helps to simplify the notation. We shall show later that the words from $\mathcal{A}_2^n$ represent asymptotically stable solutions of the GDE (3.15). The varying parameter $a \in (0,1)$ leads us to the definition of the vector $(\mathrm{w}_{|a}) \in \mathbb{R}^n$ for any $\mathrm{w} \in \mathcal{A}_3^n$

$$(\mathrm{w}_{|a})_i = \begin{cases} 0, & \mathrm{w}_i = \mathfrak{o}, \\ a, & \mathrm{w}_i = \mathfrak{a}, \\ 1, & \mathrm{w}_i = \mathfrak{1}. \end{cases}$$

Definition 3.2.5 ([32, Definition 2.1])**.** Consider a word $\mathrm{w} \in \mathcal{A}_3^n$ together with a triplet

$$(u, a, d) \in [0,1]^n \times (0,1) \times \mathbb{R}_0^+.$$

Then we say that u is an equilibrium of the type w if there exists a C^1-smooth curve

$$[0,1] \ni t \mapsto \big(\mathrm{v}(t), \alpha(t), \delta(t)\big) \in [0,1]^n \times (0,1) \times \mathbb{R}_0^+$$

so that we have

$$\begin{aligned}(\mathrm{v},\alpha,\delta)(0) &= (\mathrm{w}_{|a}, a, 0),\\ (\mathrm{v},\alpha,\delta)(1) &= (\mathrm{u}, a, d),\end{aligned}$$

together with

$$h(\mathrm{v}(t);\alpha(t),\delta(t)) = 0, \qquad \det D_1 h(\mathrm{v}(t);\alpha(t),\delta(t)) \neq 0$$

for all $0 \le t \le 1$.

This definition and some additional considerations (we refer the reader to [32] or Appendix D for further details) allow us to define a pathwise connected open set for each $\mathrm{w} \in \mathcal{A}_3^n$ by

$$\Omega_{\mathrm{w}} = \big\{(a,d) \in [0,1] \times \mathbb{R}_0^+ \,|\, \text{the system (3.18) admits a solution of type w}\big\}.$$

We further define an augmented system[5] which naturally describes the boundary portions of all Ω_{w}

$$h^*(\mathrm{u};a,d) = \begin{pmatrix} h(u;a,d) \\ \det D_1 h(\mathrm{u};a,d) \end{pmatrix} = \begin{pmatrix} 0 \\ 0 \end{pmatrix}. \tag{3.19}$$

The set Γ is then given by

$$\Gamma = \big\{(a,d) \in [0,1] \times \mathbb{R}_0^+ \,|\, \text{there exists } \mathrm{u} \in \mathbb{R}^n \text{ solving (3.18)}\big\}. \tag{3.20}$$

Note that the set Γ contains upper boundaries of the regions Ω_{w}[6].

Remark 3.2.6. The condition $D_1 h\big(\mathrm{v}(t);\alpha(t),\delta(t)\big) \neq 0$ from Definition 3.2.5 directly implies that a solution u_{w} of type preserves its stability in Ω_{w} as a stationary solution of the GDE (3.15). It is stable if $\mathrm{w} \in \mathcal{A}_2^n$ and unstable if $\mathrm{w} \in \mathcal{A}_3^n \setminus \mathcal{A}_2^n$. This also applies to the periodic stationary solutions of the LDE (3.1) via Lemma 3.2.1.

To show that our naming scheme behaves sensibly, namely that the determination of solution types is independent of the chosen continuation path we introduce three assumptions.

($A\Omega1$) For any two words $\mathrm{w}_A, \mathrm{w}_B \in \mathcal{A}_n^3$ the intersection $\Omega_{\mathrm{w}_A} \cap \Omega_{\mathrm{w}_B}$ is connected.

($A\Omega2$) For any word $\mathrm{w} \in \mathcal{A}_n^3$ the set Ω_{w} is simply connected.

($A\Omega3$) Consider any word $\mathrm{w} \in \mathcal{A}_n^3$ and any $(a,d) \in \Omega_{\mathrm{w}} \cap \Gamma$. Suppose that $h(\mathrm{u}_i;a_i,d_i)$ is a sequence of the system (3.18) solutions of type w with $(a_i,d_i) \to (a,d)$ and $\mathrm{u}_i \to \mathrm{u}$. Then we have $\det D_1 h(\mathrm{u};a,d) \neq 0$.

This enables us to state the following theorem.

Theorem 3.2.7 ([32, Corollary 2.1])**.** *Fix an integer $n \ge 2$ and suppose that ($A\Omega1$), ($A\Omega2$) and ($A\Omega3$) all hold. Then for any word $\mathrm{w} \in \mathcal{A}_3^n$ there is a smooth function $\mathrm{u}_{\mathrm{w}} : \Omega_{\mathrm{w}} \to \mathbb{R}^n$ so that $\mathrm{u}_{\mathrm{w}}(a,d)$ is the unique solution of type w for the system (3.18) for all $(a,d) \in \Omega_{\mathrm{w}}$. In addition, whenever $(a,d) \in \Omega_{\mathrm{w}_A} \cap \Omega_{\mathrm{w}_B}$ for two distinct words $\mathrm{w}_A, \mathrm{w}_B \in \mathcal{A}_3^n$ we have*

$$u_{\mathrm{w}_A}(a,d) \neq u_{\mathrm{w}_B}(a,d).$$

Remark 3.2.8. Note that we can freely extend the naming scheme to the periodic stationary solutions of the LDE (3.1) via Lemma 3.2.1 and Theorem 3.2.7 ensures that the naming scheme is well-behaved

Remark 3.2.9. There are intriguing symmetry properties of the system (3.18) solutions which are discussed later in §3.2.3. We use one rather clear fact to enlighten the notation. If we cyclically rotate any solution u_{w} of (3.18) it is still a root of $h(\,\cdot\,;a,d)$. This enables us to define classes of solutions and words, e.g., $\mathrm{u}_{[\mathfrak{oa1}]} = \{\mathrm{u}_{\mathfrak{oa1}}, \mathrm{u}_{\mathfrak{a1o}}, \mathrm{u}_{\mathfrak{1oa}}\}$ and implicitly $\Omega_{[\mathfrak{oa1}]} = \Omega_{\mathfrak{oa1}} = \Omega_{\mathfrak{a1o}} = \Omega_{\mathfrak{1oa}}$ and $[\mathfrak{oa1}] = \{\mathfrak{oa1}, \mathfrak{a1o}, \mathfrak{1oa}\}$. This rather vague definition is formalized and extended later via the tools of the finite group theory.

We are left to show that the solution type also captures the shape of the solution to a certain extent, see Figure 3.4. We demonstrate that the component-wise partial ordering of the words from $\mathcal{A}_3^n$ captures the actual partial ordering of the system (3.18) solutions. To this end, let us start with a short example of the ordering of the words.

[5] Solving this system also forms the backbone of our numerical computations, see Figures 3.6, 3.7, 3.11.

[6] In order to keep the flow of ideas commenting the naming scheme, we discuss particular properties of the sets Ω_{w} later.

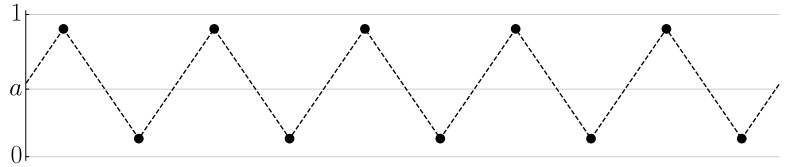

a: A two-periodic stationary solution of the type $\mathfrak{o1}$.

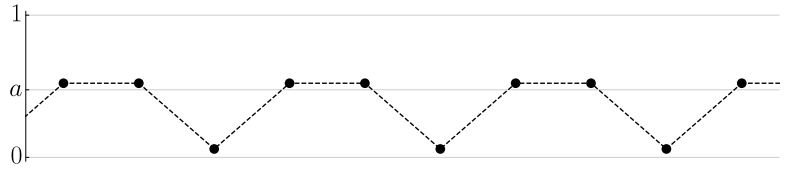

b: A three-periodic stationary solution of the type $\mathfrak{oaa}$.

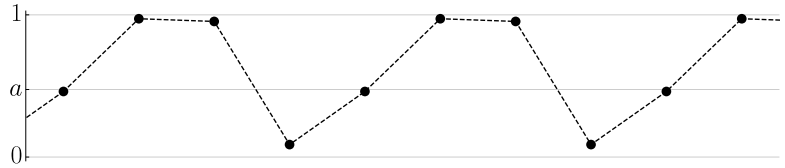

c: A four-periodic stationary solution of the type $\mathfrak{oa11}$. Source [69].

Figure 3.4: Examples of two-, three- and four-periodic stationary solutions of the LDE (3.1). The parameters $a = 0.475, d = 0.025$ are set to be identical in all three cases. See that neither of the corresponding solutions $\mathrm{u_w}$ of the system (3.18) is significantly distinct from the origin of the bifurcation branch $\mathrm{w}_{|a}$ at $d = 0$, e.g., the solution $\mathrm{u}_{\mathfrak{oa11}}$ is in close proximity to $(0, a, 1, 1) = (0, 0.475, 1, 1)$.

Example 3.2.10. Without loss of generality, we can consider the partial ordering of the classes of words defined in Remark 3.2.9. The words of length three made with the two-letter alphabet $\mathcal{A}_2$ (the stable words) can be actually totally ordered

$$[\mathfrak{o}] \lhd [\mathfrak{oo1}] \lhd [\mathfrak{o11}] \lhd [\mathfrak{1}],$$

but the words of length four can be only partially ordered

$$[\mathfrak{o}] \lhd [\mathfrak{oo01}] \begin{array}{c} \triangle \\ \\ \triangledown \end{array} \begin{array}{c} [\mathfrak{0011}] \\ \\ [\mathfrak{0101}] \end{array} \begin{array}{c} \triangledown \\ \\ \triangle \end{array} [\mathfrak{o111}] \lhd [\mathfrak{1}].$$

Theorem 3.2.11 ([32, Lemma 5.2])**.** *Assume that (AΩ1) and (AΩ2) are satisfied and consider a distinct pair* $\mathrm{w}_A, \mathrm{w}_B \in \mathcal{A}_3^n$ *that admits the ordering* $\mathrm{w}_A \leq \mathrm{w}_B$*. Suppose furthermore that at least one of these two words is contained in* $\mathcal{A}_2^n$*. Then for any* $(a, d) \in \Omega_{\mathrm{w}_A} \cap \Omega_{\mathrm{w}_B}$ *we have strict component-wise inequality*

$$\mathrm{u}_{\mathrm{w}_A}(a, d) < \mathrm{u}_{\mathrm{w}_B}(a, d).$$

The extension of the statement of Theorem 3.2.11 to the periodic stationary solutions of the LDE (3.1) is illustrated in Figure 3.5. Secondly, when fixing the detuning parameter $a \in (0, 1)$ and increasing $d > 0$ the solutions of (3.18) still preserve the partial ordering (Theorem 3.2.11), their number does not increase [71] and some of them collapse and merge into a new solution or turn into complex roots. The solution $\mathrm{u_w}$ should thus preserve the profile of the corresponding word w which is also supported by numerical experiments. Theorem 3.2.11 further plays important role in answering the question of existence of multichromatic waves in §3.3.

We continue with an overview of properties of the system (3.18) solutions (their periodic extensions as the LDE (3.1) solutions, respectively). Since the regions Ω_{w} cannot be described explicitly, we summarize asymptotic results describing their shape here.

3.2.2 N-periodic stationary solutions, $n = 2, 3, 4$

The two-periodic solutions were examined in [30] and amongst other, they are crucial elements for building the so-called *bichromatic waves*, see §3.3.

The authors proved the existence of two threshold curves in the (a, d)-plane at which the bifurcations of the problem (3.18) take place with $n = 2$, see Figure 3.6 for illustration.

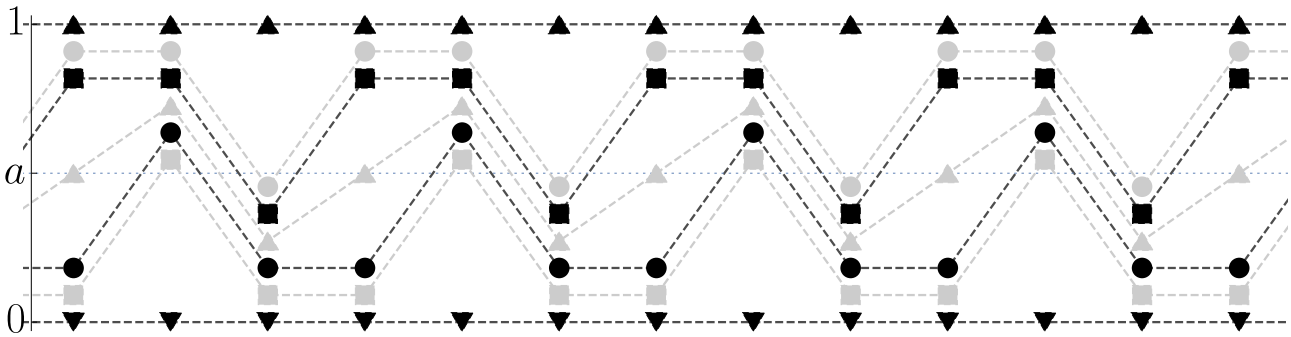

Figure 3.5: Schematic illustration of Theorem 3.2.11 statement for the LDE (3.1). The periodic extensions of the system (3.18) solutions with $n = 3$ are depicted: $\mathrm{u}_{[\mathfrak{o}]}$, $\mathrm{u}_{[\mathfrak{o}\mathfrak{o}\mathfrak{a}]}$, $\mathrm{u}_{[\mathfrak{o}\mathfrak{o}\mathfrak{1}]}$, $\mathrm{u}_{[\mathfrak{o}\mathfrak{a}\mathfrak{1}]}$, $\mathrm{u}_{[\mathfrak{o}\mathfrak{1}\mathfrak{1}]}$, $\mathrm{u}_{[\mathfrak{a}\mathfrak{1}\mathfrak{1}]}$, $\mathrm{u}_{[\mathfrak{1}]}$ (starting from bottom). Unstable solutions (the solutions of type containing the letter $\mathfrak{a}$) are displayed in grey color. Note that this picture makes sense only if (a, d) lies in the common intersection of all respective regions $\Omega_{[\mathrm{w}]}$ which, as we shall later see, is nonempty.

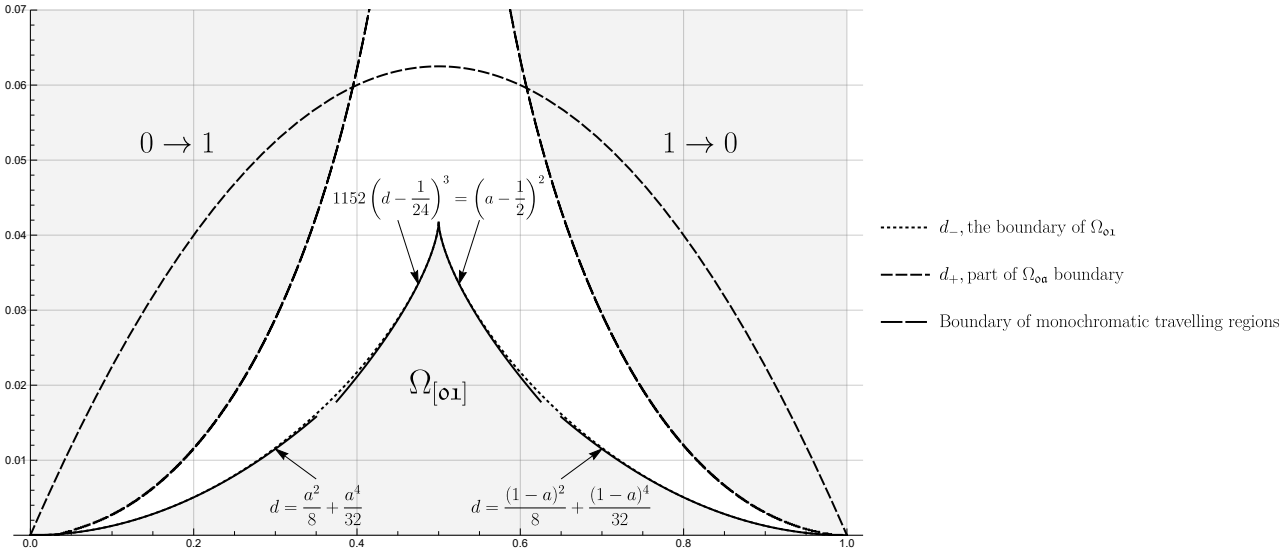

Figure 3.6: Graphical illustration of Theorem 3.2.12 statement. The pinning region consists of the white area and $\overline{\Omega}_{[\mathfrak{o}\mathfrak{1}]}$. Under the dotted line, there are 9 distinct solutions of (3.18). Between the dotted line and the parabolic line, there are 5 distinct roots and above the parabolic line, only the three homogeneous solutions $(0, 0), (a, a), (1, 1)$ remain.

Theorem 3.2.12 ([30, Proposition 3.1])**.** *There exist two continuous functions*

$$d_\pm : [0, 1] \to \mathbb{R}_0^+$$

that satisfy the following properties.

(i) For any $0 < a < 1$ we have the explicit expression

$$d_+(a) = \frac{g'(a; a)}{4}$$

together with the identities

$$d_-(a) = d_-(1 - a), \qquad d_+(a) = d_+(1 - a)$$

and the inequality $d_-(a) < d_+(a)$. In addition, we have

$$d_-(0) = d_+(0) = d_-(1) = d_+(1) = 0$$

together with $d_-(1/2) = 1/24$.

(ii) We have $d_- \in C^\infty\big([0, 1/2)\big) \cup C^\infty\big((1/2, 1]\big)$. In addition , d_- is strictly increasing on $[0, 1/2]$ and strictly decreasing on $[1/2, 1]$.

(iii) *Pick any $a \in (0,1)$. The system (3.18) has nine distinct roots for $0 \le d < d_-(a)$, five distinct roots for $d_-(a) < d < d_+(a)$, and three distinct real roots for $d > d_+(a)$.*

(iv) *Pick any $a \in (0,1)$. The equation has seven distinct roots for $d = d_-(a)$ if $a \neq 1/2$ and five if $a = 1/2$.*

(v) *We have the expansion*

$$d_-(a) = \frac{1}{8}a^2 + \frac{1}{32}a^4 + O(a^5)$$

for $a \downarrow 0$. In addition, writing $a_- : [0, 1/24] \to [0, 1/2]$ for the inverse function of d_- on $[0, 1/2]$, we have the expansion

$$a_-(d) = \frac{1}{2} - \sqrt{-1152\left(d - \frac{1}{24}\right)^3} + O\left(\left(d - \frac{1}{24}\right)^2\right)$$

as $d \uparrow 1/24$.

According to our notation, the restriction of the piecewise smooth function $d_- : [0,1] \to \mathbb{R}_0^+$ to $a \in [0, 1/2)$ describes the boundary of the region $\Omega_{[\mathtt{o1}]} = \Omega_{[\mathtt{a1}]}$. Numerical results indicate that the function $d_+ : [0,1] \to \mathbb{R}_0^+$ describes the boundary of the region $\Omega_{[\mathtt{oa}]}$ when restricted to the same interval $a \in [0, 1/2)$ See [30, Figure 6] for the bifurcation diagram.

Note that the asymptotic expansions hint, that $\Omega_{[\mathtt{o1}]}$ lies completely in the pinning region which supports the statement from [35] that the stable stationary solutions of the LDE (3.1) prevent the waves of type (3.10) from travelling.

Three-periodic solutions

We assume that $n = 3$ in this section. The system (3.18) solutions exhibit much richer behaviour compared to the two-periodic ones. The richness however goes hand in hand with increasing complexity of the system and prevents us to get results in breadth corresponding to the two-periodic case. The intuition that the increasing diffusion intensity d with fixed detuning parameter $a \in (0,1)$ makes the solutions more alike to the homogeneous ones does not hold for higher n's starting with $n = 3$. We shall show that there is a nontrivial interval $(a_c, a_f) \subset (0,1)$ for the detuning parameter a in which some solutions disappear and reappear again with increasing diffusion intensity $d > 0$. This section is commentary of results from [32] which is included in Appendix D.

Let us introduce a further distinction of the boundary set Γ defined by (3.20); the sets $\Gamma_{[\mathtt{a}]}, \Gamma_{[\mathtt{oo1}]}, \Gamma_{[\mathtt{o11}]}$ describe boundary portions of their respective $\Omega_{[\mathtt{w}]}$'s and additional two thresholds Γ_{u}^1 and Γ_{u}^2. The latter special notation is caused by the fact, that when the bifurcating roots cross their respective threshold, we cannot name them according to Definition 3.2.5. The emergence of the unlabelled branches is illustrated later. The boundary sets are depicted in Figure 3.7. We next include bifurcation diagrams with the fixed detuning parameter a in three distinct positions. Namely left of the curve $\Gamma_{[\mathtt{oo1}]}$ cusp, $a < a_f$ where $a_f \approx 0.4013889$, between the cusp and the fold $a_f < a < a_c$ where $a_c \approx 0.401476$ and right of the fold $a_f < a$, see Figures 3.8, 3.9, 3.10.

More detailed description of the threshold curves from Figure 3.7 follows. There is a symmetry present in the set of the solutions which enables us to focus on the case $a \in (0, 1/2]$ only. This will be discussed in a greater detail later in the text, namely the equality (3.22) in §3.2.3, .

The $\Gamma_{[\mathtt{o11}]}$ threshold Using a similar approach as in [30], we examine asymptotic behaviour of the curve $\Gamma_{[\mathtt{o11}]}$ near the point $(a, d) = (0, 0)$. In particular, the form of (3.18) shows that the second and the third component of the solution are equal. We can thus examine the solutions of the problem

$$h\big((x, 1+y, 1+y); a, d\big) = 0$$

for $|x| + |y| + |a| + |d|$ small. The curve can be then locally described as a function $d_{[\mathtt{o11}]}(a)$ which satisfies

$$d_{[\mathtt{o11}]}(a) = \frac{a^2}{8} + \frac{a^4}{64} + O(a^5).$$

Note that the leading term is quadratic as in the expansion for the two periodic solution of type $[\mathtt{o1}]$, Theorem 3.2.12, the function d_- but the second leading term is halved. The curve $\Gamma_{[\mathtt{o11}]}$ thus locally lies under the threshold d_-. In addition, we have

$$\mathrm{u}_{\mathtt{o11}}\big(a; d_{[\mathtt{o11}]}(a)\big) = \left(\frac{a}{2}, 1 - \frac{a^2}{8} - \frac{a^3}{16} - \frac{a^4}{64}, 1 - \frac{a^2}{8} - \frac{a^3}{16} - \frac{a^4}{64}\right) + O(a^5).$$

For detailed explanation of this approach see [30, 32] or Appendix D.

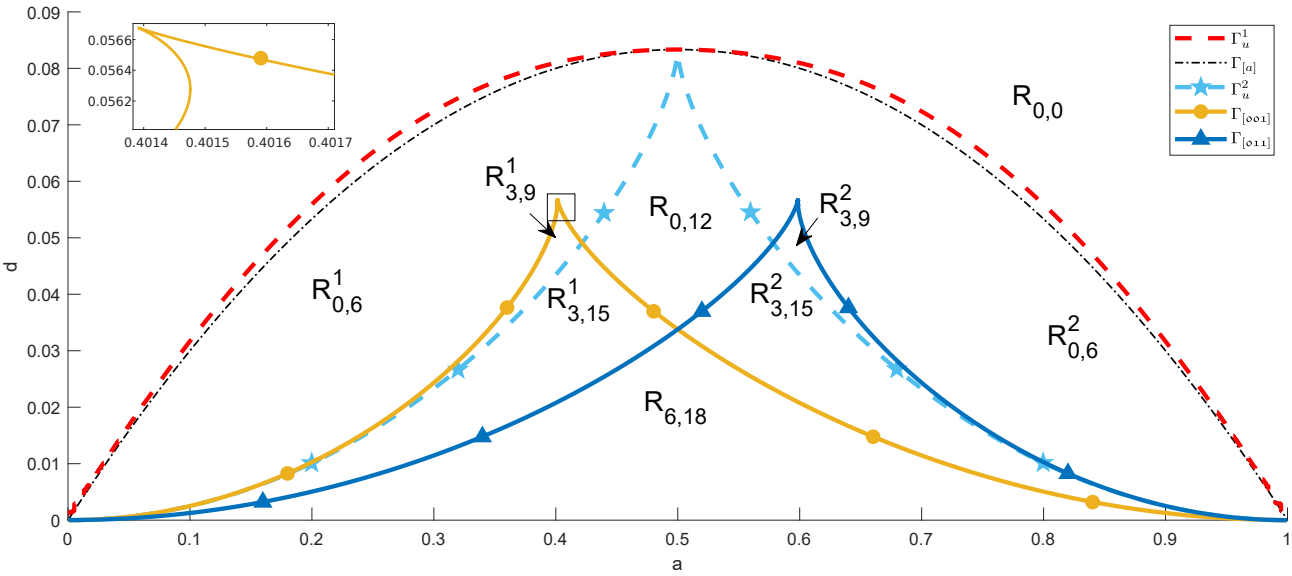

Figure 3.7: The numerically computed boundaries $\Gamma_{[\mathfrak{w}]}$ of the sets $\Omega_{[\mathfrak{w}]}$ and the two threshold curves $\Gamma^1_{\mathfrak{u}}$, $\Gamma^2_{\mathfrak{u}}$. The label in the form $R_{\#_1,\#_2}$ indicates the region in which there are $\#_2$ distinct nonhomogeneous solutions of the system (3.18) out of which $\#_1$ are asymptotically stable. Note that the curve $\Gamma_{[\mathfrak{oo1}]}$ cannot be described as a function of the detuning parameter $a \in [0,1]$ due to the cusp and fold in the interval numerically computed interval $a \in (0.4013889, 0.401476)$. Source: [32].

The Γ^2_u threshold This is the threshold on which there lies a pitchfork bifurcation of the roots of type $[\mathfrak{o a 1}], [\mathfrak{a o 1}], [\mathfrak{a a 1}]$; it takes place simultaneously at three places of the space $[0,1]^3$. Only one of the three collisions is depicted in Figures 3.8, 3.9, 3.10.

The $\Gamma_{[\mathfrak{oo1}]}$ threshold The curve $\Gamma_{[\mathfrak{oo1}]}$ cannot be expressed as a function of the detuning parameter $a \in (0, 1/2]$. Indeed, numerical experiments indicate that there exist a couple of solutions $(\mathfrak{u}_f; a_f, d_f)$, $(\mathfrak{u}_c; a_c, d_c)$ for the once again augmented system (see (3.19))

$$\begin{pmatrix} h^*(u; a, d) \\ \det D_{1,3}\, h^*(\mathfrak{u}; a, d) \end{pmatrix} = \begin{pmatrix} 0 \\ 0 \end{pmatrix}$$

with $(a_f, d_f) \approx (0.401476, 0.056275)$ and $(a_c, d_c) \approx (0.4013889, 0.05668)$. These solutions correspond to the fold and cusp points visible in the zoom frame of Figure 3.7. This manifests in the phenomenon where two solution branches collide, temporarily become complex just in order to become real again, see Figure 3.9. Nevertheless, the curve $\Gamma_{[\mathfrak{oo1}]}$ can be approximated in the proximity of $(a, d) = (0, 0)$ via the solution of the system

$$h\big((x, x, 1+y); a, d\big) = 0$$

for $|x| + |y| + |a| + |d|$ small by a function $d_{[\mathfrak{oo1}]}$ of the detuning parameter a. We have

$$d_{[\mathfrak{oo1}]}(a) = \frac{a^2}{4} + \frac{a^4}{8} + O(a^5)$$

and

$$\mathfrak{u}_{\mathfrak{o11}}(a; d_{[\mathfrak{o11}]}(a)) = \left(\frac{a}{2}, \frac{a}{2}, 1 - \frac{a^2}{8} - \frac{a^3}{16} - \frac{a^4}{64}\right) + O(a^5),$$

which shows that the curve $\Gamma_{[\mathfrak{oo1}]}$ locally lies above $\Gamma_{[\mathfrak{o11}]}$, see Figure 3.7.

The $\Gamma_{[\mathfrak{a}]}$ threshold This curve can be explicitly computed as a solution of

$$\det D_1 h(\mathbf{u}; a, d) = 0$$

to be

$$d_{[\mathfrak{a}]}(a) = \frac{a(1-a)}{3}.$$

At this threshold, there is a triple intersection of the branches $[\mathfrak{o a a}]$ which then continue to the bifurcation point at the next threshold.

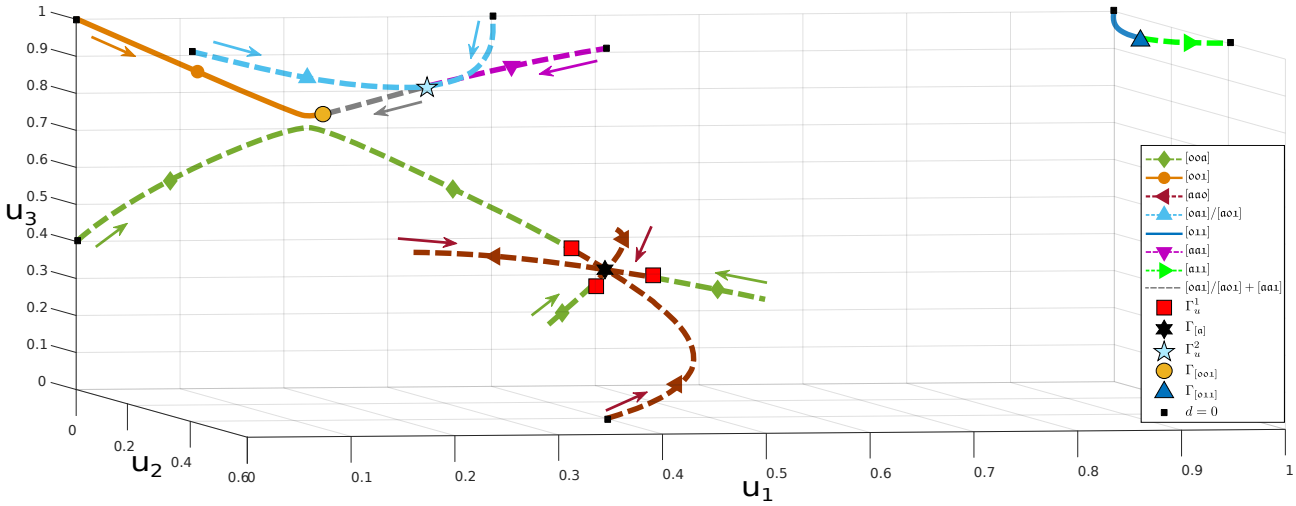

Figure 3.8: The bifurcation diagram for fixed detuning parameter $a = 0.401 < a_c$ and increasing $d \geq 0$ for the system (3.18) with $n = 3$. Wherever possible, the branches are named according to the scheme from Definition 3.2.5 but clearly, not all branches could be named that way since some of them originate from a bifurcation point, e.g., the branch $[\mathtt{oa1}]/[\mathtt{ao1}] + [\mathtt{aa1}]$. Interesting behaviour occurs when crossing the threshold $\Gamma_{[\mathtt{a}]}$ where the three roots of type $[\mathtt{oaa}]$ pass through each other and subsequently merge with the roots of type $[\mathtt{ooa}]$ at Γ^1_u. The thresholds are depicted by the dot-dashed line and the red dashed line in Figure 3.7. Source: [32].

The Γ^2_u threshold At this numerically observed threshold, the branches emerging from the triple collision of $[\mathtt{oaa}]$ meet the branches of $[\mathtt{ooa}]$. Above this threshold, only the homogeneous solutions $\mathbf{0}, \mathbf{a}$ and $\mathbf{1}$ remain.

Four-periodic solutions

The solutions of (3.18) with $n = 4$ exhibit qualitatively similar behaviour with the the case of $n = 3$, see Figure 3.11. There is however one exception which is of crucial importance later in the examination of travelling waves. The curves $\Gamma_{[\mathtt{ooo1}]}$ and $\Gamma_{[\mathtt{o111}]}$ have a nonempty intersection with the travelling region of monochromatic waves as can be seen in Figure 3.16.

Note that asymptotic expansions of the system (3.18) and the curves Γ_{w} near $(a, d) = (0, 0)$ can be computed in the virtue of the $n = 3$ case. Interested reader can see [32] or Appendix D for further details.

3.2.3 Symmetries of stationary solutions in the Nagumo LDE

The previous section focused on various properties of the existence regions for two-, three- and four-periodic stationary solutions of the LDE (3.14). Here, we investigate symmetries present in the equation and their significance for its stationary solutions. This was foreshadowed in Remark 3.2.9.

We first turn our attention to the solutions of the system (3.18). Let u be a solution of the system (3.18), it is still a solution under the transformations $\mathrm{u}_i \to \mathrm{u}_{i-1}$ and $\mathrm{u}_i \to \mathrm{u}_{n-i+1}$ (the former with a proper modulo wrapping). It can be shown by a mere relabelling of the vector's elements; the transformed solutions then have the same profile. When we want to determine the number of distinct solutions of the system (3.18) (and subsequently the stationary solutions of the GDE (3.15) and the LDE (3.1)), these symmetries must be taken into account. To this end, we define groups of transformations and count the number of their orbits (maximal subsets of words/solutions which are unreachable by the group actions) via Burnside's lemma. When we want to count the number of distinct periodic stationary solutions of the LDE (3.1) of all periods $m \in \mathbb{N}$ up to the given one $n \in \mathbb{N}$, there is one more thing to be considered. A solutions with, say, period three is also six-, nine- etc. periodic and must be thus included only once. This is taken into account via Möbius inversion formula.

Aside from counting the stationary solutions, we can use the group formulation to group together solutions whose existence regions Ω_{w} are identical or easily-transformable onto each other. If there is a solution of type w, then there surely exist a solution with type obtained by rotation $\mathrm{u}_i \to \mathrm{u}_{i-1}$ or reflection $\mathrm{u}_i \to \mathrm{u}_{n-i+1}$ and moreover, they have the same existence region Ω_{w}, e.g., $\Omega_{\mathtt{oa1}} = \Omega_{\mathtt{a1o}} = \Omega_{\mathtt{1oa}} = \Omega_{\mathtt{1ao}} = \Omega_{\mathtt{ao1}} = \Omega_{\mathtt{1oa}}$. Moreover, switch in the letter $\mathtt{o} \leftrightarrow \mathtt{1}$ gives another legitimate solution type whose region is obtained via the axial reflection. All the counting formulas are extended to include this value switch .

It is beneficial to know the number of the regions and namely the relationship between them when performing analytical computations or numerical simulations. The similarities of regions were actually used in [32] and in the previous section to reduce the number of computations.

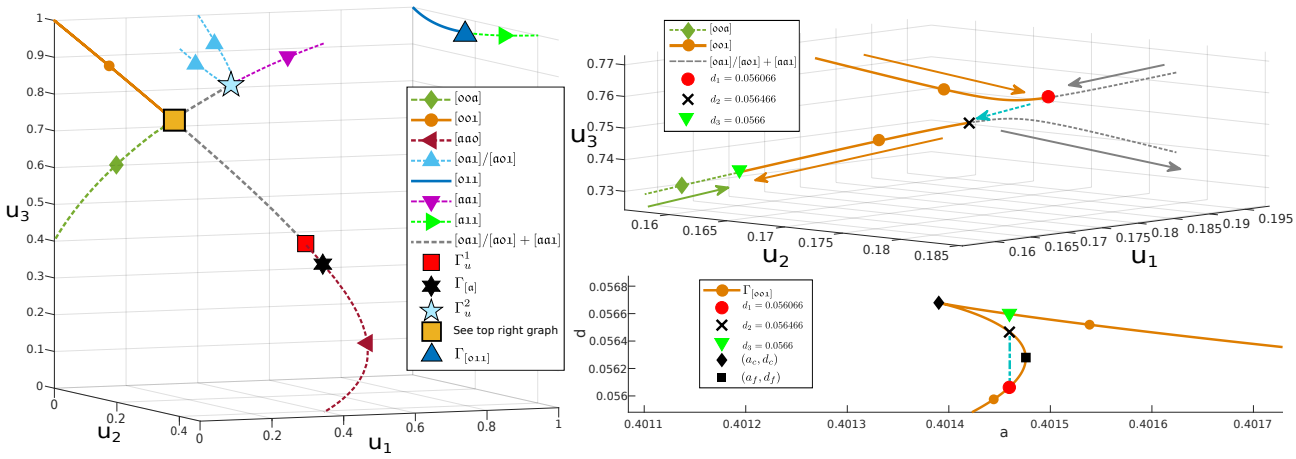

Figure 3.9: The bifurcation diagram for fixed detuning parameter $a = 0.40146 \in (a_c, a_f)$ and increasing $d \geq 0$ for the system (3.18) with $n = 3$. This is the region when the three pairs of branches collide and then reappear elsewhere. The results from [23] indicate that the solutions became complex, collide after a slight increase in d and become real again. This situation is depicted in the upper right tile. Some branches are omitted since we depict only the class representatives for the sake of clarity. Source: [32].

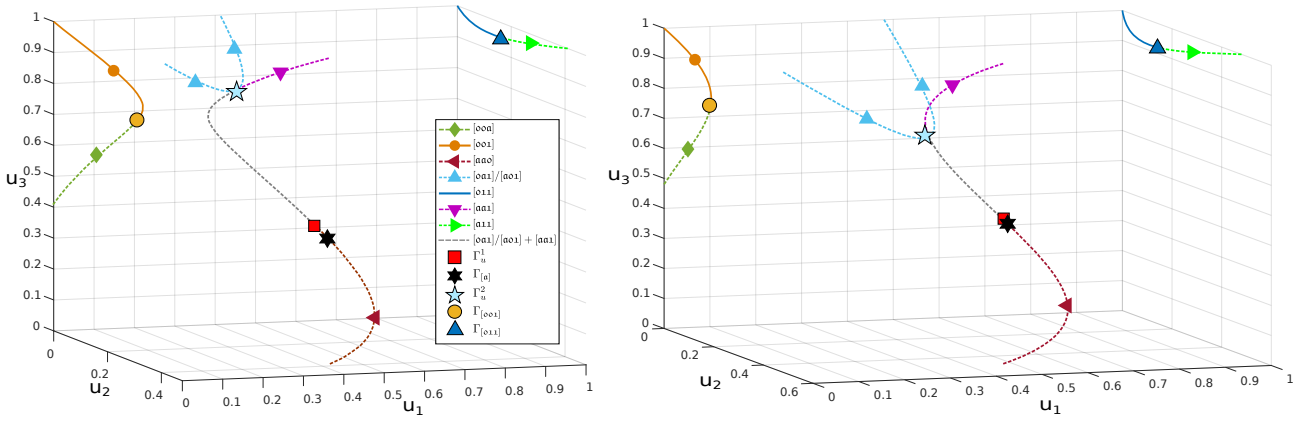

Figure 3.10: The bifurcation diagram for fixed detuning parameters $a = 0.41$ and $a = 0.48$, both greater than a_f, increasing $d \geq 0$ for the system (3.18) with $n = 3$. Note that the threshold values at $\Gamma_{[\mathrm{a}]}$ and Γ^1_u get closer to each other as $a \to 1/2$. Source: [32].

This section gathers mainly the results from [31] and [69] (Appendices E and F).

Rotation/translation Let $\mathrm{u} = (\mathrm{u}_1, \mathrm{u}_2, \ldots, \mathrm{u}_n) \in \mathbb{R}^n$ be a solution of type $\mathrm{w} = (\mathrm{w}_1, \mathrm{w}_2, \ldots, \mathrm{w}_n) \in \mathcal{A}_3^n$ of the system (3.18). Then the rotated vector $(\mathrm{u}_2, \ldots, \mathrm{u}_n, \mathrm{u}_1)$ is also a solution and moreover, it is of type $(\mathrm{w}_2, \ldots, \mathrm{w}_n, \mathrm{w}_1)$. This motivates the introduction of the rotation operator $r : \mathcal{A}_3^n \to \mathcal{A}_3^n$ defined by

$$\big(r(\mathrm{w})\big)_i = \mathrm{w}_{1+\mathrm{mod}\,(i,n)}, \tag{3.21}$$

which can be extended to work on vectors from $\mathbb{R}^n$ and on the stationary solutions of the LDE (3.1) as the translation $u_i \mapsto u_{i-1}$. Since the rotation r just relabels the vertices, we have

$$\Omega_{\mathrm{w}} = \Omega_{r(\mathrm{w})}$$

for all $\mathrm{w} \in \mathcal{A}_3^n$.

The rotation operator r is a generator of a cyclic group of order n

$$C_n = \big(\{e, r^1, \ldots, r^{n-1}\}, \circ\big).$$

. The group operation $\circ$ is composition of the rotations through the modulo sum $r^i \circ r^j = r^{\mathrm{mod}\,(i+j,n)}$.

Reflection Let $\mathrm{u} = (\mathrm{u}_1, \mathrm{u}_2, \ldots, \mathrm{u}_n) \in \mathbb{R}^n$ be a solution of type $\mathrm{w} = (\mathrm{w}_1, \mathrm{w}_2, \ldots, \mathrm{w}_n) \in \mathcal{A}_3^n$ of the system (3.18). Then the reflected vector $(\mathrm{u}_n, \mathrm{u}_{n-1}, \ldots, \mathrm{u}_1)$ is a solutions of type $(\mathrm{w}_n, \mathrm{w}_{n-1}, \ldots, \mathrm{w}_1)$. Formally, we define the

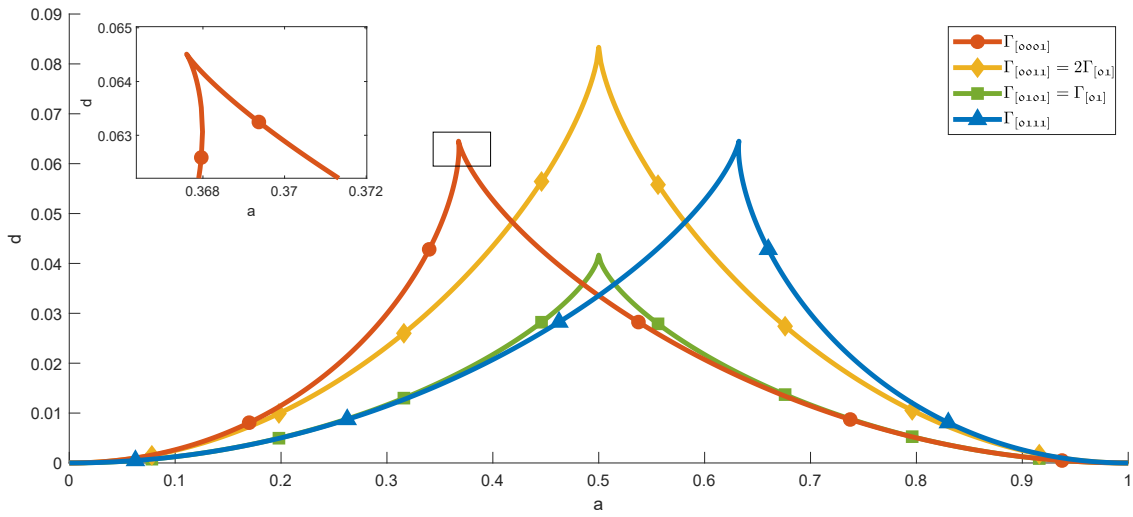

Figure 3.11: Numerically computed thresholds for the system (3.18) with $n = 4$. The curves $\Gamma_{[0001]}$, $\Gamma_{[0111]}$ exhibit fold and cusp behaviour similar to $\Gamma_{[001]}$, $\Gamma_{[011]}$, see Figure 3.7. Moreover, these curves intersect the travelling region for the waves of type (3.10) for the LDE (3.1) as can be seen in Figure 3.16. The notation $\Gamma_{[0011]} = 2\Gamma_{[01]}$ indicates that the curve $\Gamma_{[0011]}$ can be expressed as a function $d_{[0011]}(a) = 2d_-(a)$ for $a \in [0, 1]$ where d_- is defined in Theorem 3.2.12 as the threshold for existence of the system (3.18) heterogeneous two-periodic solution of type [01]. Source: [32].

reflection operator $s : \mathcal{A}_3^n \to \mathcal{A}_3^n$ by

$$\big(s(\mathrm{w})\big)_i = \mathrm{w}_{n-i+1}.$$

As the rotation r, it can be extended to vectors from $\mathbb{R}^n$ and to stationary solutions of the LDE (3.1) as $u_i \mapsto u_{-i}$. The rotation r with the reflection s generate the dihedral group

$$D_n = \big(\{e, r^1, \dots, r^{n-1}, s, sr^1, \dots, sr^{n-1}\}, \circ\big)$$

where sr^i is the composition of rotation and reflection with the subsequent rotation, i.e., $sr^i = r^i \circ s$. The action of the group D_n just relabels the vertices while preserving their incidence, we have

$$\Omega_{\mathrm{w}} = \Omega_{g(\mathrm{w})}$$

holds for all $\mathrm{w} \in \mathcal{A}_3^n$ and $g \in D_n$.

Value permutation The previous two symmetries originated from the cyclic graph structure of the GDE (3.15). This one is a consequence of certain property of the cubic bistable nonlinear term (3.9).[7] Namely,

$$f(u, a) = -f(1 - u, 1 - a)$$

holds for $u, a \in [0, 1]$. Since the transformations $u \mapsto 1 - u, a \mapsto 1 - a$ is linear, we have

$$h(\mathrm{u}; a, d) = -h(\mathbf{1} - \mathrm{u}; 1 - a, d) \tag{3.22}$$

for any $\mathrm{u} \in [0, 1]^n$ and $a \in [0, 1]$ where the subtraction $\mathbf{1} - \mathrm{u}$ is element-wise. This has two consequences. First, when $a = 1/2$, then u is a solution of type w if and only if $\mathbf{1} - \mathrm{u}$ is a solution of type $\pi(\mathrm{w})$ where

$$\big(\pi(\mathrm{w})\big)_i = \begin{cases} 1, & \mathrm{w}_i = 0, \\ a, & \mathrm{w}_i = a, \\ 0, & \mathrm{w}_i = 1. \end{cases} \tag{3.23}$$

This is however a very special case since any deviation from $a = 1/2$ destroys this symmetry. On the other hand, this still propagates to the shape of the existence regions. In particular, we have

$$\Omega_{\mathrm{w}} = \mathcal{T}\big(\Omega_{\pi(\mathrm{w})}\big)$$

[7] This property is not however exclusive to this term only; various generalizations and application are discussed in the concluding parts of [69] (included in Appendix F).

for all $\mathrm{w} \in \mathcal{A}_3^n$ where $\mathcal{T}\colon \mathcal{H} \to \mathcal{H}$ is

$$\mathcal{T}(a,d) = (1-a,d).$$

Indeed, the transformations $u \mapsto 1-u, a \mapsto 1-a$ induce a flip of the regions with respect to the line $a = 1/2$.

The transformation π generates an order-two group

$$\Pi = \big(\{e,\pi\},\circ\big),$$

whose structure is rather simple, but the group product of Π with C_n and D_n (i.e., groups of operations whose actions do not change the profile of the solution and/or the shape of the existence regions significantly) are not trivial any more and are expressed as

$$C_n^{\Pi} = \big(\{e, r, \dots, r^{n-1}, \pi, \pi r, \dots, \pi r^{n-1}\},\circ\big).$$

and

$$D_n^{\Pi} = \left(\left\{\begin{array}{l} e, r, \dots, r^{n-1}, \pi, \pi r, \dots, \pi r^{n-1}, \\ s, sr, \dots, sr^{n-1}, \pi s, \pi sr, \dots, \pi sr^{n-1} \end{array}\right\},\circ\right).$$

Formally, adding π to the group operations from C_n or D_n just mean, that we exchange $\mathtt{0} \leftrightarrow \mathtt{1}$ after (or before since the composition with π is commutative) the index permutations.

To conclude our discussion on the similarity of the regions, we provide the following definition.

Definition 3.2.13. Two regions $\Omega_{\mathrm{w}_1}, \Omega_{\mathrm{w}_2} \subset \mathcal{H}$ are called *qualitatively alike* if either

$$\Omega_{\mathrm{w}_1} = \Omega_{\mathrm{w}_2} \quad \text{or} \quad \Omega_{\mathrm{w}_1} = \mathcal{T}(\Omega_{\mathrm{w}_2}).$$

Two sets are called *qualitatively distinct* if they are not qualitatively alike.

Remark 3.2.14. Note that all of the operations can be restricted to act on the words corresponding to asymptotically stable stationary solutions of the GDE (3.15) and the LDE (3.1), the set $\mathcal{A}_2^n$. The only issue is that we have to formally restrict the value permutation π

$$\big(\pi(\mathrm{w})\big)_i = \begin{cases} \mathtt{1}, & \mathrm{w}_i = \mathtt{0}, \\ \mathtt{0}, & \mathrm{w}_i = \mathtt{1}. \end{cases}$$

Action of any group G divides its underlying set ($\mathcal{A}_3^n$ or $\mathcal{A}_2^n$ in our case) into equivalence classes (also called orbits) through the equivalence relation: $\mathrm{w}_1, \mathrm{w}_2 \in \mathcal{A}_3^n$ are equivalent if and only if there exists a group element $g \in G$ such that $g(\mathrm{w}_1) = \mathrm{w}_2$. The general group properties ensure that this is indeed an equivalence relation. The previous discussion furthermore implies that the words in one equivalence class label solutions with similar properties and whose regions are easily transformable onto each other. Let us include a short example.

Example 3.2.15 ([69, Example 2.5])**.** There are 27 words of length $n = 3$ made with the alphabet $\mathcal{A}_3 = \{\mathtt{0}, \mathtt{a}, \mathtt{1}\}$:

$$\begin{aligned} \mathrm{W}_{\mathcal{A}_3}(3) = \{&\mathtt{000}, \mathtt{00a}, \mathtt{001}, \mathtt{0a0}, \mathtt{0aa}, \mathtt{0a1}, \mathtt{010}, \mathtt{01a}, \mathtt{011}, \\ &\mathtt{a00}, \mathtt{a0a}, \mathtt{a01}, \mathtt{aa0}, \mathtt{aaa}, \mathtt{aa1}, \mathtt{a10}, \mathtt{a1a}, \mathtt{a11}, \\ &\mathtt{100}, \mathtt{10a}, \mathtt{101}, \mathtt{1a0}, \mathtt{1aa}, \mathtt{1a1}, \mathtt{110}, \mathtt{11a}, \mathtt{111}\}. \end{aligned}$$

Taking into account the action of the group C_3, there are 11 equivalence classes

$$\begin{aligned} \mathrm{W}_{\mathcal{A}_3}^{C_3}(3) = \big\{&\{\mathtt{000}\}, \{\mathtt{aaa}\}, \{\mathtt{111}\}, \\ &\{\mathtt{00a}, \mathtt{0a0}, \mathtt{a00}\}, \{\mathtt{001}, \mathtt{010}, \mathtt{100}\}, \{\mathtt{0aa}, \mathtt{a0a}, \mathtt{aa0}\}, \\ &\{\mathtt{0a1}, \mathtt{a10}, \mathtt{10a}\}, \{\mathtt{01a}, \mathtt{1a0}, \mathtt{a01}\}, \{\mathtt{011}, \mathtt{110}, \mathtt{101}\}, \\ &\{\mathtt{aa1}, \mathtt{a1a}, \mathtt{1aa}\}, \{\mathtt{a11}, \mathtt{11a}, \mathtt{1a1}\}\big\}, \end{aligned}$$

while the action of the group D_3 merges two classes

$$\begin{aligned} \mathrm{W}_{\mathcal{A}_3}^{D_3}(3) = \big\{&\{\mathtt{000}\}, \{\mathtt{aaa}\}, \{\mathtt{111}\}, \\ &\{\mathtt{00a}, \mathtt{0a0}, \mathtt{a00}\}, \{\mathtt{001}, \mathtt{010}, \mathtt{100}\}, \{\mathtt{0aa}, \mathtt{a0a}, \mathtt{aa0}\}, \\ &\{\mathtt{0a1}, \mathtt{a10}, \mathtt{10a}, \mathtt{1a0}, \mathtt{a01}, \mathtt{01a}\}, \{\mathtt{011}, \mathtt{110}, \mathtt{101}\}, \\ &\{\mathtt{aa1}, \mathtt{a1a}, \mathtt{1aa}\}, \{\mathtt{a11}, \mathtt{11a}, \mathtt{1a1}\}\big\}. \end{aligned}$$

The action of the groups C_3^{Π} and D_3^{Π} divides the set of the words into the same system of 6 equivalence classes

$$\begin{aligned}\mathrm{W}_{\mathcal{A}_3}^{C_3^{\Pi}}(3) = \mathrm{W}_{\mathcal{A}_3}^{D_3^{\Pi}}(3) = \big\{&\{\mathtt{ooo}, \mathtt{111}\}, \{\mathtt{aaa}\},\\ &\{\mathtt{ooa}, \mathtt{oao}, \mathtt{aoo}, \mathtt{11a}, \mathtt{1a1}, \mathtt{a11}\}, \{\mathtt{oo1}, \mathtt{o1o}, \mathtt{1oo},\\ &\mathtt{11o}, \mathtt{1o1}, \mathtt{o11}\}, \{\mathtt{oaa}, \mathtt{aoa}, \mathtt{aao}, \mathtt{1aa}, \mathtt{aa1}, \mathtt{a1a}\},\\ &\{\mathtt{oa1}, \mathtt{a1o}, \mathtt{1oa}, \mathtt{1ao}, \mathtt{ao1}, \mathtt{o1a}\}\big\}.\end{aligned}$$

See Figure 3.12 for a graphical illustration of the equivalence classes.

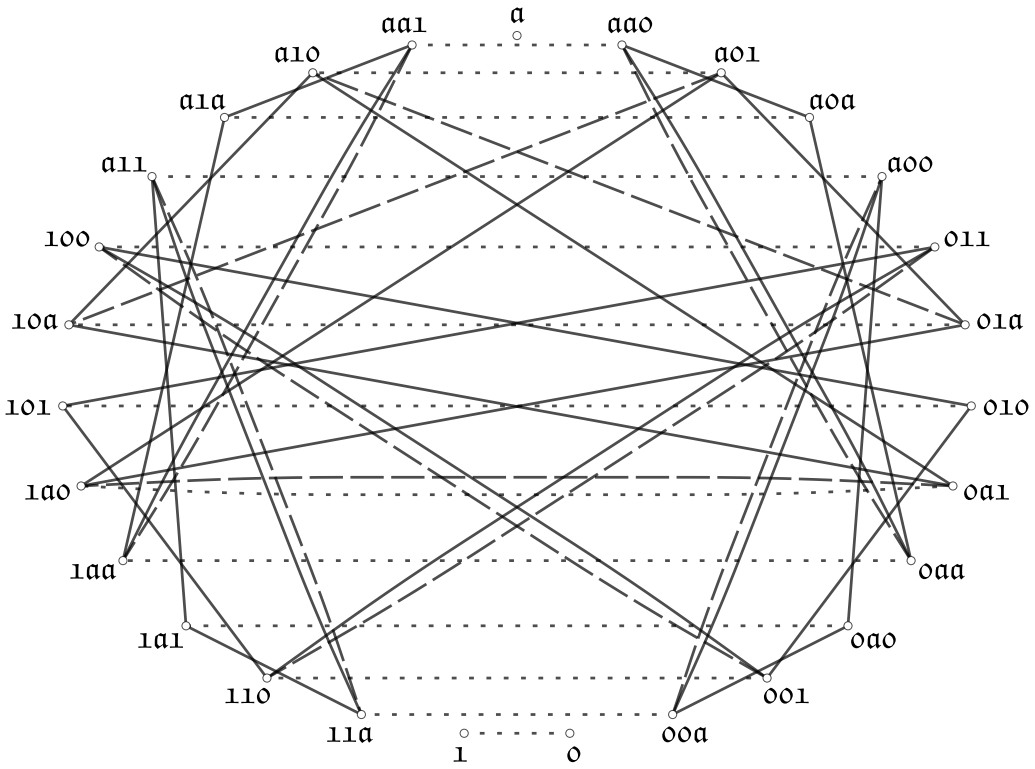

Figure 3.12: A diagram capturing the action of the groups C_3, D_3, C_3^{Π} and D_3^{Π} on the set of three-letter words made with the alphabet $\mathcal{A}_3$. The presence of a line connecting two words indicates the existence of an operation transforming the solutions onto each other. The rotation r is expressed by a solid line, the reflection s is expressed by a dashed line and the symbol permutation π is expressed by a dotted line. Every maximal connected subgraph with appropriate line types represents one equivalence class with respect to the action of a certain group, e.g., the action of C_3^{Π} is depicted by solid and dotted lines. Source [69].

There are multiple ways to determine the number of orbits generated by an action of a group, [59]. In [69], we resorted to the use of Burnside's lemma.

Theorem 3.2.16 (Burnside's lemma)**.** *Let G be a finite group operating on a finite set S. Let $I(g)$ be the number of set elements such that the group operation $g \in G$ leaves them invariant. Then the number of distinct orbits O is given by the formula*

$$O = \frac{1}{|G|} \sum_{g \in G} I(g).$$

The main advantage is such that we do not actually count the number of the orbits but number of elements fixed by each of the group operations which is significantly easier in many cases. Also, the orbits induced by action of the groups C_n or D_n represent distinct stationary solution of the GDE (3.15) and periodic stationary solutions of the LDE (3.1). With the help of Definition 3.2.13, the orbits induced by action of the groups C_n^{Π} and D_n^{Π} represent word subsets whose regions of existence are qualitatively alike.[8]

[8]To obtain a full set of symmetries present in the GDE (3.15) caused by its structure it is more reasonable to include the action of the groups D_n and D_n^{Π}. From theoretical point of view, it is convenient to consider also their simpler counterparts, i.e., C_n, C_n^{Π}.

Up until now, we assumed that the number of the equations of the system (3.18) $n \in \mathbb{N}$ is fixed. But what if we want to count for example periodic stationary solutions of the LDE (3.1) with all periods m smaller than some given $n \in \mathbb{N}$? Simple summing of all the solutions with period lengths smaller than n is not sufficient since it does not take into account the primitive period of the solutions, e.g., if $n = 4$, then the solution of type $\mathfrak{oa}$ would be counted twice since its period is two and four. To this end, we employ Möbius inversion formula, see [49].

Theorem 3.2.17 (Möbius inversion formula)**.** *Let $f, g : \mathbb{N} \to \mathbb{R}$ be two arithmetic functions such that*

$$f(n) = \sum_{d|n} g(d),$$

holds for all $n \in \mathbb{N}$. Then the values of the latter function g can be expressed as

$$g(n) = \sum_{d|n} \mu\left(\frac{n}{d}\right) f(d),$$

where μ is the Möbius function.

The Möbius function μ was first introduced in [49] as

$$\mu(n) = \begin{cases} (-1)^{P(n)}, & \text{each prime factor of } n \text{ is present at most once,} \\ 0, & \text{otherwise,} \end{cases}$$

where $P(n)$ number of the prime factors of n. In our setting, the function g expresses the number of solutions of a given primitive period, which is a-priori unknown. We are only able to obtain the values of f through Burnside's lemma. Möbius inversion formula then enables us to compute g from f.

Before stating the main theorems of this section, we include another example which takes the primitive period of the labelling words into account.

Example 3.2.18 ([69, Example 2.8])**.** We complement Example 3.2.15 with the list of equivalence classes of the length $n = 4$ words made with the alphabet $\mathcal{A}_2 = \{\mathfrak{o}, \mathfrak{1}\}$. There exist words of length 4 with the primitive period 2 and thus the set of the equivalence classes and the set of the Lyndon words will differ not by only the trivial constant words $\{\mathfrak{oooo}\}, \{\mathfrak{1111}\}$. There are 16 words of length 4

$$\begin{aligned} \mathrm{W}_{\mathcal{A}_2}(4) = \big\{&\mathfrak{oooo}, \mathfrak{ooo1}, \mathfrak{oo1o}, \mathfrak{oo11}, \mathfrak{o1oo}, \mathfrak{o1o1}, \mathfrak{o11o}, \mathfrak{o111}, \\ &\mathfrak{1ooo}, \mathfrak{1oo1}, \mathfrak{1o1o}, \mathfrak{1o11}, \mathfrak{11oo}, \mathfrak{11o1}, \mathfrak{111o}, \mathfrak{1111}\big\}. \end{aligned}$$

We next include the equivalence classes induced by the action of the groups $C_4, D_4, C_4^{\Pi}, D_4^{\Pi}$. The words with the primitive period of length lesser than 4 are highlighted by a grey color

$$\begin{aligned} \mathrm{W}_{\mathcal{A}_2}^{C_4}(4) = \mathrm{W}_{\mathcal{A}_2}^{D_4}(4) = \big\{&\{\mathfrak{oooo}\}, \{\mathfrak{1111}\}, \{\mathfrak{o1o1}, \mathfrak{1o1o}\}, \{\mathfrak{oo11}, \mathfrak{o11o}, \mathfrak{11oo}, \mathfrak{1oo1}\}, \\ &\{\mathfrak{ooo1}, \mathfrak{oo1o}, \mathfrak{o1oo}, \mathfrak{1ooo}\}, \{\mathfrak{o111}, \mathfrak{1110}, \mathfrak{1101}, \mathfrak{1011}\}\big\}, \\ \mathrm{W}_{\mathcal{A}_2}^{C_4^{\Pi}}(4) = \mathrm{W}_{\mathcal{A}_2}^{D_4^{\Pi}}(4) = \big\{&\{\mathfrak{oooo}, \mathfrak{1111}\}, \{\mathfrak{o1o1}, \mathfrak{1o1o}\}, \{\mathfrak{oo11}, \mathfrak{o11o}, \mathfrak{11oo}, \mathfrak{1oo1}\}, \\ &\{\mathfrak{ooo1}, \mathfrak{oo1o}, \mathfrak{o1oo}, \mathfrak{1ooo}, \mathfrak{o111}, \mathfrak{1110}, \mathfrak{1101}, \mathfrak{1011}\}\big\}. \end{aligned}$$

First, we assume that $d > 0$ is small enough which ensures the existence of all 3^n n-periodic stationary solutions of the LDE (3.1) via the implicit function theorem.

Theorem 3.2.19 ([31, Theorem 4.])**.** *Let $a \in (0, 1)$ and $d > 0$ be small enough. Then the LDE* (3.1) *has*

1. *3^n n-periodic stationary solutions which form*
   (a) *$N_3(n)$ equivalence classes with respect to translations C_n. Moreover, $NL_3(n)$ of these equivalence classes are formed by primitive periodic solutions.*
   (b) *$B_3(n)$ equivalence classes with respect to translations and reflections D_n. Moreover, $BL_3(n)$ of these equivalence classes are formed by primitive periodic solutions.*
2. *2^n asymptotically stable n-periodic stationary solutions which form*
   (a) *$N_2(n)$ equivalence classes with respect to translations C_n. Moreover, $NL_2(n)$ of these equivalence classes are formed by primitive periodic solutions.*

(b) $B_2(n)$ equivalence classes with respect to translations and reflections D_n. Moreover, $BL_2(n)$ of these equivalence classes are formed by primitive periodic solutions,

where

$$N_k(n) = \frac{1}{n}\sum_{d|n}\varphi(d)k^{\frac{n}{d}}, \tag{3.24}$$

$$B_k(n) = \frac{1}{2}\big[N_k(n) + X_{B,k}(n)\big], \quad X_{B,k}(n) = \begin{cases} \dfrac{k+1}{2}\,k^{\frac{n}{2}}, & n \text{ is even}, \\ k^{\frac{n+1}{2}}, & n \text{ is odd}, \end{cases} \tag{3.25}$$

$$NL_k(n) = \frac{1}{n}\sum_{d|n}\mu\left(\frac{n}{d}\right)\,k^d, \tag{3.26}$$

$$BL_k(n) = \frac{1}{2}\left[NL_k(n) + \sum_{d|n}\mu\left(\frac{n}{d}\right)\,X_{B,k}(d)\right]. \tag{3.27}$$

The function $\varphi : \mathbb{N} \to \mathbb{N}$ is the *Euler totient function*, see, e.g., [1]. Now, we consider the shapes of the regions.

Theorem 3.2.20 ([69, Theorem 2.9])**.** *Let $n \geq 2$ be given. There are at most*

$$\#^{\leq}_{\mathcal{A}_3}(n) = 1 + \sum_{m=2}^{n} BL^{\pi}_{\mathcal{A}_3}(m) \tag{3.28}$$

qualitatively distinct regions Ω_{w}, $\mathrm{w} \in \mathcal{A}_3^m$, out of which at most

$$\#^{\leq}_{\mathcal{A}_2}(n) = 1 + \sum_{m=2}^{n} BL^{\pi}_{\mathcal{A}_2}(m) \tag{3.29}$$

regions belong to the asymptotically stable stationary solutions, where

$$BL^{\pi}_{\mathcal{A}_3}(m) = \frac{1}{4m}\left[\sum_{d|m,\, d\ odd}\mu(d)\,3^{\frac{m}{d}} + X_{NL}(m) + 2m\sum_{d|m}\mu\left(\frac{m}{d}\right)X^{\pi}_{B,3}(d)\right], \tag{3.30}$$

$$BL^{\pi}_{\mathcal{A}_2}(m) = \frac{1}{4m}\left[\sum_{d|m,\, d\ odd}\mu(d)\,2^{\frac{m}{d}} + 2n\sum_{d|m}\mu\left(\frac{m}{d}\right)X^{\pi}_{B,2}(d)\right], \tag{3.31}$$

$$X_{NL}(m) = \begin{cases} 1, & m = 1, \\ -1, & m = 2^{\alpha},\ \alpha \in \mathbb{N}, \\ 0, & \text{otherwise} \end{cases}$$

and

$$X^{\pi}_{B,3}(d) = \begin{cases} \dfrac{4}{3}\cdot 3^{\frac{d}{2}}, & d \text{ is even}, \\ 2\cdot 3^{\frac{d-1}{2}}, & d \text{ is odd}, \end{cases} \qquad X^{\pi}_{B,2}(d) = \begin{cases} 2^{\frac{d}{2}}, & d \text{ is even}, \\ 2^{\frac{d-1}{2}}, & d \text{ is odd}. \end{cases} \tag{3.32}$$

Technical details of the proofs and derivations of the used formulas can be found in [69] (included in Appendix F).

3.3 Multichromatic travelling waves of the Nagumo LDE

The examined properties of the periodic stationary solutions of the LDE (3.1) form the basis of the investigation of the multichromatic waves. The waves of type (3.10) are monotone both in continuous and discrete case. On the other hand, we can consider waves connecting a homogeneous steady state and a nonhomogeneous periodic steady state of LDE (3.1). Such waves can be understood as a composition of multiple monotone waves; this phenomenon has no natural counterpart in the continuous case.

We first provide analytic results proving the existence of the multichromatic waves. Mostly numerical results are provided to determine the speed of such waves[9]. The final part of this section is devoted to the examination of the collision of compound travelling solutions. The presented results originate mainly from [30] and [32]. The latter paper is included in Appendix D.

[9]Indeed, the increasing complexity and the beauty of the behaviour comes at the cost of increasing analytical intricacy.

3.3.1 Problem formulation and general results

In this section, we study the solutions of the LDE (3.1) which connect n-periodic stationary solutions investigated in the preceding text. We call these solutions multichromatic waves. A solution of (3.1) in an *n-chromatic wave*, $n \in \mathbb{N}$, $n \geq 2$ if it has the form

$$u_j(t) = \begin{cases} \Phi_0(j - ct), & \mathrm{mod}(j,n) = 0, \\ \Phi_1(j - ct), & \mathrm{mod}(j,n) = 1, \\ \quad \vdots & \\ \Phi_{n-1}(j - ct), & \mathrm{mod}(j,n) = n-1 \end{cases} \tag{3.33}$$

for some wavespeed $c \in \mathbb{R}$ and $\mathbb{R}^n$-valued waveprofile

$$\Phi = (\Phi_0, \Phi_1, \ldots, \Phi_{n-1}) : \mathbb{R} \to \mathbb{R}^n$$

satisfying boundary conditions

$$\lim_{\xi \to -\infty} \Phi(\xi) = \mathrm{u}_{\mathrm{w}_1}, \qquad \lim_{\xi \to +\infty} \Phi(\xi) = \mathrm{u}_{\mathrm{w}_2} \tag{3.34}$$

with some system (3.18) solutions $\mathrm{u}_{\mathrm{w}_1}, \mathrm{u}_{\mathrm{w}_2}$ of type $\mathrm{w}_1, \mathrm{w}_2$, respectively[10]. See Figure 3.1 for illustration.

Substituting (3.33) into (3.1) we obtain the travelling wave system

$$\begin{aligned} -c\,\Phi_0'(\xi) &= d\big[\Phi_{n-1}(\xi-1) - 2\,\Phi_0(\xi) + \Phi_1(\xi+1)\big] + f\big(\Phi_0(\xi); a\big), \\ -c\,\Phi_1'(\xi) &= d\big[\Phi_0(\xi-1) - 2\,\Phi_1(\xi) + \Phi_2(\xi+1)\big] + f\big(\Phi_1(\xi); a\big), \\ &\vdots \\ -c\,\Phi_{n-1}'(\xi) &= d\big[\Phi_{n-2}(\xi-1) - 2\,\Phi_{n-1}(\xi) + \Phi_0(\xi+1)\big] + f\big(\Phi_{n-1}(\xi); a\big). \end{aligned} \tag{3.35}$$

If $n = 2$ then the system has the form

$$\begin{aligned} -c\,\Phi_0'(\xi) &= d\big[\Phi_1(\xi-1) - 2\,\Phi_0(\xi) + \Phi_1(\xi+1)\big] + f\big(\Phi_0(\xi); a\big), \\ -c\,\Phi_1'(\xi) &= d\big[\Phi_0(\xi-1) - 2\,\Phi_1(\xi) + \Phi_0(\xi+1)\big] + f\big(\Phi_1(\xi); a\big). \end{aligned} \tag{3.36}$$

The system can be understood as a problem of searching for a real number $c \in \mathbb{R}$ and a set of profiles $\Phi = (\Phi_0, \Phi_1, \ldots, \Phi_{n-1}) : \mathbb{R} \to \mathbb{R}^n$. Naturally, the existence and properties of the solutions depend on the parameters (a, d). As the structure of the problem suggests, there are two main questions concerning the MFDE (3.35): the existence and the properties of the profile Φ and the value of c (particularly whether $c = 0$ or $c \neq 0$).

The existence of the profile system Φ solving (3.35) was proved in [32, Theorem 2.1]. Before formulating the result, let us note that the naming scheme from Definition 3.2.5 and the properties of the cubic f ensure proper correspondence of words from $\mathcal{A}_3^n$ or $\mathcal{A}_2^n$ with n-periodic stationary solutions of the LDE (3.1). This is not always true for a general bistable nonlinearity (3.7), [50, Section 1.2]. For the sake of completeness, we include the following assumption.

(AS) Suppose that $h(\mathrm{u}; a, d) = 0$ for some $\mathrm{u} \in \mathbb{R}^n$ and $(a, d) \in [0,1] \times [0, +\infty]$. Suppose furthermore that all eigenvalues λ of $D_1 h(\mathrm{u}; a, d)$ satisfy $\lambda \leq 0$. Then we have $\mathrm{u} = \mathrm{u}_{\mathrm{w}}(a, d)$ for some $\mathrm{w} \in \mathcal{A}_2^n$ and $(a, d) \in \overline{\Omega}_{\mathrm{w}}$.

Theorem 3.3.1 ([32, Theorem 2.1])**.** *Fix an integer $n \geq 2$ and assume that (AΩ1), (AΩ2), (AΩ3) and (AS) all hold. Consider two distinct words $\mathrm{w}_-, \mathrm{w}_+ \in \mathcal{A}_2^n$ and pick $(a, d) \in \Omega_{\mathrm{w}_-} \cap \Omega_{\mathrm{w}_+}$ with $d > 0$. Suppose furthermore that one of the following conditions holds.*

1. *The words w_- and w_+ differ at precisely one location.*
2. *For each $\mathrm{w} \in \mathcal{A}_2^n \setminus \{\mathrm{w}_-, \mathrm{w}_+\}$ that satisfies $\mathrm{w}_- \leq \mathrm{w} \leq \mathrm{w}_+$ we have $(a, d) \notin \overline{\Omega}_{\mathrm{w}}$.*

Then there exists a unique $c \in \mathbb{R}$ for which the travelling system (3.35) admits a solution $\Phi : \mathbb{R} \to \mathbb{R}^n$ that satisfies the boundary conditions (3.34). If $c \neq 0$ then Φ is unique up to translation and each component is strictly increasing.

The main idea of the proof is to show that the partial ordering of the words induces the respective partial ordering of the periodic stationary solutions through Theorem 3.2.11. The ordering then allows us to apply [14, Theorem 6]. The validity of either of the two conditions ensures that there are no stable stationary solutions

[10] For the sake of simplicity, we omit the the discussion of the question whether both of the solutions $\mathrm{u}_{\mathrm{w}^1}, \mathrm{u}_{\mathrm{w}^2}$ exist for the given parameter (a, d) combination. This is treated later in a systematic manner.

"in between" the ones we want to connect. The wave connecting the two periodic steady states of type w_- and w_+ is denoted by $w_- \to w_+$. Note that the translational symmetry (3.21) is also present in the set of wave connections and for the sake of simplicity, we usually speak about classes of waves, i.e.,[11]

$$[001 \to 011] = \{001 \to 011, 010 \to 110, 100 \to 101\}.$$

The statement of Theorem 3.3.1 allows us to construct diagrams depicting the existence of respective waves, Figure 3.13.

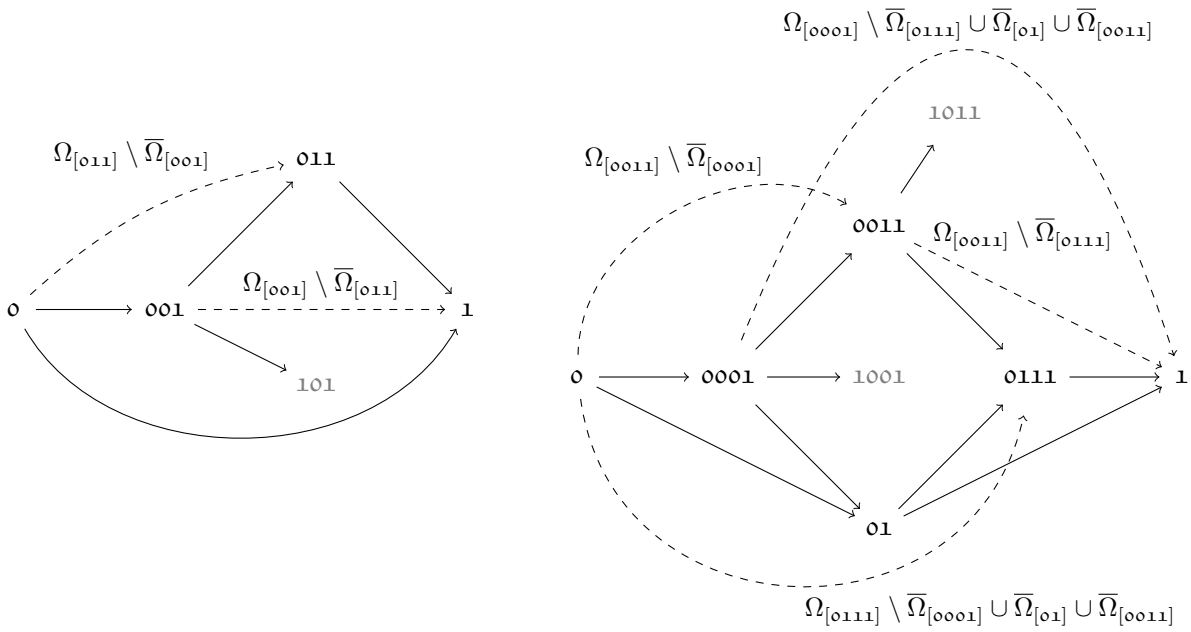

Figure 3.13: This diagram depicts the wave connections mentioned in Theorem 3.3.1. A solid arrow indicates the wave connection existing due to the validity of the first condition (i.e., the respective words differ at precisely one location). A dashed arrow indicates the wave connection existing due to the second condition including the necessary condition on the parameter (a, d) tuple. For the sake of clarity, we omit the obvious connection $0 \to 1$. The connections with words which are not minimal with respect to the rotation (3.21) are hinted in grey at proper places and omitted everywhere else. Source: [32].

As previously mentioned, the crucial question is whether the existing wave travels or not. Intuitively, the monochromatic wave (3.10) travelling speed is closely connected to the diffusion intensity d. Vaguely speaking the higher the diffusion intensity, the more likely is the wave to travel. On the other hand, the results on existence of stable periodic stationary solutions of the LDE (3.1) show that the solutions tend to lose their stability and bifurcate if the diffusion intensity exceeds some threshold. One then should expect that the solutions of the form (3.33) and (3.34) travel, i.e., $c \neq 0$, only for some small balanced parameter region inside $\Omega_{w_-} \cap \Omega_{w_+}$. Due to the complexity of the problem, no general analytic results are available so far. The nonzero speed of the bichromatic waves (waves of type $[0 \to 01]$ and $[01 \to 1]$) was however proved by Hupkes et al. in [30, Theorem 2.2, 2.3], see Figure 3.14 for illustration. Other results concerning the speed of the multichromatic waves are numerical.

3.3.2 Numerical results and wave collisions

The numerical investigation is divided into three separate sections. First, we examine the behaviour of trichromatic waves, the waves connecting the trivial stable steady state of the LDE (3.1) and some stable three-periodic steady state. We next turn out attention to quadrichromatic waves which incorporate four-periodic solutions.

Each of the paragraphs is concluded with an overview of the wave collisions. Experiments show that Theorem 3.3.1 can be applied somewhat locally which enables the construction of compound waves containing for example the wave $[0 \to 001]$ and $[001 \to 1]$, see Figure 3.19. Such waves can collide and subsequently form new waves. Closer examination of the travelling regions for tri- and quadrichromatic waves helps us to categorize the collisions and specify the parameter (a, d) regimes in which the collisions occur.

[11] Note that the stationary solutions rotate simultaneously. Analytically, an asynchronous rotation would create qualitatively distinct object. This is illustrated in Figure 3.20.

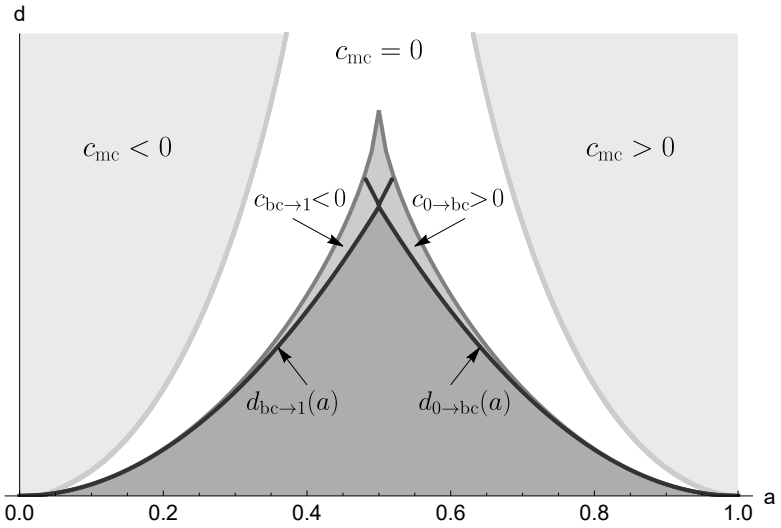

Figure 3.14: Regions of nonzero travelling speed for the bichromatic waves ([0 → 01] and [01 → 1]). The number c_{mc} indicates the speed of the monochromatic wave of type (3.10). The "tent" region is Ω_{01} as in Figure 3.6. The indices 0 → bc and bc → 1 label the values describing the wave connections [0 → 01] and [01 → 1], respectively. The regions of nonzero speed for bichromatic waves are just under the upper edge of the Ω_{01} region, see [30] for further details. Source: [32].

Each of the traveling wave simulations were performed on a path with more than 100 vertices. The initial condition was estimated as an arcus tangent approximation. A special attention was paid for the connection not to be close to the end vertices. Surprisingly, this was enough to reach the desired wave type. The actual ODE simulation was performed by the ODE45 solver in MATLAB software.

Let us note that this section is figure-heavy and it is not technically possible to include all the figures in their proper place in the text. The simulation examples are thus included in the final pages of this chapter in order to keep the flow of the text as natural as possible.

Trichromatic waves

The majority of information about the travelling regions of trichromatic waves is compiled in Figure 3.15. Let

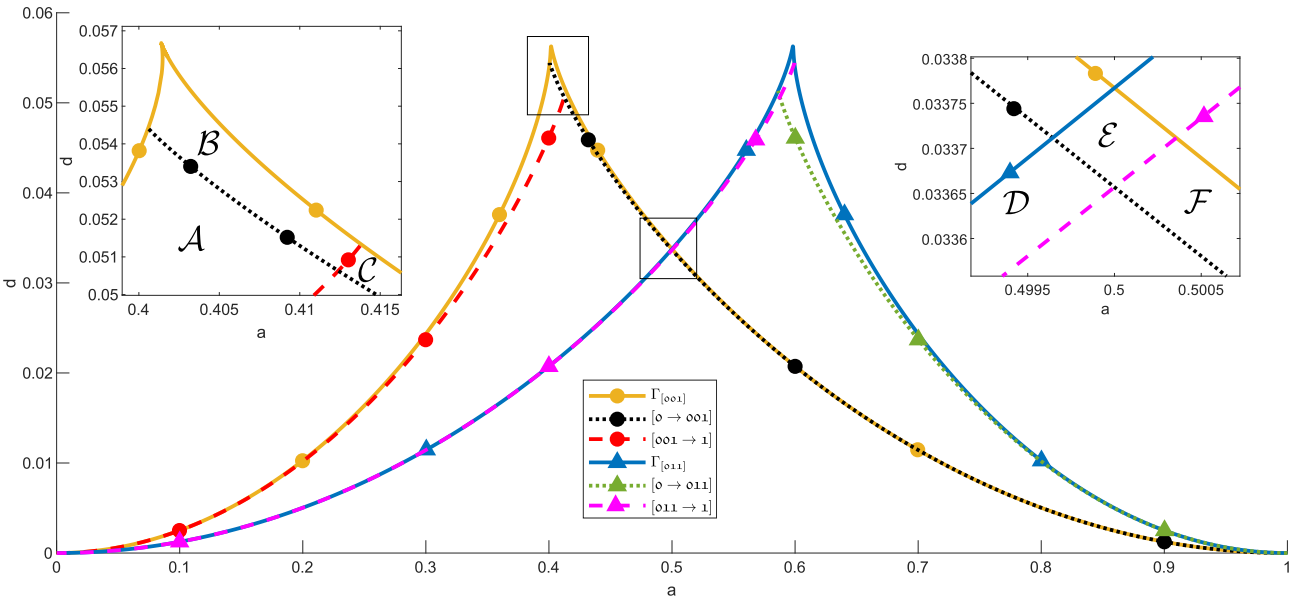

Figure 3.15: Numerically computed regions in which the trichromatic waves travel. Boundary of each of the region consists of the existence threshold of the three-periodic solution of the LDE (3.1). The lower thresholds on which the waves still exist but with zero speed $c = 0$ are depicted by non-solid lines. The travelling regions are divided into six regions (omitting the symmetry of the waves [0 → 001] and [011 → 1]) with qualitatively different behaviour. Source: [32].

us note that we examine waves of type $[0 \to 001]$, $[0 \to 011]$, $[001 \to 1]$ and $[011 \to 1]$. The other three possible wave connections as predicted by Theorem 3.3.1, i.e., $[001 \to 011]$, $[001 \to 110]$ and $[001 \to 110]$, seem to exist; they were however not observed to travel.

The travelling regions for waves in the state $[001]$ existence area can be divided into six different subregions in which the compound waves exhibit different behaviour. Note that considering other regions would be superficial because the symmetry argument (3.22) implies that the waves $[0 \to 001]$ and $[011 \to 1]$ exhibit qualitatively same behaviour for $a \mapsto 1 - a$.

In the region $\Omega_{[001]}$ both of the waves $[0 \to 001]$ and $[001 \to 1]$ exist. In the region $\mathcal{A}$ the wave $[001 \to 1]$ travels. This enables us to construct a compound wave denoted by[12] $[0 \to 001 \to 1]$ as can be seen in the second row of Figure 3.19. The travelling connection moves to left until it hits the pinned connection and created the pinned monochromatic wave. Indeed, the monochromatic wave is pinned since the region $\Omega_{[001]}$ lies exclusively in the pinning region. Another possibility occurs in the region $\mathcal{B}$ where both of the waves $[0 \to 001]$ and $[001 \to 1]$ travel, collide and form the pinned monochromatic wave, see the first line in Figure 3.19. The behaviour of the compound wave in the region $\mathcal{C}$ is just a symmetric counterpart of $\mathcal{A}$.

The most convoluted behaviour can be observed in the region $\mathcal{E}$. Since $\mathcal{E} \subset \Omega_{[001]} \cap \Omega_{[011]}$ the existence of the waves $[0 \to 001]$, $[001 \to 011]$ and $[011 \to 1]$ is ensured. Moreover, the former and the latter waves travel. In the virtue of the previous wave compositions, we can create a compound wave $[0 \to 001 \to 011 \to 1]$ where the two outer connections travel until the collision occurs. Then again the pinned monochromatic wave emerges, see the first row of Figure 3.20.

We omit the discussion of the behaviour in the other regions since the compound waves in $\mathcal{D}$ and $\mathcal{F}$ corresponds to the already discussed cases in $\mathcal{A}$ and $\mathcal{C}$.

Quadrichromatic waves

In the virtue of Figure 3.15 we include Figure 3.16 depicting the traveling regions for quadrichromatic waves. Besides higher number of waves containing trivial periodic steady states there is one significant novel behaviour.

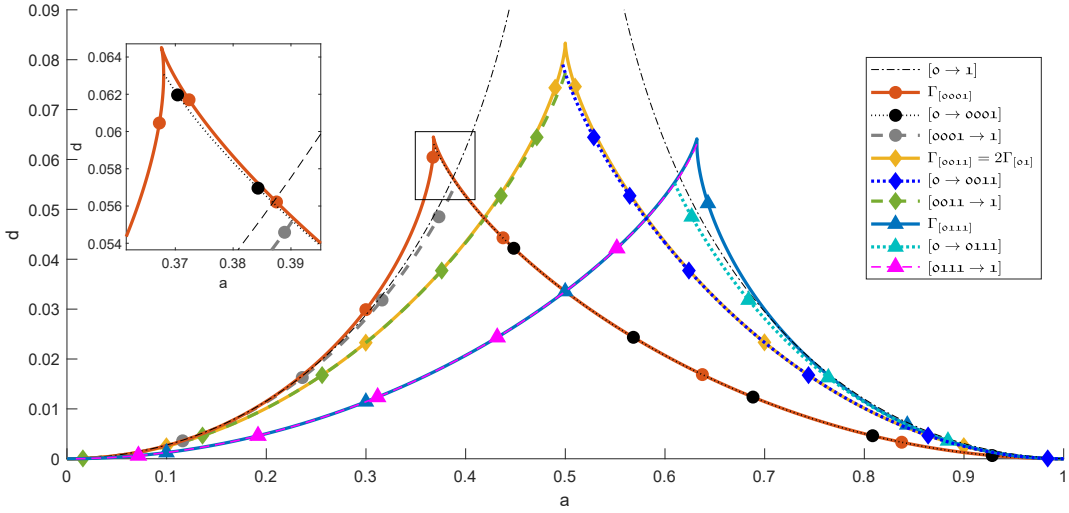

Figure 3.16: Regions in which quadrichromatic waves travel. The Γ_w thresholds are identical to the ones in Figure 3.11. The travelling regions of the waves incorporating the steady states of type $[0001]$ and $[0111]$ have nonempty intersection with the region in which the monochromatic wave $[0 \to 1]$ travels. This enables us to observe more intricate collision processes compared to trichromatic case. Source: [32].

Note that the existence regions of the 4-periodic stationary solutions of type $[0001]$ and $[0111]$ have nonempty intersection with the travelling region of the monochromatic waves. The collisions of the compound waves thus exhibit much richer phenomena. There can again be distinguished six subsets of $\Omega_{[0001]}$ in which the compound waves show qualitatively different behaviour, see Figure 3.17. Indeed, there are six possible combinations of whether the waves of type $[0 \to 0001]$, $[0001 \to 0111]$ and $[0 \to 1]$ travel. Let us closely examine the compound wave $[0 \to 0001 \to 1]$. The regions C, D, E and F correspond to the regions $\mathcal{A}, \mathcal{B}$, the region with zero speed for the waves $[0 \to 001], [001 \to 1]$ and $\mathcal{C}$, respectively, see Figure 3.15. Both in A and B, the emerging monochromatic wave travels as can be seen in Figure 3.21.

[12] Up to now, we do not have a proper definition of compound waves and thus the labelling is rather intuitive than rigorous. Figures 3.19, 3.20 and 3.21 should be informative enough to explain the concept of compound waves and its notation.

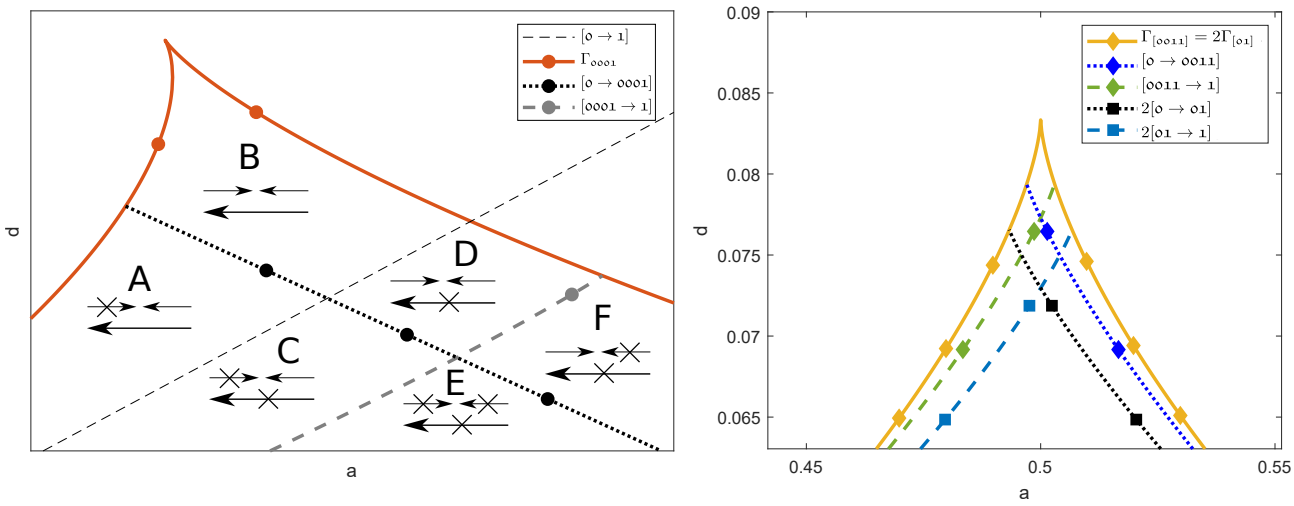

Figure 3.17: Magnifications of two sepcific parts of Figure 3.16. The first panel is illustrative depiction of the situation at the intersection of the monochromatic travelling region and $\Omega_{[0001]}$. The small arrows respectively depict whether the waves of type $[0 \to 0001]$ and $[0001 \to 1]$ travel. The big arrow relates to the monochromatic wave of type $[0 \to 1]$. The second panel illustrates a qualitative difference in the examination of periodic steady states and the travelling waves, see Remark 3.3.2. Source: [32].

More complex compound waves can also be made. For example, assuming $(a, d) \in \Omega_{[0001]} \cap \Omega_{[01]}$ the wave $[0 \to 0001 \to 01 \to 1]$ can be constructed, see Figure 3.20.

Remark 3.3.2. There is one subtlety observed which further shows the intricacy in the study of the multichromatic waves. It can be shown that $\Omega_{[01]}$ and $\Omega_{[0011]}$ coincide. Indeed, if we search for solution of type $[0011]$ we assume $u_1 = u_2$ and $u_3 = u_4$. The system (3.18) reduces to the system on two vertices with halved diffusion coefficient. This is demonstrated in the right panel of Figure 3.17 such that $\Omega_{[0011]}$ coincides with twice vertically magnified $\Omega_{[01]}$. On the other hand, the existence region of the wave $[0 \to 01]$ and the scaled region of the wave $[0 \to 0011]$ do not seem to coincide.

3.4 Open questions and further directions

The following list does not aspire to give a general overview of open questions and possible directions. It just gives few ideas which might be of interest for future research.

Travelling waves in general bistable systems The LDE (3.1) exhibits bistable behaviour; there are two asymptotically stable homogeneous steady states. This rather general property can be for example observed in Lotka-Volterra competition model. Local behaviour of stationary states of such systems were examined in [61]. In the light of §3.2, can a similar analysis be performed for such systems? What can be said about multichromatic waves in such system?

Counting of stationary solutions on general graphs with nontrivial automorphism, [69] The main objects of interests were the LDE (3.1) and the GDE (3.15) in this paper. In general, given a graph $\mathcal{G} = (V, E)$, the Nagumo graph differential equation can be written as (3.5). Provided the graph $\mathcal{G}$ has a nontrivial automorphism (a nontrivial self-map which preserves the edge-vertex connectivity) the approach used here can be extended. Indeed, the group D_n is the automorphism group of the cycle graph with n vertices and all computation can be carried out when the replacing the dihedral group D_n with the automorphism group of the graph $\mathcal{G}$.

Equivalence of the GDE and the LDE stationary solutions in general, [69] The idea of Lemma 3.2.1 is such that the restriction to the periodic stationary solutions of the LDE (3.1) allows us to formally divide the lattice into a countable number of identical finite graphs. General equivalence claim which helps to reduce the search for an arbitrary periodic patterns in sufficiently regular infinite graphs (e.g., triangular lattice, hexagonal lattice) into a finite-dimensional problem is still missing. For example, a reproduction of the proof of Lemma 3.2.1 shows that the stationary solutions of the LDE (3.14) in the form of a repeated 2x2 pattern are equivalent to the stationary solutions of the GDE (3.15) on 4 vertices with the doubled diffusion coefficient d, see Figure 3.18 for illustration.

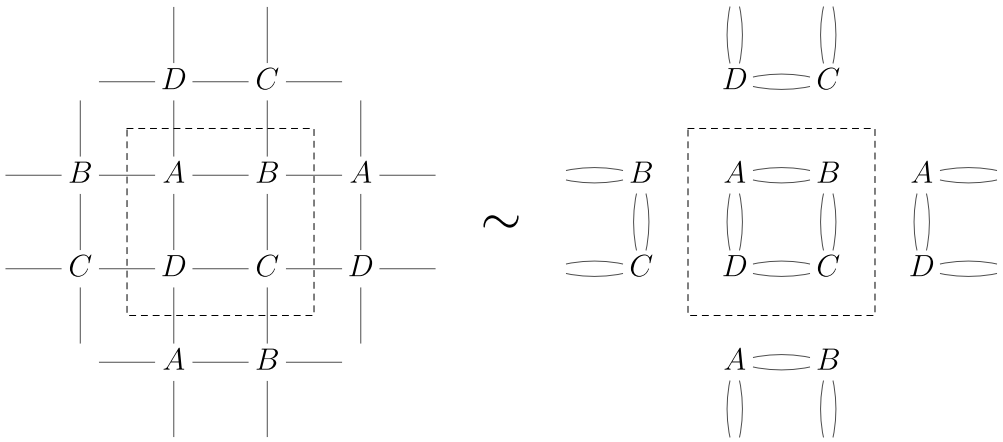

Figure 3.18: A graphical illustration of a possible extension of Lemma 3.2.1 for patterns on two-dimensional lattices. A general idea is that the edges crossing the dashed line are wrapped back inside from the opposite sides. Source: [69].

Can there be derived a more general lemma in the virtue of Lemma 2.1 for a general class of lattices, e.g., hexagonal lattice, triangular lattice, etc., and an arbitrary pattern which covers the whole lattice?

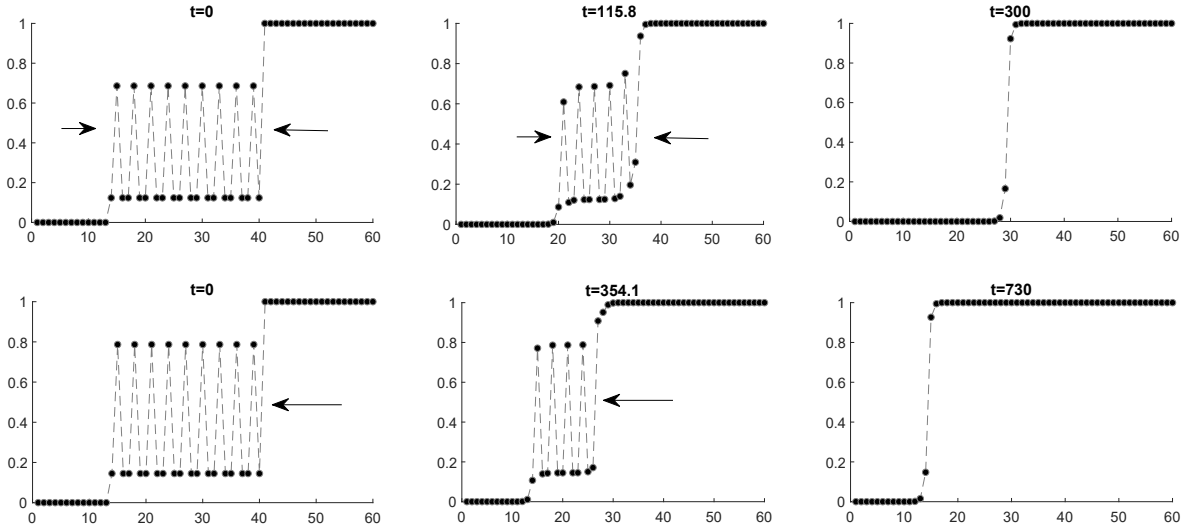

Figure 3.19: Examples of two wave collisions. The first line depicts the wave $[0 \to 001 \to 1]$. The parameters were set to $(a, d) = (0.404, 0.054)$ and they occupy the region $\mathcal{B}$, see Figure 3.15. Both the waves $[0 \to 001]$ and $[001 \to 1]$ travel here until the collision which creates a pinned monochromatic wave. The second line shows the wave of the same type but the parameters $(a, d) = (0.404, 0.05)$ lie in the region $\mathcal{A}$. Only the wave $[0 \to 001]$ travels here until hits the pinned wave $[001 \to 1]$ and create a pinned monochromatic wave. Source: [32].

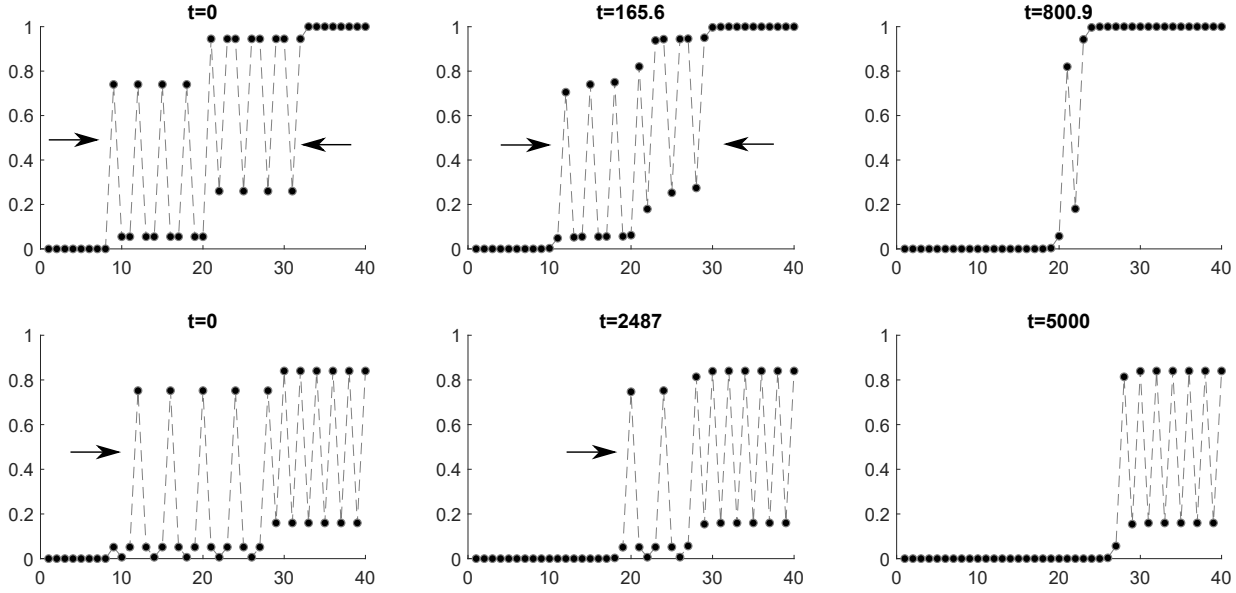

Figure 3.20: The first line depicts the wave of type $[0 \to 001 \to 011 \to 1]$. The parameters are set to be $(a, d) = (0.5, 0.0337)$ which places them in the region $\mathcal{E}$, see Figure 3.15. Both the waves $[0 \to 001]$ and $[011 \to 1]$ travel here; they collide and they form a pinned nonmonotone monochromatic wave. A monotone monochromatic wave can be obtained by replacing the first wave with $[0 \to 010]$. The second line depicts a compound quadrichromatic wave $[0 \to 0001 \to 0101]$ in the regime where the wave $[0 \to 0001]$ travels, $(a, d) = (0.5, 0.033554)$. The collision results in a pinned bichromatic wave $[0 \to 01]$. Source: [32].

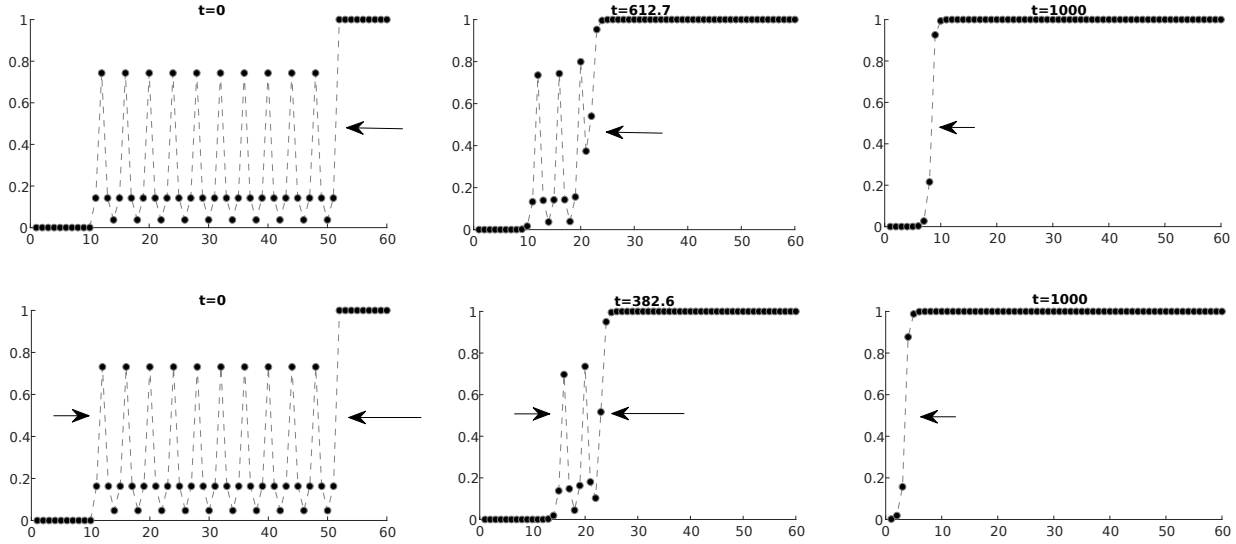

Figure 3.21: Two examples of compound quadrichromatic waves. The first line depicts the wave of type $[\mathfrak{0} \to \mathfrak{0001} \to \mathfrak{1}]$ with $(a, d) = (0.378, 0.058)$, i.e., they lie in the region A from Figure 3.17. Only the wave of type $[\mathfrak{0001} \to \mathfrak{1}]$ travels here. After the collision the monochromatic travelling wave is formed. This is a novel behaviour impossible to observe in the trichromatic case. The same wave is shown in the second line but the parameters are set to be in the region B, $(a, d) = (0.37, 0.0625)$. Now both of the waves $[\mathfrak{0} \to \mathfrak{0001}]$ and $[\mathfrak{0001} \to \mathfrak{1}]$ travel. The resulting monochromatic wave then also travels. Source: [32].

Chapter 4

Conclusion

A wide topic of dynamical systems on graphs was presented from two of many possible viewpoints. We investigated evolutionary games on graphs which are dynamical systems with discrete spatial and temporal structure and discrete (even binary) state space. Another examined field were reaction-diffusion problems which in contrary possess continuous temporal structure and state space. Generally speaking, the research focused on various types of equilibrium states.

In the evolutionary games on graphs, we investigated fixed points (constant states of the system) and periodic orbits (invariant set of states which are periodically rotating). Although not explicitly stated, all the results show that introducing a spatial structure into a system can result in much richer and less predictable behaviour. Specific spatial settings can construct fixed states whose ratio of cooperating and defecting players is in a complete contrast with the possible Nash equilibria and/or the evolutionary stable strategies of the two-player matrix game. On the other hand, the richer dynamics is balanced with increasing complexity of the problem from the mathematical point of view. To this end, we have so far neglected possible extensions such as other reproduction dynamics (death-birth, birth-death, etc., see [17]), length of player interaction [8], various update rules and other. One of the major traits of the model is such that the notion of stability is yet to be defined since even one vertex perturbation can lead to emergence of an intricate trajectory. Although this trajectory ends in the desired steady state the behaviour is still unexpected and hard to predict, see [17, Example 13]. On the other hand, even simple discrete-time models can exhibit very rich and unintuitive behaviour, see, e.g., [70].

The second part of this thesis was devoted to the Nagumo lattice differential equation. When possible, some overlap with the theory of more general bistable systems is discussed. We paid special attention to the comparison of the properties of the lattice equation and its continuous counterpart, the Nagumo partial differential equation. The lattice equation can possess travelling wave solutions similar to the spatially continuous equation but there is a non-trivial parameter region (the pinning region) in which the solutions do not travel. Moreover, the lattice equation can have an infinite number of stationary solutions; it is argued that the existence of such solutions is directly connected to the pinning phenomenon. Further, we investigated the properties of heterogeneous periodic stationary solutions of the lattice equation; again, a phenomenon with no counterpart in the continuous case. The periodic stationary solutions we used as building blocks of more intricate travelling wave solutions, the multichromatic waves, which exhibit wave collisions and even travel in the pinning area. Since the topic of emergence of the heterogeneous stationary states and the travelling structures in the Nagumo lattice differential equation is fairly complex, there is abundance of open questions and further research directions. Namelly, the multichromatic waves travelling speed has been investigated only through numerical simulations but even the knowledge of the monochromatic waves' travelling speed is not complete yet, [35, 72]. Next, our approach for investigating stationary solutions included the reduction of the countable system of algebraic equations into a finite one. This was possible due to a specific structure of the underlying structure: the one-dimensional lattice, the path graph. Further extension to other types of lattices is still missing.

We would like to finally mention an interesting link between the Nagumo lattice equation and time-discrete dynamical systems. The stationary problem for the lattice equation

$$0 = d(u_{i-1} - 2u_i - u_{i+1}) + f(u_i; a)$$

can be expressed as a two dimensional system

$$\begin{aligned} u_{i+1} &= v_i, \\ v_{i+1} &= 2v_i - u_i + \frac{1}{d} f(v_i; a), \end{aligned} \tag{4.1}$$

which is forward and backward solvable for any initial condition $(u_0, v_0) \in [0,1]^n$. The knowledge of the fixed and periodic points is crucial to understanding of the stationary solutions of the lattice equation, [7, 29].

All the mentioned directions show a similar property: the parameters of the system must be in a certain balanced setting for the equilibrium-like behaviours to emerge which makes it challenging and interesting topic for mathematical research.

Bibliography

[1] Tom M. Apostol. *Introduction to analytic number theory*. Springer New York, 1976.

[2] G. W. Beeler and H. Reuter. "Reconstruction of the action potential of ventricular myocardial fibres". In: *The Journal of Physiology* 268.1 (1977), pp. 177–210.

[3] Jonathan Bell. "Some threshold results for models of myelinated nerves". In: *Mathematical Biosciences* 54.3 (1981), pp. 181–190.

[4] Martin Bohner and Allan C. Peterson. *Advances in Dynamic Equations on Time Scales*. Ed. by Martin Bohner and Allan C. Peterson. Birkhäuser Boston, 2002. 364 pp.

[5] A. Bouzerdoum and R.B. Pinter. "Shunting inhibitory cellular neural networks: derivation and stability analysis". In: *IEEE Transactions on Circuits and Systems I: Fundamental Theory and Applications* 40.3 (1993), pp. 215–221.

[6] Jason J. Bramburger. "Rotating wave solutions to lattice synamical systems I: The anti-continuum limit". In: *Journal of Dynamics and Differential Equations* (2018), pp. 469–498.

[7] Jason J. Bramburger and Björn Sandstede. "Spatially localized structures in lattice dynamical systems". In: *Journal of Nonlinear Science* 30.2 (2019), pp. 603–644.

[8] Mark Broom and Vlastimil Křivan. "Two-strategy games with time constraints on regular graphs". In: *Journal of Theoretical Biology* (2020), p. 110426.

[9] Mark Broom and Jan Rychtář. *Game-Theoretical Models in Biology*. Chapman and Hall, 2013.

[10] Maila Brucal-Hallare and Erik Van Vleck. "Traveling Wavefronts in an Antidiffusion Lattice Nagumo Model". In: *SIAM Journal on Applied Dynamical Systems* 10.3 (2011), pp. 921–959.

[11] Claudia. Bucur. *Nonlocal diffusion and applications*. eng. Claudia Bucur. New York, NY: Springer Berlin Heidelberg, 2016.

[12] J. W. Cahn and A. Novick-Cohen. "Evolution equations for phase separation and ordering in binary alloys". In: *Journal of Statistical Physics* 76.3-4 (1994), pp. 877–909.

[13] Yunus A. Çengel and John M. Cimbala. *Fluid mechanics: fundamentals and applications*. McGraw-Hill, 2006.

[14] Xinfu Chen, Jong-Shenq Guo, and Chin-Chin Wu. "Traveling waves in discrete periodic media for bistable dynamics". In: *Archive for Rational Mechanics and Analysis* 189.2 (2008), pp. 189–236.

[15] Yan-Yu Chen, Jong-Shenq Guo, and François Hamel. "Traveling waves for a lattice dynamical system arising in a diffusive endemic model". In: *Nonlinearity* 30.6 (2017), pp. 2334–2359.

[16] L.O. Chua and L. Yang. "Cellular neural networks: theory". In: *IEEE Transactions on Circuits and Systems* 35.10 (1988), pp. 1257–1272.

[17] Jeremias Epperlein, Stefan Siegmund, and Petr Stehlík. "Evolutionary games on graphs and discrete dynamical systems". In: *Journal of Difference Equations and Applications* 21.2 (2014), pp. 72–95.

[18] Jeremias Epperlein, Stefan Siegmund, Petr Stehlík, and Vladimír Švígler. "Coexistence equilibria of evolutionary games on graphs under deterministic imitation dynamics". In: *Discrete and Continuous Dynamical Systems - Series B* 21.3 (2016), pp. 803–813.

[19] Jeremias Epperlein and Vladimír Švígler. "On arbitrarily long periodic orbits of evolutionary games on graphs". In: *Discrete and Continuous Dynamical Systems - B* 23.5 (2018), pp. 1917–1937.

[20] Paul C. Fife and J. Bryce McLeod. "The approach of solutions of nonlinear diffusion equations to travelling front solutions". In: *Archive for Rational Mechanics and Analysis* 65.4 (1977), pp. 335–361.

[21] Richard FitzHugh. "Impulses and physiological states in theoretical models of nerve membrane". In: *Biophysical Journal* 1 (1961), pp. 445–66.

[22] Paul Glendinning. “View from the pennines: analysis on time scales”. In: *Mathematics Today* 39 (2003). semanticscholar.com.

[23] M. E. Henderson and H. B. Keller. “Complex Bifurcation from Real Paths”. In: *SIAM Journal on Applied Mathematics* 50.2 (1990), pp. 460–482.

[24] Stefan Hilger. “Ein Masskettenkalkül mit Anwendung auf Zentrumsmannigfaltigkeiten”. PhD thesis. University of Würzburg, 1989.

[25] Josef Hofbauer and Karl Sigmund. *Evolutionary Games and Population Dynamics*. Cambridge University Press, 1998.

[26] Aaron Hoffman and John Mallet-Paret. “Universality of Crystallographic Pinning”. In: *Journal of Dynamics and Differential Equations* 22.2 (2010), pp. 79–119.

[27] Paul L. Houston. *Chemical Kinetics and Reaction Dynamics*. Dover Publications Inc., 2006. 352 pp.

[28] H. J. Hupkes and L. Morelli. “Travelling corners for spatially discrete reaction-diffusion systems”. In: *Communications on Pure & Applied Analysis* 19.3 (2020), pp. 1609–1667.

[29] Hermen Jan Hupkes, Leonardo Morelli, Willem M. Schouten-Straatman, and Erik S. Van Vleck. “Traveling Waves and Pattern Formation for Spatially Discrete Bistable Reaction-Diffusion Equations”. In: *Difference Equations and Discrete Dynamical Systems with Applications*. Springer International Publishing, 2020, pp. 55–112.

[30] Hermen Jan Hupkes, Leonardo Morelli, and Petr Stehlík. “Bichromatic travelling waves for lattice Nagumo equations”. In: *SIAM Journal on Applied Dynamical Systems* 18.2 (2019), pp. 973–1014.

[31] Hermen Jan Hupkes, Leonardo Morelli, Petr Stehlík, and Vladimír Švígler. “Counting and ordering periodic stationary solutions of lattice Nagumo equations”. In: *Applied Mathematics Letters* 98 (2019), pp. 398–405.

[32] Hermen Jan Hupkes, Leonardo Morelli, Petr Stehlík, and Vladimír Švígler. “Multichromatic travelling waves for lattice Nagumo equations”. In: *Applied Mathematics and Computation* 361 (2019), pp. 430–452.

[33] Hermen Jan Hupkes and Erik S. Van Vleck. “Negative diffusion and traveling waves in high dimensional lattice systems”. In: *SIAM Journal on Mathematical Analysis* 45.3 (2013), pp. 1068–1135.

[34] Hermen Jan Hupkes and Erik S. Van Vleck. “Travelling waves for complete discretizations of reaction diffusion systems”. In: *Journal of Dynamics and Differential Equations* 28.3-4 (2015), pp. 955–1006.

[35] James P. Keener. “Propagation and its failure in coupled systems of discrete excitable cells”. In: *SIAM Journal on Applied Mathematics* 47.3 (1987), pp. 556–572.

[36] Panayotis G. Kevrekidis. *The discrete nonlinear Schrödinger equation*. Springer-Verlag GmbH, 2009.

[37] István Z. Kiss, Joel C. Miller, and Péter L. Simon. *Mathematics of epidemics on networks*. Springer Science + Business Media, 2017.

[38] Jean Pierre Laplante and Thomas Erneux. “Propagation failure in arrays of coupled bistable chemical reactors”. In: *The Journal of Physical Chemistry* 96.12 (1992), pp. 4931–4934.

[39] J.P. Laplante and T. Erneux. “Propagation failure and multiple steady states in an array of diffusion coupled flow reactors”. In: *Physica A: Statistical Mechanics and its Applications* 188.1-3 (1992), pp. 89–98.

[40] Randall J. LeVeque. *Finite difference methods for ordinary and partial differential equations*. eng. Randall J. LeVeque., Includes bibliographical references (p. 329-335) and index. Philadelphia, PA: Society for Industrial and Applied Mathematics, 2007.

[41] Simon A. Levin. “Dispersion and population interactions”. In: *The American Naturalist* 108.960 (1974), pp. 207–228.

[42] Tien-Yien Li and James A. Yorke. “Period Three Implies Chaos”. In: *The American Mathematical Monthly* 82.10 (1975), pp. 985–992.

[43] John David Logan. *Introduction to Nonlinear Partial Differential Equations*. eng. 2nd ed. J. David Logan., Includes bibliographical references (p. [387]-393) and index. Hoboken, N.J: Wiley-Interscience, 2008.

[44] John Mallet-Paret. “Crystallographic pinning: direction dependent pinning in lattice differential equations”. In: (2002).

[45] John Mallet-Paret. “The Fredholm alternative for functional differential equations of mixed type”. In: *Journal of Dynamics and Differential Equations* 11.1 (1999), pp. 1–47.

[46] John Mallet-Paret. “The global structure of traveling waves in spatially discrete dynamical systems”. In: *Journal of Dynamics and Differential Equations* 11.1 (1999), pp. 49–127.

[47] Thomas Robert Malthus. *An Essay on the Principle of Population As It Affects the Future Improvement of Society, with Remarks on the Speculations of Mr. Goodwin, M. Condorcet and Other Writers*. London: J. Johnson in St Paul's Church-yard, 1798.

[48] Carsten Marr and Marc-Thorsten Hütt. "Outer-totalistic cellular automata on graphs". In: *Physics Letters A* 373.5 (2009), pp. 546–549.

[49] A.F. Möbius. "Über eine besondere Art von Umkehrung der Reihen". ger. In: *Journal für die reine und angewandte Mathematik* 9 (1832), pp. 105–123.

[50] Leonardo Morelli. "Travelling patterns on discrete media". PhD thesis. Leiden University, 2019.

[51] James D. Murray. *Mathematical Biology II*. Springer-Verlag GmbH, 2011.

[52] James Dickson Murray. *Mathematical biology*. eng. 3rd ed. J.D. Murray., Includes bibliographical references and index. New York: Springer, 2003.

[53] Roger B. Myerson. *Game Theory: Analysis of Conflict*. First Harvard University Press, 1997.

[54] J. Nagumo, S. Arimoto, and S. Yoshizawa. "An active pulse transmission line simulating nerve axon". In: *Proceedings of the IRE* 50.10 (1962), pp. 2061–2070.

[55] J. Nagumo, S. Yoshizawa, and S. Arimoto. "Bistable transmission lines". In: *IEEE Transactions on Circuit Theory* 12.3 (1965), pp. 400–412.

[56] John Forbes Nash. "Equilibrium points in n-person games". In: *Proceedings of the National Academy of Sciences* 36.1 (1950), pp. 48–49.

[57] Martin A. Nowak. "Five Rules for the Evolution of Cooperation". In: *Science* 314.5805 (2006), pp. 1560–1563.

[58] Martin A. Nowak and Robert M. May. "Evolutionary Games and Spatial Chaos". In: *Nature* 359.6398 (1992), pp. 826–829.

[59] John Riordan. *Combinatorial analysis*. London: Chapman & Hall, 1958.

[60] O. M. Sharkovsiĭ. "Coexistence of cycles of a continuous mapping of the line into itself". In: *International Journal of Bifurcation and Chaos* 05.05 (1995), pp. 1263–1273.

[61] Antonín Slavík. "Lotka–Volterra competition model on graphs". In: *SIAM Journal on Applied Dynamical Systems* 19.2 (2020), pp. 725–762.

[62] Petr Stehlík. "Exponential number of stationary solutions for Nagumo equations on graphs". In: *Journal of Mathematical Analysis and Applications* 455.2 (2017), pp. 1749–1764.

[63] Petr Stehlík. "Replicator Equations as Limits of Evolutionary Games on Complete Graphs". In: *Advances in Difference Equations and Discrete Dynamical Systems*. Springer Singapore, 2017, pp. 67–87.

[64] Petr Stehlík and Jonáš Volek. "Maximum Principles for Discrete and Semidiscrete Reaction-Diffusion Equation". In: *Discrete Dynamics in Nature and Society* 2015 (2015), pp. 1–13.

[65] I.U.M. Svirezhev and D.O. Logofet. *Stability of Biological Communities*. Mir Publishers, 1983.

[66] György Szabó and Gábor Fáth. "Evolutionary games on graphs". In: *Physics Reports* 446.4-6 (2007), pp. 97–216.

[67] A. Tychonoff. "Uber unendliche Systeme von Differentialgleichungen." German. In: *Rec. Math. Moscou* 41 (1934), pp. 551–555.

[68] P.F. Verhulst. "Recherches mathématiques sur la loi d'accroissement de la population." In: *Nouveaux mémoires de l'Académie Royale des Sciences et Belles-Lettres de Bruxelles* 18 (1845), pp. 14–54.

[69] Vladimír Švígler. "Bistable lattice equations: Symmetry groups of periodic stationary solutions". In: *Under review* (2020).

[70] Stephen Wolfram. *A New Kind of Science*. Wolfram Media Inc., 2002. 1197 pp.

[71] Alden H. Wright. "Finding all solutions to a system of polynomial equations". In: *Mathematics of Computation* 44.169 (1985), pp. 125–125.

[72] Bertram Zinner. "Existence of traveling wavefront solutions for the discrete Nagumo equation". In: *Journal of Differential Equations* 96.1 (1992), pp. 1–27.

Appendix A

Author's Publications

- Stehlík, P., Švígler, V., Volek, J., *Bifurcations in Nagumo equations on graphs and Fiedler vectors*, submitted
- Švígler, V., *Periodic stationary solutions of the Nagumo lattice differential equation: existence regions and their number*, Electronic Journal of Qualitative Theory of Differential Equations, No. 23, 2021.
- Hupkes, H. J., Morelli, L., Stehlík, P., Švígler, V., *Counting and ordering periodic stationary solutions of lattice Nagumo equations*, Applied Mathematics Letters, Volume 98, December 2019.
- Hupkes, H. J., Morelli, L., Stehlík, P., Švígler, V., *Multichromatic travelling waves for lattice Nagumo equations*, Applied Mathematics and Computation, Volume 361, November 2019.
- Pospíšil, J., Švígler, V., *Isogeometric analysis in option pricing*, International Journal of Computer Mathematics, published online 16th July, 2018.
- Epperlein, J., Švígler, V., *On arbitrarily long periodic orbits of evolutionary games on graphs*, Discrete and Continuous Dynamical Systems Series B, Volume 25, Number 5, July 2018. (included)
- Epperlein, J., Siegmund, S., Stehlík, P., Švígler, V., *Coexistence Equilibria of Evolutionary Games on Graphs Under Deterministic Imitation Dynamics*, Discrete and Continuous Dynamical Systems Series B, Volume 21, Number 3, May 2016. (included, published before the start of the doctoral study)
- Švígler, V., *Qualitative Study of Problems for Elliptic (Possibly Also Parabolic) Equations with Measure Data – Solvability, Bifurcation, Approximation of Solutions*, Pilsen: Faculty of Applied Sciences, University of West Bohemia, 2016. Rigorous thesis (supervisor Petr Girg, in English).
- Švígler, V., *Qualitative Study of Problems for Elliptic (Possibly Also Parabolic) Equations with Measure Data – Solvability, Bifurcation, Approximation of Solutions*, Pilsen: Faculty of Applied Sciences, University of West Bohemia, 2016. Diploma thesis (supervisor Petr Girg, in English).
- Švígler, V., *Mathematical Models of Evolution of Cooperation*, Pilsen: Faculty of Applied Sciences, University of West Bohemia, 2013. Bachelor's thesis (supervisor Petr Stehlík, in English).

Publications included in the appendices are typed in black.

Appendix B

Paper: Coexistence equilibria of evolutionary games on graphs under deterministic imitation dynamics

DISCRETE AND CONTINUOUS
DYNAMICAL SYSTEMS SERIES B
Volume **21**, Number **3**, May **2016**

doi:10.3934/dcdsb.2016.21.803

pp. **803–813**

COEXISTENCE EQUILIBRIA OF EVOLUTIONARY GAMES ON GRAPHS UNDER DETERMINISTIC IMITATION DYNAMICS

Jeremias Epperlein and Stefan Siegmund*

Center for Dynamics & Institute for Analysis
Dept. of Mathematics
Technische Universität Dresden, 01062
Dresden, Germany

Petr Stehlík and Vladimír Švígler

Dept. of Mathematics and NTIS
Faculty of Applied Sciences
University of West Bohemia
Univerzitni 8, 30614 Pilsen
Pilsen, Czech Republic

(Communicated by Peter E. Kloeden)

Abstract. Cooperative behaviour is often accompanied by the incentives to defect, i.e., to reap the benefits of others' efforts without own contribution. We provide evidence that cooperation and defection can coexist under very broad conditions in the framework of evolutionary games on graphs under deterministic imitation dynamics. Namely, we show that for all graphs there exist coexistence equilibria for certain game-theoretical parameters. Similarly, for all relevant game-theoretical parameters there exists a graph yielding coexistence equilibria. Our proofs are constructive and robust with respect to various utility functions which can be considered. Finally, we briefly discuss bounds for the number of coexistence equilibria.

1. **Introduction.** Cooperative behaviour in complex systems and natural networks is an exciting phenomenon occurring in groups of cells, animals [4, 6, 11] and, most importantly, human societies [1], social organizations and related networks [10]. Increased levels of cooperation can lead to advanced organizational structures. It has been suggested that cooperation is the third fundamental driving force of evolution besides mutation and natural selection [12]. Naturally, in most cases, cooperative actions are accompanied by the presence of defective ones (i.e., free-riding behaviour in which individuals collect the benefits of cooperation of others without contributing themselves) and both coexist in various forms [7, 9]. The goal of this paper is to formally show that in a simple framework of evolutionary games on graphs one can easily observe omnipresence of configurations in which cooperation and defection coexist.

In standard evolutionary game theory [8, 9], infinite homogeneous populations are considered and cooperation and defection coexist in the case of Stag hunt and

2010 *Mathematics Subject Classification.* 05C90, 37N25, 37N40, 91A22.

Key words and phrases. Evolutionary games on graphs, game theory, coexistence, equilibrium, cooperation.

* Corresponding author.

Hawk and dove games (whereby the coexistence equilibrium is unstable in the former and stable in the latter case). In recent years, numerous studies of finite and heterogenous populations (modelled by evolutionary games on graphs) revealed that the introduction of spatial structure could extend the areas of coexistence of cooperation and defection to other social-dilemma games, especially prisoner's dilemma [5, 7, 13, 14, 15, 16]. We contribute to this line of research and provide constructive proofs showing that, under deterministic imitation dynamics, for every social dilemma parameter cooperation and defection can coexist. Similarly, we show that for each graph/network there exist game-theoretical parameters such that cooperation and defection can coexist (we find these parameters in SH and FC parameter regions). Finally, in order to quantify the ubiquity of the states in which cooperation and defection coexist, we construct a specific class of graphs such that the number of coexistence equilibria grows exponentially with the number of vertices of underlying graphs.

The paper is organized as follows. Firstly, in Section 2 we introduce our formal model of an evolutionary game on a graph as well as the concept of coexistence equilibria. Next, in Section 3, we study the stationary boundaries of clusters of cooperators and defectors. Based on this knowledge, we are able to show in Section 4 that coexistence equilibria (or fixed points) exist for all social-dilemma game parameters as well as for all graphs. Finally, we estimate the possible number of coexistence equilibria on graphs in Section 5. In Section 6 we provide a robustness analysis for our constructions to show that they could be used also if another utility function is considered. We conclude with final remarks and open problems in Section 7.

2. Evolutionary games on graphs.

We consider undirected graphs whose vertices represent players and the edges/links represent the interaction between the players. Each player can either cooperate C or defect D, the set of possible states for each vertex is thus $S = \{D, C\} = \{0, 1\}$. We use the following notation for neighbourhoods on graphs. $N_1(i)$ denotes all vertices with distance 1 from vertex i and $N_{\leq 1}(i)$ includes all vertices whose distance is at most one (similarly $N_2(i)$ denotes all vertices with distance 2 etc.).

In each time step each vertex (player) determines its utility u from interactions with its neighbours. This utility is given by the underlying game-theoretical parameters:

	C	D
C	a	b
D	c	d

Based on the values of its utility and the utilities of its neighbours it then chooses its next state (following a dynamical rule φ).

Putting those ideas together, we can formulate formally an evolutionary game on a graph as a dynamical system in the following way (see [5] for more details):

Definition 2.1. An *evolutionary game on a graph* is a quintuple $(G, p, u, \mathcal{T}, \varphi)$, where

(a) $G = (V, E)$ is a connected graph,
(b) $p = (a, b, c, d)$ are game-theoretical parameters,
(c) $u : S^V \to \mathbb{R}^V$ is a utility function,
(d) $\mathcal{T} : \mathbb{N}_0 \to 2^V$ is an update order,
(e) $\varphi : (\mathbb{N}_0)^2_{\geq} \times S^V \to S^V$ is a (generally nonautonomous) dynamical system.

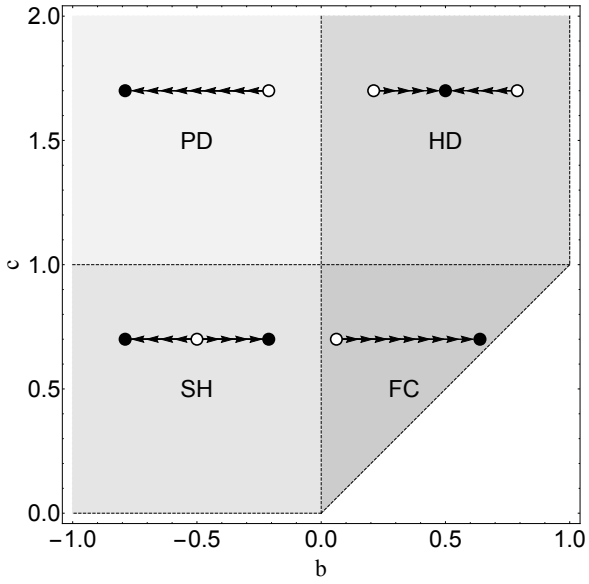

FIGURE 1. Game-theoretical parameters b, d and underlying social-dillemas (for $a = 1$, $d = 0$). Stability diagrams show the standard replicator dynamics on the interval $[0, 1]$ for spatially homogenenous and well-mixed populations. Coexistence equilibria exist only in Stag-hunt (unstable, white) and Hawk and dove (stable, black).

Remark 1. (a) We assume that the game-theoretical parameters $p = (a, b, c, d)$ satisfy $\min\{a, c\} > \max\{b, d\}$, i.e. we consider the so-called social-dilemmas which include Prisoner's dilemma (PD, $c > a > d > b$), Stag hunt (SH, $a > c > d > b$), Hawk and dove (HD, $c > a > b > d$) and Full cooperation (FC, $a > c > b > d$), see Figure 1. Without loss of generality one could assume that $a = 1$ and $d = 0$, see [5, Remark 9] for details.

(b) There are two most common choices of utility functions, either the *aggregate utility*

$$\begin{aligned} u_i^A(x) =& a \sum_{j\in N_1(i)} x_i x_j + b \sum_{j\in N_1(i)} x_i(1-x_j) + c \sum_{j\in N_1(i)} (1-x_i)x_j \\ &+ d \sum_{j\in N_1(i)} (1-x_i)(1-x_j), \end{aligned} \tag{1}$$

for $x \in S^V$ or the *mean utility*

$$u_i^M(x) = \frac{1}{|N_1(i)|} u_i^A(x). \tag{2}$$

In the case of regular graphs, the dynamics is the same, but it differs for irregular graphs, see [5].

(c) Two major examples of update orders (for others see [5, Section 5]) are *synchronous* ($\mathcal{T}(t) = V$ for each $t \in \mathbb{N}_0$), and *sequential* (vertices can be ordered

so that $\mathcal{T}(t) = \{(t+1)(\mathrm{mod}\, n)\}$). However, in this paper we deal with fixed points and our results apply to any update order.

(d) In this paper we use the (deterministic) imitation dynamics φ^{ID}, in which a vertex follows the strategy in its 1-neighbourhood which currently yields the highest utility. For other dynamics (birth-death, death-birth), see [5, Remark 4].

Mathematically, we define φ^{ID} via its components $\varphi_i^{ID} := \mathrm{proj}_i \circ \varphi : (\mathbb{N}_0)^2_{\geq} \times S^V \to S$ by

$$\varphi_i^{ID}(t+1,t,x) = \begin{cases} x_{\max} & \text{if } i \in \mathcal{T}(t), |A_i(x)| = 1 \text{ and } A_i(x) = \{x_{\max}\}, \\ x_i & \text{otherwise,} \end{cases} \tag{3}$$

where $A_i(x)$ is the set of strategies in the neighbourhood of x which yield the highest utility and is given by

$$A_i(x) = \{x_k : k \in \mathrm{argmax}\,\{u_j(x) : j \in N_{\leq 1}(i)\}\}. \tag{4}$$

The cardinality of $A_i(x)$ is used to ensure that all vertices with the highest utility have the same state. If that is not the case, the vertex preserves its current state (in order to keep the dynamics deterministic).

In this paper we study states in which cooperation and defection coexist and which remain unchanged by the dynamics φ.

Definition 2.2. We say that a state $x \in S^V$ is a *coexistence equilibrium* (coexistence fixed point) of the evolutionary game on a graph $(G, p, u, \mathcal{T}, \varphi)$ if

(a) it is a fixed point, i.e., $\varphi(t+1,t,x) = x$ for all $t \in \mathbb{N}_0$,
(b) it is a coexistence state, i.e., $0 < \sum_{i \in V} x_i < |V|$.

The following observation enables us to easily consider all update orders $\mathcal{T}$ at once.

Lemma 2.3. *Let $\mathcal{T} : \mathbb{N}_0 \to 2^V$ be the synchronous update order, i.e., $\mathcal{T}(t) = V$ for all $t \in \mathbb{N}_0$. If a state $x \in S^V$ is a coexistence equilibrium of the evolutionary game on a graph $(G, p, u, \mathcal{T}, \varphi)$ then it is a coexistence equilibrium of any evolutionary game $(G, p, u, \tilde{\mathcal{T}}, \varphi)$, where $\tilde{\mathcal{T}}$ is an arbitrary update order.*

Proof. Indeed, if $\varphi(t+1,t,x) = x$ in the synchronous case, all vertices $i \in V = \mathcal{T}(t)$ preserve their strategy x_i. Thus, if $\tilde{\mathcal{T}}(t) \subset V$ (only a subset of vertices is being updated) we have $\varphi(t+1,t,x) = x$ as well. □

Remark 2. (i) Consequently, we consider the synchronous update order throughout the paper and shorten the nonautonomous notation $\varphi(t+1,t,x)$ and write autonomously $\varphi(x)$ instead. However, note that the dynamical properties like the stability of fixed points (which we do not study in this paper) need not be preserved when we move from the synchronous (autonomous) to the general (nonautonomous) update order, see examples in [5].

(ii) Following the idea of the proof, we could replace synchronous update order by any fair update order in Lemma 2.3. An update order $\mathcal{T} : \mathbb{N}_0 \to 2^V$ is fair if for each vertex $v \in V$ and each time $t_0 \in \mathbb{N}_0$ there exists $t > t_0$ such that $v \in \mathcal{T}(t)$ (i.e., v is updated at time t). See [5, Definition 15] for more details.

3. **Cluster boundaries.** In a deterministic imitation dynamics φ^{ID} which we introduced above, the vertices which only have neighbours with the same state never change their strategy. Consequently, we introduce clusters of cooperators and defectors and study their boundaries on which the change of strategies could occur, see Figure 2 for the illustration and note that the importance of clusters has been already pointed out [13]. For a given state $x \in S^V$ we introduce the sets of inner cooperators (abbreviated by IC, cooperators with only cooperative neighbours) and inner defectors (ID, defectors with only defective neighbours)

$$V_{IC}(x) := \{i \in V : x_i = 1, \text{ and } x_j = 1 \text{ for all } j \in N_1(i)\},$$
$$V_{ID}(x) := \{i \in V : x_i = 0, \text{ and } x_j = 0 \text{ for all } j \in N_1(i)\}.$$

In contrast, if a cooperator has at least one defective neighbour, we call it a boundary cooperator (BC). Similarly, boundary defectors (BD) have at least one cooperative neighbour. For a given state $x \in S^V$ we define the set of boundary cooperators by

$$V_{BC}(x) := \{i \in V : x_i = 1, \text{ and there exists } j \in N_1(i) \text{ with } x_j = 0\},$$

and the set of boundary defectors by

$$V_{BD}(x) := \{i \in V : x_i = 0, \text{ and there exists } j \in N_1(i) \text{ with } x_j = 1\}.$$

Obviously, for all $x \in S^V$ we have $V = V_{IC}(x) \cup V_{BC}(x) \cup V_{ID}(x) \cup V_{BD}(x)$.

This definition of cluster boundaries enables us to prove the following simple sufficient condition for a state x to be a coexistence equilibrium. This statement is the cornerstone of our later constructions.

Lemma 3.1. *Let $(G, p, u, \mathcal{T}, \varphi^{ID})$ be an evolutionary game on a graph and let $x \in S^V$ be a coexistence state. If for each $i \in V_{BD}(x)$ and each $j \in V_{BC}(x) \cap N_1(i)$ there exists $v \in V_{IC}(x) \cap N_1(j)$ such that*

$$u_v > u_i > u_j, \tag{5}$$

then x is a coexistence equilibrium of $(G, p, u, \mathcal{T}, \varphi^{ID})$.

Proof. We need to prove that neither boundary cooperators nor boundary defectors change states. Indeed, the fact that for all $i \in V_{BD}(x)$ and each $j \in V_{BC}(x) \cap N_1(i)$ we have $u_i > u_j$ implies that (see (3)-(4))

$$A_i(x) = \{0\} \text{ and consequently } \varphi_i^{ID}(x) = 0 \ (= x_i).$$

Similarly, each $j \in V_{BC}(x)$ has a cooperative neighbour $v \in V_{IC}(x) \cap N_1(j)$ such that for all $i \in V_{BD}(x) \cap N_1(j)$ inequalities (5) hold, which implies that

$$A_j(x) = \{1\} \text{ and consequently } \varphi_j^{ID}(x) = 1 \ (= x_j).$$

□

Remark 3. The inequalities (5) are not necessary (only sufficient) for x to be a fixed point. For example, the boundary defector i could have a cooperating neighbour $j \in V_{BC}(x)$ with a higher utility as long as it has a defective neighbour $k \in V_{BD}(x)$ such that

$$u_k > u_j > u_i.$$

4. **Construction of coexistence equilibria.** First, we show that for any given game-theoretical parameters $p = (a, b, c, d)$ there exists a graph such that the evolutionary game has a coexistence equilibrium.

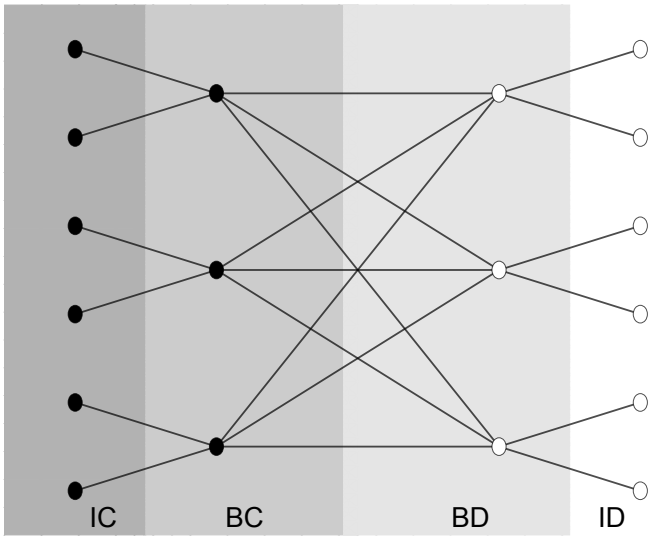

FIGURE 2. Construction of a graph with a coexistence equilibrium for any given parameters, see Theorem 4.1. Black vertices represent cooperators, white vertices defect.

Theorem 4.1. *For each $p = (a, b, c, d)$ and any update order $\mathcal{T}$ there exists a connected graph G such that the evolutionary game on a graph $(G, p, u^M, \mathcal{T}, \varphi^{ID})$ has a coexistence equilibrium.*

Proof. We construct a graph G and a state configuration $x \in S^V$ of the coexistence equilibrium at once. We have four vertex types (see Figure 2). In our construction, inner cooperators (IC) and inner defectors (ID) are always vertices of degree 1 (i.e., leaf vertices). On the other hand, m boundary cooperators (BC) and m boundary defectors (BD) form a complete bipartite graph $K_{m,m}$ so that each boundary cooperator is connected to all m boundary defectors and vice versa. Moreover, each boundary defector has exactly ℓ neighbouring inner defectors and each boundary cooperator has exactly n neighbouring inner cooperators (see Figure 2 for illustration of this construction). For given parameters $p = (a, b, c, d)$ the respective utilities are

$$\begin{aligned} u^M_{\mathrm{IC}} &= a, \\ u^M_{\mathrm{BC}} &= \frac{na + mb}{n + m}, \\ u^M_{\mathrm{BD}} &= \frac{\ell d + mc}{\ell + m}, \\ u^M_{\mathrm{ID}} &= d. \end{aligned}$$

The inequalities (5) hold if

$$a > \frac{\ell d + mc}{\ell + m} > \frac{na + mb}{n + m}. \tag{6}$$

Since $a > b$ we have that $a > \frac{na+mb}{n+m}$ for all $m > 0$. Moreover, the fact that $a > d$ and $b < c$ imply that we can find ℓ and m such that (6) hold. □

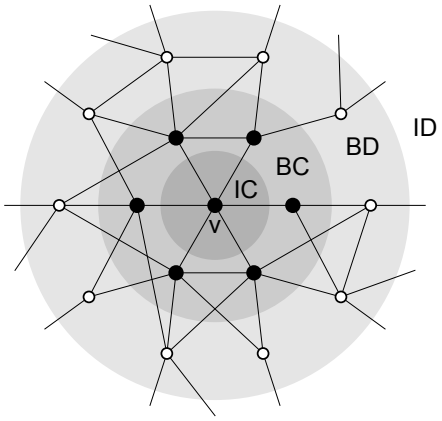

FIGURE 3. Construction of a coexistence equilibrium on an arbitrary graph, see Theorem 4.2.

So far, we showed that for any $p = (a, b, c, d)$ there exists a graph such that a coexistence equilibrium exists. Next, we prove that for any given graph we can find a suitable parameter vector such that the evolutionary game on this graph yields a coexistence equilibrium.

Theorem 4.2. *For each connected graph G and any update order $\mathcal{T}$ there exists a parameter vector $p = (a, b, c, d)$ such that the evolutionary game on a graph $(G, p, u^M, \mathcal{T}, \varphi^{ID})$ has a coexistence equilibrium.*

Proof. Firstly, we construct a coexistence equilibrium for noncomplete graphs, then for complete graphs.

1. If the graph is not complete, we can pick any vertex v which is not connected to all the other vertices. We define the states of vertices $x \in S^V$ by

$$x_i = \begin{cases} 1 & i \in N_{\leq 1}(v), \\ 0 & i \notin N_{\leq 1}(v), \end{cases}$$

i.e., we define a cluster of cooperators (vertices which are at most at distance one from v) and a set of defectors (vertices whose distance from v is at least 2, this set is not necessarily a connected subgraph of G). In other words, we have (see Figure 3):

$$\begin{aligned} V_{IC}(x) &:= \{v\}, \\ V_{BC}(x) &:= \{j \in V : j \in N_1(v)\}, \\ V_{BD}(x) &:= \{i \in V : i \in N_2(v)\}. \end{aligned}$$

If we denote by $k_{\max}$ the maximal degree of the graph G, the utilities of the relevant vertices satisfy

$$\begin{aligned} u_v^M &= a, \\ u_j^M &\leq \frac{(k_{\max} - 1)a + b}{k_{\max}}, \\ u_i^M &\leq c, \end{aligned}$$

$$u_i^M \geq \frac{c + (k_{\max} - 1)d}{k_{\max}},$$

for all $j \in V_{BC}(x)$ and $i \in V_{BD}(x)$.

Consequently, the former inequality in (5) holds if we choose

$$a > c,$$

and the latter if we choose

$$c > (k_{\max} - 1)(a - d) + b.$$

2. If the graph is complete, i.e. $G = K_n$ and we pick arbitrary m vertices as cooperators and the remaining $n - m$ as defectors, we have the following utilities for cooperators and defectors (note that $V_{ID}(x) = V_{IC}(x) = \emptyset$ in this case)

$$u_C^M = (m-1)a + (n-m)b,$$
$$u_D^M = mc + (n-m-1)d.$$

If $u_C = u_D$, we have that $\varphi_i(x) = x_i$. This situation occurs if

$$(m-1)a + (n-m)b = mc + (n-m-1)d.$$

□

Remark 4. Note that, with the exception of the complete graph, the coexistence equilibria are stable with respect to small perturbations of parameters (since the construction is based on inequalities rather than equalities as in the case of complete graphs).

5. **Number of coexistence equilibria.** In this section, we construct a special narrow class of graphs which shows that there can be an exponential number of coexistence equilibria.

Theorem 5.1. *For each $n \geq 6$, there exists a connected graph G with n vertices such that the evolutionary game on a graph $(G, p, u^M, \mathcal{T}, \varphi^{ID})$ has at least $2^{\lfloor n/3 \rfloor}$ coexistence equilibria for some parameter vector $p = (a, b, c, d)$ and any update order $\mathcal{T}$.*

Proof. Consider the undirected cycle $G = C_n$ of length n with vertices numbered $0, \ldots, n-1$. Let X be the set of states x on C_n such that each cluster of defectors and cooperators has at least size 3, that is

$$X = \{x \in \{0,1\}^n \mid W(x) \cap \{(1,0,1), (1,0,0,1), (0,1,0), (0,1,1,0)\} = \emptyset\}$$

where we write

$$W(x) = \{(x_{j \bmod n}, x_{j+1 \bmod n}, \ldots, x_{j+k-1 \bmod n}) \mid j, k \in \{0, \ldots, n-1\}\}.$$

We calculate the following mean utilities

$$u_j^M = \frac{a+b}{2} \qquad \text{for all } j \in V_{BC}(x),$$
$$u_i^M = \frac{c+d}{2} \qquad \text{for all } i \in V_{BD}(x).$$

Thus for $a > \frac{c+d}{2} > \frac{a+b}{2}$ the inequalities (5) hold and we get a coexistence equilibrium. It remains to estimate the cardinality of X. Since for $n = 3k$ we have $\{(1,1,1),(0,0,0)\}^k \subseteq X$, $|X| > 2^{\frac{n}{3}}$ holds. Consequently, for general n, we have $|X| > 2^{\lfloor n/3 \rfloor}$. □

Remark 5. The parameter range that we used in the proof is a subset of SH, HD and PD. We can get a parameter range intersecting all 4 scenarios by considering the lexicographic product $L = C_n[G]$ where G is a k regular graph with ℓ vertices (i.e., $k < \ell$). Thus L has vertex set $\{1, \dots, n\} \times V(G)$ and $((i_1, j_1), (i_2, j_2)) \in E(L)$ if $(i_1, i_2) \in E(C_n)$ or $i_1 = i_2, (j_1, j_2) \in E(G)$. Then L is a $k + 2\ell$ regular graph. Each state on x can be mapped to a state $f(x)$ with $f(x)_{(i,j)} := x_i$. Define $T = \{x \in \{0,1\}^n \mid W(x) \cap \{(0,0),(0,1,0),(0,1,1,0)\} = \emptyset\}$. Then for a state y in $f(T)$ we have

$$u_j^M = \frac{(k+\ell)a + \ell b}{k+2\ell} \qquad \text{for all } j \in V_{BC}(x),$$
$$u_i^M = \frac{2\ell c + kd}{k+2\ell} \qquad \text{for all } i \in V_{BD}(x).$$

Hence y is a fixed point, if

$$(k+2\ell)a > 2\ell c + kd > (k+\ell)a + \ell b. \tag{7}$$

For $a = 1$ and $d = 0$ this is $1 + \frac{k}{2\ell} > c > \frac{k+\ell}{2\ell} + \frac{b}{2}$. Again for fixed k and ℓ the number of elements in $f(T)$ is exponential in n, but for every admissible (a, b, c, d) with $\frac{1+b}{2} < c < 3/2$ we can find k and ℓ such that the inequalities in (7) are fulfilled.

Remark 6. Considering equivalence classes of states under automorphisms of the graph can heavily reduce the number of states. In this sense, it is worth noting that our constructions which yield the exponential number of coexistence equilibria are based on symmetric graphs. Notice however that the number of coexistence equilibria which differ under automorphisms in our example is at least $\frac{2^{\lfloor n/3 \rfloor}}{2n}$ (the automorphism group of the cycle has size $2n$), so we still get an exponential lower bound. Also some of these equilibria cannot be attained from other states (the influence of graph automorphisms and the problem of attainabilty has been studied in the case of stochastic evolutionary dynamics on graphs in [2, 3]).

6. **Aggregate utility function.** All above results can relatively simply be formulated for the aggregate utility function u^A given by (1). First, for any given parameters there exists a graph such that the evolutionary game has a coexistence equilibrium (counterpart of Theorem 4.1).

Theorem 6.1. *For each $p = (a, b, c, d)$ and any update order $\mathcal{T}$ there exists a connected graph G such that the evolutionary game on a graph $(G, p, u^A, \mathcal{T}, \varphi^{ID})$ has a coexistence equilibrium.*

Proof. We only have to modify the construction in the proof of Theorem 4.1 slightly by adding a set of k cooperators to every inner cooperator (see Figure 2). In that case, the required inequalities (6) turn into

$$(k+1)a > \ell d + mc > na + mb.$$

The former inequality will always be satisfied if k is large enough (i.e., if we add sufficiently many cooperating neighbours to inner cooperators in Figure 2. The latter inequality will be satisfied if m is large enough (since $b < c$), i.e., if each boundary cooperator will have enough boundary cooperators. □

Also in the case of the aggregate utility function, for each graph we can find admissible parameters for which the evolutionary game on a graph has a coexistence equilibrium.

Theorem 6.2. *For each connected graph G and any update order $\mathcal{T}$ there exists a parameter vector $p = (a, b, c, d)$ such that the evolutionary game on a graph $(G, p, u^A, \mathcal{T}, \varphi^{ID})$ has a coexistence equilibrium.*

Proof. In this case, the construction is the same as in the proof of Theorem 4.2, we only assume that $\max\{b, d\} \leq 0$ and $\min\{a, c\} > 0$. Considering the worst case scenarios we observe that a vertex $j \in V_{BC}(x)$ can be connected to every vertex from the cooperating cluster and must be connected to at least one boundary defector. A vertex $i \in V_{BD}(x)$ can be connected to all vertices from the cooperating cluster except the vertex v (yielding the highest utility). On the other hand, the vertex i could be connected to exactly one cooperator and to every other defecting vertex in the graph (yielding the lowest utility). Consequently,

$$\begin{aligned} u_v^A &\geq a, \\ u_j^A &\leq (k_{\max} - 1)a + b, \\ u_i^A &\leq k_{\max} c, \\ u_i^A &\geq c + (k_{\max} - 1)d. \end{aligned}$$

These estimates imply that (5) hold if $a > k_{\max} c$ and $c + (k_{\max} - 1)d > (k_{\max} - 1)a + b$. Thus, if we set $a > k_{\max} c$ and $b \ll d$ both inequalities are satisfied. □

Finally, in Theorem 5.1 we showed that there is an exponential growth of the number of coexistence equilibria with respect to the number of vertices of the underlying graph. Since the construction in the proof was based on 2-regular graphs (on which the mean and aggregate utility functions u^M and u^A satisfy $u^A = 2u^M$), we can straightforwardly claim the same statement for the aggregate utility function.

Theorem 6.3. *For each $n \geq 6$, there exists a connected graph G with n vertices such that the evolutionary game on a graph $(G, p, u^A, \mathcal{T}, \varphi^{ID})$ has at least $2^{\lfloor n/3 \rfloor}$ coexistence equilibria for some parameter vector $p = (a, b, c, d)$ and any update order $\mathcal{T}$.*

7. **Final remarks.** Evolutionary games on graphs have been studied in very complex settings under more general assumptions (large random nonconstant graphs, random updating, etc.). In this paper, we showed analytically that even in the deterministic settings the theory offers rich behaviour and yields coexistence equilibria for all graphs and for all game theoretical parameters. Consequently, we answered problems (A) and (D) which we posed in [5, Section 9]. Besides the other questions listed there we mention other issues related to coexistence equilibria worth investigation.

(A) **Cluster dynamics:** Our results are based on a simple observation, Lemma 3.1. This result could indicate that deeper analysis of dynamics on cluster boundaries could provide finer insight into the behaviour of evolutionary games on graphs. Specifically, since Lemma 3.1 is a sufficient condition for x being a coexistence equilibrium can we, e.g., obtain a helpful necessary condition?

(B) **Stability and attractivity:** A natural and surprisingly nontrivial question concerns the stability of equilibria of evolutionary games on graphs. In [5, Definition 7] we defined stability via perturbation of a single vertex in a state x and provided simple results for complete and k-regular graphs. However, it seems that this concept is very difficult to study on general graphs. Is there a sophisticated way to analyze stability of equilibria in this sense? Alternatively,

is there a better concept of stability/attractivity for evolutionary games on graphs?

(C) **Nonexistence:** Describe conditions under which there is no coexistence equilibrium for an evolutionary game on a graph.

(D) **Periodic coexistence:** In this paper we studied coexistence equilibria, i.e., fixed points. Note that we could ask similar questions related to coexistence cycles, in which we could observe periodic dynamics. Most importantly, given game-theoretical parameters (a, b, c, d) (see Figure 2), can we find a graph G such that the evolutionary game on G yields a cycle (or even a cycle of given length)?

Acknowledgments. The first and second author were partly supported by the German Research Foundation (DFG) through the Cluster of Excellence (EXC 1056), Center for Advancing Electronics Dresden (cfaed). The third author acknowledges the support by the Czech Science Foundation 15-00735S. We thank the anonymous referee for valuable comments.

REFERENCES

[1] R. Albert and A.-L. Barabási, Statistical mechanics of complex networks, *Rev. Mod. Phys.*, **74** (2002), 47–97.

[2] M. Broom and J. Rychtář, An analysis of the fixation probability of a mutant on special classes of non-directed graphs, *Proc. Royal. Soc., Ser. A*, **464** (2008), 2609–2627.

[3] M. Broom, C. Hadjichrysanthou, J. Rychtář and B. T. Stadler, Two results on evolutionary processes on general non-directed graphs, *Proc. Royal. Soc., Ser. A*, **466** (2010), 2795–2798.

[4] T. Clutton-Brock, Cooperation between non-kin in animal societies, *Nature*, **462** (2009), 51–57.

[5] J. Epperlein, S. Siegmund and P. Stehlík, Evolutionary games on graphs and discrete dynamical systems, *J. Difference Eq. Appl.*, **21** (2015), 72–95.

[6] W. D. Hamilton, The genetical evolution of social behaviour, *J. Theor. Biol.*, **7** (1964), 1–16.

[7] C. Hauert and M. Doebeli, Spatial structure often inhibits the evolution of cooperation in the snowdrift game, *Nature*, **428** (2004), 643–646.

[8] J. Hofbauer and K. Sigmund, Evolutionary game dynamics, *Bull. Amer. Math. Soc.*, **40** (2003), 479–519.

[9] J. Hofbauer and K. Sigmund, *The Theory of Evolution and Dynamical Systems*, Cambridge University Press, 1988.

[10] J. Libich and P. Stehlík, Monetary policy facing fiscal indiscipline under generalized timing of actions, *Journal of Institutional and Theoretical Economics*, **168** (2012), 393–431.

[11] J. Maynard Smith, The theory of games and the evolution of animal conflicts, *Journal of Theoretical Biology*, **47** (1974), 209–221.

[12] M. A. Nowak, Five rules for the evolution of cooperation, *Science*, **314** (2006), 1560–1563.

[13] M. A. Nowak and R. M. May, Evolutionary games and spatial chaos, *Nature*, **359** (1992), 826–829.

[14] H. Ohtsuki and M. A. Nowak, Evolutionary games on cycles, *Proc. R. Soc. B*, **273** (2006), 2249–2256.

[15] H. Ohtsuki and M. A. Nowak, Evolutionary stability on graphs, *Journal of Theoretical Biology*, **251** (2008), 698–707.

[16] G. Szabó and G. Fáth, Evolutionary games on graphs, *Phys. Rep.*, **446** (2007), 97–216.

Received July 2015; revised November 2015.

E-mail address: jeremias.epperlein@tu-dresden.de
E-mail address: stefan.siegmund@tu-dresden.de
E-mail address: pstehlik@kma.zcu.cz
E-mail address: sviglerv@kma.zcu.cz

Appendix C

Paper: On arbitrarily long periodic orbits of evolutionary games on graphs

DISCRETE AND CONTINUOUS
DYNAMICAL SYSTEMS SERIES B
Volume **23**, Number **5**, July **2018**

doi:10.3934/dcdsb.2018187

pp. **1895–1915**

ON ARBITRARILY LONG PERIODIC ORBITS OF EVOLUTIONARY GAMES ON GRAPHS

Jeremias Epperlein*

Center for Dynamics & Institute for Analysis
Dept. of Mathematics
Technische Universität Dresden, 01062
Dresden, Germany

Vladimír Švígler

Department of Mathematics and NTIS
Faculty of Applied Sciences
University of West Bohemia
Univerzitní 8, 30614
Pilsen, Czech Republic

Abstract. A periodic behavior is a well observed phenomena in biological and economical systems. We show that evolutionary games on graphs with imitation dynamics can display periodic behavior for an arbitrary choice of game theoretical parameters describing social-dilemma games. We construct graphs and corresponding initial conditions whose trajectories are periodic with an arbitrary minimal period length. We also examine a periodic behavior of evolutionary games on graphs with the underlying graph being an acyclic (tree) graph. Astonishingly, even this acyclic structure allows for arbitrary long periodic behavior.

1. **Introduction.** Evolutionary game theory on graphs in the spirit of Nowak and May [14] studies the evolution of social behavior in spatially structured populations. In our setting, each vertex of a graph is assigned a strategy. In every time step, each vertex plays a matrix game with its imminent neighbors. The resulting game utilities together with the update order (certain vertices can remain rigid) and the update function result in the change of strategy to the subsequent time step. Here, we focus on the case of synchronous update order and deterministic imitation dynamics - every vertex copies the strategy of the most successful neighbor including itself. From a biological point of view, it is natural to consider a stochastic update rule leading mathematically to a Markov chain. This is also the approach taken by most rigorous investigations of such systems, see for example [4] and [2]. Randomness can also be used to introduce mutations of the individuals into the model, see for example [2]. However, questions about the dynamical behavior of these models often become intractable because of the stochastic nature of the system. Different authors therefore also studied deterministic versions of the model, see for example

2010 *Mathematics Subject Classification.* Primary: 91A22, 05C57, 91A43; Secondary: 37N40.
Key words and phrases. Evolutionary games on graphs, game theory, periodic orbit, deterministic imitation dynamics, discrete dynamical systems.

* Corresponding author.

[1, 5, 10, 12, 14, 15]. The results regarding this deterministic version, however, are almost all obtained by simulations.

One of the factors influencing dynamics heavily are the parameters of the underlying matrix game. We consider a two strategy game (Cooperation, Defection) whose interpretation leads to a natural division of the parameter space into 4 scenarios Prisoner's dilemma, Stag hunt, Hawk and dove, Full cooperation. The equilibria of the replicator dynamics based on matrix games with such parameters are already well known, [9].

In [14] it was shown by simulations that even on lattices these dynamical systems can show very complicated behavior starting from a very simple initial condition, see also Chapter 9 in [13]. Nowak and May show for example that the systems can exhibit cascading behavior. Most of the time, such constructions work for very specific choices of parameters.

Our main questions is thus: Can arbitrarily long periodic behavior happen for all parameter choices? For example, the replicator dynamics with parameters of HD scenario tend to a stable mixed equilibrium but only pure equilibria are attractive for the other scenarios. The spatial structure of the game must be thus thoroughly examined. We will answer the question positively by explicitly constructing the graphs demonstrating the required behavior for each set of parameters.

In this paper, we focus on evolutionary games on a graph with periodic trajectories along which the strategy profiles (number of cooperators and defectors) change. Periodic behavior with no change in the strategy profiles was observed for example in [13] by Nowak and May in a structure they called a walker (spaceship in cellular automata terms). Moreover, such a structure is automorphism invariant in a certain sense; for each time step, there exists a graph automorphism which keeps the moving walker in one place. Such structures may be of interest for future research. We note, that our constructions introduce a periodic behavior of arbitrary length both in strategy vectors (distribution of strategies) and strategy profiles.

Evolutionary games on graphs also form a very interesting class of cellular automata. Cellular automata on a lattice can take into account the relative spatial position of a neighbor. The dependence on the neighbor on the left might differ from the dependence on the neighbor on the right. On an arbitrary graph this is only possible if the edges carry some kind of label. A cellular automaton in which the new state of a cell depends only on its own state and the number of neighboring cells in each state is called totalistic. Such cellular automata are naturally defined also on unlabeled graphs. While evolutionary games as considered here are not totalistic, they nevertheless are defined on unlabeled graphs in an obvious way. See [11] for a discussion of cellular automata on graphs.

The paper is organized as follows. We introduce basic notation and the dynamics of evolutionary games on a graph in Section 2. In Section 3, Theorem 3.1, answering the main question of this paper, is stated and proved. The proof is carried out for two separate cases depending on the parameter scenario. Periodic behavior of evolutionary games on a graph with the underlying graph being a tree is examined in Section 4. We conclude our results in Section 5.

2. **Preliminaries.**

We are considering undirected connected graphs $\mathcal{G}$ as the spatial structure of our game with the vertices V being players. The interactions between vertices are defined by a set of edges E (no edge means no direct interaction). The m-neighborhood of the vertex i (the set of all vertices having distance

to i exactly m) is denoted by $N_m(i)$. We also define

$$N_{\leq m}(v) := \bigcup_{n=1}^{m} N_n(v) \cup \{v\}.$$

The strategy set of the game is simply $S = \{\text{“Cooperate”}, \text{“Defect”}\} = \{C, D\} = \{1, 0\}$. The neighboring vertices play a matrix game where the resulting utilities are defined by the matrix

	C	D
C	a	b
D	c	d

and the utility function u. For example, if player A cooperates and player B defects, player A gets utility b and player B gets utility c. In each time step, a certain subset of players is allowed to change their strategy based on the update order $\mathcal{T}$. Finally, the strategy update is defined by a function φ. A general framework of evolutionary games on graphs was developed in [7]. An evolutionary game on a graph can be formally defined as follows.

Definition 2.1. An *evolutionary game on a graph* is a quintuple $(\mathcal{G}, \pi, u, \mathcal{T}, \varphi)$, where

(i) $\mathcal{G} = (V, E)$ is a connected graph,
(ii) $\pi = (a, b, c, d)$ are game-theoretical parameters,
(iii) $u : S^V \to \mathbb{R}^V$ is a utility function,
(iv) $\mathcal{T} : \mathbb{N}_0 \to 2^V$ is an update order,
(v) $\varphi : (\mathbb{N}_0)^2_{\geq} \times S^V \to S^V$ is a dynamical system.

The strategy vector (the state of the system) will be denoted $X = (x_1, \ldots, x_{|V|}) \in S^V$. For a strategy vector $X \in S^V$, the strategy of the vertex v is X_v. The utility of a player v is given by $u_v(X)$.

Our main focus lies in social dilemma games and we are thus interested in the game-theoretical parameters $\mathcal{P}$ describing such games. In particular, it is more advantageous if the opponent cooperates than if it defects for each player, i.e.

$$\min\{a, c\} > \max\{b, d\}\,.$$

This results into four possible scenarios: Prisoner's dilemma (PD): $c > a > d > b$, Stag hunt (SH): $a > c > d > b$, Hawk and dove (HD): $c > a > b > d$ and Full cooperation (FC): $a > c > b > d$. Demanding the inequalities to be strict only excludes sets of measure zero. This *generic payoff assumption* is common in examining game-theoretical models (see e.g. [3]). From now on, we consider the *mean utility function*

$$u_i(X) = \frac{1}{|N_1(i)|}\left(a \sum_{j \in N_1(i)} X_i X_j + b \sum_{j \in N_1(i)} X_i(1 - X_j) + \right.$$
$$\left. + c \sum_{j \in N_1(i)} (1 - X_i) X_j + d \sum_{j \in N_1(i)} (1 - X_i)(1 - X_j)\right)$$

which is an averaged sum of the outcomes of the matrix games played with direct neighbors. Without loss of generality, we can now assume $a = 1, d = 0$ and thus the parameter regions can be depicted in the plane (see Figure 1).

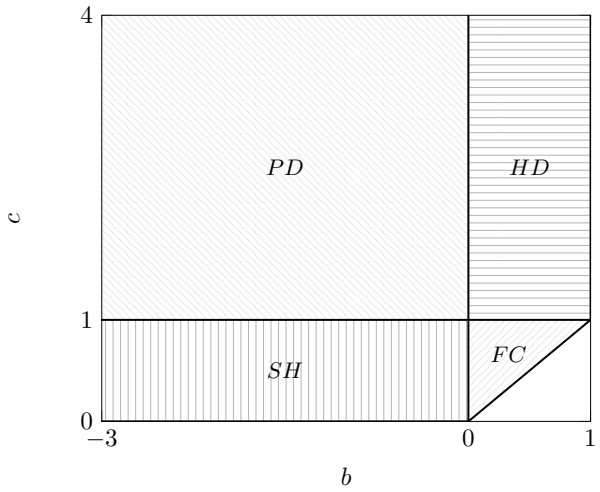

FIGURE 1. Regions of admissible parameters $\mathcal{P}$ with normalization $a = 1, d = 0$.

This simplification can be done thanks to the averaging property of the mean utility function (see [6, Remark 8.]). In Question 1, Theorem 3.1 and Theorem 4.1 we assume a synchronous update order only, i.e. $\mathcal{T}(t) = V$ for all $t \in \mathbb{N}_0$. In other words, all vertices are updated simultaneously at every time step. However, the definitions from Section 2 make sense for an arbitrary update order. Finally, the dynamical system φ follows the deterministic imitation dynamics; namely, each vertex adopts the strategy of its most successful neighbor (including itself). Formally,

$$\varphi_i(t+1, t, X) = \begin{cases} X_{\max} & i \in \mathcal{T}(t),\ |A_i(X)| = 1 \text{ and } A_i(X) = \{X_{\max}\}\ , \\ X_i & \text{otherwise}\,, \end{cases}$$

where

$$A_i(x) = \{X_k \,|\, k \in \operatorname{argmax}\{u_j(X) \,|\, j \in N_1(i) \cup \{i\}\}\}\ .$$

We refer to [6] for further discussion on the utility function, update order and the dynamics.

Considering a deterministic dynamical system, the natural interest lies in examining the existence and properties of *fixed points* – strategy vectors $X^* \in S^V$ for which $\varphi(t, 0, X^*) = X^*$ for $t \in \mathbb{N}_0$. This topic was studied in [7]. Another notion is the one of a *periodic trajectory*, a periodic behavior of a game on a graph.

Definition 2.2. Given an evolutionary game $\mathcal{E} = (\mathcal{G}, \pi, u, \mathcal{T}, \varphi)$ on a graph and an initial state X_0, the sequence of strategy vectors $\mathcal{X} = (X(0), X(1), \ldots) \in \left[S^V\right]^{\mathbb{N}_0}$ is called the *trajectory* of $\mathcal{E} = (\mathcal{G}, \pi, u, \mathcal{T}, \varphi)$ with initial state X_0 if for all $t \in \mathbb{N}_0$ we have

$$\begin{aligned} X(0) &= X_0\,, \\ X(t+1) &= \varphi(t+1, t, X(t)). \end{aligned}$$

The trajectory is called *periodic with period* $p \in \mathbb{N}$ if $X(t+p) = X(t)$ for $t \in \mathbb{N}_0$.

The previous definition admits an arbitrary choice of the update order. In general, two games $\mathcal{E}_1 = (\mathcal{G}, \pi, u, \mathcal{T}_1, \varphi)$, $\mathcal{E}_2 = (\mathcal{G}, \pi, u, \mathcal{T}_2, \varphi)$ with the same initial condition X_0 may not have the same trajectory.

Note that a vertex playing a certain strategy will keep its strategy if surrounded by vertices playing the same strategy. Thus, it is reasonable to define a cluster of cooperators and defectors and their inner and boundary vertices. The inner (IC) and boundary (BC) cooperators are defined by

$$V_{IC} = \{i \in V \mid X_i = 1 \text{ and } X_j = 1 \text{ for all } j \in N_1(i)\},$$
$$V_{BC} = \{i \in V \mid X_i = 1 \text{ and there exists } j \in N_1(i) \text{ with } X_j = 0\}.$$

Boundary (BD) and inner (ID) defectors are defined analogously.

The basic question we are answering in this paper can now be formulated using the notation introduced in this section:

Question 1. *Given admissible parameters $\pi = (a, b, c, d) \in \mathcal{P}$, a utility function u, an update order $\mathcal{T}$, dynamics φ and a number $p \in \mathbb{N}$, does there exist a connected graph $\mathcal{G}$ and an initial state X_0 such that $\mathcal{X}$ is a periodic trajectory of the evolutionary game $\mathcal{E} = (\mathcal{G}, \pi, u, \mathcal{T}, \varphi)$ on a graph with minimal period p?*

3. Existence of a periodic orbit of arbitrary length.

In the following, graphs and subgraphs are denoted by big calligraphic letters (e.g., $\mathcal{G}$), sets of vertices are denoted by capital letters (e.g., K) and single vertices are denoted by lower case letters (e.g., v).

Theorem 3.1. *Let $\pi = (a, b, c, d) \in \mathcal{P}$ be admissible parameters, u the mean utility function, $\mathcal{T}$ the synchronous update order, φ deterministic imitation dynamics and $p \in \mathbb{N}$. Then there exists a graph $\mathcal{G}$ and an initial state X_0 such that $\mathcal{X} = (X(0), X(1), \ldots)$ is a periodic trajectory of minimal length p of the evolutionary game $\mathcal{E} = (\mathcal{G}, \pi, u, \mathcal{T}, \varphi)$ on a graph with initial state X_0.*

Theorem 3.1 formally answers Question 1. The proof will be carried out for the cases $a > c$ (FC and SH scenario) and $c > a$ (HD and PD scenario) separately. We construct a connected graph, define an initial state and show, that the resulting trajectory is periodic with the required minimal period length p.

3.1. Proof of Theorem 3.1 for FC and SH scenarios.

3.1.1. *The graph and initial state.* The construction of our graph depends on p and three parameters $q, r, s \in \mathbb{N}$ which we will choose later. See Figure 2 for an illustration of the graph structure. Let $\mathcal{S}$ be the bipartite graph with classes S_1 and S_2 each having s vertices. Add a vertex $h_{\mathcal{S}}$ incident with all vertices in S_1 and a vertex $f_{\mathcal{S}}$ incident with exactly one vertex in S_2.

Now take $2p - 1$ copies of the complete graph with q vertices, denoted by $\mathcal{K}_{-(p-1)}, \ldots, \mathcal{K}_{p-1}$, and chain them together to form a ladder-like structure. Add one vertex g connected to all vertices in $\mathcal{K}_0$. Denote the vertices in $\mathcal{K}_n$ by $\{k_{n,\ell} \mid \ell = 1, \ldots, q\}$ for $n = -(p-1), \ldots, p-1$ such that $k_{n,\ell}$ and $k_{n+1,\ell}$ are connected by an edge for $n = -(p-1), \ldots, p-2$ and $\ell = 1, \ldots, q$. Add $q \cdot r$ many copies of $\mathcal{S}$ and denote them by $\mathcal{S}_{\ell,m}$ for $\ell = 1, \ldots, q$ and $m = 1, \ldots, r$. Connect $f_{\mathcal{S}_{\ell,m}}$ to all vertices in $\{k_{n,\ell} \mid n = -(p-1), \ldots, p-1\}$ for $m = 1, \ldots, r$ and $\ell = 1, \ldots, q$. We denote the graph thus obtained $\mathcal{G}$.

Set $H := \{h_{\mathcal{S}_{\ell,m}} \mid \ell = 1, \ldots, q,\ m = 1, \ldots, r\}$. Let I be the set of all neighbors of vertices in H, let J be the set of all neighbors of vertices in I which are not

already in H, and set $F := \{f_{\mathcal{S}_{\ell,m}} \mid \ell = 1,\dots,q,\ m = 1,\dots,r\}$. Finally set $K_n := \{k_{n,\ell} \mid \ell = 1,\dots,q\} \cup \{k_{-n,\ell} \mid \ell = 1,\dots,q\}$ for $n = 0,\dots,p-1$ and $K := K_0 \cup \dots \cup K_{p-1}$.

Let X_0 be the state in which all vertices in $H \cup I \cup K_0 \cup \{g\}$ are cooperating and all other vertices are defecting, that is,

$$\begin{aligned} (X_0)_v &:= 1, && v \in I \cup H \cup K_0 \cup \{g\}\,, \\ (X_0)_v &:= 0, && v \in F \cup J \cup (K_1 \cup \dots \cup K_{p-1})\,. \end{aligned}$$

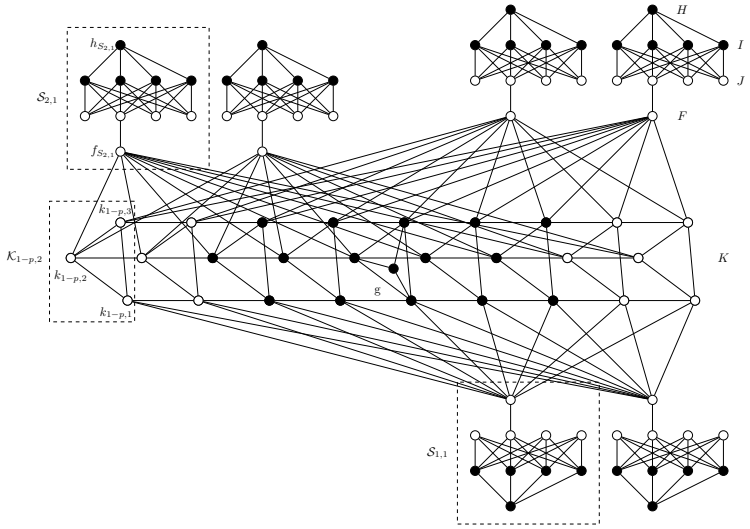

FIGURE 2. Example of the graph $\mathcal{G}$ with parameters $p = 5$, $q = 3$, $r = 2$ and $s = 4$. Cooperators are depicted by full circles.

3.1.2. *Dynamics.* Let $\mathcal{X} = (X(0), X(1), \dots)$ be the trajectory of the evolutionary game with parameters (a, b, c, d), synchronous update order, mean utility and imitation dynamics on the graph $\mathcal{G}$ constructed above with initial state X_0. Let $u_v(t) := u(X_v(t))$ be the utility of the vertex v at time t. We will show that for suitable parameters q, r, s the dynamics with initial value X_0 is the following. All vertices not in K do not change their strategy and cooperation spreads along the ladder for p time steps. After p time steps, we reach again the initial state X_0 since all vertices in $K \setminus K_0$ switch back to defection. More precisely, for $t = 0,\dots,p-1$ we have

$$\begin{aligned} X_v(t) &= X_v(0)\,, && v \in F \cup H \cup I \cup J \cup K_0 \cup \{g\}\,, \\ X_v(t) &= 1\,, && v \in K_0 \cup \dots \cup K_t\,, \\ X_v(t) &= 0\,, && v \in K_{t+1} \cup \dots \cup K_{p-1} \end{aligned}$$

and $X(p) = X(0)$. We first ensure that all vertices not in K do not change their strategy. The vertices in H have utility a, the highest achievable one, and therefore all vertices in $I \cup H$ always cooperate. By the same argument, the vertex g and its neighbors K_0 stay cooperators at all time steps. We want the vertices in J to stay

defectors by never imitating the strategy of their neighbors in I, hence we want

$$u_j(t) > u_i(t)\,, \qquad t = 0,\dots,p-1,\ i \in I,\ j \in J\,. \tag{1}$$

Every vertex in F should stay defecting. This is ensured if

$$u_j(t) > u_{k_n}(t)\,, \qquad t = 0,\dots,p-1,\ j \in J,\ n = 0,\dots t,\ k_n \in K_n\,. \tag{2}$$

We now want cooperation to spread along the ladder for $t = 0,\dots,p-2$. At time t, the vertices in K_{t+1} should copy the strategy from the vertices in K_t and all vertices in K_n with $n = 0,\dots,t$ should keep cooperating. Defecting vertices without cooperating neighbors always have a lower utility than defecting vertices with cooperating neighbors, hence the later never imitate the former. It is therefore sufficient to have

$$u_{k_n}(t) > u_f(t)\,, \qquad t = 0,\dots,p-2,\ n = 0,\dots,t,\ k_n \in K_n,\ f \in F\,, \tag{3}$$

$$u_{k_t}(t) > u_{k_{t+1}}(t)\,, \qquad t = 0,\dots,p-2,\ k_t \in K_t,\ k_{t+1} \in K_{t+1}\,. \tag{4}$$

In the time step from $p-1$ to p, we want the big reset to occur. The utility of the vertices in F should be greater than the utilities of all vertices in K, in other words,

$$u_f(p-1) > u_k(p-1)\,, \qquad f \in F,\ k \in K\,. \tag{5}$$

3.1.3. *Bounds for the utilities and the resulting inequalities.* We now give bounds for the utilities involved in the inequalities (1) to (5).

$$\begin{aligned}
u_j(t) &> \frac{sc+d}{s+1}\,, && t = 0,\dots,p-1,\ j \in J\,,\\
u_i(t) &= \frac{a+sb}{s+1}\,, && t = 0,\dots,p-1,\ i \in I\,,\\
u_f(t) &< \frac{(2p-3)c+3d}{2p}\,, && t = 0,\dots,p-2,\ f \in F\,,\\
u_f(p-1) &= \frac{(2p-1)c+d}{2p}\,, && f \in F\,,\\
u_{k_n}(t) &< \frac{(q+2)a+rb}{q+2+r}\,, && t = 0,\dots,p-1,\ n = 0,\dots,t,\ k_n \in K_n\,,\\
u_{k_n}(t) &> \frac{qa+(r+2)b}{q+2+r}\,, && t = 0,\dots,p-2,\ n = 0,\dots,t,\ k_n \in K_n\,,\\
u_{k_{t+1}}(t) &< \frac{c+(q+r-1)d}{q+r}\,, && t = 0,\dots,p-2,\ k_{t+1} \in K_{t+1}\,,\\
u_k(p-1) &< \frac{(q+2)a+rb}{q+r+2}\,, && k \in K\,.
\end{aligned}$$

A set of inequalities sufficient for (1) to (5) to hold is therefore given by

$$\frac{sc+d}{s+1} > \frac{a+sb}{s+1}\,, \tag{6}$$

$$\frac{sc+d}{s+1} > \frac{(q+2)a+rb}{q+r+2}\,, \tag{7}$$

$$\frac{qa+(r+2)b}{q+r+2} > \frac{(2p-3)c+3d}{2p}\,, \tag{8}$$

$$\frac{qa+(r+2)b}{q+r+2} > \frac{c+(q+r-1)d}{q+r}\,, \tag{9}$$

$$\frac{(2p-1)c+d}{2p} > \frac{(q+2)a+rb}{q+r+2}\,. \tag{10}$$

3.1.4. *Choosing parameters.* We start by choosing r and q in order to satisfy the inequalities (8) – (10). Since $c > d$ we also have $\frac{(2p-1)c+d}{2p} > \frac{(2p-3)c+3d}{2p}$ and $\frac{(2p-1)c+d}{2p} - \frac{(2p-3)c+3d}{2p} = \frac{c-d}{p} > 0$. Choose m large enough such that $\frac{6(a-b)}{m+2} < \frac{c-d}{p}$ and $\frac{c+(m-1)d}{m} < \frac{(2p-3)c+3d}{2p}$. We can then find $r \in \{1,\dots,m-1\}$ and set $q := m-r$ such that

$$\frac{(2p-1)c+d}{2p} > \frac{(q+2)a+rb}{m+2} > \frac{qa+(r+2)b}{m+2} > \frac{(2p-3)c+3d}{2p}\,.$$

This directly implies (8) and (10). The inequality (9) follows from

$$\frac{(2p-3)c+3d}{2p} > \frac{c+(q+r-1)d}{q+r}\,.$$

Finally choose s large enough such that (6) is fulfilled and such that

$$\frac{sc+d}{s+1} > \frac{(2p-1)c+d}{2p}\,,$$

which implies (7) by (10). □

3.2. **Proof Theorem 3.1 for HD and PD scenarios.**

3.2.1. *The graph and initial state.* Let us define a graph $\mathcal{G}$ depending on p and four parameters $o,q,r,s \in \mathbb{N}$ as depicted in Figure 3. We start with p complete graphs $\mathcal{K}_1,\dots,\mathcal{K}_p$ on o vertices. Again, the subgraphs $\mathcal{K}_n$ for $n=1,\dots,p$ are connected in series to form a ladder-like structure. There is a subgraph $\mathcal{K}_{p+1}$ which is a complement of a complete graph on o vertices (isolated vertices) connected to the ladder in the same manner. The vertices of $\mathcal{K}_n$ are denoted $k_{n,m}$ for $n=1,\dots,p+1$ and $m=1,\dots,o$, forming the sets K_n. Every vertex in the interior of the ladder (the vertices in K_2 to K_p) is connected to a vertex g_R. Additionally, the vertex g_R has $q+1$ other neighbors. It has q neighboring vertices of degree one forming the set H and a neighbor which we call g_D. The vertex g_D has r neighboring vertices of degree one forming the set I and s neighboring vertices of degree two forming the set J. Each vertex in J is connected to a vertex g_C.

Let X_0 be the initial state defined by

$$(X_0)_v = 1\,, \qquad v \in K_1 \cup J \cup \{g_C\}\,,$$

$$(X_0)_v = 0\,, \qquad v \in \bigcup_{n=1}^{p+1} K_n \cup H \cup I \cup \{g_D, g_R\}\,.$$

3.2.2. *Dynamics.* Let $\mathcal{X} = (X(0), X(1), \dots)$ be the trajectory of the evolutionary game with parameters (a,b,c,d), synchronous update order, mean utility and imitation dynamics on the graph $\mathcal{G}$ constructed above with initial state X_0. We will show that for suitable parameters o,q,r,s the dynamics with initial value X_0 is the

following. Cooperation spreads along the ladder of vertices in $\mathcal{K}_n$ to $\mathcal{K}_p$ and at time $t = p - 1$ the strategy of all vertices of $\mathcal{K}_2$ to $\mathcal{K}_p$ is reset to defection. Formally

$$X_v(t) = 1\,, \qquad v \in \bigcup_{n=1}^{t+1} K_n\,, \tag{11}$$

$$X_v(t) = X_v(t-1)\,, \qquad \text{otherwise}\,, \tag{12}$$

for $t = 1, \dots, p-1$ and $X(t+p) = X(t)$ for $t \in \mathbb{N}_0$. See again Figure 3 for an illustration.

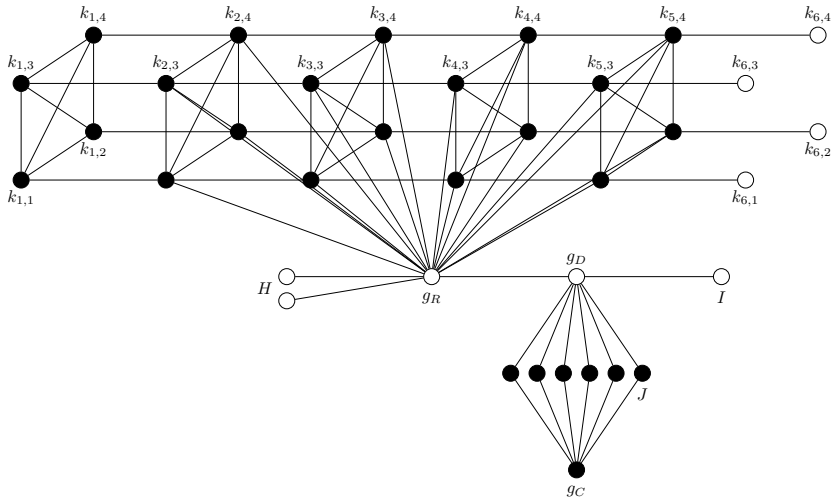

FIGURE 3. Example of the graph $\mathcal{G}$ with parameters $p = 5, o = 4, s = 6, r = 1, q = 2$ with strategy vector $X(4)$. Cooperators are depicted by full circles. Note, that this graph exhibits periodic behavior as described in Section 3.2 for $(a, b, c, d) = (1, 0.45, 1.24, 0)$.

The following conditions must be satisfied in order for $\mathcal{X}$ to fulfill (11) and (12).

- The vertices g_R, g_C, g_D and all vertices in H, I, J keep their strategy. The defector g_D must prevent the vertex g_R from changing its strategy, must not change its own strategy and must not change the strategy of the cooperators in J. This is guaranteed by satisfying the inequalities

$$\frac{(o+1)a + b}{o+2} < \frac{sc + (r+1)d}{s+r+1} < a\,, \tag{13}$$

  where a is the utility of the vertex g_C and the fraction on the left hand side of (13) is an upper bound for the utilities of the cooperating neighbors of g_D and g_R.
- For the cooperation to spread at time t, $t = 0, \dots, p-2$, the boundary cooperators in K_{t+1} must have greater utility than the boundary defectors in K_{t+2}, that is,

$$\min\left\{\frac{(o-1)a + b}{o}, \frac{oa + 2b}{o+2}\right\} > \frac{c + (o+1)d}{o+2}\,. \tag{14}$$

Here the first term on the left is the utility of the cooperators in K_1 at $t = 0$ and the second term is the utility of boundary cooperators in subsequent time steps.

- The vertex g_R must not be stronger than the cooperators in K_m for $t = 0, \dots, p-2$ and $1 \leq m \leq t+1$ for the cooperation to be able to spread, hence

$$\frac{oa + 2b}{o+2} > \frac{(p-2)oc + (o+q+1)d}{(p-1)o + q + 1}\,. \tag{15}$$

Simultaneously, the defecting vertex g_R must be able to change the strategy of all neighboring cooperators to defection at time $p-1$, thus

$$a < \frac{(p-1)oc + (q+1)d}{(p-1)o + q + 1}\,. \tag{16}$$

3.2.3. *Choosing parameters.* We now show that there exists a choice of parameters $o, q, r, s \in \mathbb{N}$ such that the inequalities (13) – (16) are satisfied.

Without loss of generality, we assume $a = 1, d = 0$ (see [6], Remark 8.). Since the denominators in (15), (16) are positive, we can multiply both sides by the product of the denominators and express q in the terms of o. The inequality (15) gives

$$q > \frac{o^2\left((1-p)(1-c) - c\right) - o\left(2(p-1)b - 2(p-2)c + 1\right) - 2b}{o + 2b} \tag{17}$$

and the inequality (16) gives

$$q < o(p-1)(c-1) - 1\,. \tag{18}$$

If we depict both inequalities in the first quadrant of the o-q plane, the inequality (17) is satisfied above the line given by the function on the right hand side. The function on the right hand side asymptotically approaches the line with slope

$$\sigma_1 = (1-p)(1-c) - c\,.$$

The inequality (18) is satisfied below the line with positive slope

$$\sigma_2 = (p-1)(c-1) > 0\,.$$

The difference of the slopes $\sigma_2 - \sigma_1 = c > 0$ is always positive and we are therefore able to find $o, q \in \mathbb{N}$ such that the inequalities (15) and (16) are satisfied, see Figure 4. Furthermore, we can choose o, q arbitrarily big. Since $a > d$ holds, the number o can be chosen great enough such that (14) is satisfied.

Since $c > a > d$ holds, we can find integers $r, s \in \mathbb{N}$ (possibly very big ones) such that (13) is satisfied (implicitly using the density of rational numbers and the fact that our parameters are generic).

Thus, we are able to find parameters $o, q, r, s \in \mathbb{N}$ such that the equations (13) – (16) are satisfied and subsequently, $\mathcal{X}$ is a periodic trajectory of $\mathcal{E} = (\mathcal{G}, \pi, u, \mathcal{T}, \varphi)$ with initial state X_0 having minimal period length p. □

4. **Periodic orbits on an acyclic graph.** Interestingly, periodic behavior of an evolutionary game on a graph can be observed even in the case when the underlying graph is a tree. The absence of cycles demands a new view on the periodic dynamics since the information (strategy change) can spread only gradually through the graph; for example there is no way of "resetting" vertex strategies. Nevertheless, for specific parameter regions arbitrary long periodic behavior can occur.

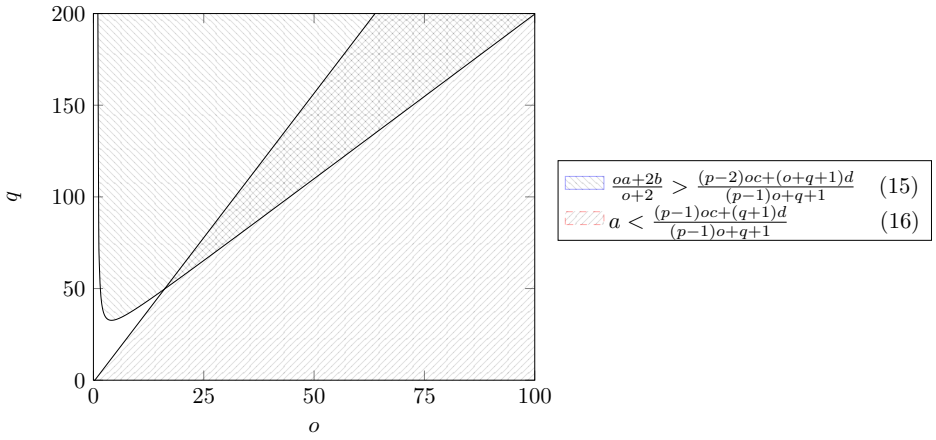

FIGURE 4. Regions of parameters o, q satisfying the inequalities (15)and (16). The regions are depicted for $(a, b, c, d) = (1, -0.45, 1.35, 0)$ and $p = 10$.

Theorem 4.1. *Let $\pi = (a, b, c, d) \in \mathcal{P}$ be admissible parameters satisfying the conditions of the HD scenario, $c > a > b > d$, u the mean utility function, $\mathcal{T}$ the synchronous update order, φ deterministic imitation dynamics and $p_0 \in \mathbb{N}$. There exists an acyclic graph $\mathcal{G}$, a number $p \in \mathbb{N}_0$ such that $p \geq p_0$ and an initial state X_0 such that $\mathcal{X} = (X(0), X(1), \ldots)$ is a periodic trajectory of minimal length p of the evolutionary game $\mathcal{E} = (\mathcal{G}, \pi, u, \mathcal{T}, \varphi)$ on a graph with initial state X_0.*

4.1. Proof of Theorem 4.1.

4.1.1. *The graph and initial state.* Let us define a graph $\mathcal{G}$ whose structure is dependent on two parameters q, r. The graph $\mathcal{G}$ is a rooted r-nary tree such that

- the root h_0 has only one child h_1,
- every vertex in level 1 to $q-2$ has exactly r children,
- exactly r^2 vertices in level $q-1$ with pairwise different predecessors at level 3 are leaves,
- every other vertex in level $q-1$ has r children which are leaves.

See Figure 5 for an illustration.

For the sake of simplicity, we focus only on one branch of the tree $\mathcal{G}$ rooted in a fixed vertex h_3 at level 3. The vertices in the other branches follow the same dynamics by symmetry reasons (the initial state and the graph $\mathcal{G}$ are invariant with respect to an automorphism exchanging the whole branches rooted at level 3). The descendant of h_1 at level $q-1$ in the fixed branch which is a leaf is denoted by h_{q-1}. The vertices in a path from h_1 to h_{q-1} will be denoted by $h_1, h_2, \ldots, h_{q-1}$ in an increasing manner. The vertices in $\{h_1, \ldots, h_{q-1}\} = H$ are called *special vertices*. The set of all descendants of h_m for $m = 3, \ldots, q-2$ which are not in H will be denoted by I_m. Vertices in $I := \bigcup_{m=3}^{q-2} I_m$ are called *ordinary vertices*.

Let the initial condition X_0 be such that every vertex in levels $0, \ldots, q-2$ is cooperating and every other vertex is defecting, that is,

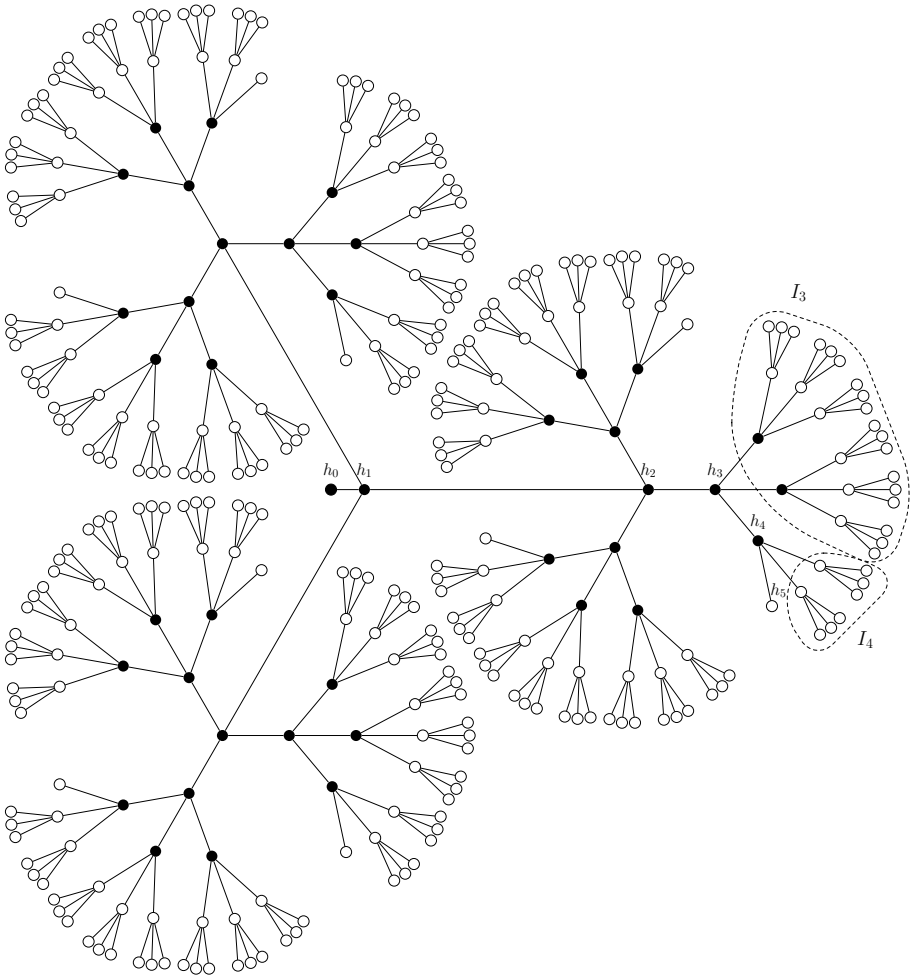

FIGURE 5. Example of the graph constructed in the proof of Theorem 4.1 with an initial condition. The cooperators are depicted by filled black circles, defectors by white ones. The parameters are $r = 3, q = 6$

$$(X_0)_v = 1\,, \qquad v \in N_{\leq q-2}(h_0)\,,$$
$$(X_0)_v = 0\,, \qquad \text{otherwise}\,.$$

See Figure 5 for illustration of the graph construction and initial condition.

4.1.2. *The dynamics.* The dynamics of the system in one period can be divided into three qualitatively different phases. There are three important events that occur during one period. At time $t = 0$, all vertices at level at most $q-2$ cooperate and all vertices at the levels $q-1$ and q defect. From here, defection is spreading along the special vertices to the root and outward towards the boundary along the ordinary vertices. We call this phase the *shrinking phase*. At time step $t = q - 3$, the only special vertices which cooperate are those at level 0 and 1. There are however a few

clusters of cooperating ordinary vertices left in the higher levels. Starting from the root, the central cooperating cluster is growing again and at time $t = (q-3)+(q-5)$ there is only this central cluster of cooperators left which encompasses all vertices at level at most $q-4$. Two time steps later, at $t = 2(q-3)$, this cluster encompasses all vertices at level at most $q-2$ and we are back at the initial state. Please refer to the example in Section 4.2 and Figures 10–15 for an illustration of the dynamics.

The local dynamics is essentially governed by the following two lemmas.

Lemma 4.2. *Consider parameters $(a, b, c, d) \in \mathcal{P}$ such that*

$$\frac{a+rb}{r+1} > \frac{c+rd}{r+1}\,. \tag{19}$$

Let i be a vertex which is a boundary cooperator at time t. If i is connected to one cooperator and r boundary defectors, whose defecting neighbors have utility lower that $\frac{a+rb}{r+1}$ and whose only cooperating neighbor is i, then i and all of its defecting neighbors will cooperate in the next time step.

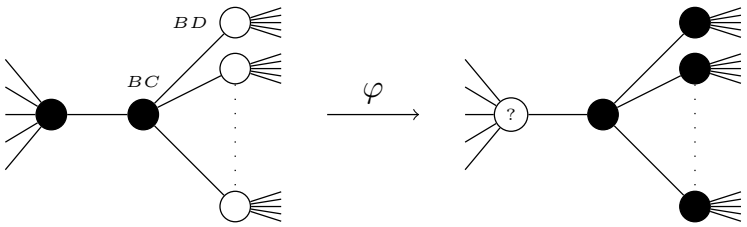

FIGURE 6. Illustration of the local situation in Lemma 4.2. Generally, nothing can be stated about the behavior of the cooperating neighbor on the left.

Proof. The defecting neighbors of i have utility $\frac{c+rd}{r+1}$, and their defecting neighbors have utility smaller than $\frac{a+rb}{r+1}$. Both of these quantities are lower then the utility of i, which is $\frac{a+rb}{r+1}$. □

See Figure 6 for an illustration of Lemma 4.2.

Lemma 4.3. *Consider parameters $(a, b, c, d) \in \mathcal{P}$ such that*

$$a < \frac{rc+d}{r+1}\,. \tag{20}$$

Let i be a vertex which is a boundary defector at time t. If i is connected to one defector and r boundary cooperators, then i and all its neighbors will defect in the next time step.

Proof. At time t, the vertex i has utility $\frac{rc+d}{r+1}$ which is larger then a, the largest utility that a cooperator can achieve. □

See Figure 7 for an illustration of Lemma 4.3.

Let $\mathcal{X} = (X(0), X(1), \dots)$ be the trajectory of the evolutionary game on a graph described above with initial state X_0. We start with some simple observations.

Lemma 4.4. *Let i be an ordinary vertex and let $t \in \mathbb{N}$. All children of i have the same state at time t.*

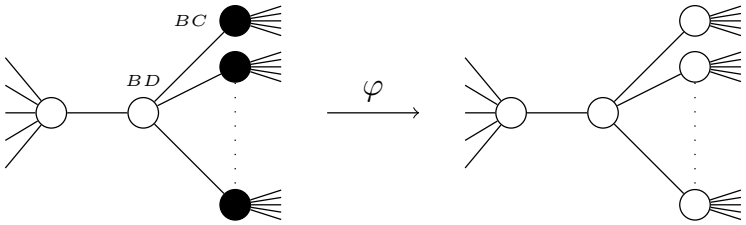

FIGURE 7. Illustration of the local situation in Lemma 4.3.

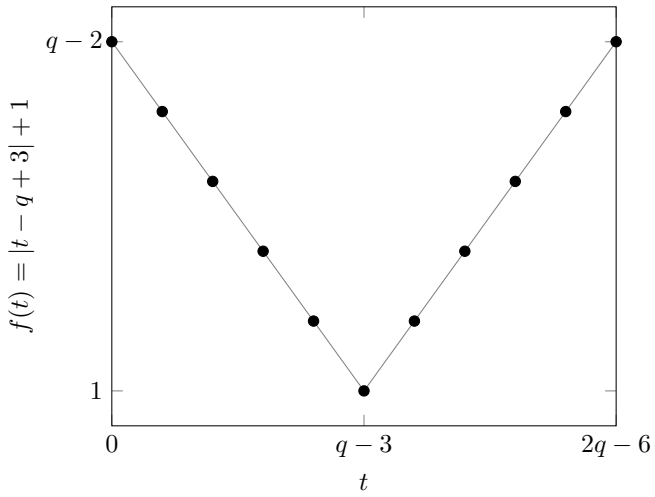

FIGURE 8. The function f governing the shrinking and expansion of cooperation among the special vertices for $q = 8$.

Proof. This follows directly by a symmetry argument. For every pair of children j_1 and j_2 of i there is an automorphism of the graph $\mathcal{G}$ that exchanges j_1 and j_2. The initial state and the functions defining the dynamics are invariant under such automorphisms of the graph, hence the same must hold for every state in the trajectory. □

Lemma 4.5. *Let i be an ordinary vertex. If $X_i(t) = 0$, then $X_j(t+1) = 0$ for all children j of i.*

Proof. Based on Lemma 4.4 we have to differentiate between only three cases. In the first case all children of i are cooperators. By Lemma 4.3 they will switch to defection. In the second case they are boundary defectors. Therefore all of their children must be cooperators and again Lemma 4.3 shows that they will switch to defection. In the last case the children are inner defectors which can not change their strategy. □

The dynamics along the special vertices is very simple to describe. Let $f : \{0, \dots, 2q-6\} \to \mathbb{N}$ be the function given by $f(t) := |t - q + 3| + 1$, see Figure 8. A special vertex h_ℓ is cooperating at time t if and only if $\ell \le f(t)$. This is shown together with a description of the dynamics of the strategies of the ordinary vertices

in the following theorem. Notice that property (f) and property (g) in Theorem 4.6 immediately imply that $\mathcal{X}$ has period $2q-6$ and property (a) implies that $\mathcal{X}$ has no shorter period.

Theorem 4.6. *The following invariants hold for the dynamics when* $0 \leq t \leq 2q-6$

(a)

$$X_{h_\ell}(t) = \begin{cases} 1 & \text{if } \ell \leq f(t) \\ 0 & \text{otherwise} \end{cases}, \qquad \text{for all } h_\ell \in H_\ell.$$

(b) h_ℓ *is an inner cooperator if and only if* $\ell < f(t)$.
(c) h_ℓ *is an inner defector if and only if* $\ell > f(t)+1$.

In the shrinking phase $(0 \leq t < q-3)$ *additionally the following properties hold.*

(d) For $m \leq f(t)+1$ *and* $i \in I_m \cap N_1(h_m)$ *we have* $X_i(t) = 1$.
(e) For $m > f(t)+1$ *and* $i \in I_m \cap N_{\leq m-f(t)-1}(h_m)$ *we have* $X_i(t) = 0$.

In the expanding phase $(q-3 \leq t \leq 2q-6)$*, we have*

(f) All vertices at level at most $f(t)$ *are cooperating.*
(g) All vertices at level n *with* $f(t) < n \leq f(t)+3$ *are defecting.*

Proof. We show by induction that these invariants are true throughout the course of the dynamics. Let $s \in \mathbb{N}$ and assume that the theorem holds for all $t \leq s$.

Initial state; i.e. $s = 0$: Obviously, all of the points (a) - (e) hold true. Since all of the vertices h_ℓ for $\ell \leq q-3$ are inner cooperators by (b), they preserve their strategy at time 1. The defecting vertex h_{q-1} has utility c. Thus, the vertex h_{q-2} changes its strategy to defection at time $s+1$ while changing the strategy of vertices in $I_{q-2} \cap N_1(h_{q-2})$ to cooperation as a consequence of Lemma 4.2. Every other vertex preserve its strategy at time $s = 0$ and thus, the points (a) - (e) hold true at time 1.

Shrinking phase; i.e. $0 < s < q-3$: The vertex $h_{f(s)+1}$ is defecting and has one defecting neighbor $h_{f(s)+2}$ by (a). The children of $h_{f(s)+1}$ are cooperating by (d). Thus, using Lemma 4.3, the vertex $h_{f(s)+1}$ and all of his neighbors are defecting in the next time step. Together with (c), this proves the point (a) for time $s+1$. Using (d), this also immediately implies (b) (the boundary cooperators closest to the root h_0 of the cluster containing h_0 are at level $q-2-s$).

The vertices h_ℓ for $\ell \geq f(s)+1$ are inner defectors by (c). Moreover, their children are all defecting by (e). Thus, h_ℓ stay inner defectors for $\ell \geq f(s)+1$. The vertex $h_{f(s)}$ is a boundary defector by (b) and has r cooperating neighbors ((d) and (a)). Lemma 4.3 implies the vertex $h_{f(s)}$ is an inner defector at time $s+1$ which is (c) for the next time step.

The invariant (a) implies that the predecessors of all vertices in $I_m \cap N_1(h_m)$ are cooperating for $m \leq f(s)+1$. The children of a specific vertex v in $I_m \cap N_1(h_m)$ are either all defecting (Lemma 4.4) and then Lemma 4.2 ensures the preservation of cooperation in $s+1$. If the children of v are cooperating then the vertex v is an inner cooperator and preserves its strategy.

As a trivial consequence of Lemma 4.5, if all vertices in $I_m \cap N_{\leq m-f(s)-1}(h_m)$ are defecting for $m > f(s)+1$ then all vertices in $I_m \cap N_{\leq m-f(s)}(h_m)$ are defecting in the next time step. Furthermore, by (c) and (d) we can apply Lemma 4.2 to the

vertex h_{q+s-2}. This gives (e).

Phase switch; i.e. $s = q-2$: We already established (a) - (e) at time $s+1$. We still have to show, that (f) and (g) hold at time $s+1$. We have $f(q-3) = 1$. There are no ordinary vertices at level one, hence (d) holds at time $s+1$ by (a). This also shows (g) for special vertices. There is also no ordinary vertex at level two and three, hence we only have to show (g) for ordinary vertices at level four. They are contained in $N_{\leq m-2} \cap I_m$ for some $m = 3$, hence they are defecting at time $s+1$ by (e).

Growing phase; i.e. $q-3 \leq s < 2q-6$: Lemma 4.2 together with (f) and (g) implies that all vertices at level at most $f(s)+1$ will cooperate at time $s+1$, hence (f) holds. This also implies (b).

The special vertices $h_{f(s)+2}, \dots, h_{q-1}$ are inner defectors by (c) and hence also defect at time $s+1$. Therefore (a) is satisfied. If $f(s)+3 < q$, property (g) automatically holds at time $s+1$. Consider s with $f(s)+3 < q$. An ordinary vertex at level $f(s)+4$ is either an inner defector at time s and hence defects at time $s+1$ or it has only cooperating children and hence defects by Lemma 4.3. All in all this shows that (g) is also fulfilled. Let v be a child of a special vertex h_ℓ with $\ell > s+1$. By (c) it is defecting at time s. Either it is an inner defector and hence also defects at time $s+1$ or all its children are cooperators and it defects at time $s+1$ by Lemma 4.3. This established in particular that h_ℓ is an inner defector at time $s+1$, in other words, (g). □

4.1.3. *Parameter choice.* The only assumptions we needed in the dynamics section were the inequalities (19), (20) and the assumption that the parameters (a, b, c, d) satisfy the conditions of the HD scenario ($c > a > b > d$). Let such a, b, c, d be given. Clearly, r can be chosen great enough such that the inequalities (19) and (20) hold.

The minimal period of the constructed trajectory is $2(q-3)$. Setting $q := \max\{5, \lceil p_0/2 \rceil + 3\}$ the period is at least p_0. □

Remark 1. In the constructions in Sections 3.1 and 3.2, the behaviour of the number of cooperators or more precisely the sequence $(|\{v \in V \mid X_v(t) = 1\}|)_{t \in \mathbb{N}_0}$ was rather boring. During one period of the trajectory it was growing and reset to the initial value at the end of the period. The behaviour of this sequence is much more interesting for our tree construction as shown in Figure 9.

4.2. **Example.** Figures 10 – 15 depict an example of a trajectory on an evolutionary game on a graph constructed in Section 4.1. Cooperators are depicted with black circles, defectors are depicted with white ones. The players changing strategy in the current time step are highlighted with a dashed circle. The parameters of this graph are $r = 3, q = 6$. This trajectory can be observed for example for parameter vector $(a, b, c, d) = (1, 0.6, 2, 0)$ satisfying the inequalities (19), (20). Note that the inequality

$$b > \frac{c + rd}{r+1} \tag{21}$$

holds for such a choice of parameters. Cooperation then spreads from outer cooperators towards the leaves between $X(2)$ and $X(3)$. In contrary, for $b \in (0, 0.5)$ the inequality (21) does not hold anymore. The outer cooperators (cooperators not

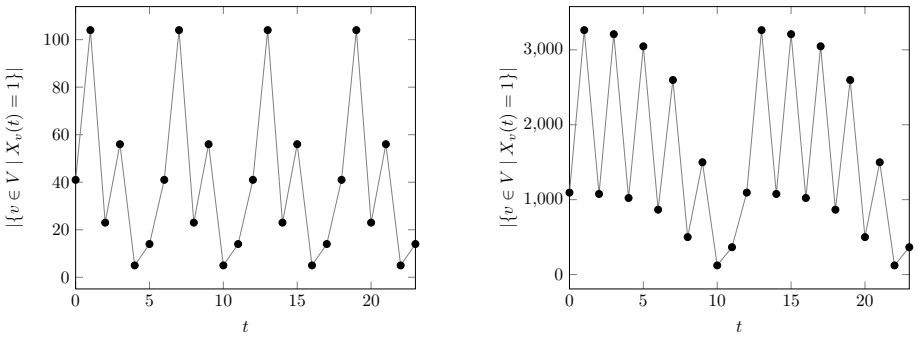

FIGURE 9. Development of the number of cooperators for the evolutionary game on the tree $\mathcal{G}$ in Section 4 with $r = 3$ and game theoretic parameters $(a, b, c, d) = (1, 0.7, 2, 0)$. On the left the tree has depth $q = 6$, on the right $q = 9$.

in the cluster containing the root h_0) then vanish in $X(3)$ and they do not spread cooperation further. The strategy vectors $X(t)$ and $X(t + 6)$ coincide for $t \in \mathbb{N}_0$.

This example and an example of an evolutionary game on a graph with $q = 7$ and all other parameters remaining unchanged can be found online in [8].

5. **Conclusion.** We showed that on arbitrary graphs the game theoretic parameters can not exclude periodic behavior with long periods. Our proofs hold also true for a small perturbation of the game-theoretical parameters a, b, c, d as a consequence of the generic payoff assumption.

Our constructions rely heavily on the fact that we can choose the graph parameters arbitrarily. This no longer works if we restrict to certain classes of graphs. For example Theorem 4.1 partially answers Question 1 while restricting to the parameters (a, b, c, d) satisfying the conditions of the HD scenario, $c > a > b > d$, and the class of acyclic graphs.

Natural classes of graphs we might restrict ourselves to are k-regular graphs (every vertex has exactly k neighbors), vertex-transitive graphs (every pair of vertices can be exchanged by a graph automorphism) or planar graphs (the graph can be drawn in the plane without edge crossings). This leads for example to the following question.

Question 2. *For which game theoretic parameters (a, b, c, d) and positive integers k, p is there a k-regular graph $\mathcal{G}$ such that the corresponding evolutionary game with synchronous update and imitation dynamics on $\mathcal{G}$ has a periodic trajectory with minimal period p?*

Acknowledgments. The first author would like to acknowledge the project LO1506 of the Czech Ministry of Education, Youth and Sports for supporting his visit at the research centre NTIS (New Technologies for the Information Society of the Faculty of Applied Sciences, University of West Bohemia). The second author was supported by the Grant Agency of the Czech Republic Project No. 15-07690S.

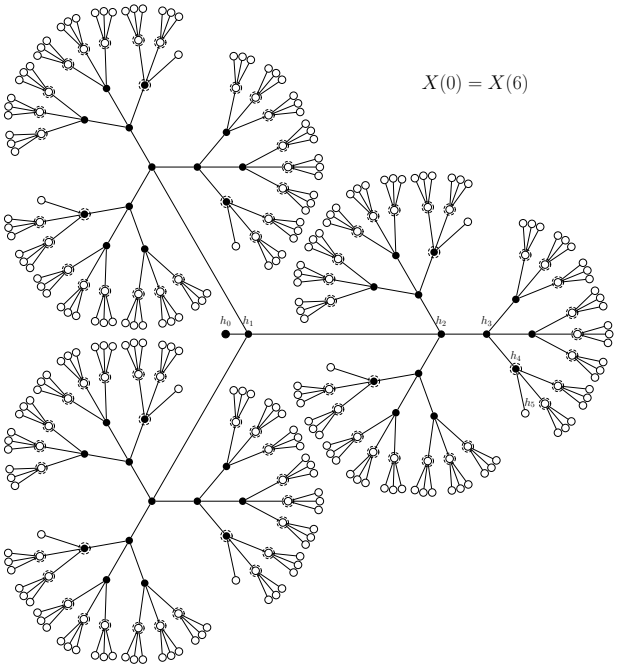

FIGURE 10. The example from Section 4.2.

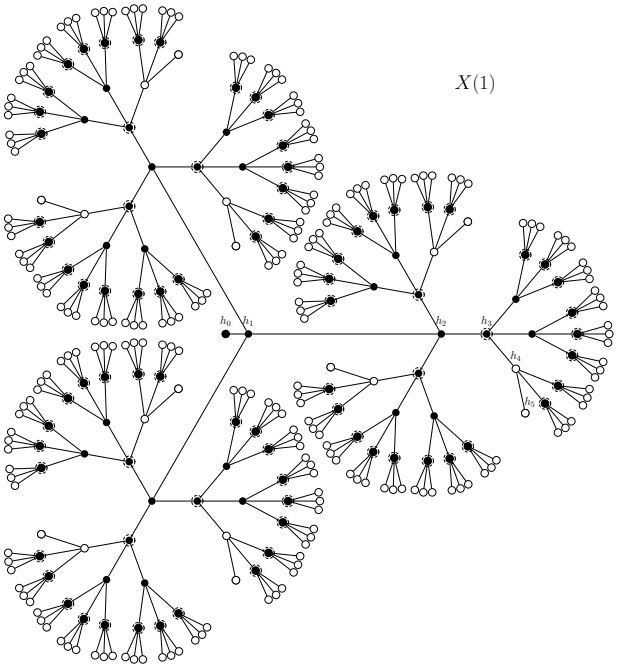

FIGURE 11. The example from Section 4.2.

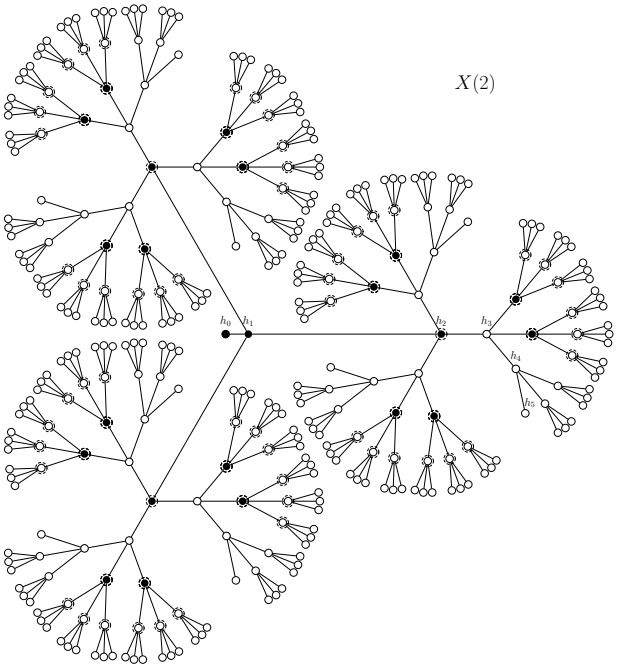

FIGURE 12. The example from Section 4.2.

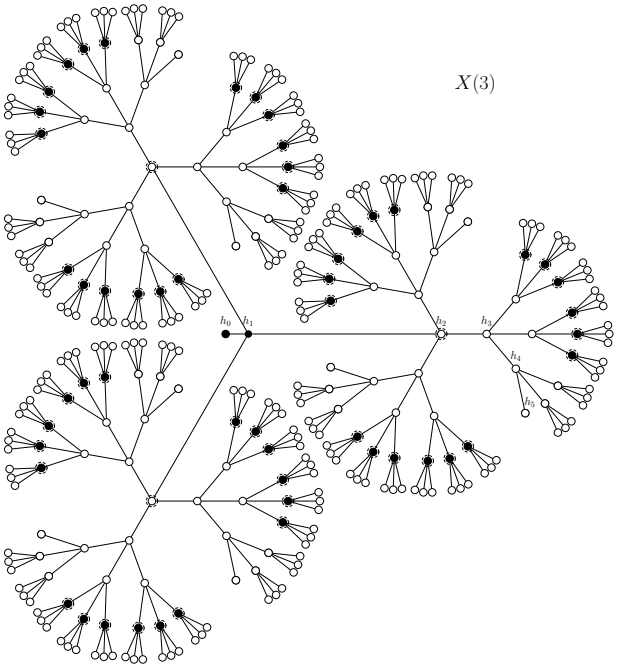

FIGURE 13. The example from Section 4.2.

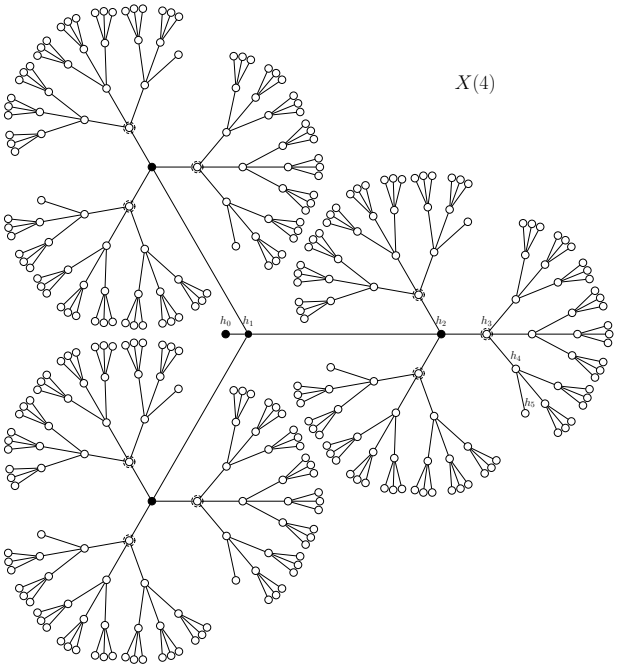

FIGURE 14. The example from Section 4.2.

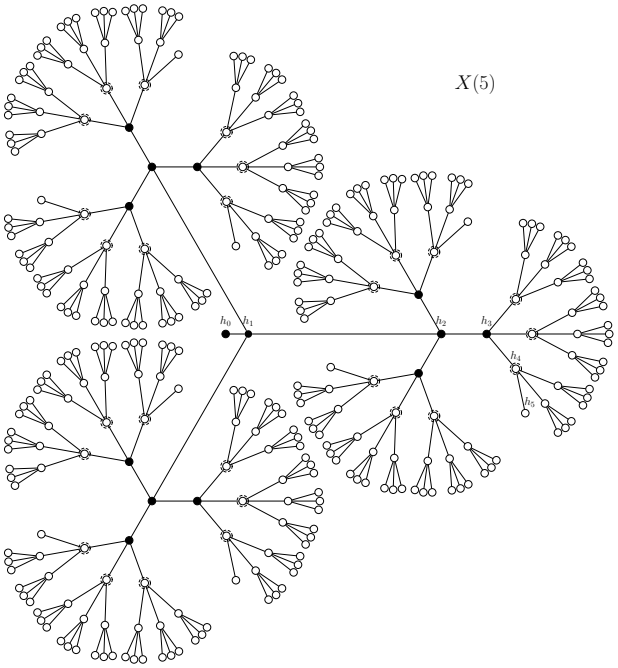

FIGURE 15. The example from Section 4.2.

REFERENCES

[1] G. Abramson and M. Kuperman, Social games in a social network, *Physical Review E*, **63** (2001), 030901.

[2] B. Allen and M. A. Nowak, Games on graphs, *EMS Surv. Math. Sci.,* **1** (2014), 113–151.

[3] M. Broom and J. Rychtář, *Game-Theoretical Models in Biology*, 1st edition, CRC Press, Taylor & Francis Group, 2013.

[4] J. T. Cox, R. Durrett and E. A. Perkins, *Voter Model Perturbations and Reaction Diffusion Equations*, vol. 349 of Astérisque, Société Mathématique de France, 2013.

[5] O. Durán and R. Mulet, Evolutionary prisoner's dilemma in random graphs, *Physica D: Nonlinear Phenomena*, **208** (2005), 257–265.

[6] J. Epperlein, S. Siegmund and P. Stehlík, Evolutionary games on graphs and discrete dynamical systems, *Journal of Difference Equations and Applications*, **21** (2015), 72–95.

[7] J. Epperlein, S. Siegmund, P. Stehlík and V. Švígler, Coexistence equilibria of evolutionary games on graphs under deterministic imitation dynamics, *Discrete and Continuous Dynamical Systems - Series B*, **21** (2016), 803–813.

[8] J. Epperlein and V. Švígler, Periodic orbits of an evolutionary game on a tree, `https://figshare.com/articles/6-periodic_orbit_of_an_evolutionary_game_on_a_tree/5110981`, June 2017, DOI: 10.6084/m9.figshare.5110981.

[9] J. Hofbauer and K. Sigmund, *Evolutionary Games and Population Dynamics*, Cambridge University Press, 1998.

[10] B. J. Kim, A. Trusina, P. Holme, P. Minnhagen, J. S. Chung and M. Y. Choi, Dynamic instabilities induced by asymmetric influence: Prisoners' dilemma game in small-world networks, *Physical Review E*, **66** (2002), 021907.

[11] C. Marr and M.-T. Hütt, Outer-totalistic cellular automata on graphs, *Physics Letters A*, **373** (2009), 546–549.

[12] N. Masuda and K. Aihara, Spatial prisoner's dilemma optimally played in small-world networks, *Physics Letters A*, **313** (2003), 55–61.

[13] M. A. Nowak, *Evolutionary Dynamics: Exploring the Equations of Life*, Belknap Press of Harvard University Press, 2006.

[14] M. A. Nowak and R. M. May, Evolutionary games and spatial chaos, *Nature*, **359** (1992), 826–829.

[15] M. Tomochi, Defectors' niches: Prisoner's dilemma game on disordered networks, *Social Networks*, **26** (2004), 309–321.

Received April 2017; revised August 2017.

E-mail address: `jeremias.epperlein@gmail.com`
E-mail address: `sviglerv@ntis.zcu.cz`

Appendix D

Paper: Multichromatic travelling waves for lattice Nagumo equations

Applied Mathematics and Computation 361 (2019) 430–452

Contents lists available at ScienceDirect

Applied Mathematics and Computation

journal homepage: www.elsevier.com/locate/amc

Multichromatic travelling waves for lattice Nagumo equations

Hermen Jan Hupkes[a], Leonardo Morelli[a], Petr Stehlík[b,*], Vladimír Švígler[b]

[a] Mathematisch Instituut, Universiteit Leiden, P.O. Box 9512, Leiden, RA 2300, The Netherlands
[b] Department of Mathematics and NTIS, Faculty of Applied Sciences, University of West Bohemia, Univerzitní 8, Plzeň 306 14 Czech Republic

ARTICLE INFO

MSC:
34A33
37L60
39A12
65M22

Keywords:
Reaction-diffusion equations
Lattice differential equations
Travelling waves
Wave collisions

ABSTRACT

We discuss multichromatic front solutions to the bistable Nagumo lattice differential equation. Such fronts connect the stable spatially homogeneous equilibria with spatially heterogeneous n-periodic equilibria and hence are not monotonic like the standard monochromatic fronts. In contrast to the bichromatic case, our results show that these multichromatic fronts can disappear and reappear as the diffusion coefficient is increased. In addition, these multichromatic waves can travel in parameter regimes where the monochromatic fronts are also free to travel. This leads to intricate collision processes where an incoming multichromatic wave can reverse its direction and turn into a monochromatic wave.

1. Introduction

In this paper we are interested in the Nagumo lattice differential equation (LDE)

$$\dot{u}_j(t) = d[u_{j-1}(t) - 2u_j(t) + u_{j+1}(t)] + u_j(t)(1-u_j(t))(u_j(t)-a), \tag{1.1}$$

posed on the one-dimensional lattice $j \in \mathbb{Z}$, for small and intermediate values of the diffusion coefficient $d > 0$. This regime features spatially periodic equilibria for (1.1) that can serve as buffer zones between regions of space where the homogeneous stable equilibria $u \equiv 0$ and $u \equiv 1$ dominate the dynamics. Our goal here is to continue the program initiated in [1] where two-periodic patterns and their connection to bichromatic waves were rigorously analyzed.

In particular, we build a classification framework that also allows larger periods to be considered. We also construct so-called multichromatic (or n-chromatic) waves, which connect heterogeneous n-periodic rest-states to each other or their homogeneous counterparts $u \equiv 0$ and $u \equiv 1$. We numerically analyze these multichromatic waves for $n \in \{3, 4\}$ and show that they exhibit richer behaviour than the bichromatic versions. Indeed, these multichromatic waves can disappear and reappear as the diffusion d is increased. In addition, open sets of parameters (a, d) exist where monochromatic and multichromatic waves can travel simultaneously. This allows us to explore various new types of wave collisions.

Reaction-diffusion systems

The LDE (1.1) can be seen as the spatial discretization of the Nagumo PDE

$$u_t = u_{xx} + u(1-u)(u-a) \tag{1.2}$$

* Corresponding author.
E-mail addresses: hhupkes@math.leidenuniv.nl (H.J. Hupkes), leonardo.morelli@gmail.com (L. Morelli), pstehlik@kma.zcu.cz (P. Stehlík), sviglerv@kma.zcu.cz (V. Švígler).

https://doi.org/10.1016/j.amc.2019.05.036
0096-3003/

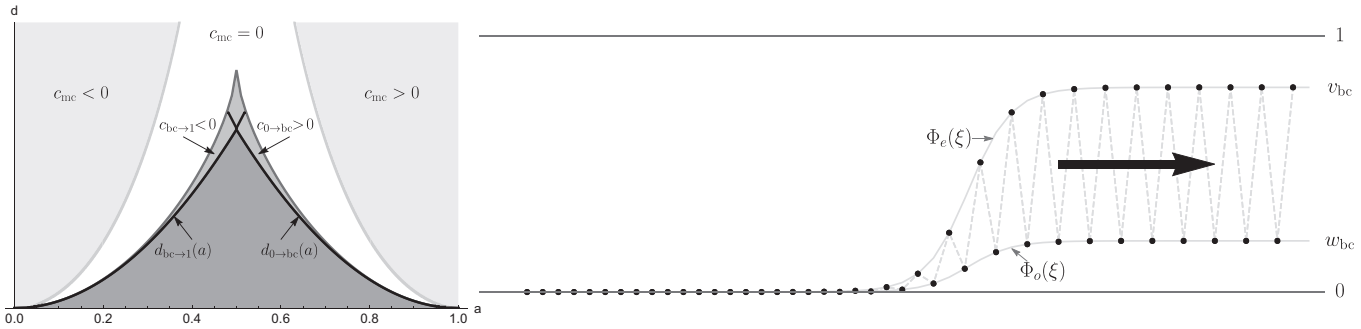

Fig. 1. The left panel depicts the parameter regions where (1.1) admits monochromatic and bichromatic wave solutions. Monochromatic waves (1.5) exist for all pairs (a, d) but travel only inside the light gray regions (with either $c_{mc} < 0$ or $c_{mc} > 0$). Inside the region where monochromatic waves are pinned ($c_{mc} = 0$), there exist a (gray/dark gray) set where the bichromatic waves (1.8) exist. Above the black bounds $d_{0\to bc}(a)$ and $d_{bc\to 1}(a)$, bichromatic waves travel with $c_{0\to bc} > 0$ or $c_{bc\to 1} < 0$ respectively. The right panel shows a bichromatic wave (1.8) connecting the homogeneous solution (0,0) with the nonhomogeneous 2-periodic solution (v_{bc}, w_{bc}).

onto a uniform grid with node-spacing $h = d^{-1/2}$. This scalar reaction-diffusion PDE can serve as a highly simplified model to describe the interaction between two species or states (described by $u = 0$ and $u = 1$) that compete for dominance in a spatial domain [2]. It admits a comparison principle and can be equipped with a variational structure [3], but it also has a rich global attractor. As such, it has served as a prototype system to investigate many of the key concepts in the field of pattern formation, such as spreading speeds for compact disturbances [4], the existence and stability of travelling waves [5,6] and other non-trivial entire solutions [7,8].

The semi-discrete version (1.1) has acted as a playground to investigate the impact of the transition from a spatially continuous to a spatially discrete domain. From a mathematical point of view, interesting questions and complications arise due to the broken translational invariance [9]. From the practical point of view, it is highly desirable to be able to incorporate the natural spatial discreteness present in many physical systems such as myelinated nerve fibres [10], meta-materials [11–13] and crystals [14,15].

Monochromatic waves

Substitution of the travelling wave Ansatz $u(x, t) = \Phi(x - ct)$ into the PDE (1.2) yields the travelling wave ODE

$$-c\Phi' = \Phi'' + \Phi(1 - \Phi)(\Phi - a). \tag{1.3}$$

On the other hand, substitution of the discrete analog $u_j(t) = \Phi(j - ct)$ into the LDE (1.1) yields the monochromatic wave equation

$$-c\Phi'(\xi) = d[\Phi(\xi - 1) - 2\Phi(\xi) + \Phi(\xi + 1)] + \Phi(\xi)(1 - \Phi(\xi))(\Phi(\xi) - a), \tag{1.4}$$

which is a functional differential equation of mixed type (MFDE). We use the term monochromatic here to refer to the fact that each spatial index j follows the same waveprofile Φ. We are specially interested in waves that connect the two stable equilibria $u = 0$ and $u = 1$. In particular, we impose the boundary conditions

$$\lim_{\xi\to-\infty} \Phi(\xi) = 0, \quad \lim_{\xi\to+\infty} \Phi(\xi) = 1. \tag{1.5}$$

The ODE (1.3) with (1.5) can be analyzed by phase-plane analysis [5] (and even solved explicitly) to yield the existence of solutions that increase monotonically and have $\text{sign}(c) = \text{sign}(a - \frac{1}{2})$. These waves have a large basin of attraction [5] and can be used as building blocks to construct and analyze more complicated solutions [4].

More advanced techniques are required to analyze (1.4), but again it is possible to show that non-decreasing solutions exist [16]. However, it is now a very delicate question to determine whether the uniquely determined wavespeed $c = c_{mc}(a, d)$ satisfies $c_{mc}(a, d) = 0$ or $c_{mc}(a, d) \neq 0$. Indeed, the broken translational invariance causes an energy-barrier that must be overcome before waves are able to travel. As such, there is an open region in the (a, d)-plane for which $c_{mc}(a, d) = 0$ holds; see Fig. 1. This pinning phenomenon is generic[1] [17–24] but not omnipresent [25,26] in discrete systems and has received considerable attention.

Bichromatic waves

The spatial second difference allows (1.1) to have a much larger class of equilibrium solutions than the PDE (1.2). For example, two-periodic equilibria of the form

$$u_j = \begin{cases} v & j \text{ is even}, \\ w & j \text{ is odd}. \end{cases} \tag{1.6}$$

[1] In a sense that is made formally precise in [17].

can be found by solving the nonlinear algebraic two-component system $G(v, w; a, d) = 0$ given by

$$G(v, w; a, d) = \begin{pmatrix} 2d(w - v) + v(1 - v)(v - a) \\ 2d(v - w) + w(1 - w)(w - a) \end{pmatrix}. \tag{1.7}$$

The variable w can be readily eliminated, leading to a ninth-order polynomial equation for the remaining component v. For $0 < d \ll 1$ this polynomial has nine roots, leading to two stable and four unstable spatially heterogeneous two-periodic equilibria for (1.1) besides the three spatially homogeneous equilibria $\{0, a, 1\}$.

In [1] we performed a full rigorous analysis of this system, which shows that the number of these two-periodic equilibria decreases as $d > 0$ is increased. In particular, there exist two functions $0 < d_s(a) < d_u(a)$ defined for $a \in (0, 1)$ so that the two stable patterns $(v_{\mathrm{bc}}, w_{\mathrm{bc}})$ and $(w_{\mathrm{bc}}, v_{\mathrm{bc}})$ collide with two (or all four) unstable patterns and disappear as d crosses $d_s(a)$. The remaining two unstable patterns subsequently collide with (a, a) as d crosses $d_u(a)$, leaving only the three spatially homogeneous equilibria. We emphasize that all these two-periodic equilibria only exist in the region where monochromatic waves are pinned, i.e. $c_{\mathrm{mc}}(a, d) = 0$; see Fig. 1.

Based on general results in [27] we showed that for $0 < d < d_s(a)$ the system (1.1) admits two types of bichromatic waves

$$u_j(t) = \begin{cases} \Phi_e(j - ct) & j \text{ is even}, \\ \Phi_o(j - ct) & j \text{ is odd}. \end{cases} \tag{1.8}$$

The first class satisfies the lower limits (see Fig. 1 for an example)

$$\lim_{\xi \to -\infty} (\Phi_e(\xi), \Phi_o(\xi)) = (0, 0), \quad \lim_{\xi \to +\infty} (\Phi_e(\xi), \Phi_o(\xi)) = (v_{\mathrm{bc}}, w_{\mathrm{bc}}), \tag{1.9}$$

and has wavespeed $c_{0 \to \mathrm{bc}} \geq 0$, while the second class satisfies the upper limits

$$\lim_{\xi \to -\infty} (\Phi_e(\xi), \Phi_o(\xi)) = (v_{\mathrm{bc}}, w_{\mathrm{bc}}), \quad \lim_{\xi \to +\infty} (\Phi_e(\xi), \Phi_o(\xi)) = (1, 1), \tag{1.10}$$

and has $c_{\mathrm{bc} \to 1} \leq 0$. In [1] we showed that there exist two thresholds

$$0 < d_{0 \to \mathrm{bc}}(a) \leq d_s(a), \quad 0 < d_{\mathrm{bc} \to 1}(a) \leq d_s(a), \tag{1.11}$$

so that in fact $c_{0 \to \mathrm{bc}} > 0$ respectively $c_{\mathrm{bc} \to 1} < 0$ holds as d is increased above these thresholds; see Fig. 1. In addition, for all $a \in (0, 1)$ one or both of the inequalities in (1.11) is strict, indicating the presence of one or more *travelling* bichromatic waves for d sufficiently close to $d_s(a)$; see Fig. 1.

Numerical results indicate that these two types of bichromatic waves can be glued together via an intermediate buffer zone that displays the two-periodic pattern $(v_{\mathrm{bc}}, w_{\mathrm{bc}})$. This buffer zone is consumed as the waves move towards each other and eventually collide to form a trapped monochromatic wave; see Fig. 10 for the trichromatic analogue.

Multichromatic waves

The main purpose of the present paper is to illustrate the novel behaviour that arises for (1.1) when considering wave connections to/from stable n-periodic patterns with $n \geq 3$. Our two main conclusions are that the monotonicity properties described above are no longer valid and that travelling multichromatic waves can co-exist with travelling monochromatic waves. In particular, travelling multichromatic waves can appear, disappear and reappear as $d > 0$ is increased and can collide with other multichromatic waves to form travelling monochromatic waves.

Since the degree of the polynomial that governs the n-periodic equilibria is given by 3^n, it is essential to develop an appropriate classification system to keep track of all the roots and their ordering properties. We develop such a system in this paper, using words from the set $\{\mathfrak{o}, \mathfrak{a}, \mathfrak{1}\}^n$ to classify roots that bifurcate off the corresponding sequence of zeroes of the cubic at $d = 0$. The lack of monotonicity with respect to d leads to complications and forces us to allow both parameters (a, d) to vary when tracking the roots, unlike in [1]. Although the general theory in [27] also applies to our setting, it is still a challenge to check the conditions in a systematic fashion.

For concreteness, the cubic nonlinearity was used for our numerical investigations. However, we emphasize that the principle behind our bookkeeping and ordering techniques can also be applied to versions of (1.1) with general bistable nonlinearities. In fact, we only need the derivatives of g in stationary points to be nonzero, allowing us to apply the implicit function theorem. That said, it is possible to construct examples [28, Section 1.2] featuring stable periodic equilibria that emerge from the complex plane and *cannot* be classified in this fashion.

Periodicity

The presence of multiple characteristic length scales in spatially discrete systems often leads to the formation of periodic patterns. Examples include phase boundaries in binary solids [29,30], domain-wall microstructures in dielectric crystals [31], oscillations in neural networks [32] and phase transitions in martensitic materials [13]. At present a serious effort is underway to start analyzing the dynamics of these patterns, which has already led to several subtle and counterintuitive results.

For example, bichromatic waves have been found in several spatially discrete settings. The results in [33,34] apply to an anti-diffusion version of (1.1) where $d < 0$. Although PDEs of this type are ill-posed, this LDE can be reformulated as a two-component problem with positive alternating diffusion coefficients, allowing the general results in [27] to be applied. Several versions of the two-periodic FPU problem are considered in [35–37]. Using a different palette of techniques, the authors obtain so-called nanopteron solutions. Such solutions can have exponentially small high-frequency oscillations in their tails, which are poorly understood at present. Finally, the two-periodic FitzHugh-Nagumo problem was considered in [38] using a modified spectral-convergence argument.

The common feature in all the examples above is that the periodicity is already built into the underlying system parameters. By contrast, the periodic structures considered here and in [1] are *intrinsic*, in the sense that they emerge from the spatially *homogeneous* LDE (1.1). In particular, equilibria of different (possibly coprime) periods can coexist and influence the general behaviour of (1.1). For example, the early work in [23] for small $d > 0$ already examines how the existence of such equilibria can cause wave pinning.

An important longer-term motivation for the current paper is that we wish to explore the reverse point of view. In particular, the standing wave solutions to (1.4)–(1.5) with $c = 0$ can be combined with their spatial mirror images to form so-called heteroclinic cycles between zero and one. Based on the theory described in [39, Section 3], one expects stable n-periodic solutions with $n \gg 1$ to exist in the neighbourhood of such limit cycles. In particular, the pinning boundary could potentially be better understood by analyzing the behaviour of the parameter regions where stable n-periodic patterns exist for large values of n. In order to work towards this goal, we show in this paper how asymptotic expansions can be obtained for the boundaries of these regions for $n = 3, 4$. These curves already track the pinning boundary much more closely than their bichromatic counterparts.

Spreading phenomena

From a modelling perspective, the various travelling waves considered here are robust mechanisms by which the two species represented by the stable states zero and one can spread through the spatial domain. The novel feature here as compared to [1] is that zero can 'win' against stable phase mixtures, even if it would 'lose' in a direct confrontation with one (cf. Fig. 16 and Supplement A.3). This presents a clear violation of the general rule of thumb, which states that the LDE (1.1) and the PDE (1.2) have qualitatively similar behaviour as long as one avoids the pinning region. Stated more generally, multiple types of transport mechanisms can be available simultaneously for (1.1), both *inside* and *outside* the pinning region.

From a population control or material design perspective this opens up numerous interesting possibilities. For example, one could pre-process the center of the underlying medium to exhibit one of the stable n-periodic phase mixtures. This could then be used to increase the spreading speed of the energetically favoured phase ($n \geq 4$). Or alternatively, it could act as a waveguide to 'draw in' the two stable phases from opposite sides and force a collision between the two incoming waves ($n \geq 2$). We will see here that the end-product of such a collision is typically a wave of a different type, which is highly likely to be trapped. However, it can be forced to move by carefully tuning the system parameters ($n \geq 4$).

Wave collisions

Understanding the interaction between waves is an important topic that is attracting considerable attention, primarily in the spatially continuous setting at present. The so-called weak interaction regime where the waves are far apart is relatively well-understood; see e.g. the exit manifold developed by Wright and Hoffman [40] for the discrete setting and the numerous studies on renormalization techniques for the continuous setting [41–43].

However, at present there is no general theory to understand strong interactions, where the core of the waves approach each other and deform significantly. Early numerical results by Nishiura et al. [44] for the Gray–Scott and a three-component FitzHugh–Nagumo system suggest that the fate of colliding waves (annihilation, combination or scattering) is related to the properties of a special class of unstable solutions called separators. Even the internal dynamics of a single pulse under the influence of essential spectrum (a proxy for the advance of a second wave) can be highly complicated, see e.g. [45] for the (partial) unfolding of a butterfly catastrophe.

Naturally, more information can be obtained in the presence of a comparison principle. Indeed, for the PDE (1.2) one can show that monostable waves can merge to form a bistable wave [7] and that counterpropagating waves can annihilate [8,46]. If one modifies the nonlinearity to allow more zero-crossings, one can stack waves that connect a chain of equilibria to form so-called propagating terraces [47].

We emphasize that the collisions described in this paper are far richer than those described above for (1.2). This is a direct consequence of the delicate structure of the set of equilibria for (1.1). By exploiting the comparison principle, our hope is that this system can serve as a playground for generating and understanding complicated collision processes.

Organization

In Section 2 we discuss the algebraic problem that n-periodic equilibria must satisfy, develop a naming scheme for its roots and formulate a result concerning the existence of travelling waves. In Section 3 we discuss trichromatic waves and focus on the fact that for certain values of a three-periodic stable equilibria can disappear and reappear as the diffusion

parameter d is increased. We move on to quadrichromatic waves in Section 4, highlighting the fact that quadrichromatic and monochromatic waves can travel simultaneously in certain parameter regions. This allows us to study various types of wave collisions. Finally, in Section 5 we prove our main result Theorem 2.1, which establishes the existence of multichromatic waves.

2. Multichromatic Root Naming and Ordering

The main focus of this paper is the Nagumo lattice differential equation (LDE)

$$\dot{u}_j(t) = d\big[u_{j-1}(t) - 2u_j(t) + u_{j+1}(t)\big] + g\big(u_j(t); a\big), \qquad j \in \mathbb{Z}, \tag{2.1}$$

in which the parameters (a, d) are taken from the half-strip

$$\mathcal{H} = [0, 1] \times [0, \infty) \tag{2.2}$$

and the nonlinearity is given by the cubic

$$g(u; a) = u(1 - u)(u - a). \tag{2.3}$$

Our results focus on n-periodic stationary solutions to (2.1) and the waves that connect them.

In Section 2.1 we develop a naming system that allows us to partially classify these stationary solutions in an intuitive fashion. We proceed in Section 2.2 by formulating a result for the existence of waves that uses our naming system to decide which equilibria can be connected. Finally, equivalence classes for these waves are introduced in Section 2.3 by exploiting the symmetries present in (2.1).

2.1. Equilibrium types

We will write n-periodic equilibria for the LDE (2.1) in the form

$$u_i = \mathrm{u}_{\mathrm{mod}(i,n)} \tag{2.4}$$

for some vector $\mathrm{u} \in \mathbb{R}^n$, where we let the modulo operator take values in

$$\mathrm{mod}(i, n) \in \{1, \dots, n\}. \tag{2.5}$$

We remark that u can be interpreted as a solution of the Nagumo equation posed on a cyclic graph of length n; see [48]. Taking $n \geq 3$ and introducing the nonlinear mapping

$$G(\mathrm{u}; a, d) := \begin{pmatrix} d(\mathrm{u}_n - 2\mathrm{u}_1 + \mathrm{u}_2) + g\big(\mathrm{u}_1; a\big) \\ d(\mathrm{u}_1 - 2\mathrm{u}_2 + \mathrm{u}_3) + g\big(\mathrm{u}_2; a\big) \\ \vdots \\ d(\mathrm{u}_{n-1} - 2\mathrm{u}_n + \mathrm{u}_1) + g\big(\mathrm{u}_n; a\big) \end{pmatrix} \in \mathbb{R}^n, \tag{2.6}$$

we see that any such equilibrium must satisfy $G(\mathrm{u}; a, d) = 0$.

For any $a \in (0, 1)$ and $\mathrm{u} \in \{0, a, 1\}^n$, it is easy to see that $G(\mathrm{u}; a, 0) = 0$ and to confirm that the diagonal matrix

$$D_1\, G(\mathrm{u}; a, 0) = \mathrm{diag}\big(g'(\mathrm{u}_1; a), \dots, g'(\mathrm{u}_n; a)\big) \tag{2.7}$$

has non-zero entries. In particular, the implicit function theorem implies that each of these 3^n roots is part of a smooth one-parameter family of roots that exists whenever $|d|$ is small. In fact, one can track the location of each of these roots as d is increased, up until the point where the root in question disappears by colliding with another root. This procedure forms the heart of the naming scheme that we develop here, which will allow us to refer to different types of roots in an efficient manner.

In particular, we set out to label solutions of the equation $G(\cdot\,; a, d) = 0$ with words w taken from the set $\{\mathfrak{o}, \mathfrak{a}, \mathfrak{1}\}^n$. We emphasize that we are using the fixed symbol $\mathfrak{a}$ as placeholder for the parameter $a \in (0, 1)$, which is allowed to vary. Indeed, for any $\mathrm{w} \in \{\mathfrak{o}, \mathfrak{a}, \mathfrak{1}\}^n$ we introduce the vector $\mathrm{w}_{|a} \in \mathbb{R}^n$ by writing

$$\big(\mathrm{w}_{|a}\big)_i = \begin{cases} 0 & \text{if } \mathrm{w}_i = \mathfrak{o}, \\ a & \text{if } \mathrm{w}_i = \mathfrak{a}, \\ 1 & \text{if } \mathrm{w}_i = \mathfrak{1}. \end{cases} \tag{2.8}$$

Definition 2.1. Consider a word $\mathrm{w} \in \{\mathfrak{o}, \mathfrak{a}, \mathfrak{1}\}^n$ together with a triplet

$$(\mathrm{u}, a, d) \in [0, 1]^n \times (0, 1) \times [0, \infty). \tag{2.9}$$

Then we say that u is an equilibrium of type w if there exists a C^1-smooth curve

$$[0, 1] \ni t \mapsto \big(\mathrm{v}(t), \alpha(t), \delta(t)\big) \in [0, 1]^n \times (0, 1) \times [0, \infty) \tag{2.10}$$

so that we have

$$(\mathrm{v},\alpha,\delta)(0) = (\mathrm{w}_{|a}, a, 0),$$
$$(\mathrm{v},\alpha,\delta)(1) = (\mathrm{u}, a, d), \tag{2.11}$$

together with

$$G\big(\mathrm{v}(t);\alpha(t),\delta(t)\big) = 0, \quad \det D_1 G\big(\mathrm{v}(t);\alpha(t),\delta(t)\big) \neq 0 \tag{2.12}$$

for all $0 \leq t \leq 1$.

We note that substituting $t = 1$ in (2.12) shows that indeed $G(\mathrm{u}; a, d) = 0$, justifying the terminology of an equilibrium. In addition, the second requirement in (2.12) allows us to apply the implicit function theorem to conclude that $G(\cdot\,; \tilde{a}, \tilde{d}) = 0$ also has equilibria of type w for all pairs $(\tilde{a}, \tilde{d})$ sufficiently close to (a, d). In particular, these observations allow us to introduce the pathwise connected set

$$\Omega_{\mathrm{w}} = \{(a,d) \in \mathcal{H} : \text{the system } G(\cdot\,; a, d) = 0 \text{ admits an equilibrium of type w}\}, \tag{2.13}$$

which is open in the half-strip $\mathcal{H} = [0,1] \times [0,\infty)$.

We now impose several conditions on the structure of these sets Ω_{w} in order to ensure that our classification scheme behaves sensibly. The main issue is to show that the specific shape of the paths (2.10) do not play a role, which involves ruling out loops with non-trivial behaviour. As a preparation, we introduce the set

$$\Gamma = \{(a,d) \in \mathcal{H} : \text{ there exists } u \in \mathbb{R}^n \text{ for which } G(u;a,d) = 0 \text{ and } \det D_1 G(u;a,d) = 0\}, \tag{2.14}$$

which by continuity is a closed subset of $\mathcal{H} = [0,1] \times [0,\infty)$ that contains the upper boundaries of each Ω_{w}.

(HΩ1) For any two words $\mathrm{w}_A, \mathrm{w}_B \in \{\mathfrak{o}, \mathfrak{a}, \mathfrak{1}\}^n$ the intersection $\Omega_{\mathrm{w}_A} \cap \Omega_{\mathrm{w}_B}$ is connected.
(HΩ2) For any word $\mathrm{w} \in \{\mathfrak{o}, \mathfrak{a}, \mathfrak{1}\}^n$ the set Ω_{w} is simply connected.
(HΩ3) Consider any word $\mathrm{w} \in \{\mathfrak{o}, \mathfrak{a}, \mathfrak{1}\}^n$ and any $(a, d) \in \Omega_{\mathrm{w}} \cap \Gamma$. Suppose that $G(\mathrm{u}_i; a_i, d_i) = 0$ is a sequence of equilibria of type w with $(a_i, d_i) \to (a, d)$ and $\mathrm{u}_i \to \mathrm{u}$. Then we have $\det D_1 G(u; a, d) \neq 0$.

We remark that (HΩ3) can be checked by looking at one-dimensional curves instead of two-dimensional sets. It implies that equilibria of type w can be smoothly extended through the parts of the critical set Γ that lie inside Ω_{w}. This allows us to perturb the interior of the curve (2.10) freely within Ω_{w} without changing the value of the equilibrium u.

Lemma 2.1. *Suppose that* (HΩ2) *and* (HΩ3) *are satisfied. Pick a word* $\mathrm{w} \in \{\mathfrak{o}, \mathfrak{a}, \mathfrak{1}\}^n$, *together with a pair of parameters* $(a, d) \in \Omega_{\mathrm{w}}$ *and a pair of curves*

$$[0,1] \ni t \mapsto (\alpha_A, \delta_A)(t) \in \Omega_{\mathrm{w}}, \quad [0,1] \ni t \mapsto (\alpha_B, \delta_B)(t) \in \Omega_{\mathrm{w}} \tag{2.15}$$

that have

$$(\alpha_A, \delta_A)(0) = (\alpha_B, \delta_B)(0) = (a, 0), \quad (\alpha_A, \delta_A)(1) = (\alpha_B, \delta_B)(1) = (a, d). \tag{2.16}$$

Then there exist unique functions

$$[0,1] \ni t \mapsto (\mathrm{v}_A, \mathrm{v}_B)(t) \in \mathbb{R}^n \times \mathbb{R}^n \tag{2.17}$$

so that the triplets $(\mathrm{v}_A, \alpha_A, \delta_A)$ *and* $(\mathrm{v}_B, \alpha_B, \delta_B)$ *both satisfy (2.12) for all* $0 \leq t \leq 1$, *together with the identities*

$$\mathrm{v}_A(0) = \mathrm{v}_B(0) = \mathrm{w}_{|a}, \quad \mathrm{v}_A(1) = \mathrm{v}_B(1). \tag{2.18}$$

Proof. Consider the curve $(\mathrm{v}, \alpha, \delta)$ given in (2.10). Since Ω_{w} is simply connected, this curve can be continuously deformed to either (α_A, δ_A) or (α_B, δ_B) without leaving Ω_{w}. The assumption (*H*Ω3) and the implicit function theorem allow us to modify the curve v in such a way that (2.12) is maintained throughout this deformation. The desired identities (2.18) now follow from the fact that the values v(0) and v(1) remain unchanged. □

In the sequel we will not use (HΩ2) and (HΩ3) directly, but only the conclusion of Lemma 2.1. In particular, if these conditions fail one can still set out to verify the desired path independence 'by hand'. For example, let us assume that $\mathcal{H} \setminus \Gamma$ consists of a finite number N_Γ of components $\{V_i\}_{i=1}^{N_\Gamma}$ that are open in $\mathcal{H}$ and *simply connected*. On account of a global implicit function theorem [49, Theorem 3], there exist non-negative integers $\{m_i\}_{i=1}^{N_\Gamma}$ together with smooth functions

$$\mathrm{u}_{i,j} : V_i \to \mathbb{R}^n, \qquad 1 \leq i \leq N_\Gamma, \quad 1 \leq j \leq m_i \tag{2.19}$$

so that $G(\mathrm{u}_{i,j}(a,d); a, d) = 0$ for each $(a, d) \in V_i$. In addition, $\mathrm{u}_{i,j_1}(a,d) \neq \mathrm{u}_{i,j_2}(a,d)$ whenever $j_1 \neq j_2$ and every solution $G(\cdot; a, d) = 0$ with $(a, d) \in V_i$ can be written in this way.

The path independence can now be verified by checking which of these functions can be connected continuously through the boundaries of adjacent components. Indeed, the conclusion of Lemma 2.1 still holds if there is no sequence of connections that starts in u_{i,j_1} and ends in u_{i,j_2} for some $1 \leq i \leq N_\Gamma$ and some pair $1 \leq j_1 \neq j_2 \leq m_i$. Such a sequence would allow a closed loop to be formed that does not map an equilibrium onto itself.

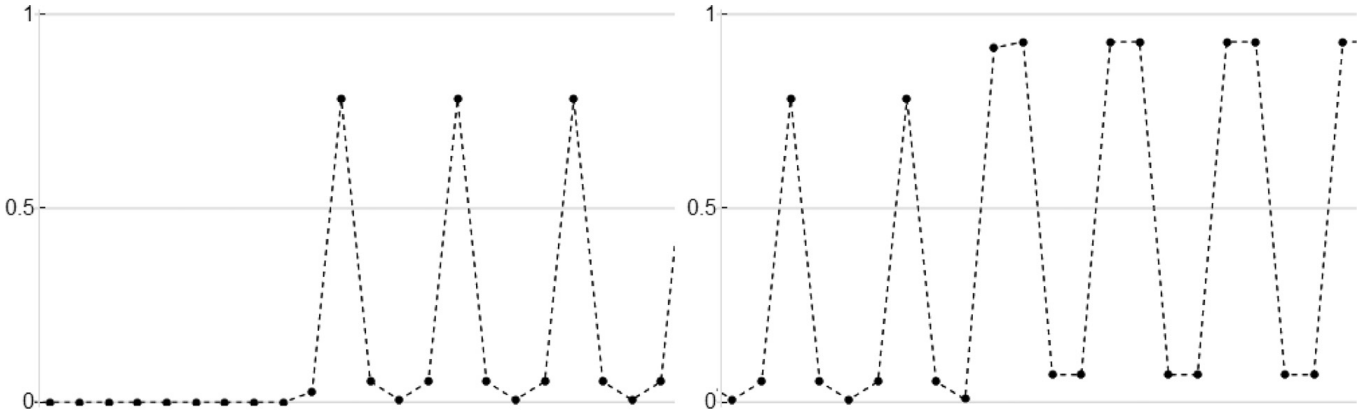

(a) $\mathrm{w}_- = 0000, \mathrm{w}_+ = 0001.$ (b) $\mathrm{w}_- = 0001, \mathrm{w}_+ = 0011.$

Fig. 2. Two examples of 4-chromatic waves as described in Theorem 2.1.

In any case, writing V_* for the component of $\mathcal{H} \setminus \Gamma$ that contains the horizontal segment $(0, 1) \times \{0\}$, (HΩ2) and (HΩ3) can always be achieved if one replaces Ω_{w} by subsets of the form

$$\Omega^*_{\mathrm{w}} = \{(a, d) \in V_* : \text{the system } G(\cdot; a, d) = 0 \text{ admits an equilibrium of type w}\}. \tag{2.20}$$

However, we emphasize that these two conditions appear to be valid without this artificial restriction for the regions that we have numerically computed in this paper.

Corollary 2.1. *Fix an integer $n \geq 2$ and suppose that* (HΩ1), (HΩ2) *and* (HΩ3) *all hold. Then for any word $\mathrm{w} \in \{0, a, 1\}^n$ there is a smooth function $\mathrm{u}_{\mathrm{w}} : \Omega_{\mathrm{w}} \to \mathbb{R}^n$ so that $\mathrm{u}_{\mathrm{w}}(a, d)$ is the unique equilibrium of type w for the system $G(\cdot; a, d) = 0$ for all $(a, d) \in \Omega_{\mathrm{w}}$. In addition, whenever $(a, d) \in \Omega_{\mathrm{w}_A} \cap \Omega_{\mathrm{w}_B}$ for two distinct words $\mathrm{w}_A, \mathrm{w}_B \in \{0, a, 1\}^n$ we have*

$$\mathrm{u}_{\mathrm{w}_A}(a, d) \neq \mathrm{u}_{\mathrm{w}_B}(a, d). \tag{2.21}$$

Proof. The first statement is a consequence of Lemma 2.1 and the implicit function theorem. For the second statement, let us argue by contradiction and assume that both vectors in (2.21) are equal to $\mathrm{u} \in \mathbb{R}^n$. Condition (HΩ1) allows us to pick a path from $(a, 0)$ to (a, d) that lies entirely within $\Omega_{\mathrm{w}_A} \cap \Omega_{\mathrm{w}_B}$. Applying Lemma 2.1 shows that u can be continued as an equilibrium along this path back to both $(\mathrm{w}_A)_{|a}$ and $(\mathrm{w}_B)_{|a}$. However, the implicit function theorem implies that this continuation should be unique. □

We emphasize that our classification scheme only track roots until the first time the associated Jacobian becomes singular and the implicit function theorem can no longer be applied. We will encounter several different types of behaviour at such points. It is possible for two roots to collide and become complex and sometimes even recombine at 'later' parameter values. We will also encounter multi-root collisions where one or more roots survive the collision process. In such cases, we often use an ad-hoc naming system, where we label the emerging branch by reusing or combining the types of the original colliding branches.

2.2. Waves

In this section we focus on wave solutions to (2.1) that connect the n-periodic stationary solutions investigated in the previous section. These so-called multichromatic waves (see Fig. 2) can be written as

$$u_j(t) = \Phi_{\mathrm{mod}(j,n)}(j - ct) \tag{2.22}$$

for some wavespeed $c \in \mathbb{R}$ and $\mathbb{R}^n$-valued waveprofile

$$\Phi = (\Phi_1, \Phi_2, \ldots, \Phi_n) : \mathbb{R} \to \mathbb{R}^n \tag{2.23}$$

that satisfies the boundary conditions

$$\lim_{\xi \to -\infty} \Phi(\xi) = \mathrm{u}_{\mathrm{w}_-}, \quad \lim_{\xi \to +\infty} \Phi(\xi) = \mathrm{u}_{\mathrm{w}_+} \tag{2.24}$$

for some pair of words $\mathrm{w}_\pm \in \{0, a, 1\}^n$; see Corollary 2.1.

Substituting this Ansatz into (2.1) yields the traveling wave functional differential equation

$$\begin{aligned} -c\Phi_1'(\xi) &= d\big[\Phi_n(\xi - 1) - 2\Phi_1(\xi) + \Phi_2(\xi + 1)\big] + g\big(\Phi_1(\xi); a\big), \\ -c\Phi_2'(\xi) &= d\big[\Phi_1(\xi - 1) - 2\Phi_2(\xi) + \Phi_3(\xi + 1)\big] + g\big(\Phi_2(\xi); a\big), \end{aligned}$$

$$\vdots$$

$$-c\Phi_n'(\xi) = d\big[\Phi_{n-1}(\xi-1) - 2\Phi_n(\xi) + \Phi_1(\xi+1)\big] + g\big(\Phi_n(\xi); a\big), \tag{2.25}$$

which has positive coefficients on all shifted terms and also has diagonal nonlinearities. This system hence fits into the framework developed in [27], provided that the assumptions pertaining to the boundary conditions (2.24) can also be validated.

This is in fact the key question that we address in our main result below. This result requires the following assumption, which states that our root tracking scheme captures all (marginally) stable[2] n-periodic equilibria of the LDE. In particular, the types of these equilibria correspond with words from the *stable* subset $\{0,1\}^n$. This assumption is satisfied for all the cases considered in this paper, but the example in [28, Section 1.2] shows how it can fail for non-cubic bistable nonlinearities.

(HS) Recall the definitions (2.2) and (2.14) and suppose that $G(\mathrm{u}; a, d) = 0$ for some $\mathrm{u} \in \mathbb{R}^n$ and $(a, d) \in \mathcal{H}$. Suppose furthermore that all eigenvalues λ of $D_1 G(\mathrm{u}; a, d)$ satisfy $\lambda \leq 0$. Then we have[3] $\mathrm{u} = \mathrm{u}_{\mathrm{w}}(a, d)$ for some $\mathrm{w} \in \{0,1\}^n$ and $(a, d) \in \overline{\Omega}_{\mathrm{w}}$.

Theorem 2.1 (see Section 5). *Fix an integer $n \geq 2$ and assume that* (HΩ1), (HΩ2), (HΩ3) *and* (HS) *all hold. Consider two distinct words $\mathrm{w}_-, \mathrm{w}_+ \in \{0,1\}^n$ with $\mathrm{w}_- \leq \mathrm{w}_+$ and pick $(a, d) \in \Omega_{\mathrm{w}_-} \cap \Omega_{\mathrm{w}_+}$ with $d > 0$. Suppose furthermore that one of the following conditions holds.*

(a) *The words w_- and w_+ differ at precisely one location.*
(b) *For each $\mathrm{w} \in \{0,1\}^n \setminus \{\mathrm{w}_-, \mathrm{w}_+\}$ that satisfies $\mathrm{w}_- \leq \mathrm{w} \leq \mathrm{w}_+$ we have $(a, d) \notin \overline{\Omega}_{\mathrm{w}}$.*

Then there exists a unique $c \in \mathbb{R}$ for which the travelling system (2.25) admits a solution $\Phi : \mathbb{R} \to \mathbb{R}^n$ that satisfies the boundary conditions

$$\lim_{\xi \to -\infty} \Phi(\xi) = \mathrm{u}_{\mathrm{w}_-}(a, d), \quad \lim_{\xi \to +\infty} \Phi(\xi) = \mathrm{u}_{\mathrm{w}_+}(a, d). \tag{2.26}$$

If $c \neq 0$, then Φ is unique up to translation and each component is strictly increasing.

The main task in Section 5 is to show that the ordering $\mathrm{w}_- \leq \mathrm{w}_+$ extends to the boundary conditions (2.26), i.e. $\mathrm{u}_{\mathrm{w}_-}(a, d) \leq \mathrm{u}_{\mathrm{w}_+}(a, d)$. Indeed, one does not expect wave connections to exist between states that cannot be ordered. The main reason for this is that the leading order spatial eigenvalue for the linearization of (2.25) around a stable equilibrium has an eigenvector with strictly positive components (see e.g. the Krein–Rutman theorem). This is no longer a natural orientation when attempting to connect non-ordered limiting states, leading to oscillatory behaviour that conflicts with the comparison principle.

2.3. Symmetries

There are a number of useful symmetries present in the equilibrium equation $G(\mathrm{u}; a, d) = 0$ and the travelling wave MFDE (2.25). We explore three important transformations here that significantly reduce the number of cases that need to be considered.

We first note that the identity $g(1-u; a) = -g(u; 1-a)$ implies that

$$G(\mathbf{1} - \mathrm{u}; a, d) = -G(\mathrm{u}; 1-a, d) \tag{2.27}$$

holds for all $\mathrm{u} \in \mathbb{R}^n$, with $\mathbf{1} = (1, \dots, 1)^\top \in \mathbb{R}^n$. In order to exploit this, we pick $\mathrm{w} \in \{0, \mathfrak{a}, 1\}^n$ and write $\mathrm{w}_{0 \leftrightarrow 1} \in \{0, \mathfrak{a}, 1\}^n$ for the 'inverted' word

$$(\mathrm{w}_{0 \leftrightarrow 1})_i = \begin{cases} 1 & \text{if } \mathrm{w}_i = 0, \\ \mathfrak{a} & \text{if } \mathrm{w}_i = \mathfrak{a}, \\ 0 & \text{if } \mathrm{w}_i = 1. \end{cases} \tag{2.28}$$

The identity (2.27) directly implies the reflection relation

$$\Omega_{\mathrm{w}_{0 \leftrightarrow 1}} = \{(a, d) : (1-a, d) \in \Omega_{\mathrm{w}}\}, \tag{2.29}$$

together with

$$\mathrm{u}_{\mathrm{w}_{0 \leftrightarrow 1}}(a, d) = \mathbf{1} - \mathrm{u}_{\mathrm{w}}(1-a, d). \tag{2.30}$$

We proceed by introducing the coordinate-shifts $\{T_k\}_{k=1}^n : \mathbb{R}^n \to \mathbb{R}^n$ and reflection $R : \mathbb{R}^n \to \mathbb{R}^n$ that act as

$$(T_k \mathrm{u})_i = \mathrm{u}_{\mathrm{mod}(i+k,n)}, \qquad \big(R\mathrm{u}\big)_i = \mathrm{u}_{\mathrm{mod}(1-i,n)}. \tag{2.31}$$

[2] We use the eigenvalues of the matrix $D_1 G(\mathrm{u}; a, d)$ to characterize the stability of u. Using the comparison principle this can be easily transferred to the full LDE (1.1).

[3] If $(a, d) \in \partial\Omega_{\mathrm{w}}$ this identity should be interpreted as a limit.

It is easy to verify that the identity $G(\mathrm{u}; a, d) = 0$ implies that also

$$G(T_k \mathrm{u}; a, d) = G(R\mathrm{u}; a, d) = 0. \tag{2.32}$$

In addition, when (c, Φ) is a solution to the travelling wave MFDE (2.25), the same holds for the coordinate-shifted pair $(c, T_k\Phi)$ and the reflected version $(-c, \tilde{\Phi})$ with

$$\tilde{\Phi}(\xi) = R\Phi(-\xi). \tag{2.33}$$

These identities are all consequence of the invariance of the Nagumo LDE (2.1) under the transformations $j \mapsto j + k$ and $j \mapsto -j$.

Our choice to only consider waves where $\Phi(-\infty) \leq \Phi(+\infty)$ breaks the reflection invariance (2.33), which allows us to focus solely on the symmetry caused by the coordinate shifts T_k. In particular, for any word $\mathrm{w} \in \{0, a, 1\}^n$, we write

$$\Omega_{[\mathrm{w}]} = \Omega_{\mathrm{w}} = \Omega_{T_1\mathrm{w}} = \ldots = \Omega_{T_{n-1}\mathrm{w}}. \tag{2.34}$$

In addition, we introduce the shorthand notation

$$[\mathrm{w}] = \{\mathrm{u}_{\mathrm{w}}, T_1\mathrm{u}_{\mathrm{w}}, \ldots, T_{n-1}\mathrm{u}_{\mathrm{w}}\} \tag{2.35}$$

to refer to all the roots in the corresponding equivalence class, which are defined for $(a, d) \in \Omega_{[\mathrm{w}]}$.

Note that we are hence treating $[0a1]$ and $[01a]$ as separate classes, even though they correspond with equivalent equilibria of $G(\cdot; a, d) = 0$. Interestingly enough, when restricting attention to the alphabet $\{0, 1\}^n$, this distinction only plays a role for $n \geq 6$. For example, 001011 is not shift-related to its reflection 110100, but all shorter binary sequences are.

Whenever we are referring to an equivalence class of roots, we will use the word that is the smallest in the lexicographical[4] sense (the so-called Lyndon word) as a class representative. For example, $0a11$ is the Lyndon word for the class

$$[0a11] = \{\mathrm{u}_{0a11}, \mathrm{u}_{10a1}, \mathrm{u}_{110a}, \mathrm{u}_{a110}\}. \tag{2.36}$$

We note that shorter words with a length that divides n can also be interpreted as a word of length n by periodic extension. For example, we write

$$[01] = [0101] = \{\mathrm{u}_{0101}, \mathrm{u}_{1010}\}. \tag{2.37}$$

For any pair $\mathrm{w}_\pm \in \{0, 1\}^n$ with $\mathrm{w}_- \leq \mathrm{w}_+$, we will use the shorthand notation $\mathrm{u}_{\mathrm{w}_-} \to \mathrm{u}_{\mathrm{w}_+}$ to refer to any pair (c, Φ) that satisfies the travelling wave MFDE (2.25) together with the boundary conditions (2.26). The observations above show that $T_k\mathrm{u}_{\mathrm{w}_-} \to T_k\mathrm{u}_{\mathrm{w}_+}$ then corresponds with the pair $(c, T_k\Phi)$.

In order to refer to an equivalence class of wave solutions, we pick $\mathrm{w}_- \leq \mathrm{w}_+$ and introduce the notation

$$[\mathrm{w}_- \to \mathrm{w}_+] = \{\mathrm{u}_{\mathrm{w}_-} \to \mathrm{u}_{\mathrm{w}_+}, T_1\mathrm{u}_{\mathrm{w}_-} \to T_1\mathrm{u}_{\mathrm{w}_+}, \ldots, T_{n-1}\mathrm{u}_{\mathrm{w}_-} \to T_{n-1}\mathrm{u}_{\mathrm{w}_+}\}. \tag{2.38}$$

Here we always take w_- to be the Lyndon representative for its equivalence class, but we emphasize that w_+ *cannot* always be chosen in this way. For example,

$$[001 \to 011] = \{\mathrm{u}_{001} \to \mathrm{u}_{011}, \mathrm{u}_{100} \to \mathrm{u}_{101}, \mathrm{u}_{010} \to \mathrm{u}_{110}\} \tag{2.39}$$

refers to a different set of waves than

$$[001 \to 101] = \{\mathrm{u}_{001} \to \mathrm{u}_{101}, \mathrm{u}_{100} \to \mathrm{u}_{110}, \mathrm{u}_{010} \to \mathrm{u}_{011}\}. \tag{2.40}$$

Naturally, this distinction disappears when considering waves that connect to or from one of the monochromatic states $[0]$ and $[1]$.

3. Trichromatic waves

In this section we apply our results to the trichromatic case $n = 3$. As in the bichromatic case considered in [1], we observe that stable 3-periodic equilibria can only exist inside the parameter region where the monochromatic $[0 \to 1]$ wave is pinned. The novel behaviour as compared to the bichromatic case is that there exist intervals of the parameter a in which the number of (stable) equilibria can actually increase as d is increased (e.g., for $a = 0.40146$, see Figs. 4 and 6). In addition, for values of a in these intervals, there are two disjoint intervals of parameters d for which *travelling* trichromatic waves exist that connect the homogeneous states $[0]$ and $[1]$ to a stable 3-periodic equilibrium. Similarly, for a fixed d, the number of (stable) equilibria can increase as $\left|a - \frac{1}{2}\right|$ is increased (e.g., for $d = 0.04$, see Fig. 4).

3.1. Equilibria

Fig. 3 illustrates several trichromatic equilibria for (2.1), which correspond to roots $\mathrm{u} \in \mathbb{R}^3$ of the nonlinear function

$$G(\mathrm{u}; a, d) = \begin{pmatrix} d(\mathrm{u}_3 - 2\mathrm{u}_1 + \mathrm{u}_2) + g(\mathrm{u}_1; a) \\ d(\mathrm{u}_1 - 2\mathrm{u}_2 + \mathrm{u}_3) + g(\mathrm{u}_2; a) \\ d(\mathrm{u}_2 - 2\mathrm{u}_3 + \mathrm{u}_1) + g(\mathrm{u}_3; a) \end{pmatrix}. \tag{3.1}$$

[4] For ordering purposes we assume that $0 < a < 1$ holds.

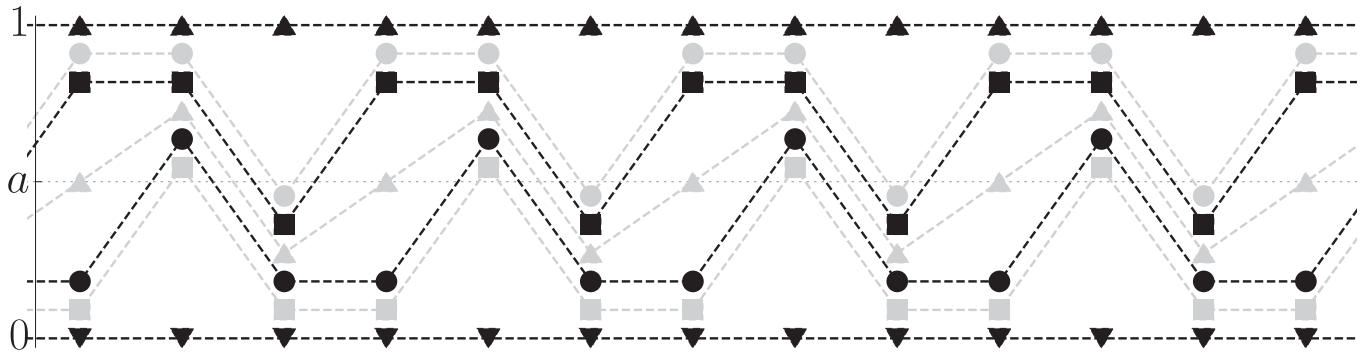

Fig. 3. Schematic illustration of several stable (black) and unstable (gray) 3-periodic equilibria for (2.1), namely $u_{\circ}$, $u_{\circ\circ a}$, $u_{\circ\circ 1}$, $u_{\circ a 1}$, $u_{\circ 11}$, u_{a11} and u_{1} (bottom to top). The values were adjusted for presentation purposes without changing the ordering properties which follow from Lemma 5.2.

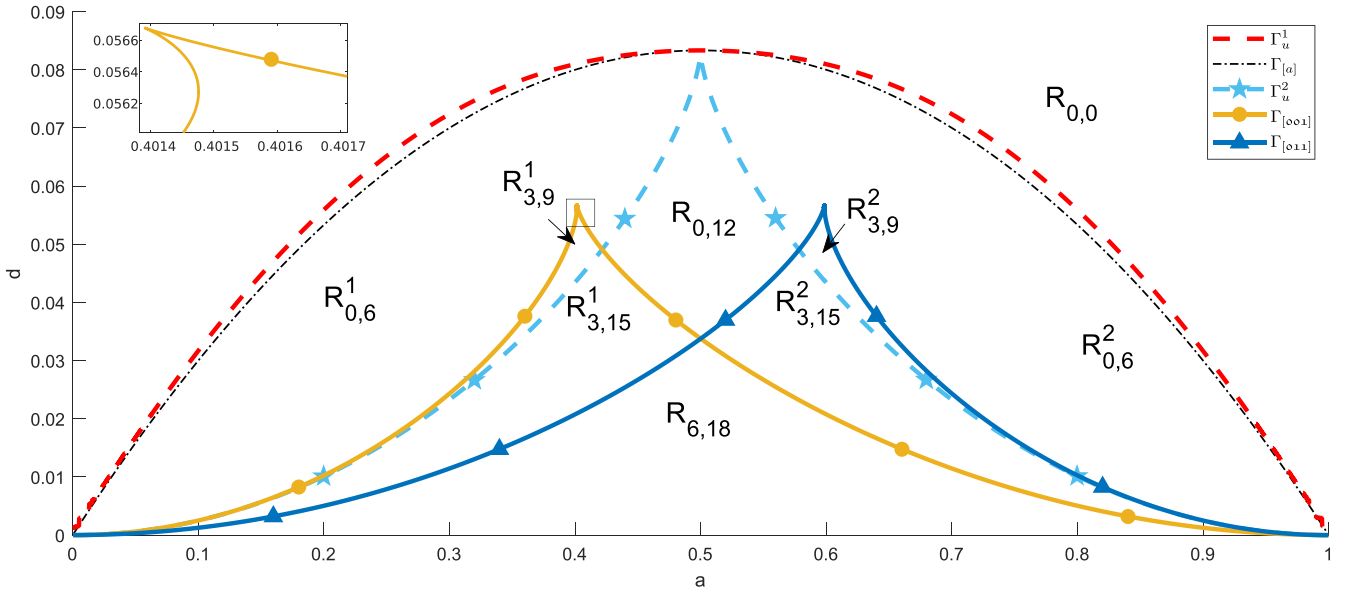

Fig. 4. Bifurcation thresholds for the number of roots of (3.1). The subscripts in the regions R indicate the number of stable and unstable roots present in each region, counting their multiplicities but excluding the homogeneous roots $[\circ]$, $[a]$ and $[1]$.

Inspection of this system shows that one component can be removed if one enforces either $u_1 = u_2$, $u_2 = u_3$ or $u_1 = u_3$.

In Fig. 4 we numerically computed the critical set Γ defined in (2.14) by searching for roots of the augmented system

$$G_*(u; a, d) = \begin{pmatrix} G(u; a, d) \\ \det D_1 G(u; a, d) \end{pmatrix}. \tag{3.2}$$

The results show that Γ can be decomposed into 5 piecewise-smooth curves that we label as $\Gamma_{[a]}$, $\Gamma_{[\circ\circ 1]}$, $\Gamma_{[\circ 11]}$, Γ_u^1 and Γ_u^2. The labels of the form $\Gamma_{[w]}$ imply that $\Gamma_{[w]} \subset \partial\Omega_{[w]}$. We emphasize that this naming scheme is ambiguous by its very nature. Indeed, collisions between roots occur precisely on these curves, which also intersect each other.

These 5 curves divide the remaining parameter space $\mathcal{H} \setminus \Gamma$ into 11 open and simply connected components. Ignoring the three homogeneous roots[5] $[\circ]$, $[a]$ and $[1]$, the bottom region $R_{6,18}$ contains 6 stable roots and 18 unstable roots. The stable roots are represented by the equivalence classes $[\circ\circ 1]$ and $[\circ 11]$, while all the remaining equivalence classes generate the unstable roots. We recall the identity (2.27,) which explains the reflection symmetry through the line $a = \frac{1}{2}$ and allows us to focus on the case $a \in (0, \frac{1}{2}]$.

In the discussion below we indicate how this configuration changes as each of the critical curves is crossed. In addition, we obtain asymptotic expansions for the curves $\Gamma_{[\circ\circ 1]}$ and $\Gamma_{[\circ 11]}$ associated to the stable trichromatic roots near the corner $(a, d) = (0, 0)$. This allows us to confirm the assumptions in Section 2 in the regions where the curves cannot easily be distinguished numerically. As explained in Section 1, we are also interested in the properties of such curves for large n. Hopefully the insights gained here for $n = 3$ could help with this endeavour.

[5] In the current trichromatic context, these roots are given by (0,0,0), (a, a, a) and (1,1,1).

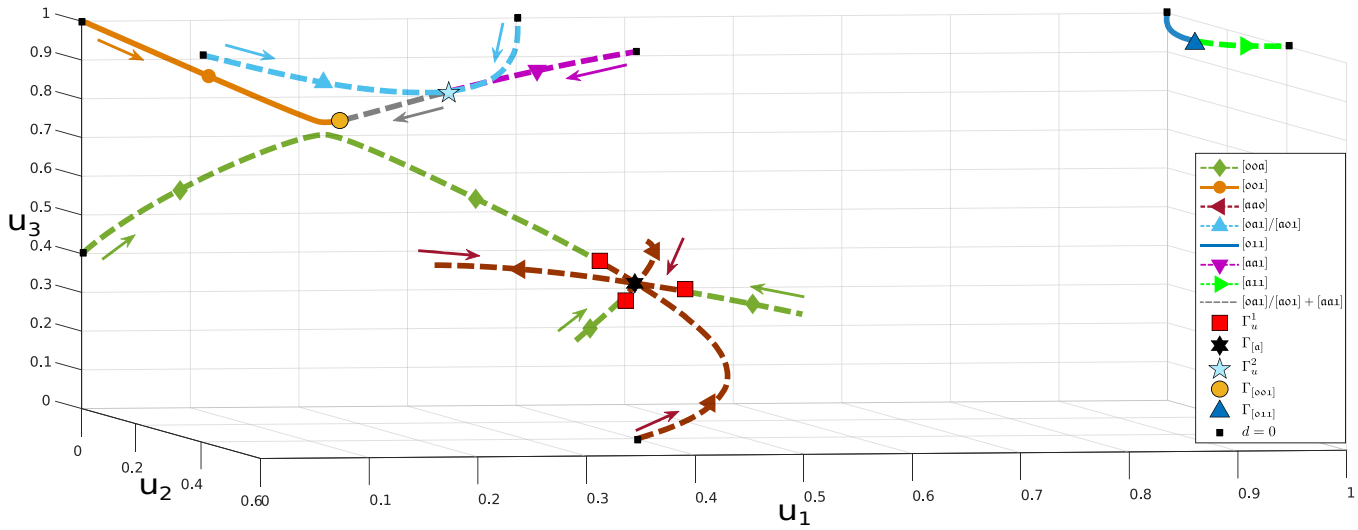

Fig. 5. Root trajectories as d is increased for $a = 0.401 < a_c$. The continuous lines represent stable roots branches, while the dashed ones are unstable. In principle only one element of each root class is displayed. However, we (locally) plot all three permutations of $\mathtt{oaa}$ to show how they all collide with (a, a, a) at $\Gamma_{[\mathtt{a}]}$ and subsequently pass through each other. Finally, they hit the three permutations of $\mathtt{ooa}$ at Γ^1_u and disappear. We emphasize that $\mathtt{aoi}$ is not a Lyndon word, but we need to use it here to describe the Γ^2_u collision.

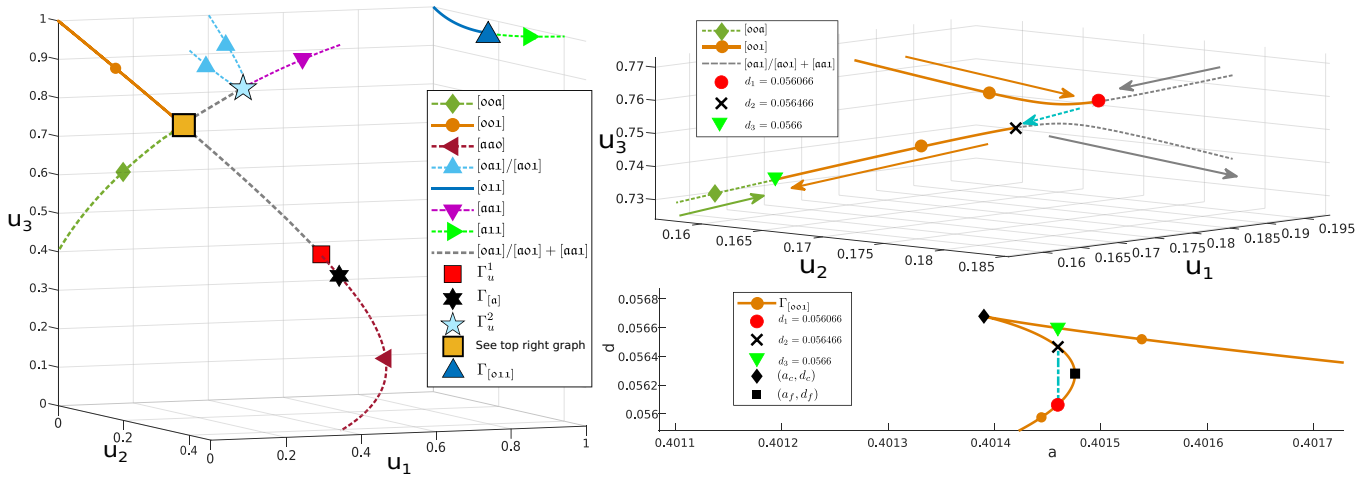

Fig. 6. Behaviour of the root branches near the cusp of the yellow $\Gamma_{[\mathtt{oo1}]}$ curve from Fig. 4, which is magnified in the bottom right panel. In particular, we fix $a = 0.40146 \in (a_c, a_f)$ and note that $\Gamma_{[\mathtt{oo1}]}$ is crossed three times as d is increased. The top right panel contains a zoom of the yellow square from the left panel, which is impacted by these crossings. The blue dashed line between the red circle and black cross represents the region where two of the roots are temporarily complex. These plots illustrate the mechanism by which the stable branch $[\mathtt{oo1}]$ switches its unstable connecting branch as a is increased through the cusp and fold points a_c and a_f. (For interpretation of the references to colour in this figure legend, the reader is referred to the web version of this article.)

3.1.1. *The* $\Gamma_{[\mathtt{o11}]}$ *threshold*

The first threshold that is encountered when increasing d for $a \in (0, \frac{1}{2})$ is the curve $\Gamma_{[\mathtt{o11}]}$. Here the stable roots $[\mathtt{o11}]$ collide with the unstable roots $[\mathtt{a11}]$, after which both branches disappear. This collision is visible in Figs. 5–7.

In order to find an expansion for this threshold near the corner $(a, d) = (0, 0)$, we exploit the observations above which allow us to consider equilibria close to (0,1,1) for which the second and third components are equal. In particular, we construct solutions to the problem

$$G\big((x, 1+y, 1+y); a, d\big) = 0 \tag{3.3}$$

for which $|x| + |y| + |a| + |d|$ is small. The resulting system has a structure that is very similar to that encountered in [1], allowing us to follow the exact same procedure to unfold the saddle node bifurcations. In particular, viewing $\Gamma_{[\mathtt{o11}]}$ locally as the graph of the function $d_{[\mathtt{o11}]}$, we obtain the expansion

$$d_{[\mathtt{o11}]}(a) = \frac{a^2}{8} + \frac{a^4}{64} + O(a^5), \tag{3.4}$$

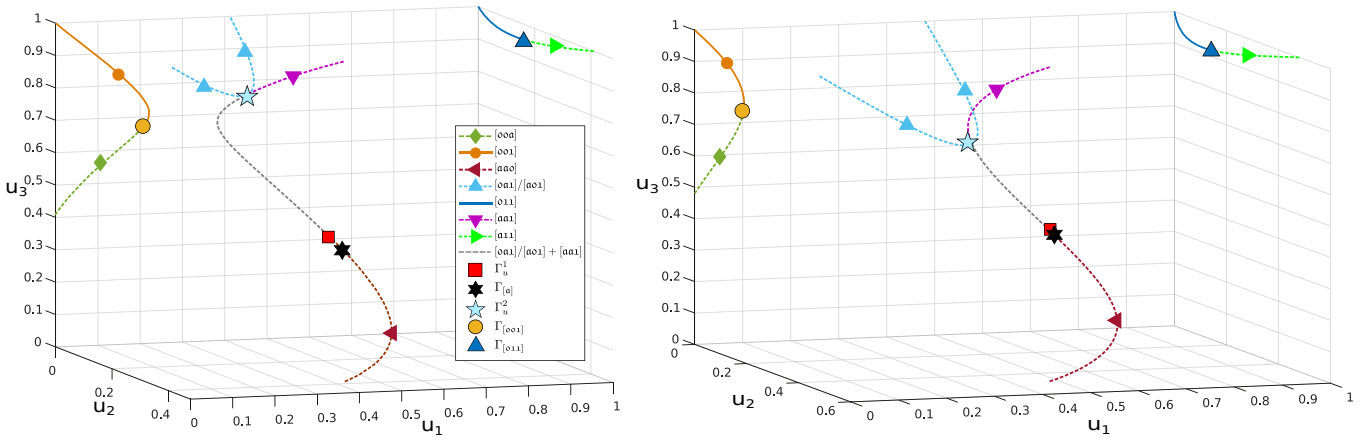

Fig. 7. Root branches for $a = 0.41 > a_f$ (left) and $a = 0.48 > a_f$ (right). The branch $[\circ\circ\mathtt{1}]$ now collides with $[\circ\circ\mathtt{a}]$, while the unstable branch spawned by the Γ_u^2 collision collides with $[\circ\mathtt{a}\mathtt{a}]$ at Γ_u^1. The collision points Γ_u^1 and Γ_u^2 slide through (a, a, a) as a is increased beyond $a = \frac{1}{2}$.

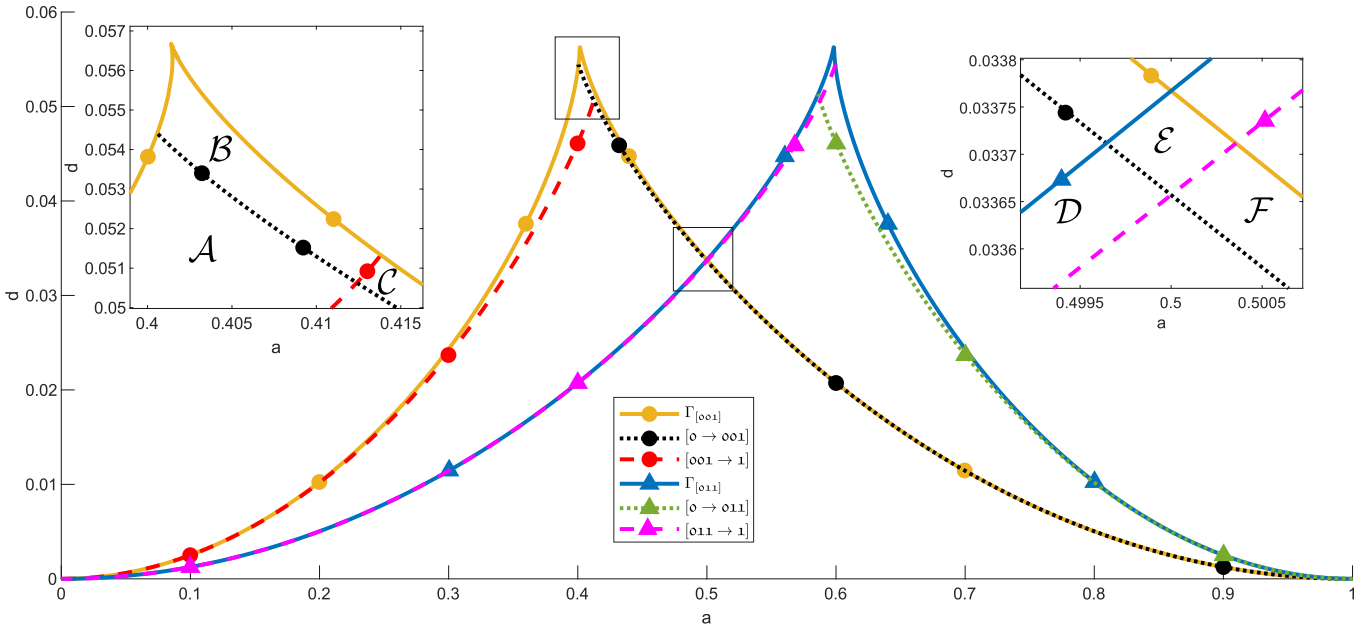

Fig. 8. Thresholds where standing waves ($c = 0$) transition to travelling waves ($c \neq 0$) for the connections to and from the homogeneous equilibria $[\circ]$ and $[\mathtt{1}]$. The labels $\mathcal{A} - \mathcal{F}$ are used to describe wave collisions in Section 3.9.

together with

$$\mathrm{u}_{\circ\mathtt{11}}\left(a; d_{[\circ\mathtt{11}]}(a)\right) = \left(\frac{a}{2}, 1 - \frac{a^2}{8} - \frac{a^3}{16} - \frac{a^4}{64}, 1 - \frac{a^2}{8} - \frac{a^3}{16} - \frac{a^4}{64}\right) + O(a^5). \tag{3.5}$$

This curve hence (locally) lies below the bichromatic threshold discussed in Section 21.

3.1.2. *The* Γ_u^2 *threshold*

This curve features the triple collision of the unstable branches $[\circ\mathtt{a}\mathtt{1}]$, $[\mathtt{a}\circ\mathtt{1}]$ and $[\mathtt{a}\mathtt{a}\mathtt{1}]$ when $a \in (0, \frac{1}{2})$. One unstable branch of roots emerges from this collision. This collision is visible in Figs. 5–7.

3.1.3. *The* $\Gamma_{[\circ\circ\mathtt{1}]}$ *threshold*

The important feature of this curve is that d cannot be expressed as a function of a. Indeed, the function

$$G_{**}(\mathrm{u}; a, d) = \begin{pmatrix} G_*(\mathrm{u}; a, d) \\ \det D_{1,3} G_*(\mathrm{u}; a, d) \end{pmatrix} \tag{3.6}$$

has the (numerically computed) roots

$$(a_c, d_c) \approx (0.4013889, 0.05668), \qquad (a_f, d_f) \approx (0.401476, 0.056275), \tag{3.7}$$

which correspond with a cusp respectively fold point for the curve $\Gamma_{[\mathfrak{001}]}$; see Figs. 4 and 6.

When $a \in (0, a_c)$, the root $[\mathfrak{001}]$ hits the branch spawned by the Γ_u^2 collision and disappears; see Fig. 5. On the other hand, for $a \in (a_f, 1)$ the root $[\mathfrak{001}]$ hits $[\mathfrak{00a}]$; see Fig. 7. This corresponds with the scenario described above for $\Gamma_{[\mathfrak{011}]}$ after applying the $\mathfrak{0} \leftrightarrow \mathfrak{1}$ swap.

The intermediate case $a \in (a_c, a_f)$ is illustrated in Fig. 6. In this case the root $[\mathfrak{001}]$ again hits the branch spawned by the Γ_u^2 collision and disappears, but this pair reappears and splits off from each other after d crosses the $\Gamma_{[\mathfrak{001}]}$ threshold a second time. The stable branch of this pair collides with $[\mathfrak{00a}]$ and disappears when d crosses $\Gamma_{[\mathfrak{001}]}$ for the third and final time, while the unstable branch emerges as the survivor of the full triple crossing process.

The black cross and green triangle in Fig. 6 overlap when $a = a_c$, in which case the $[\mathfrak{00a}]$ branch has a triple root at the critical value $d = d_c$. On the other hand, the black cross and red circle in this figure overlap when $a = a_f$, in which case the branch $[\mathfrak{001}]$ and the branch spawned by the Γ_u^2 collision can be said to bounce off each other at $d = d_f$.

In order to find an expansion for this threshold near the corner $(a, d) = (0, 0)$, we now look for solutions to

$$G\big((x, x, 1+y); a, d\big) = 0 \tag{3.8}$$

for which $|x| + |y| + |a| + |d|$ is small. Viewing $\Gamma_{[\mathfrak{001}]}$ locally as the graph of the function $d_{[\mathfrak{001}]}$, we may again use the same procedure as in [1] to obtain the expansion

$$d_{[\mathfrak{001}]}(a) = \frac{a^2}{4} + \frac{a^4}{8} + O(a^5), \tag{3.9}$$

together with

$$\mathrm{u}_{\mathfrak{001}}(a; d_{[\mathfrak{001}]}(a)) = \left(\frac{a}{2}, \frac{a}{2}, 1 - \frac{a^2}{8} - \frac{a^3}{16} - \frac{a^4}{64}\right) + O(a^5). \tag{3.10}$$

The fact that this curve (locally) lies above $\Gamma_{[\mathfrak{011}]}$ is hence already visible at leading order.

3.1.4. *The* $\Gamma_{[\mathfrak{a}]}$ *threshold*

This curve is characterized by the relation $\det D_1 G([\mathfrak{a}]; a, d) = 0$, which can be explicitly solved to yield $d_{[\mathfrak{a}]}(a) = a(1 - a)/3$. As shown in Fig. 5, the three branches of roots contained in the equivalence class $[\mathfrak{0a0}]$ all pass through (a, a, a) at $d = d_{[\mathfrak{a}]}$ and survive the collision.

3.1.5. *The* Γ_u^1 *threshold*

On this threshold the unstable branch that survived the Γ_u^2 and $\Gamma_{[\mathfrak{001}]}$ collisions hits the branch $[\mathfrak{0a0}]$ that passed through (a, a, a); see Figs. 5–7. Above this threshold the only remaining equilibria are the homogeneous states $[\mathfrak{0}][\mathfrak{a}]$ and $[\mathfrak{1}]$.

3.1.6. *The critical case* $a = \frac{1}{2}$

The right panel in Fig. 7 describes the situation just before a reaches the critical value $a = \frac{1}{2}$. Upon increasing a through this value, the collisions at Γ_u^2 and Γ_u^1 both cross through the center $(\frac{1}{2}, \frac{1}{2}, \frac{1}{2})$ at $a = \frac{1}{2}$ and $d = d_{[a]}(\frac{1}{2}) = \frac{1}{12}$, transitioning to occur on the $[\mathfrak{0a0}]$ branch.

3.2. Wave connections

Our numerical results strongly suggest that (HΩ1) – (HΩ3) and (HS) are satisfied, allowing us to apply the results in Section 2. Fig. 9 represents the equivalence classes of wave connections between neighbouring words. We note that we are not drawing an edge from $\mathfrak{101}$ because this is not a Lyndon word.

We recall that Theorem 2.1 does not provide any information about the speed c of the travelling wave. We therefore resorted to numerics to find parameter values where $c \neq 0$ for the waves discussed in the diagram above. This was done by connecting the two endstates with a tanh profile and letting this initial profile evolve under the flow of 2.1. Exploiting the stability of the moving waves, one can test whether $c = 0$ by determining whether movement ceases after an initial transient period.

For the $[\mathfrak{001} \to \mathfrak{011}]$ and $[\mathfrak{001} \to \mathfrak{101}]$ connections we were not able to find any regions where $c \neq 0$. However, in Fig. 8 we can observe the numerically computed minimum threshold for d where we in fact have $c \neq 0$ for the waves that connect to and from the homogeneous states $[\mathfrak{0}]$ and $[\mathfrak{1}]$. Although these threshold curves are often very close to the boundary of the existence region for the associated stable trichromatic root, our numerical results strongly suggest that they touch only in the corners $d = 0$. This was rigorously established for the bichromatic case in [1].

Notice that the $[\mathfrak{0} \to \mathfrak{001}]$ and $[\mathfrak{001} \to \mathfrak{1}]$ waves both have non-zero speed in region $\mathcal{B}$, which contains the fold and cusp points of $\Gamma_{[\mathfrak{001}]}$. This indicates that travelling waves can appear and disappear twice as the diffusion coefficient is increased, which does not happen in the bichromatic case.

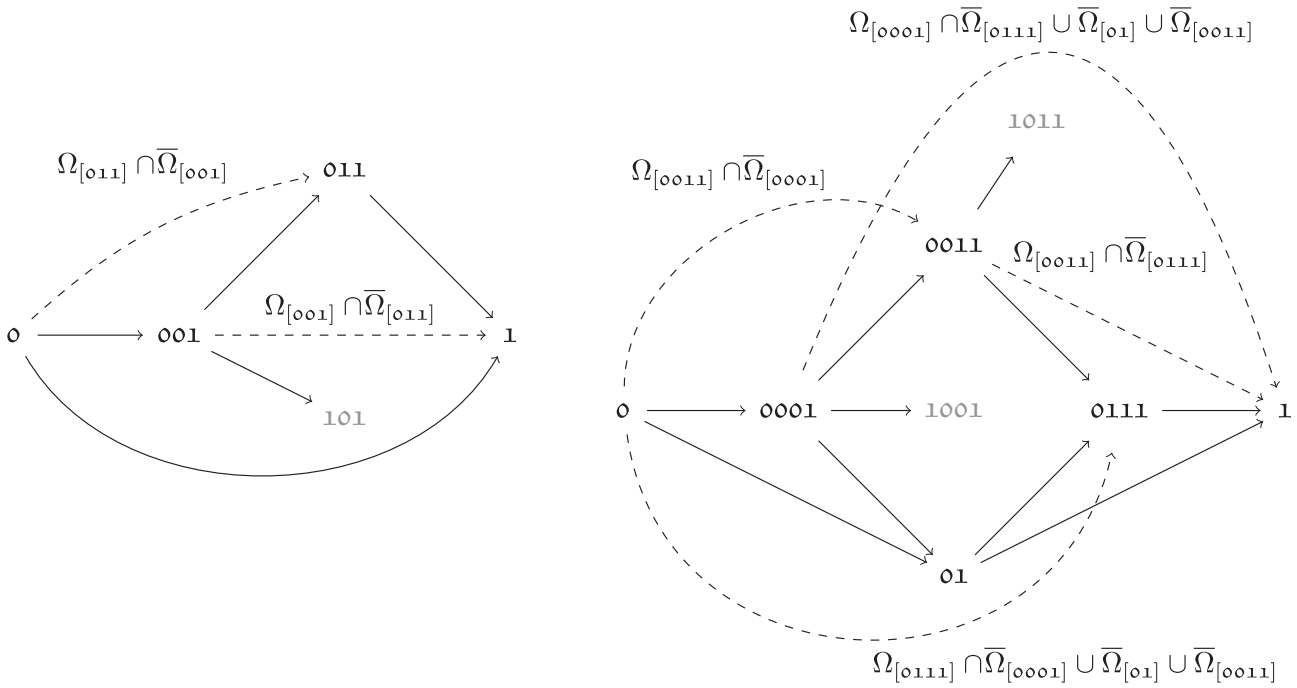

Fig. 9. This diagram depicts the trichromatic (left) and quadrichromatic (right) wave connections predicted by the theory in Section 2. A solid edge from w_- to w_+ indicates that waves of type $[w_- \to w_+]$ exist for $(a, d) \in \Omega_{[w_+]} \cap \Omega_{[w_-]}$ with $d > 0$ by applying Theorem 2.1 with option (a). A dashed edge indicates that this connection is covered by option (b). In this case, the connection is only guaranteed to exist in the parameter region displayed next to the edge, because intermediate stable roots have to be ruled out. The asymptotics in Sections 3.1 and 4.1 guarantee that all the relevant parameter regions are non-empty. In addition, the connections $[0001 \to 1101]$, $[0001 \to 0111]$ and $[0001 \to 1011]$ are not listed because $\Omega_{[0001]} \cap \Omega_{[0111]}$ is contained in $\Omega_{[0011]}$. To prevent clutter, we have also left out the monochromatic $[0 \to 1]$ connection in the diagram on the right. The words that are gray are *not* Lyndon words and as such do not have any outgoing arrows; see the discussion in Section 2.3.

3.3. Wave collisions

In order to investigate interactions between waves, we set out to find ordered triplet of words $w_A \leq w_B \leq w_C$ from the stable set $\{0, 1\}^n$, for which the waves $[w_A \to w_B]$ and $[w_B \to w_C]$ both exist. In addition, we demand that at least one of these two waves has non-zero speed. One can then construct an initial condition that resembles the two waveprofiles separated by a buffer-zone containing the stable equilibrium $[w_B]$ and study the resulting dynamics.

Zooming in near the cusp of $\Gamma_{[001]}$, Fig. 8 identifies three regions $\mathcal{A} - \mathcal{C}$ that are relevant for collisions between $[0 \to 001]$ and $[001 \to 1]$ waves. In Fig. 10 we give snapshots of the collision process occurring in regions $\mathcal{A}$ and $\mathcal{B}$. In both cases the buffer-zone containing $[001]$ is consumed by one ($\mathcal{A}$) or both ($\mathcal{B}$) of the incoming trichromatic waves, leading eventually to a pinned monochromatic wave. This type of collision can also be observed in the bichromatic setting.

A novel feature in this trichromatic setting is that one can make longer collision chains. Indeed, let us consider parameter values in regions $\mathcal{D} - \mathcal{F}$ of Fig. 8. We can then construct initial conditions resembling a $[0 \to 001]$ wave on the left, a $[001 \to 011]$ standing wave in the center and a $[011 \to 1]$ wave on the right. The intermediate wave is consumed from the left ($\mathcal{F}$), right ($\mathcal{D}$) or both directions ($\mathcal{E}$), again resulting in a pinned monochromatic wave that can be non-monotonic. An illustration of a type $\mathcal{E}$ collision can be found in Fig. 11.

3.4. Example

In order to illustrate all the concepts discussed in this section, we examine the curve $d \mapsto u_{001}(a, d)$ for the fixed parameter value $a = 0.40146 \in (a_c, a_f)$. In particular, we discuss all the changes in behaviour that occur as the diffusion coefficient d is increased from zero. The three components of this curve are plotted in Fig. 12, along with several other equilibria that interact with u_{001}. This figure can be seen as an alternative visualization of the setting in Fig. 6, with matching colour codes and symbols.

The first change occurs as we cross through $\Gamma_{[011]}$ at $d = 0.0209$ (blue triangle), where the stable root u_{011} disappears. Here the standing waves $u_{001} \to u_{011}$ and $u_{001} \to u_{101}$ are replaced by standing waves $u_{001} \to 1$. These latter waves start to travel after crossing $d = 0.046615$ (orange line). In particular, we are in region $\mathcal{A}$ of Fig. 4, which features the standing-moving wave collisions featured in the lower panes of Fig. 10.

Moving beyond $d = 0.05405$ (gray line), the $u_0 \to u_{001}$ waves also start to travel, placing us in region $\mathcal{B}$ of Fig. 4 and allowing the collisions in the upper panes of Fig. 10 to occur. At $d = 0.056066$ (red dot) however, u_{001} disappears by colliding with the branch of roots that emerges from the collision at Γ_u^2 (blue stars).

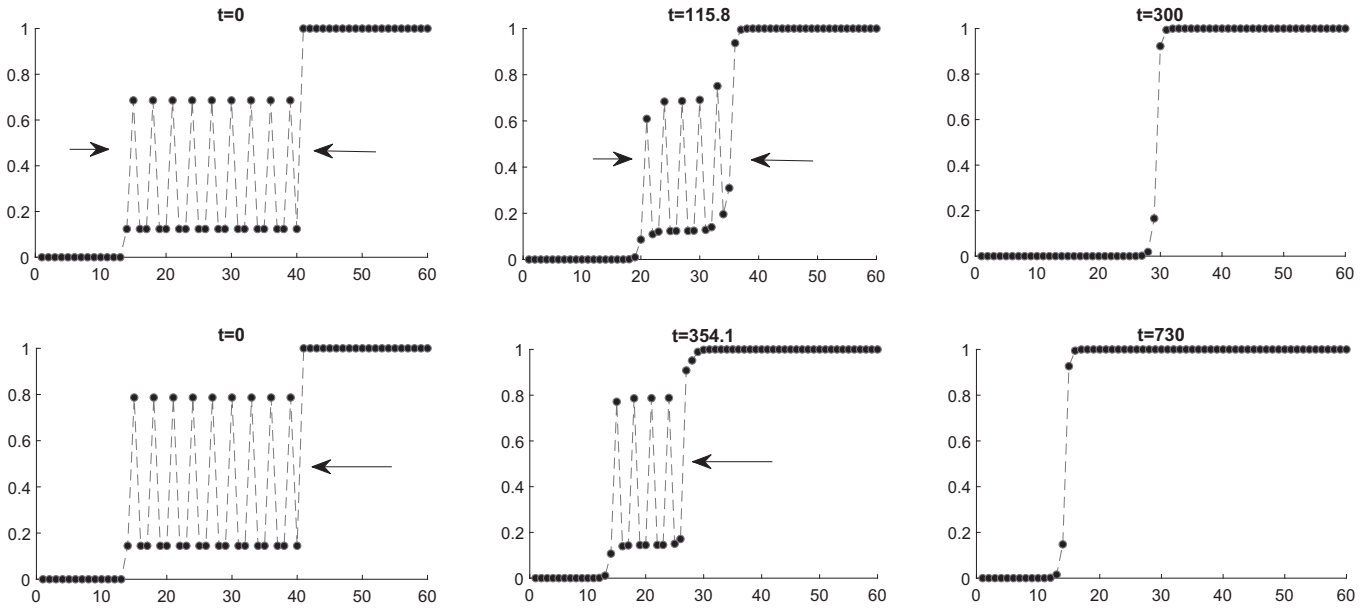

Fig. 10. These panels describe two simulations of the LDE (2.1) that feature a collision between a $[0 \to 001]$ wave and a $[001 \to 1]$ wave. For the top three panels we have $a = 0.404$ and $d = 0.054$, which is inside region $\mathcal{B}$. However, it is still below the monochromatic threshold. In particular, the buffer zone is now consumed from both sides, but the end result is again a pinned monochromatic front. For the bottom three panels we have $a = 0.404$ and $d = 0.05$, which is in region $\mathcal{A}$. Here the $[001]$ buffer zone is consumed from the right, resulting in a pinned monochromatic front.

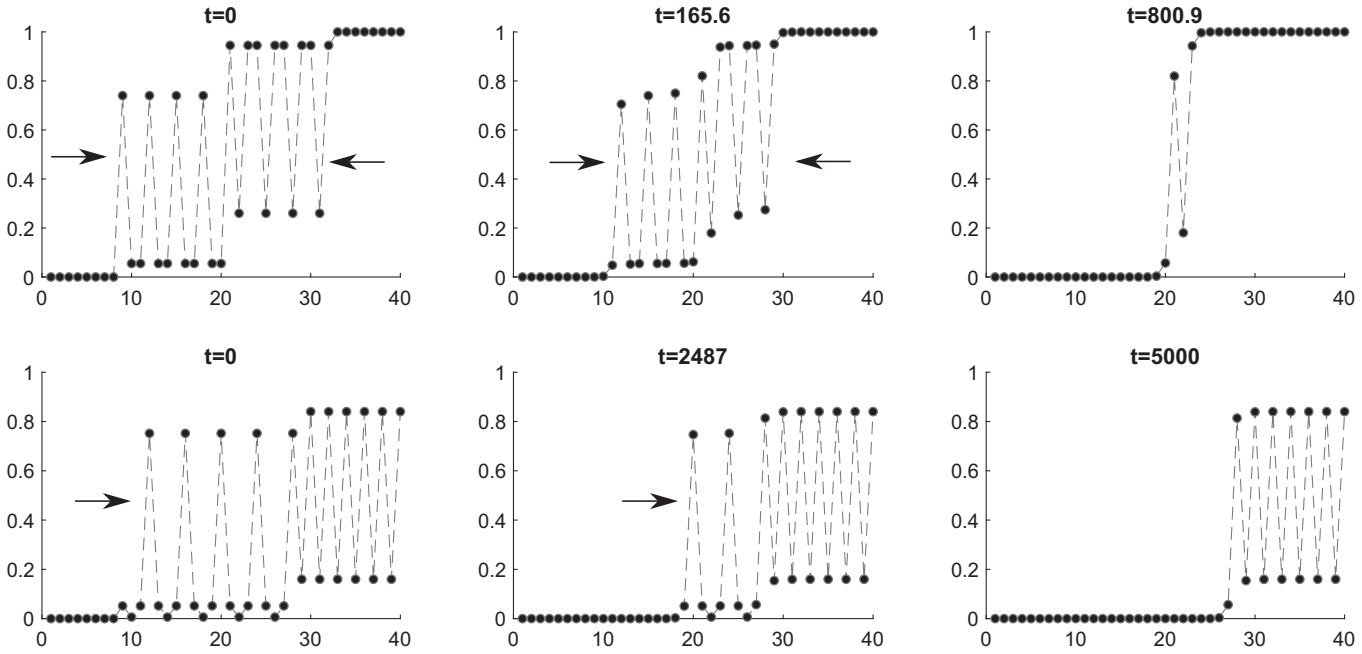

Fig. 11. The top panels describe a collision where a standing $[001 \to 011]$ wave is sandwiched between incoming $[0 \to 001]$ and $[011 \to 1]$ waves. Here we are in region $\mathcal{E}$ of Fig. 8, with $a = 0.5$ and $d = 0.0337$. The end-product is a non-monotonic pinned monochromatic wave. The monotonicity of the final state can be recovered by replacing the left wave with $[0 \to 010]$. The bottom panels describe a collision between $[0 \to 0001]$ and $[0001 \to 0101]$ at $a = 0.5$ and $d = 0.033554$. The end-product is now a trapped bichromatic wave.

No stable three-periodic patterns exist until we cross through $\Gamma_{[001]}$ for the second time at $d = 0.56466$ (black cross). Here u_{001} reappears together with the associated waves $u_0 \to u_{001}$ and $u_{001} \to u_1$, which all have non-zero speed. This situation is short-lived however, as u_{001} collides with u_{00a} and disappears at $d = 0.0566$ (green triangle), where $\Gamma_{[001]}$ is crossed for the third and final time.

4. Quadrichromatic waves

In this section we discuss the quadrichromatic case $n = 4$. As in the trichromatic case, stable 4-periodic equilibria can disappear and reappear as d is increased for a fixed a. The novel behaviour in this setting is that *travelling* quadrichromatic

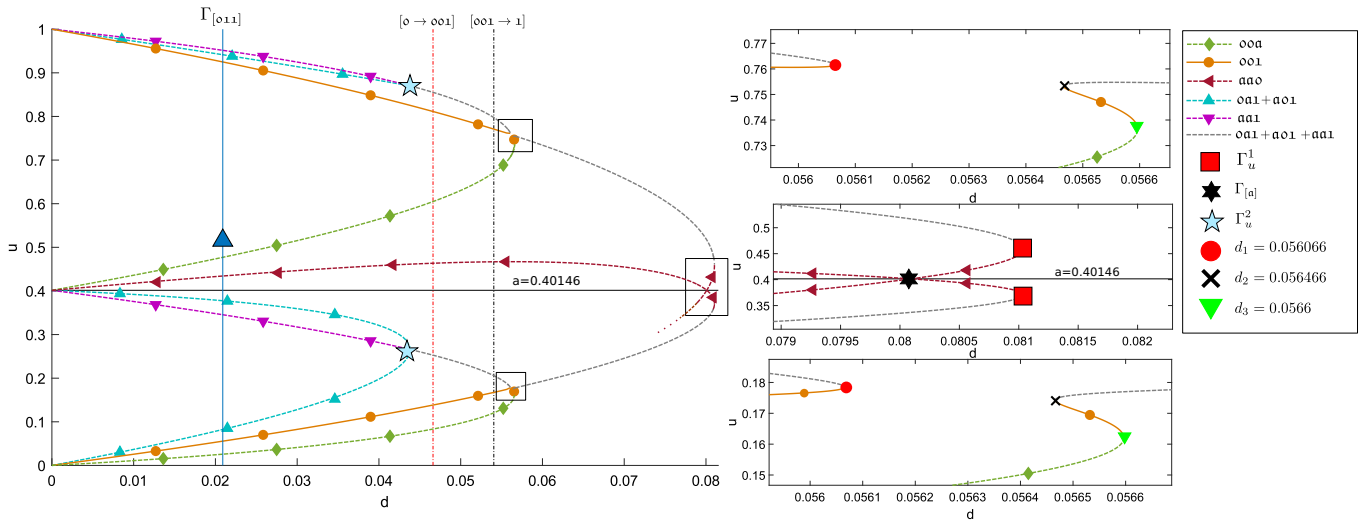

Fig. 12. These graphs display the d-dependence of the three components of all trichromatic roots that interact with u_{001}, for the fixed value $a = 0.40146$ that was also used in Fig. 6. Note that the first two coordinates of u_{001} are equal, which is why there are only two orange curves. Note also that both roots u_{011} and u_{101} have the same third component (and flipped first and second components). In particular, the blue stars indeed describe the triple root collision at Γ_u^2. The unstable root emerging from the black cross survives the triple crossing of $\Gamma_{[001]}$ and collides with u_{111} at Γ_u^1 (red squares). The last component of this latter branch is only partially plotted to prevent clutter. (For interpretation of the references to colour in this figure legend, the reader is referred to the web version of this article.)

waves can co-exist with *travelling* monochromatic waves or pinned *bichromatic* waves for an open set of parameters (a, d). This allows several new types of collisions to occur. For example, two incoming connections with intermediate quadrichromatic states can collide to form a monochromatic travelling wave.

4.1. Equilibria

The relevant nonlinearity that governs quadrichromatic equilibria to (2.1) is now given by

$$G(\mathrm{u}; a, d) := \begin{pmatrix} d(\mathrm{u}_4 - 2\mathrm{u}_1 + \mathrm{u}_2) + g(\mathrm{u}_1; a) \\ d(\mathrm{u}_1 - 2\mathrm{u}_2 + \mathrm{u}_3) + g(\mathrm{u}_2; a) \\ d(\mathrm{u}_2 - 2\mathrm{u}_3 + \mathrm{u}_4) + g(\mathrm{u}_3; a) \\ d(\mathrm{u}_3 - 2\mathrm{u}_4 + \mathrm{u}_1) + g(\mathrm{u}_4; a) \end{pmatrix}. \tag{4.1}$$

Inspecting this system shows that one component can be removed by enforcing either $\mathrm{u}_1 = \mathrm{u}_3$ or $\mathrm{u}_2 = \mathrm{u}_4$. Of course, this problem reduces to the bichromatic case $n = 2$ if both these identities are enforced. On the other hand, if one takes

$$\mathrm{u}_1 = \mathrm{u}_2 = \mathrm{u}_A, \qquad \mathrm{u}_3 = \mathrm{u}_4 = \mathrm{u}_B, \tag{4.2}$$

the system $G(\mathrm{u}; a, d) = 0$ reduces to

$$d(\mathrm{u}_B - \mathrm{u}_A) + g(\mathrm{u}_A; a) = d(\mathrm{u}_A - \mathrm{u}_B) + g(\mathrm{u}_B; a) = 0. \tag{4.3}$$

This again corresponds to the bichromatic case $n = 2$ but now with the halved diffusion coefficient $d_{\mathrm{bc}} = \frac{1}{2}d$.

In Fig. 13 we display several numerically computed curves $\Gamma_{[\mathrm{w}]}$ in the critical set Γ that correspond with the upper boundaries of the sets $\Omega_{[\mathrm{w}]}$. For visual clarity, we only consider the words

$$\mathrm{w} \in \{0001, 0011, 01, 0111\}, \tag{4.4}$$

which correspond with the stable non-homogeneous equilibria for $G(\mathrm{u}; a, d) = 0$.

The curves $\Gamma_{[0001]}$ and $\Gamma_{[0111]}$ again contain cusp and fold points. However, all four curves can *locally* be described as a graph $d = d_{[\mathrm{w}]}(a)$ near the corner $(a, d) = (0, 0)$. As in Section 3 we now set out to compute the first two terms in the asymptotic expansion of each of these curves. We especially wish to highlight the structural difference between two of these computations. Indeed, the inequality $g'(1;\, 0) < 0$ allows us to handle $\Gamma_{[0111]}$ using techniques similar to those in Section 3 and [1]. However, the identity $g'(0; 0) = 0$ forces us to tackle $\Gamma_{[0001]}$ in a different fashion. This leads to the appearance of a cubic term that places us *above* the monochromatic pinning region.

4.1.1. The $\Gamma_{[0111]}$ threshold

In view of the symmetries discussed above we consider solutions where the second and fourth component are equal. In particular, we consider the problem

$$G\big((x, 1 + y, 1 + z, 1 + y); a, d\big) = 0, \tag{4.5}$$

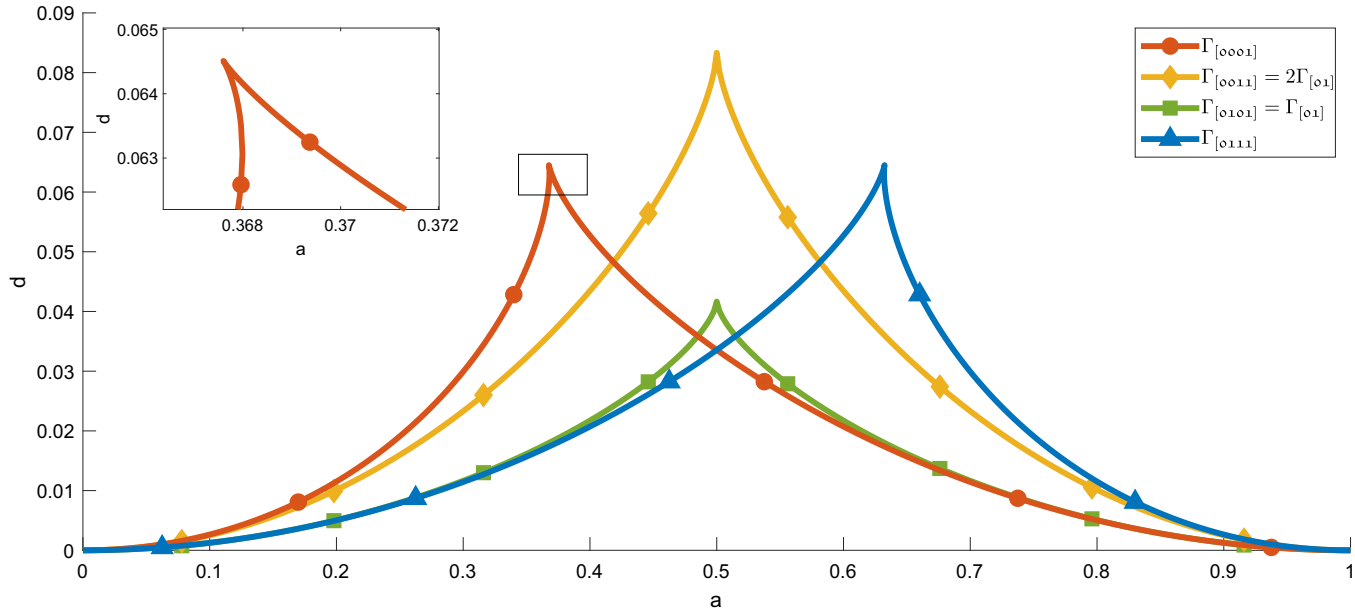

Fig. 13. Bifurcation thresholds for the four stable quadrichromatic root classes. The $\Gamma_{[0001]}$ and $\Gamma_{[0111]}$ curves again feature slanted cusps; see the inset.

which can be written as

$$(H_1, H_2, H_3)(x, y, z; a, d) = 0 \tag{4.6}$$

with

$$\begin{aligned} H_1(x, y, z; a, d) &= 2d(1 + y - x) + x(1 - x)(x - a), \\ H_2(x, y, z; a, d) &= d(x + z - 2y - 1) - y(1 + y)(y + 1 - a), \\ H_3(x, y, z; a, d) &= 2d(y - z) - z(1 + z)(z + 1 - a). \end{aligned} \tag{4.7}$$

Notice that H_2 and H_3 feature terms of order $O(y)$ respectively $O(z)$, which corresponds with the fact that the root $g(1; a) = 0$ is simple when $a = 0$. In addition, H_3 is independent of x. Setting $H_3 = 0$ hence allows us to write $z = z_*(y; a, d)$, which can be substituted into $H_2 = 0$ to yield $y = y_*(x; a, d)$. Plugging these expressions into H_1 by writing

$$\tilde{H}_1(x; a, d) = H_1\big(x, y_*(x; a, d), z_*(y; a, d); a, d\big), \tag{4.8}$$

we find

$$\tilde{H}_1(x; a, d) = x^2 + O\big(x^3 + ax + d\big). \tag{4.9}$$

This allows us to uncover the saddle-node bifurcations in a fashion analogous to [1]. In particular, we obtain the expansion

$$d_{[0111]}(a) = \frac{a^2}{8} + \frac{a^4}{64} + O(a^5), \tag{4.10}$$

together with

$$\mathrm{u}_{0111}(a; d_{[0111]}(a)) = \left(\frac{a}{2}, 1 - \frac{a^2}{8} - \frac{a^3}{16}, 1, 1 - \frac{a^2}{8} - \frac{a^3}{16}\right) + O(a^4). \tag{4.11}$$

Notice that the two leading order terms in (4.10) agree with those for the trichromatic curve $d_{[011]}$.

4.1.2. *The* $\Gamma_{[0101]}$ *and* $\Gamma_{[0011]}$ *thresholds*

The discussion above implies that the threshold $\Gamma_{[0101]}$ is identical to the corresponding threshold $\Gamma_{[01]}$ for the bichromatic case $n = 2$. In addition, the identity (4.3) allows us to write

$$d_{[0011]}(a) = 2d_{[01]}(a). \tag{4.12}$$

We can hence copy the results from [1, Prop 3.6] and write

$$\begin{aligned} d_{[0101]}(a) &= \frac{a^2}{8} + \frac{a^4}{32} + O(a^5), \\ d_{[0011]}(a) &= \frac{a^2}{4} + \frac{a^4}{16} + O(a^5), \end{aligned} \tag{4.13}$$

together with

$$\mathrm{u}_{\mathtt{0101}}\big(a; d_{[\mathtt{0101}]}(a)\big) = \Big(\frac{a}{2}, 1 - \frac{a^2}{4} - \frac{a^3}{8}, \frac{a}{2}, 1 - \frac{a^2}{4} - \frac{a^3}{8}\Big) + O(a^4),$$
$$\mathrm{u}_{\mathtt{0011}}\big(a; d_{[\mathtt{0011}]}(a)\big) = \Big(\frac{a}{2}, \frac{a}{2}, 1 - \frac{a^2}{4} - \frac{a^3}{8}, 1 - \frac{a^2}{4} - \frac{a^3}{8}\Big) + O(a^4). \tag{4.14}$$

Note that the curve $\Gamma_{[\mathtt{0011}]}$ is (locally) beneath the trichromatic $\Gamma_{[\mathtt{001}]}$ threshold.

4.1.3. *The* $\Gamma_{[\mathtt{0001}]}$ *threshold*

The symmetries discussed above allow us to consider solutions where the first and third component are equal. In particular, we consider the problem

$$G\big((x, y, x, 1 + z); a, d\big) = 0, \tag{4.15}$$

which can be written as

$$(H_1, H_2, H_3)(x, y, z; a, d) = 0 \tag{4.16}$$

with

$$\begin{aligned} H_1(x, y, z; a, d) &= d(y + z + 1 - 2x) + x(1 - x)(x - a), \\ H_2(x, y, z; a, d) &= 2d(x - y) + y(1 - y)(y - a), \\ H_3(x, y, z; a, d) &= 2d(x - z - 1) - z(1 + z)(z + 1 - a). \end{aligned} \tag{4.17}$$

Notice that H_3 features a term of order $O(z)$ and is independent of y. In fact, it is very similar to the second line of [1, Eq. (3.30)], which allows us to write

$$z = z_*(x; a, d) = -2d - 2ad + 2dx + O(d^2 + da^2). \tag{4.18}$$

However H_2 features $O((a + d)y)$ terms, which prevents us from expressing y in terms of x as before. This corresponds with the fact that the root $g(0; a) = 0$ is double at $a = 0$. On the other hand, setting $H_2 = 0$ and introducing the scalings

$$y = a\tilde{y}, \quad d = d_*(a, \tilde{d}) = \frac{1}{4}a^2(1 + \tilde{d}) \tag{4.19}$$

does allow us to write

$$x = x_*(\tilde{y}; a, \tilde{d}) = a\tilde{y} - \frac{2\tilde{y}}{1 + 4\tilde{d}}(1 - a\tilde{y})(\tilde{y} - 1). \tag{4.20}$$

Substituting these expressions into H_1, we write

$$\tilde{H}_1(\tilde{y}; a, \tilde{d}) = H_1\big(x_*(\tilde{y}; a, \tilde{d}), a\tilde{y}, z_*(x_*(\tilde{y}; a, \tilde{d}); a, d_*(a, \tilde{d})); a, d_*(a, \tilde{d})\big) \tag{4.21}$$

and find

$$\tilde{H}_1(\tilde{y}; a, \tilde{d}) = 4\tilde{y}^2 + O\big(\tilde{y}^3 + (a + \tilde{d})\tilde{y}^2 + a\tilde{y} + a^2\big). \tag{4.22}$$

The saddle-node bifurcations can now be unfolded by examining the terms in this equation using the procedure in [1]. In particular, we find

$$d_{[\mathtt{0001}]}(a) = \frac{a^2}{4} + \frac{a^3}{8} + O(a^4), \tag{4.23}$$

together with

$$\mathrm{u}_{\mathtt{0001}}\big(a; d_{[\mathtt{0001}]}(a)\big) = \Big(\frac{a}{2} + \frac{a^2}{8} + \frac{3a^3}{16}, \frac{a^2}{4} + \frac{a^3}{8}, \frac{a}{2} + \frac{a^2}{8} + \frac{3a^3}{16}, 1 - \frac{a^2}{2} - \frac{a^3}{2}\Big) + O(a^4). \tag{4.24}$$

The main point of interest here is that $d_{[\mathtt{0001}]}(a)$ contains a cubic term. In fact, our expansion here agrees with the expansion of the formula [23, Eq. (5.1)], which provides a (non-sharp) upper bound for the values of d where monochromatic waves are pinned. As indicated in Fig. 14, our numerical results confirm that $\Omega_{[\mathtt{0001}]}$ intersects the region in (a, d) space where monochromatic waves can travel.

4.2. Waves

As in the trichromatic case, a visual inspection confirms that assumptions (HΩ1) – (HΩ3) and (HS) are satisfied. The connections predicted by Theorem 2.1 are depicted in Fig. 9. In Fig. 14 we provide the numerically computed minimal values for d for which the waves connecting to and from the spatially homogeneous equilibria $[\mathtt{0}]$ and $[\mathtt{1}]$ have a non-zero speed. A dynamic illustration of such a wave can be found in Supplement A.1. The novel feature here is that there is overlap with the region where the monochromatic $[\mathtt{0} \to \mathtt{1}]$ wave has non-zero speed. This allows for situations where

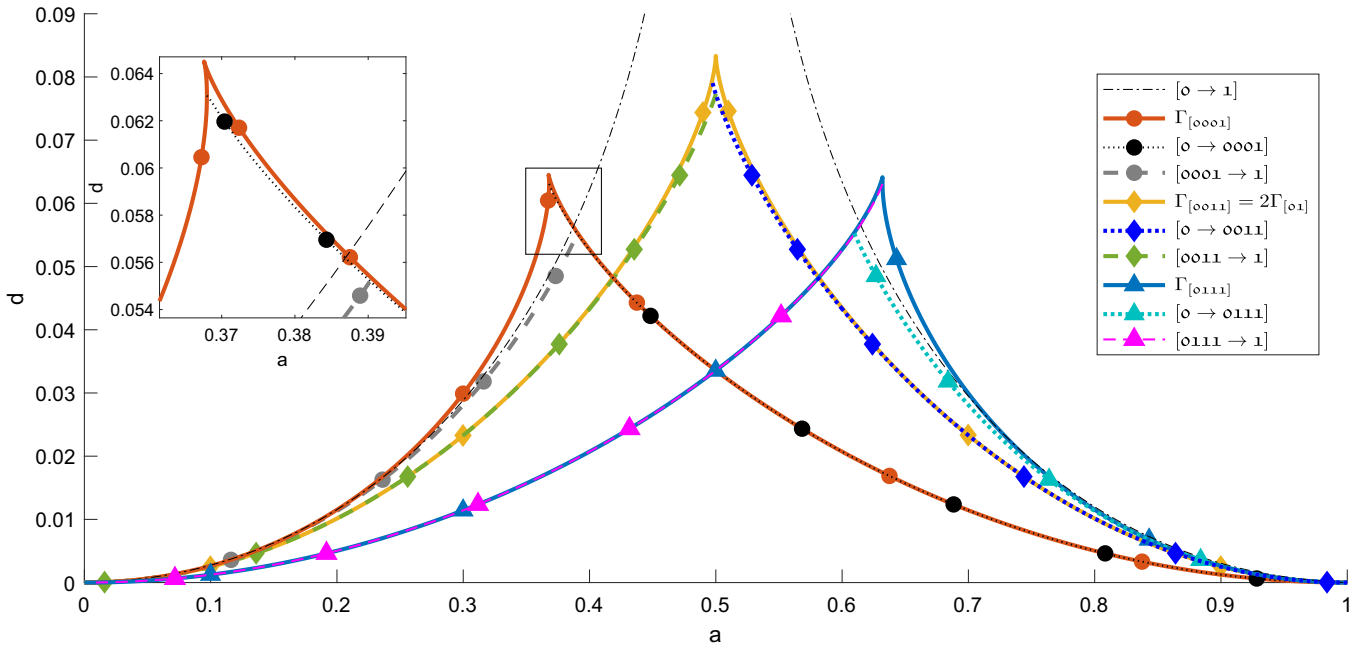

Fig. 14. Speed thresholds for the wave connections to and from the stable roots [0001], [0011] and [0111]. The thresholds for [0101] are not shown, as they coincide with the bichromatic results obtained in [1]. Supplement A.1 contains an animation of the quadrichromatic wave [0 → 0001].

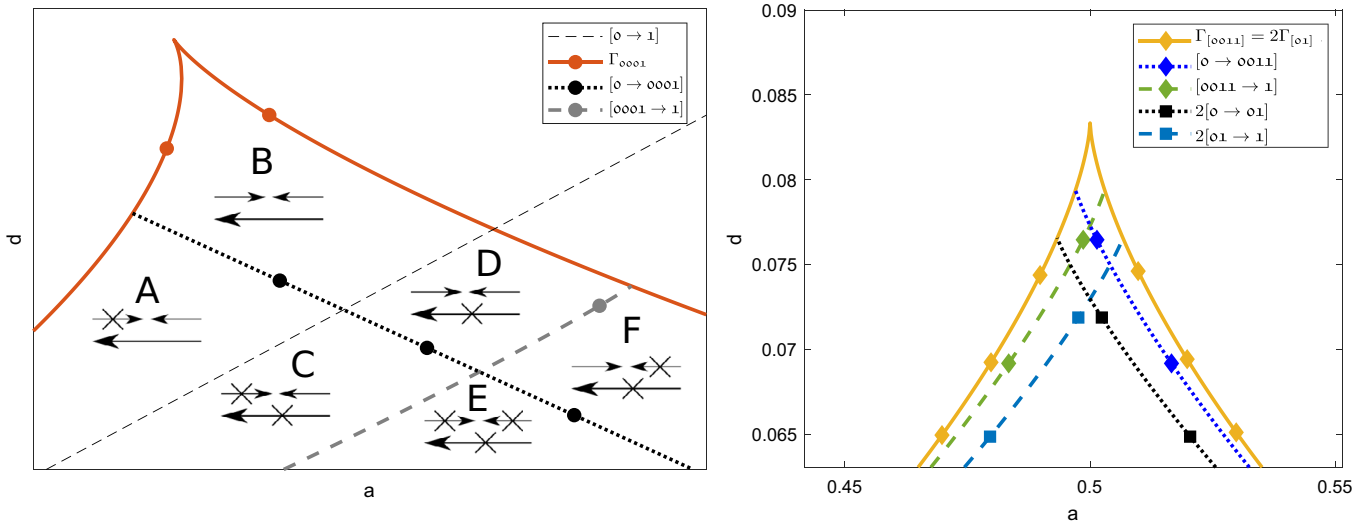

Fig. 15. The left panel contains a schematic exaggeration of the area around the cusp of $\Gamma_{[0001]}$, together with a description of the collision type that can be expected in each region. The top two arrows indicate the nature of the [0 → 0001] and [0001 → 1] connections that move towards each other. The bottom arrow describes whether or not the resulting monochromatic wave is pinned. Supplements A.2–A.4 provide animations of collision types A, B and D. The right panel compares the speed threshold for the connections involving [0011] with the doubled bichromatic thresholds. One can see that the reduction (4.2) respects the equilibrium structure but not the wave structure of the system.

the end-product of a collision between two quadrichromatic wave is no longer a pinned monochromatic wave but in fact a travelling monochromatic wave.

Indeed, let us focus first on the neighbourhood of the cusp of $\Gamma_{[0001]}$. Fig. 15 distinguishes several parameter regions where collisions between [0 → 0001] and [0001 → 1] waves can occur. Types C-F closely resemble those encountered in the bichromatic and trichromatic cases. Types A and B are new however and indeed feature travelling monochromatic end-products. Type B is especially interesting since the left side of the domain experiences a reversal in the direction of propagation. Supplements A.2–A.4 provide animations of quadrichromatic collisions of type A, B and D.

Furthermore, two examples with snapshots of such collisions are provided in Fig. 16. We remark that in both cases the speed of the [0001 → 1] wave is significantly faster than the speed of the monochromatic wave. In particular, the spreading speed of the stable state $u = 1$ can be increased by using [0001] as a buffer.

We do not give an exhaustive description of all possible collisions here. However, we do wish to point out a second novelty that arises for $n = 4$, which is depicted in the bottom panels of Fig. 11. Here a moving [0 → 0001] wave collides with

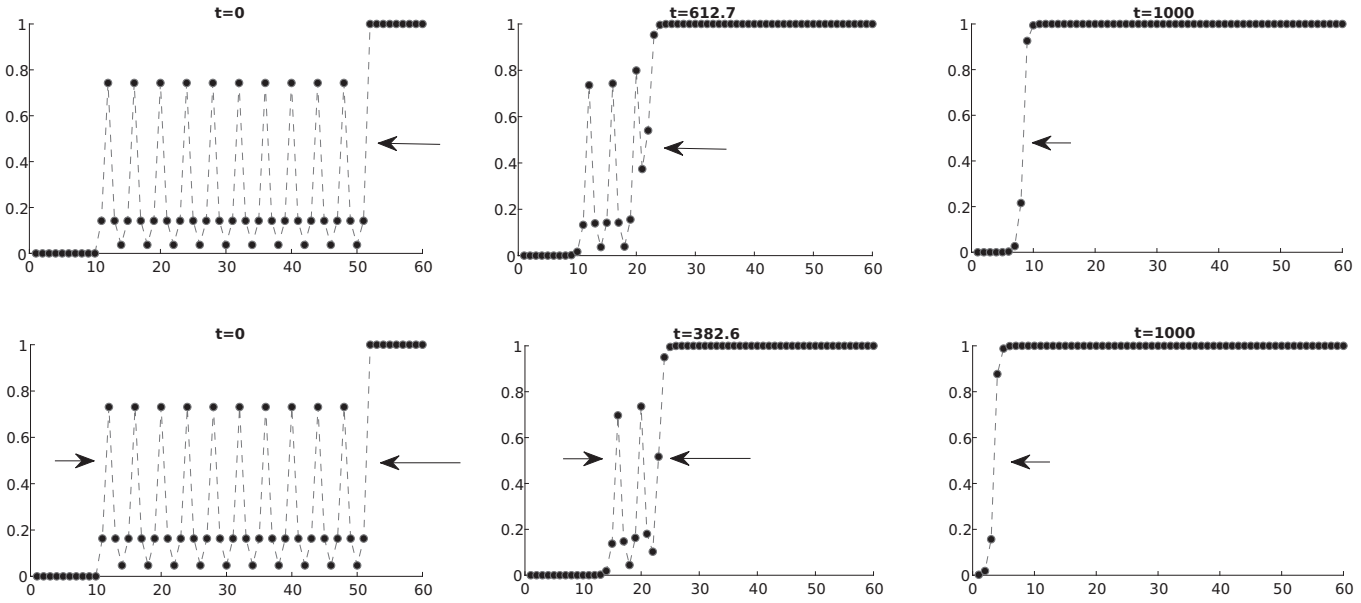

Fig. 16. These panels describe two simulations of the LDE (2.1) that feature a collision between a $[0 \to 0001]$ wave and a $[0001 \to 1]$ wave. The top three panels feature a collision of type A, with $a = 0.378$ and $d = 0.058$. The quadrichromatic buffer zone is invaded from the right, forming a travelling monochromatic wave once it is extinguished. The bottom three panels feature a collision of type B, with $a = 0.37$ and $d = 0.0625$. Here the left part of the buffer zone is first pulled towards zero by the incoming wave on the left, but then gets pulled towards one by the final travelling monochromatic wave. Dynamic animations of collisions of type A and B can be seen in Supplements A.2–A.3.

a standing $[0001 \to 0101]$ wave to form a standing *bichromatic* $[0 \to 01]$ wave. This leads us to suspect that a wide range of possibilities exist to construct collision sequences involving sets of n-chromatic waves with multiple separate values of $n > 1$.

5. Proof of Theorem 2.3

Here we provide the proof of our main result, which allows us to establish the existence of wave connections between equilibria by simply comparing their types.

We first show that a pair of distinct ordered stationary solutions cannot have two equal components. Throughout this section we assume that expressions such as $i-1$ or $i+1$ should be evaluated within the modulo arithmetic on indices $\{1, 2, \dots, n\}$.

Lemma 5.1. *Assume that* $\mathrm{u}, \mathrm{v} \in \mathbb{R}^n$ *satisfy* $G(\mathrm{u}; a, d) = G(\mathrm{v}; a, d) = 0$ *for some pair* $a \in (0, 1)$ *and* $d > 0$. *Assume furthermore that* $\mathrm{u} \leq \mathrm{v}$ *and that* $\mathrm{u}_i = \mathrm{v}_i$ *for some* $i \in \{1, \dots, n\}$. *Then in fact* $\mathrm{u} = \mathrm{v}$.

Proof. Since $\mathrm{u}_i = \mathrm{v}_i$ we have

$$0 = d(\mathrm{u}_{i-1} - 2\mathrm{u}_i + \mathrm{u}_{i+1}) + g(\mathrm{u}_i; a) = d(\mathrm{u}_{i-1} - 2\mathrm{v}_i + \mathrm{u}_{i+1}) + g(\mathrm{v}_i; a) = d(\mathrm{v}_{i-1} - 2\mathrm{v}_i + \mathrm{v}_{i+1}) + g(\mathrm{v}_i; a), \tag{5.1}$$

which implies that

$$\mathrm{u}_{i-1} + \mathrm{u}_{i+1} = \mathrm{v}_{i-1} + \mathrm{v}_{i+1}. \tag{5.2}$$

Since $\mathrm{u}_{i-1} \leq \mathrm{v}_{i-1}$ and $\mathrm{u}_{i+1} \leq \mathrm{v}_{i+1}$ we obtain $\mathrm{u}_{i-1} = \mathrm{v}_{i-1}$ and $\mathrm{u}_{i+1} = \mathrm{v}_{i+1}$. This argument can subsequently be repeated a number of times to yield $\mathrm{u} = \mathrm{v}$. □

The main ingredient in our proof of Theorem 2.1 is that the ordering of any pair of words from the full set $\{0, a, 1\}^n$ and the stable subset $\{0, 1\}^n$ is preserved for the equilibria that have the corresponding types. For example, for $n = 4$ we have the partial ordering

$$\begin{array}{ccccccccccc} & & & & [00a1] & \lhd & [0011] & \lhd & [0a11] & & \\ & & & \rhd & & & & & & \triangledown & \\ [0] & \lhd & [000a] & \lhd & [0001] & & & & & & [0111] \lhd [a111] \lhd [1] \\ & & & \triangledown & & & & & & \rhd & \\ & & & & [0a01] & \lhd & [01] & \lhd & [01a1] & & \end{array}$$

whereby each $[\mathrm{w}_A] \lhd [\mathrm{w}_B]$ connection in this diagram indicates that $\mathrm{u}_{\mathrm{w}_A}(a, d) < \mathrm{u}_{\mathrm{w}_B}(a, d)$ whenever $(a, d) \in \Omega_{\mathrm{w}_A} \cap \Omega_{\mathrm{w}_B}$ with $d > 0$. For $n = 3$ we can similarly write

$$[0] \lhd [00a] \lhd [001] \lhd [0a1] \lhd [011] \lhd [a11] \lhd [1],$$

which explains the ordering in Fig. 3. These ideas are summed up in the following key statement.

Lemma 5.2. *Assume that* (HΩ1) *and* (HΩ2) *are satisfied and consider a distinct pair* $\mathrm{w}_A, \mathrm{w}_B \in \{\mathfrak{o}, \mathfrak{a}, \mathfrak{1}\}^n$ *that admits the ordering* $\mathrm{w}_A \leq \mathrm{w}_B$. *Suppose furthermore that at least one of these two words is contained in* $\{\mathfrak{o}, \mathfrak{1}\}^n$. *Then for any* $(a, d) \in \Omega_{\mathrm{w}_A} \cap \Omega_{\mathrm{w}_B}$ *we have the strict component-wise inequality*

$$\mathrm{u}_{\mathrm{w}_A}(a, d) < \mathrm{u}_{\mathrm{w}_B}(a, d). \tag{5.3}$$

Proof. Fixing $(a, d) \in \Omega_{\mathrm{w}_A} \cap \Omega_{\mathrm{w}_B}$, we note that (HΩ1) and Lemma 2.1 allow us to pick a curve

$$[0, 1] \ni t \mapsto (\mathrm{v}_A(t), \mathrm{v}_B(t), \alpha(t), \delta(t)) \in [0, 1]^n \times [0, 1]^n \times (0, 1) \times [0, \infty) \tag{5.4}$$

so that we have

$$\begin{aligned} (\mathrm{v}_A, \mathrm{v}_B, \alpha, \delta)(0) &= ([\mathrm{w}_A]_{|a}, [\mathrm{w}_B]_{|a}, a, 0), \\ (\mathrm{v}_A, \mathrm{v}_B, \alpha, \delta)(1) &= (\mathrm{u}_{\mathrm{w}_A}(a, d), \mathrm{u}_{\mathrm{w}_B}(a, d), a, d), \end{aligned} \tag{5.5}$$

while the inclusion

$$(\alpha(t), \delta(t)) \in \Omega_{\mathrm{w}_A} \cap \Omega_{\mathrm{w}_B} \tag{5.6}$$

and the identities

$$G\big(\mathrm{v}_A(t); \alpha(t), \delta(t)\big) = G\big(\mathrm{v}_B(t); \alpha(t), \delta(t)\big) = 0 \tag{5.7}$$

all hold for $0 \leq t \leq 1$. By slightly modifying the path and picking a small $\epsilon > 0$, we can also ensure that $\alpha(t) = a$ and $\delta(t) = t$ for all $t \in [0, \epsilon)$.

Upon introducing the graph Laplacian $B : \mathbb{R}^n \to \mathbb{R}^n$ and the nonlinearity $\Psi : \mathbb{R}^n \to \mathbb{R}^n$ that act as

$$(B\mathrm{u})_i = \mathrm{u}_{i-1} - 2\mathrm{u}_i + \mathrm{u}_{i+1}, \quad \Psi(\mathrm{u})_i = g(\mathrm{u}_i; a), \tag{5.8}$$

we see that

$$0 = G(\mathrm{v}_\#(t); a, t) = tB\mathrm{v}_\#(t) + \Psi\big(\mathrm{v}_\#(t)\big) \tag{5.9}$$

for t small and $\# \in \{A, B\}$. Taking implicit derivatives of (5.9), we find

$$tB\frac{d^k}{dt^k}\mathrm{v}_\#(t) + kB\frac{d^{k-1}}{dt^{k-1}}\mathrm{v}_\#(t) + \mathcal{R}^{(k)}_\#(t) = -D\Psi\big(\mathrm{v}_\#(t)\big)\frac{d^k}{dt^k}\mathrm{v}_\#(t), \tag{5.10}$$

in which we have defined

$$\mathcal{R}^{(k)}_\#(t) = \sum_{j=1}^{k-1}\binom{k-1}{j-1}\Big[\frac{d^{k-j}}{dt^{k-j}}D\Psi\big(\mathrm{v}_\#(t)\big)\Big]\frac{d^j}{dt^j}\mathrm{v}_\#(t) \tag{5.11}$$

for $k \geq 2$, setting this expression to zero for $k = 1$.

For any index i we define the quantity

$$\ell_i = \min\{j' \geq 0 : (\mathrm{w}_A)_{i+j'} < (\mathrm{w}_B)_{i+j'} \text{ or } (\mathrm{w}_A)_{i-j'} < (\mathrm{w}_B)_{i-j'}\}, \tag{5.12}$$

which measures the distance to the closest index where w_A and w_B are unequal. We now claim that for any $k \geq 0$ we have

$$\frac{d^k}{dt^k}(\mathrm{v}_A)_i(0) \leq \frac{d^k}{dt^k}(\mathrm{v}_B)_i(0) \tag{5.13}$$

if $\ell_i \geq k$, with the inequality being strict if and only if $\ell_i = k$. For $k = 0$ this is obvious. Assuming this holds for $k - 1$, consider any index with $\ell_i \geq k \geq 1$. Our alphabet assumption implies that

$$(\mathrm{w}_A)_i = (\mathrm{w}_B)_i \neq \mathfrak{a}, \tag{5.14}$$

which implies that the i-component of the two diagonal matrices $D\Psi(\mathrm{v}_A(0))$ and $D\Psi(\mathrm{v}_B(0))$ are strictly negative; see (2.7). In addition, our induction hypothesis implies that

$$\mathcal{R}^{(k)}_A(0) = \mathcal{R}^{(k)}_B(0). \tag{5.15}$$

By definition, we have

$$\ell_{i\pm1} \geq \ell_i - 1 \geq k - 1. \tag{5.16}$$

In addition, we have $\ell_i = k$ if and only if $\ell_{i+1} = k - 1$ or $\ell_{i-1} = k - 1$ holds. Our induction hypothesis hence implies

$$\Big(B\frac{d^{k-1}}{dt^{k-1}}\mathrm{v}_A(0)\Big)_i \leq \Big(B\frac{d^{k-1}}{dt^{k-1}}\mathrm{v}_B(0)\Big)_i, \tag{5.17}$$

with strict inequality if and only if $\ell_i = k$. Our claim now follows immediately from (5.10).

The argument above shows that $v_A(t) < v_B(t)$ for all $t \in (0, \epsilon)$. If (5.3) fails to hold, this hence means that there exists $t_* \in [\epsilon, 1]$ for which $v_A(t_*) \leq v_B(t_*)$, with also $(v_A(t_*))_i = (v_B(t_*))_i$ for some $i \in \{1, \dots, n\}$. Lemma 5.1 now implies $v_A(t_*) = v_B(t_*)$ and hence

$$u_{w_A}\big(\alpha(t_*), \delta(t_*)\big) = u_{w_B}\big(\alpha(t_*), \delta(t_*)\big), \tag{5.18}$$

which violates Corollary 2.1. □

By combining Lemma 5.1 and 5.2 we can control all the (marginally) stable equilibria in the box $[u_{w_-}, u_{w_+}]$. This allows us to finally prove our main result.

Proof of Theorem 2.3. Pick any distinct pair $w_\pm \in \{0, 1\}^n$ with $w_- \leq w_+$ and any $(a, d) \in \Omega_{w_-} \cap \Omega_{w_+}$ with $d > 0$. Lemma 5.2 implies that the cuboid

$$\mathcal{K} = \{u \in \mathbb{R}^n : u_{w_-}(a, d) \leq u \leq u_{w_+}(a, d)\} \subset [0, 1]^n \tag{5.19}$$

has non-empty volume. In addition, for any $w \in \{0, 1\}^n$ that does not satisfy $w_- \leq w \leq w_+$ and for which $(a, d) \in \overline{\Omega}_w$, we have $u_w(a, d) \notin \mathcal{K}$ on account of Lemma 5.1, the connectedness of $\Omega_{w_\pm} \cap \Omega_w$ and continuity considerations.

In view of (HS), all equilibria inside the cube $\mathcal{K}$ besides the two corner points $u_{w_\pm}(a, d)$ hence have a strictly positive eigenvalue. The existence of the wave (c, Φ) now follows from [27, Theorem. 6]. □

Acknowledgments

HJH acknowledges support from the Netherlands Organization for Scientific Research (NWO) (grant 639.032.612). LM acknowledges support from the Netherlands Organization for Scientific Research (NWO) (grant 613.001.304). PS and VŠ acknowledge the support of the project LO1506 of the Czech Ministry of Education, Youth and Sports under the program NPU I. Moreover, VŠ was supported by the project SGS-2016-003 of the University of West Bohemia. The authors are grateful to three anonymous referees and Antonín Slavík for their valuable suggestions.

Supplementary material

Supplementary material associated with this article can be found, in the online version, at doi:10.1016/j.amc.2019.05.036.

References

[1] H.J. Hupkes, L. Morelli, P. Stehlík, Bichromatic travelling waves for lattice Nagumo equations, SIAM J. Appl. Dyn. Syst. 18 (2) (2019) 973–1014.
[2] D.G. Aronson, H.F. Weinberger, Nonlinear diffusion in population genetics, combustion, and nerve pulse propagation, in: Partial differential equations and related topics, Springer, 1975, pp. 5–49.
[3] T. Gallay, E. Risler, et al., A variational proof of global stability for bistable travelling waves, Differ. Integral Equ. 20 (8) (2007) 901–926.
[4] H.F. Weinberger, Genetic wave propagation, convex sets, and semi-infinite programming, in: Constructive approaches to mathematical models (Proc. Conf. in honor of R. J. Duffin, Pittsburgh, Pa., 1978), Academic Press, New York, 1979, pp. 293–317.
[5] P.C. Fife, J.B. McLeod, The approach of solutions of nonlinear diffusion equations to travelling front solutions, Arch. Ration. Mech. Anal. 65 (4) (1977) 335–361.
[6] D. Sattinger, Weighted norms for the stability of traveling waves, J. Differ. Equ. 25 (1) (1977) 130–144.
[7] Y. Morita, H. Ninomiya, Entire solutions with merging fronts to reaction–diffusion equations, J. Dyn. Differ. Equ. 18 (4) (2006) 841–861.
[8] H. Yagisita, Backward Global Solutions Characterizing Annihilation Dynamics of Travelling Fronts, 39, Publications of the Research Institute for Mathematical Sciences, 2003, pp. 117–164.
[9] J. Mallet-Paret, Spatial patterns, spatial chaos and traveling waves in lattice differential equations, in: Stochastic and Spatial Structures of Dynamical Systems, volume 45, Royal Netherlands Academy of Sciences. Proceedings, Physics Section. Series 1, Amsterdam, 1996, pp. 105–129.
[10] L.A. Ranvier, Leçons sur l'Histologie du Système Nerveux, par M. L. Ranvier, recueillies par M. Ed. Weber, F. Savy, Paris, 1878.
[11] J.W. Cahn, A. Novick-Cohen, Evolution equations for phase separation and ordering in binary alloys, J. Stat. Phys. 76 (1994) 877–909.
[12] J.W. Cahn, E.S. Van Vleck, On the co-existence and stability of trijunctions and quadrijunctions in a simple model, Acta Materialia 47 (1999) 4627–4639.
[13] A. Vainchtein, E.S. Van Vleck, Nucleation and propagation of phase mixtures in a bistable chain, Phys. Rev. B 79 (2009) 144123.
[14] V. Celli, N. Flytzanis, Motion of a screw dislocation in a crystal, J. Appl. Phys. 41 (11) (1970) 4443–4447.
[15] S.V. Dmitriev, K. Abe, T. Shigenari, Domain wall solutions for EHM model of crystal: structures with period multiple of four, Physica D 147 (1–2) (2000) 122–134.
[16] J. Mallet-Paret, The global structure of traveling waves in spatially discrete dynamical systems, J. Dyn. Diff. Equ. 11 (1999) 49–128.
[17] A. Hoffman, J. Mallet-Paret, Universality of crystallographic pinning, J. Dyn. Diff. Equ. 22 (2010) 79–119.
[18] P.W. Bates, A. Chmaj, A discrete convolution model for phase transitions, Arch. Rational Mech. Anal. 150 (1999) 281–305.
[19] J.W. Cahn, J. Mallet-Paret, E.S. Van Vleck, Traveling wave solutions for systems of ODE's on a two-dimensional spatial lattice, SIAM J. Appl. Math. 59 (1999) 455–493.
[20] C.E. Elmer, E.S. Van Vleck, A variant of Newton's method for the computation of traveling waves of bistable differential-difference equations, J. Dyn. Diff. Equ. 14 (2002) 493–517.
[21] C.E. Elmer, E.S. Van Vleck, Spatially discrete FitzHugh-Nagumo equations, SIAM J. Appl. Math. 65 (2005) 1153–1174.
[22] H.J. Hupkes, S.M. Verduyn-Lunel, Analysis of Newton's method to compute travelling waves in discrete media, J. Dyn. Diff. Equ. 17 (2005) 523–572.
[23] J.P. Keener, Propagation and its failure in coupled systems of discrete excitable cells, SIAM J. Appl. Math. 47 (1987) 556–572.
[24] J. Mallet-Paret, Crystallographic pinning: direction dependent pinning in lattice differential equations, Preprint (2001).
[25] C.E. Elmer, Finding stationary fronts for a discrete Nagumo and wave equation; construction, Physica D 218 (2006) 11–23.
[26] H.J. Hupkes, D. Pelinovsky, B. Sandstede, Propagation failure in the discrete Nagumo equation, Proc. Amer. Math. Soc. 139 (10) (2011) 3537–3551, doi:10.1090/S0002-9939-2011-10757-3.
[27] X. Chen, J.S. Guo, C.C. Wu, Traveling waves in discrete periodic media for bistable dynamics, Arch. Ration. Mech. Anal. 189 (2008) 189–236.
[28] L. Morelli, Travelling patterns on discrete media, Ph.D Thesis, 2019 available at http://pub.math.leidenuniv.nl/~morellil/Thesis.pdf.
[29] M. Hillert, A solid-solution model for inhomogeneous systems, Acta Met. 9 (1961) 525–535.

[30] H. Cook, D. de Fontaine, J. Hilliard, A model for diffusion on cubic lattices and its application to the early stages of ordering, Acta Met. 17 (1969) 765–773.
[31] A.K. Tagantsev, L.E. Cross, J. Fousek, Domains in Ferroic Crystals and Thin Films, Springer, 2010.
[32] B. Ermentrout, Neural networks as spatio-temporal pattern-forming systems, Rep. pProg.Phys. 61 (4) (1998) 353.
[33] M. Brucal-Hallare, E.S. Van Vleck, Traveling wavefronts in an antidiffusion lattice Nagumo model, SIAM J. Appl. Dyn. Syst. 10 (2011) 921–959.
[34] A. Vainchtein, E.S. Van Vleck, A. Zhang, Propagation of periodic patterns in a discrete system with competing interactions, SIAM J. Appl. Dyn. Syst. 14 (2) (2015) 523–555.
[35] T.E. Faver, Nanopteron-stegoton traveling waves in spring dimer Fermi-Pasta-Ulam-Tsingou lattices, arXiv:1710.07376 (2017).
[36] T.E. Faver, J.D. Wright, Exact diatomic Fermi–Pasta–Ulam–Tsingou solitary waves with optical band ripples at infinity, SIAM J. Math. Anal. 50 (1) (2018) 182–250.
[37] A. Hoffman, J.D. Wright, Nanopteron solutions of diatomic Fermi–Pasta–Ulam–Tsingou lattices with small mass-ratio, Physica D 358 (2017) 33–59.
[38] W.M. Schouten, H.J. Hupkes, Nonlinear stability of pulse solutions for the discrete Fitzhugh–Nagumo equation with infinite-range interactions, arXiv:1807.11736 (2018).
[39] A.J. Homburg, B. Sandstede, Homoclinic and Heteroclinic Bifurcations in Vector Fields, Handbook of Dynamical Systems, 3, 2010, pp. 379–524.
[40] A. Hoffman, J.D. Wright, Exit manifolds for lattice differential equations, Proc. R. Soc. Edinb. Sect. A 141 (1) (2011) 77–92, doi:10.1017/S0308210509001498.
[41] T. Bellsky, A. Doelman, T.J. Kaper, K. Promislow, Adiabatic stability under semi-strong interactions: the weakly damped regime, Indiana Univ. Math. J. (2013) 1809–1859.
[42] A. Doelman, T.J. Kaper, K. Promislow, Nonlinear asymptotic stability of the semistrong pulse dynamics in a regularized Gierer–Meinhardt model, SIAM J. Math. Anal. 38 (6) (2007) 1760–1787.
[43] P. van Heijster, A. Doelman, T.J. Kaper, K. Promislow, Front interactions in a three-component system, SIAM J. Appl. Dyn. Syst. 9 (2) (2010) 292–332.
[44] Y. Nishiura, T. Teramoto, K.-I. Ueda, Scattering and separators in dissipative systems, Phys. Rev. E 67 (5) (2003) 056210.
[45] M. Chirilus-Bruckner, A. Doelman, P. van Heijster, J.D. Rademacher, Butterfly catastrophe for fronts in a three-component reaction–diffusion system, J. Nonlinear Sci. 25 (1) (2015) 87–129.
[46] Y. Morita, K. Tachibana, An entire solution to the Lotka–Volterra competition-diffusion equations, SIAM J. Math. Anal. 40 (6) (2009) 2217–2240.
[47] P. Poláčik, Propagating terraces and the dynamics of front-like solutions of reaction-diffusion equations on r, Mem. Am. Math. Soc. (2016).
[48] P. Stehlík, Exponential number of stationary solutions for nagumo equations on graphs, J. Math. Anal. Appl. 455 (2) (2017) 1749–1764.
[49] J. Blot, On global implicit functions, Nonlinear Anal. 17 (10) (1991) 947–959.

Appendix E

Paper: Counting and ordering periodic stationary solutions of lattice Nagumo equations

Applied Mathematics Letters 98 (2019) 398–405

Contents lists available at ScienceDirect

Applied Mathematics Letters

www.elsevier.com/locate/aml

Counting and ordering periodic stationary solutions of lattice Nagumo equations

Hermen Jan Hupkes [a], Leonardo Morelli [a], Petr Stehlík [b,*], Vladimír Švígler [b]

[a] *Mathematisch Instituut, Universiteit Leiden, P.O. Box 9512, 2300 RA Leiden, The Netherlands*
[b] *Department of Mathematics and NTIS, University of West Bohemia, Univerzitní 8, 30100 Pilsen, Czech Republic*

ARTICLE INFO

Article history:
Received 21 May 2019
Accepted 25 June 2019
Available online 4 July 2019

Keywords:
Reaction diffusion equation
Lattice differential equation
Graph differential equations
Periodic solutions
Travelling waves

ABSTRACT

We study the rich structure of periodic stationary solutions of Nagumo reaction diffusion equation on lattices. By exploring the relationship with Nagumo equations on cyclic graphs we are able to divide these periodic solutions into equivalence classes that can be partially ordered and counted. In order to accomplish this, we use combinatorial concepts such as necklaces, bracelets and Lyndon words.

1. Introduction

In this paper we explore the structure of periodic stationary solutions of the lattice Nagumo equation

$$\dot{u}_i(t) = d(u_{i-1}(t) - 2u_i(t) + u_{i+1}(t)) + g(u_i(t); a), \quad i \in \mathbb{Z}, \quad t \in \mathbb{R}. \tag{LDE}$$

We assume $d > 0$ and consider the cubic bistable nonlinearity $g(u; a) := u(1 - u)(u - a)$, $a \in (0, 1)$. This equation has been extensively studied as the simplest model describing the competition between two stable states $u = 0$ and $u = 1$ in a spatially discrete environment. One of its key features is the existence of nondecreasing travelling waves $u_j(t) = \Phi(j - ct)$, and the fact that these waves do not move ($c = 0$) for small values of d. This phenomenon (called pinning) is caused by the existence of heterogeneous stationary solutions, which prevent the dominance of the two stable homogeneous states $u = 0$ and $u = 1$. Our goal is to show that the periodic stationary solutions of (LDE), which exist mainly inside the pinning region, form equivalence classes that can be partially ordered and counted.

* Corresponding author.
E-mail addresses: hhupkes@math.leidenuniv.nl (H.J. Hupkes), l.morelli@math.leidenuniv.nl (L. Morelli), pstehlik@kma.zcu.cz (P. Stehlík), sviglerv@kma.zcu.cz (V. Švígler).

https://doi.org/10.1016/j.aml.2019.06.038
0893-9659/

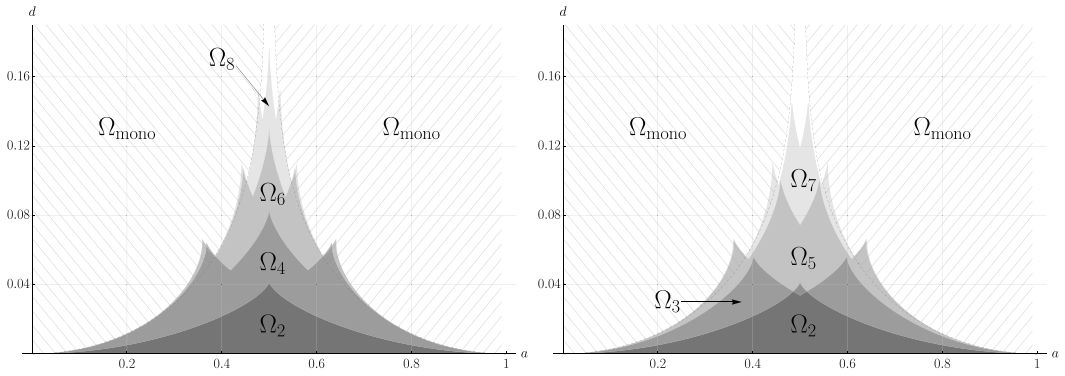

Fig. 1. Existence regions Ω_n of stable n-periodic stationary solutions of (LDE). The left panel depicts even periods, the right one odd periods. The hatched regions Ω_{mono} correspond to parameter values for which the monochromatic waves of (LDE) travel.

Eq. (LDE) is a discrete-space version of the famous Nagumo reaction–diffusion PDE $u_t = du_{xx} + g(u; a)$, with $x \in \mathbb{R}$. The lattice counterpart (LDE) has a richer set of equilibria [1] which in turn implies more complex behaviour of travelling and standing front solutions [2,3]. Mallet-Paret [2] established that for each $a \in [0, 1]$ and $d > 0$ there exists a unique $c = c(a, d)$ for which the wave Φ exists. However, if we fix $a \in (0, 1) \setminus \{\frac{1}{2}\}$, Zinner [3] showed that $c(a, d) \neq 0$ for $d \gg 1$ and Keener [4] proved that $c(a, d) = 0$ for $0 < d \ll 1$. Moreover, for fixed $d > 0$ the results in [5] suggest the existence of $\delta(d) > 0$ so that $c(a, d) = 0$ whenever $\left|a - \frac{1}{2}\right| \leq \delta(d)$. This above mentioned pinning is typical for lattice equations [6–8]. Since the pinning region is dominated by heterogeneous (periodic and aperiodic) stationary solutions, our paper contributes to the understanding of this important feature (see Fig. 1 for a simple illustration).

A second important motivation for understanding the periodic stationary solutions of (LDE) is that this knowledge aids us in the search for so-called multichromatic waves. These non-monotone travelling waves connect two or more n-periodic stationary solutions of (LDE) (in contrast to standard monochromatic waves which are monotone). In our companion papers [9,10] we have shown that these waves exist mainly inside the pinning region, appearing and disappearing as d increases. The waves that exist outside of the pinning region can be combined to form complex collision waves that involve direction changes.

In this paper we name, partially order and count the equivalence classes of periodic stationary solutions of (LDE) based on the connection between (LDE) and the Nagumo equation posed on cyclic graphs. For an arbitrary undirected graph $\mathcal{G} = (V, E)$ with the set of vertices $V = \{1, 2, 3, \ldots, n\}$ and a set of edges E, the Nagumo equation on a graph $\mathcal{G}$ is[1]

$$\dot{\mathrm{u}}_i(t) = d \sum_{j \in \mathcal{N}(i)} \big(\mathrm{u}_j(t) - \mathrm{u}_i(t)\big) + g(\mathrm{u}_i(t); a), \quad i \in V, t \in \mathbb{R}, \tag{GDE}$$

where $\mathcal{N}(i)$ denotes the 1-neighbourhood of vertex $i \in V$.

In Section 2 we establish the connection between the stationary solutions of (GDE) and the periodic stationary solutions of (LDE). In Section 3 we use this connection and the implicit function theorem to build a naming scheme for periodic stationary solutions of (LDE). In Section 4 we discuss their symmetries, which allows us to define and count their equivalence classes in Section 5. This is achieved by establishing a link with combinatorial concepts such as necklaces, bracelets and Lyndon words. Our main result is formulated in Theorem 4 and illustrated by simple examples.

[1] We use italic letters for double sequences (e.g., u for solutions of (LDE)) and roman ones for vectors (e.g., u for solutions of (GDE)).

2. Periodic solutions and solutions of graph Nagumo equation

We here consider $\mathcal{G} = \mathcal{C}_n$, where $\mathcal{C}_n$ is a cycle graph on n vertices. Eq. (GDE) can now be written as $\dot{\mathrm{u}}(t) = G(\mathrm{u}(t); a, d)$, where $G : \mathbb{R}^n \to \mathbb{R}^n$ is given by

$$G(\mathrm{u}; a, d) := \begin{pmatrix} d(\mathrm{u}_n - 2\mathrm{u}_1 + \mathrm{u}_2) + g\big(\mathrm{u}_1; a\big) \\ d(\mathrm{u}_1 - 2\mathrm{u}_2 + \mathrm{u}_3) + g\big(\mathrm{u}_2; a\big) \\ \vdots \\ d(\mathrm{u}_{n-1} - 2\mathrm{u}_n + \mathrm{u}_1) + g\big(\mathrm{u}_n; a\big) \end{pmatrix}. \tag{1}$$

Our key results are based on the correspondence of stationary solutions of (GDE) on $\mathcal{G} = \mathcal{C}_n$ and periodic stationary solutions of (LDE)[2]. We say that a double sequence $u = (u_i)_{i\in\mathbb{Z}}$ is a periodic extension of a vector $\mathrm{u} \in \mathbb{R}^n$ if $u_i = \mathrm{u}_{\mathrm{mod}(i,n)}$ (we assume that the modulo operator takes values $\mathrm{mod}(i, n) \in \{1, \dots, n\}$). We remark that (LDE) is well-posed as an evolution equation on the space $\ell^\infty(\mathbb{Z}; \mathbb{R})$. However, we caution the reader that lattice equations do not necessarily have unique solutions if one drops this boundedness condition, even in the linear case [13,14].

Lemma 1. *Let $\mathcal{G} = \mathcal{C}_n$, $n \geq 3$, be a cycle graph on n vertices. The vector $\mathrm{u} = (\mathrm{u}_1, \mathrm{u}_2, \dots, \mathrm{u}_n)$ is a stationary solution of (GDE) on $\mathcal{G} = \mathcal{C}_n$ if and only if its periodic extension u is an n-periodic stationary solution of (LDE). Moreover, u is an asymptotically stable solution of (GDE) if and only if u is an asymptotically stable solution of (LDE) with respect to the ℓ^∞-norm.*

Proof. A short inspection readily yields the desired equivalence between solutions of (GDE) and (LDE)[3]. Turning to their stability, let us assume that $\mathrm{u}^* = (\mathrm{u}_1^*, \mathrm{u}_2^*, \dots, \mathrm{u}_n^*)$ is an asymptotically stable solution of (GDE). There hence exists $\gamma > 0$ such that for each $\mathrm{u}_0 \in \mathbb{R}^n$ with $\|\mathrm{u}_0 - \mathrm{u}^*\| < \gamma$ we have

$$\lim_{t\to\infty} \mathrm{u}(t, \mathrm{u}_0) = \mathrm{u}^*,$$

in which $\mathrm{u}(t, \mathrm{u}_0)$ denotes the solution of (GDE) with the initial condition u_0. Consequently, there exists $\delta > 0$ so that the vectors $\mathrm{w}_0, \mathrm{z}_0 \in \mathbb{R}^n$ defined by

$$(\mathrm{w}_0)_i = \mathrm{u}_i^* + \delta, \quad (\mathrm{z}_0)_i = \mathrm{u}_i^* - \delta \quad \text{for all } i = 1, 2, \dots, n,$$

satisfy $\lim_{t\to\infty} \mathrm{w}(t, \mathrm{w}_0) = \mathrm{u}^*$, $\lim_{t\to\infty} \mathrm{z}(t, \mathrm{z}_0) = \mathrm{u}^*$.

Let us now consider the periodic extensions u^*, w_0 and z_0 of the vectors u^*, w_0 and z_0. Then the corresponding solutions $w(t, w_0)$, $z(t, w_0)$ of (LDE) satisfy

$$w_i(t, w_0) = \mathrm{w}_{\mathrm{mod}(i,n)}(t, \mathrm{w}_0), \quad z_i(t, w_0) = \mathrm{z}_{\mathrm{mod}(i,n)}(t, \mathrm{z}_0),$$

for each $t \geq 0$, which implies

$$\lim_{t\to\infty} w(t, w_0) = u^*, \quad \lim_{t\to\infty} z(t, z_0) = u^*.$$

Using the comparison principle (e.g., Chen et al. [13, Lemma 1]) we can hence conclude that all solutions u of (LDE) with an initial condition u_0 that satisfies $\|u_0 - u^*\|_\infty < \delta$ indeed have $\lim_{t\to\infty} u(t, u_0) = u^*$, since

$$u^* \leftarrow z(t, z_0) \leq u(t, u_0) \leq w(t, w_0) \to u^*.$$

The opposite implication can be proved similarly. □

---

[2] Additionally, it is well-known that the problem of finding stationary solutions of graph differential equations on cycles $\mathcal{G} = \mathcal{C}_n$ is actually equivalent to periodic discrete boundary value problems [11,12].

[3] We omit the case of $n = 2$. In this case, a slightly modified version of Lemma 1 holds. The reduced version of (1) for $n = 2$

$$G(\mathrm{u}; a, d) := \begin{pmatrix} d(\mathrm{u}_2 - 2\mathrm{u}_1 + \mathrm{u}_2) + g\big(\mathrm{u}_1; a\big) \\ d(\mathrm{u}_1 - 2\mathrm{u}_2 + \mathrm{u}_1) + g\big(\mathrm{u}_2; a\big) \end{pmatrix} = \begin{pmatrix} 2d(\mathrm{u}_2 - \mathrm{u}_1) + g\big(\mathrm{u}_1; a\big) \\ 2d(\mathrm{u}_1 - \mathrm{u}_2) + g\big(\mathrm{u}_2; a\big) \end{pmatrix}.$$

implies that solutions of (GDE) and (LDE) are equivalent if one considers the double value of d in (LDE).

3. Naming scheme for stationary periodic solutions

The equivalence between n-periodic solutions of (LDE) and solutions of (GDE) on $\mathcal{G} = \mathcal{C}_n$ (see Lemma 1) allows us to focus on the latter in order to establish our naming scheme for the former solutions. First, let us observe that $G(\mathrm{u}; a, 0) = 0$ for any $a \in (0,1)$ and $\mathrm{u} \in \{0, a, 1\}^n$. Moreover, the fact that

$$D_1 G(\mathrm{u}; a, 0) = \operatorname{diag}\Big(g'\big(\mathrm{u}_1; a\big), \dots, g'\big(\mathrm{u}_n; a\big)\Big) \tag{2}$$

has non-zero entries allows us to employ the implicit function theorem to conclude that there are 3^n solution branches emanating out of the roots $\{0, a, 1\}^n$ for d small. These branches can be tracked up until the first collision with another branch. This justifies the use of the following naming scheme for n-periodic stationary solutions.

We introduce an alphabet $A = \{\mathfrak{o}, \mathfrak{a}, \mathfrak{1}\}$ and call $\mathrm{u}_\mathrm{w} \in [0,1]^n$ a stationary solution of type $\mathrm{w} \in A^n = \{\mathfrak{o}, \mathfrak{a}, \mathfrak{1}\}^n$ if it satisfies $G(\mathrm{u}_\mathrm{w}; a, d) = 0$ and lies on the branch emanating from the root w_a at $d = 0$, where $\mathrm{w}_a : \{\mathfrak{o}, \mathfrak{a}, \mathfrak{1}\}^n \to \{0, a, 1\}^n$ is defined by

$$(\mathrm{w}_a)_i = \begin{cases} 0 & \text{if } \mathrm{w}_i = \mathfrak{o}, \\ a & \text{if } \mathrm{w}_i = \mathfrak{a}, \\ 1 & \text{if } \mathrm{w}_i = \mathfrak{1}. \end{cases}$$

Using this definition we introduce connected sets

$$\Omega_\mathrm{w} = \{(a, d) \in \mathcal{H} : \text{the system } G(\cdot\,; a, d) = 0 \text{ admits an equilibrium of type } \mathrm{w}\}, \tag{3}$$

which are open in the half-strip $\mathcal{H} = [0,1] \times [0, \infty)$. While a full analysis of the sets Ω_w can be very tricky (for a fixed $a \in (0,1)$, solutions of type w can disappear and then reappear, see [10]), we are only interested in small values of d here in this paper.

Lemma 2. *Let $a \in (0,1)$ and $d > 0$ be small enough. Then (LDE) has 3^n stationary n-periodic solutions. These solutions are asymptotically stable if and only if they belong to the 2^n solutions of type $\mathrm{w} \in \{\mathfrak{o}, \mathfrak{1}\}^n$.*

Proof. The existence of 3^n stationary n-periodic solutions follows from Lemma 1 and the 3^n solution branches for (GDE) supplied by the implicit function theorem. The stability properties follow from (2) and the fact that $g'(0; a) = -a < 0$, $g'(1; a) = a - 1 < 0$ and $g'(a; a) = a(1-a) > 0$. □

Moreover, pairs of stable solutions can be ordered if the corresponding words are ordered.

Lemma 3. *Let $a \in (0,1)$ and $d > 0$ be small enough and consider a distinct pair $\mathrm{w}_A, \mathrm{w}_B \in \{\mathfrak{o}, \mathfrak{a}, \mathfrak{1}\}^n$ with $(\mathrm{w}_A)_i \leq (\mathrm{w}_B)_i$ for all i. Suppose furthermore that at least one of these two words is contained in $\{\mathfrak{o}, \mathfrak{1}\}^n$. Then the solutions $u_{\mathrm{w}_A}, u_{\mathrm{w}_B}$ of (LDE) satisfy the strict component-wise inequality $(u_{\mathrm{w}_A})_i < (u_{\mathrm{w}_B})_i$, for all $i \in \mathbb{Z}$.*

Proof. The proof follows from [10, Lemma 5.2] and Lemma 1. □

4. Symmetries of stationary periodic solutions

The naming scheme introduced above allows us to study two key symmetries among the 3^n stationary solutions of (GDE) and the corresponding n-periodic stationary solutions of (LDE).

Translation (rotation). If (u_i) is an n-periodic stationary solution of (LDE) then this also holds for (u_{i+k}). We define the translation (rotation) operator on words (and more generally on any vectors of length n) by

$$(\mathcal{T}_\ell \mathrm{w})_i := \mathrm{w}_{\mathrm{mod}(i+\ell,n)}.$$

Reflection. If (u_i) is an n-periodic stationary solution of (LDE) then the same is true for (u_{1-i}). We define the reflection operator by

$$(\mathcal{R}\mathrm{w})_i := \mathrm{w}_{\mathrm{mod}(1-i,n)}.$$

Trivially, if u is a solution of type w for $G(\mathrm{u}; a, d) = 0$ then $\mathcal{T}_\ell \mathrm{u}$ is a solution of type $\mathcal{T}_\ell \mathrm{w}$ and $\mathcal{R}\mathrm{u}$ is a solution of type $\mathcal{R}\mathrm{w}$, which immediately implies that

$$\Omega_{\mathrm{w}} = \Omega_{\mathcal{T}_1 \mathrm{w}} = \cdots = \Omega_{\mathcal{T}_{n-1} \mathrm{w}} = \Omega_{\mathcal{R}\mathrm{w}}.$$

Naturally, other symmetries can be considered as well. For example, in the case of $a = 1/2$, it makes sense to consider symbol swapping $\mathfrak{0} \leftrightarrow \mathfrak{1}$. However, the existence of solution of type w for a given pair (a, d) does not imply the existence of solutions for the "swapped" word $\tilde{\mathrm{w}}$ for general $a \neq 1/2$, see Fig. 1. Therefore, we only focus on the simplest symmetries—translations $\mathcal{T}_\ell$ and reflections $\mathcal{R}$.

5. Counting equivalence classes of stationary periodic solutions

We can now define equivalence classes of n-periodic solutions to (LDE) by factoring out one or both of the symmetries discussed above. If we consider translations $\mathcal{T}_\ell$ and the word $\mathrm{w} = \mathfrak{00a1}$ we have the following equivalence class of stationary 4-periodic solutions of (LDE):

$$[u_{\mathfrak{00a1}}]_{\mathcal{T}} = \{u_{\mathfrak{00a1}}, \mathcal{T}_1 u_{\mathfrak{00a1}}, \mathcal{T}_2 u_{\mathfrak{00a1}}, \mathcal{T}_3 u_{\mathfrak{00a1}}\} = \{u_{\mathfrak{00a1}}, u_{\mathfrak{0a10}}, u_{\mathfrak{a100}}, u_{\mathfrak{100a}}\}.$$

If we consider both translations $\mathcal{T}_\ell$ and reflections $\mathcal{R}$, we have for example $\mathcal{R} u_{\mathfrak{00a1}} = u_{\mathfrak{1a00}}$ and thus

$$[u_{\mathfrak{00a1}}]_{\mathcal{T}\mathcal{R}} = \{u_{\mathfrak{00a1}}, u_{\mathfrak{0a10}}, u_{\mathfrak{a100}}, u_{\mathfrak{100a}}, u_{\mathfrak{1a00}}, u_{\mathfrak{01a0}}, u_{\mathfrak{001a}}, u_{\mathfrak{a001}}\}.$$

We always use the smallest word in the lexicographical sense (the so called Lyndon word) as a class representative. If the word is not primitive (i.e., it is periodic itself), we take the primitive (aperiodic) subword, e.g., $[\mathfrak{01}]_{\mathcal{T}} = [\mathfrak{0101}]_{\mathcal{T}}$.

If one is simply interested in the periodic solutions themselves then it is reasonable to factor out both translation and reflection symmetries and consider the full alphabet $\{\mathfrak{0}, \mathfrak{a}, \mathfrak{1}\}$. However, in special circumstances (e.g., when connecting these solutions via multichromatic waves [10]) it only makes sense to factor out the translation symmetries and to consider the reduced alphabet $\{\mathfrak{0}, \mathfrak{1}\}$.

We can now use the combinatorial theory of words [15,16] to count the equivalence classes and to get the number of qualitatively different n-periodic stationary solutions. To this end, we define the quantities

$$N_k(n) = \frac{1}{n} \sum_{d:d|n} \varphi(d) k^{\frac{n}{d}}, \quad L_k(n) = \frac{1}{n} \sum_{d:d|n} \mu(d) k^{\frac{n}{d}}, \tag{4}$$

$$B_k(n) = \begin{cases} \frac{1}{2}\left(N_k(n) + \frac{k+1}{2} k^{n/2}\right) & \text{for } n \text{ even}, \\ \frac{1}{2}\left(N_k(n) + k^{(n+1)/2}\right) & \text{for } n \text{ odd}, \end{cases} \tag{5}$$

$$BL_k(n) = \sum_{d:d|n} \mu(d) B_k(n/d), \tag{6}$$

where $\varphi(d)$ is the Euler's totient function and $\mu(d)$ is the Möbius function [17, Chapter 2]. We can use these quantities to formulate our main result, which describes the number of equivalence classes of n-periodic stationary solutions.

Table 1
Number of equivalence classes of n-periodic stationary solutions of (LDE). In each pair, the former number corresponds to all equivalence classes and the latter number in the parentheses to the equivalence classes formed by asymptotically stable solutions.

Period	All solutions	Translation $\mathcal{T}$		Translation $\mathcal{T}$+refection $\mathcal{R}$	
n	k^n	All $N_k(n)$	Primitive $L_k(n)$	All $B_k(n)$	Primitive $BL_k(n)$
1	3(2)	3(2)	3(2)	3(2)	3(2)
2	9(4)	6(3)	3(1)	6(3)	3(1)
3	27(8)	11(4)	8(2)	10(4)	7(2)
4	81(16)	24(6)	18(3)	21(6)	15(3)
5	243(32)	51(8)	48(6)	39(8)	36(6)
6	729(64)	130(14)	116(9)	92(13)	79(8)
...					

Theorem 4. *Pick an integer $n \geq 2$ and a parameter $a \in (0,1)$. Then for $d > 0$ small enough (LDE) has exactly*

(1) 3^n n-periodic stationary solutions which form

(a) $N_3(n)$ equivalence classes with respect to translations $\mathcal{T}_\ell$. Moreover, $L_3(n)$ of these equivalence classes are formed by primitive periodic solutions.
(b) $B_3(n)$ equivalence classes with respect to translations $\mathcal{T}_\ell$ and reflections $\mathcal{R}$. Moreover, $BL_3(n)$ of these equivalence classes are formed by primitive periodic solutions.

(2) 2^n asymptotically stable n-periodic stationary solutions which form

(a) $N_2(n)$ equivalence classes with respect to translations $\mathcal{T}_\ell$. Moreover, $L_2(n)$ of these equivalence classes are formed by primitive periodic solutions.
(b) $B_2(n)$ equivalence classes with respect to translations $\mathcal{T}_\ell$ and reflections $\mathcal{R}$. Moreover, $BL_2(n)$ of these equivalence classes are formed by primitive periodic solutions.

Proof. A k-ary necklace of length n is an equivalence class of words of length n formed by k letters which are equivalent with respect to translations (rotations) $\mathcal{T}_\ell$. There are $N_k(n)$ different necklaces [16, Eq. (2.1)]. There are $L_k(n)$ distinct primitive (aperiodic) necklaces—Lyndon words [16, Eq. (2.2)].

A k-ary bracelet of length n is an equivalence class of words of length n formed by k letters which are equivalent with respect to translations (rotations) $\mathcal{T}_\ell$ and refection $\mathcal{R}$. There are $B_k(n)$ different bracelets [16, Eq. (2.4)]. A primitive (aperiodic) bracelet is called a Lyndon bracelet. There are $BL_k(n)$ distinct Lyndon bracelets, which can be proved by the direct application of the Möbius inversion formula (e.g., [17, Theorem 2.9]). The result for n-periodic stationary solutions of (LDE) then follows directly from Lemma 2. □

Table 1 provides a summary of these results for small periods. As an example, we give a detailed description of the equivalence classes for $n = 3$ and $n = 4$.

Example 5. There are 27 distinct 3-periodic stationary solutions of (LDE). Considering translations $\mathcal{T}_\ell$, they form 11 equivalence classes:

$$
\begin{aligned}
[u_{\mathtt{o}}]_{\mathcal{T}} &= \{u_{\mathtt{o}}\},\ [u_{\mathtt{a}}]_{\mathcal{T}} = \{u_{\mathtt{a}}\},\ [u_{\mathtt{1}}]_{\mathcal{T}} = \{u_{\mathtt{1}}\};\\
[u_{\mathtt{ooa}}]_{\mathcal{T}} &= \{u_{\mathtt{ooa}}, u_{\mathtt{oao}}, u_{\mathtt{aoo}}\},\ [u_{\mathtt{oo1}}]_{\mathcal{T}} = \{u_{\mathtt{oo1}}, u_{\mathtt{o1o}}, u_{\mathtt{1oo}}\},\\
[u_{\mathtt{oaa}}]_{\mathcal{T}} &= \{u_{\mathtt{oaa}}, u_{\mathtt{aao}}, u_{\mathtt{aoa}}\},\ [u_{\mathtt{oa1}}]_{\mathcal{T}} = \{u_{\mathtt{oa1}}, u_{\mathtt{a1o}}, u_{\mathtt{1oa}}\},\\
[u_{\mathtt{o1a}}]_{\mathcal{T}} &= \{u_{\mathtt{o1a}}, u_{\mathtt{1ao}}, u_{\mathtt{ao1}}\},\ [u_{\mathtt{o11}}]_{\mathcal{T}} = \{u_{\mathtt{o11}}, u_{\mathtt{11o}}, u_{\mathtt{1o1}}\},\\
[u_{\mathtt{aa1}}]_{\mathcal{T}} &= \{u_{\mathtt{aa1}}, u_{\mathtt{a1a}}, u_{\mathtt{1aa}}\},\ [u_{\mathtt{a11}}]_{\mathcal{T}} = \{u_{\mathtt{a11}}, u_{\mathtt{11a}}, u_{\mathtt{1a1}}\}.
\end{aligned}
$$

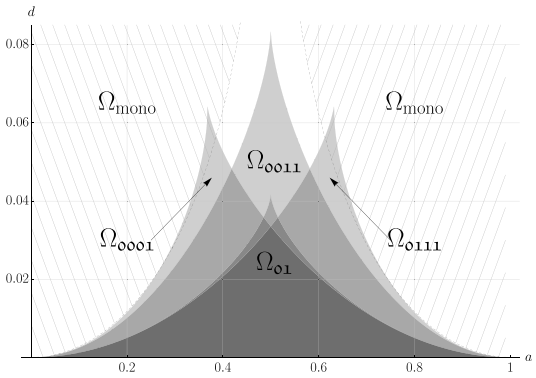

Fig. 2. Regions Ω_{w} defined in (3) corresponding to asymptotically stable spatially heterogeneous 4-periodic solutions of (LDE): $u_{\mathfrak{o}\mathfrak{o}\mathfrak{o}\mathfrak{1}}, u_{\mathfrak{o}\mathfrak{o}\mathfrak{1}\mathfrak{1}}, u_{\mathfrak{o}\mathfrak{1}}, u_{\mathfrak{o}\mathfrak{1}\mathfrak{1}\mathfrak{1}}$. The hatched regions Ω_{mono} correspond to pairs (a, d) for which the monochromatic waves of (LDE) travel.

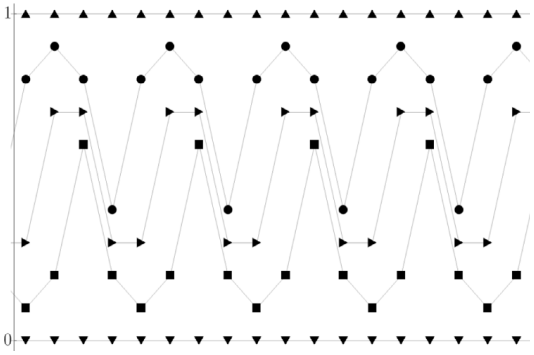

Fig. 3. Lyndon representatives of 5 ordered classes of asymptotically stable stationary 4-periodic solutions of (LDE): ▼ - $u_{\mathfrak{o}}$, ■ - $u_{\mathfrak{o}\mathfrak{o}\mathfrak{o}\mathfrak{1}}$, ▶ - $u_{\mathfrak{o}\mathfrak{o}\mathfrak{1}\mathfrak{1}}$, ● - $u_{\mathfrak{o}\mathfrak{1}\mathfrak{1}\mathfrak{1}}$, ▲ - $u_{\mathfrak{1}}$ (the values are slightly modified for better visualisation).

The former 3 classes correspond to constant solutions and are thus not primitive 3-periodic solutions, while the remaining 8 classes correspond to primitive stationary 3-periodic solutions. Upon taking reflections $\mathcal{R}$ into consideration, there are only 10 equivalence classes and 7 corresponding to primitive periodic solutions, since $[u_{\mathfrak{o}\mathfrak{a}\mathfrak{1}}]_{\mathcal{T}}$ and $[u_{\mathfrak{o}\mathfrak{1}\mathfrak{a}}]_{\mathcal{T}}$ form one equivalence class

$$[u_{\mathfrak{o}\mathfrak{a}\mathfrak{1}}]_{\mathcal{T}\mathcal{R}} = \{u_{\mathfrak{o}\mathfrak{a}\mathfrak{1}}, u_{\mathfrak{a}\mathfrak{1}\mathfrak{o}}, u_{\mathfrak{1}\mathfrak{o}\mathfrak{a}}, u_{\mathfrak{1}\mathfrak{a}\mathfrak{o}}, u_{\mathfrak{o}\mathfrak{1}\mathfrak{a}}, u_{\mathfrak{a}\mathfrak{o}\mathfrak{1}}\}.$$

The 8 asymptotically stable solutions form 4 equivalence classes with respect to translations and 2 are primitive - $[u_{\mathfrak{o}\mathfrak{o}\mathfrak{1}}]_{\mathcal{T}}$ and $[u_{\mathfrak{o}\mathfrak{1}\mathfrak{1}}]_{\mathcal{T}}$. These classes are not affected by the reflection $\mathcal{R}$ and can be ordered as

$$[u_{\mathfrak{o}}]_{\mathcal{T}} \lhd [u_{\mathfrak{o}\mathfrak{o}\mathfrak{1}}]_{\mathcal{T}} \lhd [u_{\mathfrak{o}\mathfrak{1}\mathfrak{1}}]_{\mathcal{T}} \lhd [u_{\mathfrak{1}}]_{\mathcal{T}}.$$

where $[u_{\text{w}_A}] \lhd [u_{\text{w}_B}]$ means that the Lyndon representatives satisfy $u_{\text{w}_A} < u_{\text{w}_B}$.

The ordering of asymptotically stable n-periodic solutions is only partial for periods with $n > 3$. For example, Lemma 3 implies that 6 equivalence classes of 4-periodic solutions can be partially ordered in the following way.

$$\begin{array}{ccccc} & & [u_{\mathfrak{o}\mathfrak{o}\mathfrak{1}\mathfrak{1}}]_{\mathcal{T}} & & \\ & \triangle & & \triangledown & \\ [u_{\mathfrak{o}}]_{\mathcal{T}} \lhd [u_{\mathfrak{o}\mathfrak{o}\mathfrak{o}\mathfrak{1}}]_{\mathcal{T}} & & & & [u_{\mathfrak{o}\mathfrak{1}\mathfrak{1}\mathfrak{1}}]_{\mathcal{T}} \lhd [u_{\mathfrak{1}}]_{\mathcal{T}} \\ & \triangledown & & \triangle & \\ & & [u_{\mathfrak{o}\mathfrak{1}}]_{\mathcal{T}} & & \end{array}$$

The existence regions of the four spatially heterogeneous equivalence classes are depicted in Fig. 2 and the respective Lyndon representatives of five classes corresponding to the "upper path" in this diagram are sketched in Fig. 3.

Remark 6. Finally, let us note that analysing the sums in (4)–(6) we arrive at the asymptotic estimates

$$N_k(n) \sim L_k(n) \sim \frac{k^n}{n}, \text{ and } B_k(n) \sim BL_k(n) \sim \frac{k^n}{2n} \text{ as } n \to \infty.$$

Acknowledgements

HJH and LM acknowledge support from the Netherlands Organization for Scientific Research (NWO) (grants 639.032.612, 613.001.304). PS and VŠ acknowledge the support of the project LO1506 of the Czech Ministry of Education, Youth and Sports under the program NPU I.

References

[1] J. Mallet-Paret, Spatial patterns, spatial chaos and traveling waves in lattice differential equations, in: Stochastic and Spatial Structures of Dynamical Systems, in: Proceedings, Physics Section. Series 1, vol. 45, Royal Netherlands Academy of Sciences, Amsterdam, 1996, pp. 105–129.
[2] J. Mallet-Paret, The global structure of traveling waves in spatially discrete dynamical systems, J. Dynam. Differential Equations 11 (1999) 49–128.
[3] B. Zinner, Existence of traveling wavefront solutions for the discrete nagumo equation, J. Differential Equations 96 (1992) 1–27.
[4] J.P. Keener, Propagation and its failure in coupled systems of discrete excitable cells, SIAM J. Appl. Math. 47 (1987) 556–572.
[5] A. Hoffman, J. Mallet-Paret, Universality of crystallographic pinning, J. Dynam. Differential Equations 22 (2010) 79–119.
[6] C.E. Elmer, E.S. Van Vleck, Spatially discrete FitzHugh–Nagumo equations, SIAM J. Appl. Math. 65 (2005) 1153–1174.
[7] J.-S. Guo, C.-H. Wu, Wave propagation for a two-component lattice dynamical system arising in strong competition models, J. Differential Equations 250 (8) (2011) 3504–3533.
[8] H.J. Hupkes, S.M. Verduyn-Lunel, Analysis of Newton's method to compute travelling waves in discrete media, J. Dynam. Differential Equations 17 (2005) 523–572.
[9] H.J. Hupkes, L. Morelli, P. Stehlík, Bichromatic travelling waves for lattice Nagumo equations, SIAM J. Appl. Dyn. Syst. 18 (2) (2019) 973–1014.
[10] H.J. Hupkes, L. Morelli, P. Stehlík, V. Švígler, Multichromatic travelling waves for lattice Nagumo equations, Appl. Math. Comput. 361 (2019) 430–452.
[11] P. Stehlík, P. Vaněk, Sign-changing diagonal perturbations of Laplacian matrices of graphs, Linear Algebra Appl. 531 (2017) 64–82.
[12] J. Volek, Landesman–Lazer conditions for difference equations involving sublinear perturbations, J. Difference Equ. Appl. 22 (11) (2016) 1698–1719.
[13] X. Chen, J.-S. Guo, C.-C. Wu, Traveling waves in discrete periodic media for bistable dynamics, Arch. Ration. Mech. Anal. 189 (2) (2008) 189–236.
[14] A. Slavík, P. Stehlík, Dynamic diffusion-type equations on discrete-space domains, J. Math. Anal. Appl. 427 (1) (2015) 525–545.
[15] M. Lothaire, Combinatorics on Words, Cambridge University Press, 1997.
[16] J. Sawada, Generating bracelets in constant amortized time, SIAM J. Comput. 31 (1) (2001) 259–268.
[17] T.M. Apostol, Introduction to Analytic Number Theory, Springer, New York, 1998.

Appendix F

Paper: Periodic stationary solutions of the Nagumo lattice differential equation: existence regions and their number

Electronic Journal of Qualitative Theory of Differential Equations
2021, No. **23**, 1–31; https://doi.org/10.14232/ejqtde.2021.1.23 www.math.u-szeged.hu/ejqtde/

Periodic stationary solutions of the Nagumo lattice differential equation: existence regions and their number

Vladimír Švígler✉

Department of Mathematics and NTIS, Faculty of Applied Sciences, University of West Bohemia, Technická 8, Pilsen 30100, Czech Republic

Received 3 September 2020, appeared 30 March 2021
Communicated by Sergei Trofimchuk

Abstract. The Nagumo lattice differential equation admits stationary solutions with arbitrary spatial period for sufficiently small diffusion rate. The continuation from the stationary solutions of the decoupled system (a system of isolated nodes) is used to determine their types; the solutions are labelled by words from a three-letter alphabet. Each stationary solution type can be assigned a parameter region in which the solution can be uniquely identified. Numerous symmetries present in the equation cause some of the regions to have identical or similar shape. With the help of combinatorial enumeration, we derive formulas determining the number of qualitatively different existence regions. We also discuss possible extensions to other systems with more general nonlinear terms and/or spatial structure.

Keywords: reaction-diffusion equation, lattice differential equation, graph differential equation, stationary solutions, enumeration, symmetry groups.

2020 Mathematics Subject Classification: 34A33, 39A12, 05A05, 34B45.

1 Introduction

In this paper, we consider the Nagumo lattice differential equation (LDE)

$$u_i'(t) = d\big(u_{i-1}(t) - 2u_i(t) + u_{i+1}(t)\big) + f\big(u_i(t); a\big) \tag{1.1}$$

for $i \in \mathbb{Z}, t > 0$ with $d > 0$, where the nonlinear term f is given by

$$f(s; a) = s(1-s)(s-a), \tag{1.2}$$

with $a \in (0,1)$. The LDE (1.1) is used as a prototype bistable equation arising from the modelling of a nerve impulse propagation in a myelinated axon [4]. The bistable equations have their use in modelling of active transmission lines [32,33], cardiophysiology [3], neurophysiology [4], nonlinear optics [25], population dynamics [28] and other fields.

✉Corresponding author. Email: sviglerv@kma.zcu.cz

Throughout this paper, we shall use correspondence of the LDE (1.1) and the Nagumo graph differential equation on a cycle (1.6). The graph and lattice reaction-diffusion differential equations are used in modelling of dynamical systems whose spatial structure is not continuous but can be described by individual vertices (possibly infinitely many) and their interaction via edges. The main difference is such that a lattice (the underlying structure of (1.1)) is infinite but there are strong assumptions on its regularity whereas graphs are usually (but not exclusively) finite and nothing is assumed about their structure in general. Such models arise in population dynamics [1], image processing [29], chemistry [27], epidemiology [26] and other fields. Alternative focus lies in the numerical analysis where the graph differential equations describe spatial discretizations of partial differential equations [17, 23]. Mathematically, the interaction between analytic and graph theoretic properties represent new and interesting challenges. The graph and lattice reaction-diffusion differential equations exhibit behaviour which cannot be observed in their partial differential equation counterparts such as a rich structure of stationary solutions [36], or other phenomena described in the forthcoming text such as pinning, multichromatic waves and other.

The LDE (1.1) is known to possess travelling wave solutions of the form

$$\begin{gathered} u_i(t) = \varphi(i - ct), \\ \lim_{s\to-\infty} \varphi(s) = 0, \quad \lim_{s\to+\infty} \varphi(s) = 1. \end{gathered} \tag{1.3}$$

As the authors in [24] and [38] had shown, there are nontrivial parameter (a, d)-regimes preventing the solutions of type (1.3) from travelling ($c = 0$) creating the so-called *pinning region*. This propagation failure phenomenon can be partially clarified by the existence of countably many stable stationary solutions (including the periodic ones) of (1.1) which inhabit mainly the pinning region, see Figure 1.1. This pinning phenomenon was observed in other lattice systems [10], experimentally in chemistry [27] and also hinted in systems of coupled oscillators [6]. It is worth mentioning that the equation (1.1) can be obtained via spatial discretization of the Nagumo partial differential equation

$$u_t(x,t) = du_{xx}(x,t) + f\big(u(x,t); a\big),$$

which possesses travelling wave solutions of type

$$\begin{gathered} u(x,t) = \varphi(x - ct), \\ \lim_{s\to-\infty} \varphi(s) = 0, \quad \lim_{s\to+\infty} \varphi(s) = 1; \end{gathered} \tag{1.4}$$

the waves are pinned if and only if $\int_0^1 f(s;a)\,\mathrm{d}s = 0$.

The waves of type (1.3) (whether the travelling or the pinned ones) can be perceived as solutions connecting two homogeneous stable states of the LDE (1.1); constant 0 and constant 1. This concept can be generalized to the solutions connecting the nonhomogeneous periodic steady states. Let $\mathrm{u}, \mathrm{v} \in \mathbb{R}^n$ be two vectors such that their periodic extensions are asymptotically stable stationary solutions of the LDE (1.1). The multichromatic wave is then a solution of a form

$$\begin{gathered} u_i(t) = \phi(i - ct), \\ \lim_{s\to-\infty} \phi(s) = \mathrm{u}, \quad \lim_{s\to+\infty} \phi(s) = \mathrm{v}, \end{gathered} \tag{1.5}$$

where

$$\phi = (\phi_1, \phi_2, \dots, \phi_n) : \mathbb{R} \to \mathbb{R}^n.$$

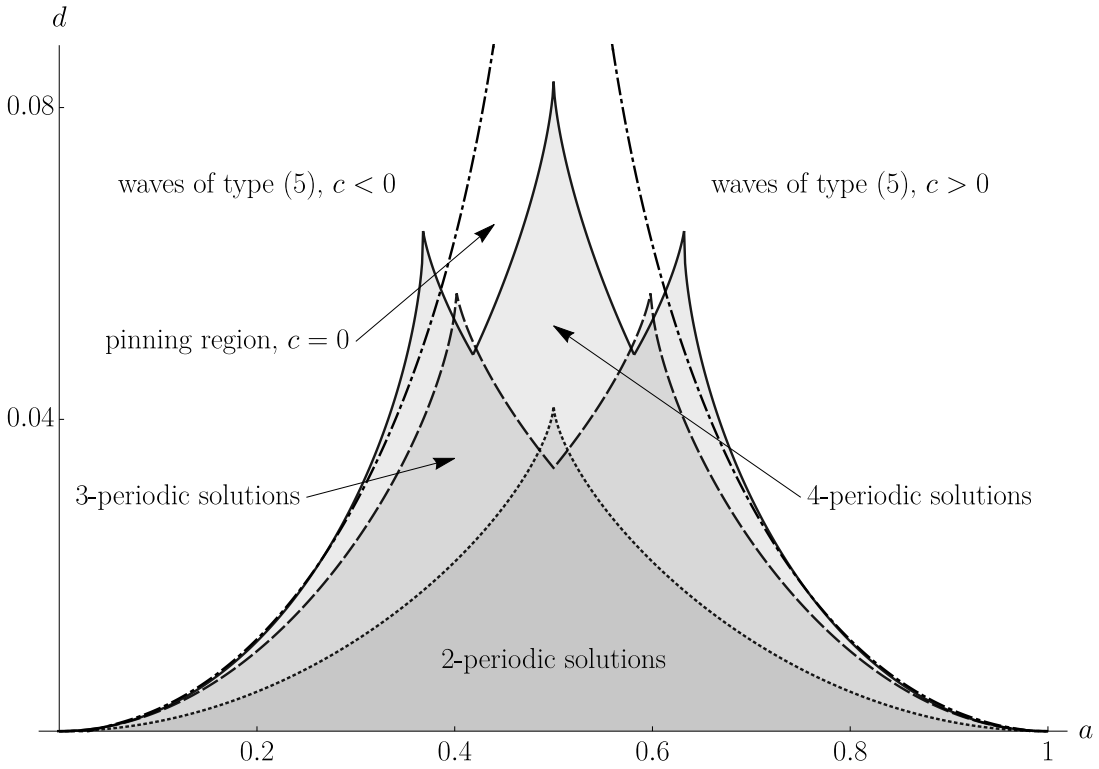

Figure 1.1: Numerically computed regions in the (a, d)-plane in which the waves of the type (1.3) travel (the regions above the two dot-dashed curves) and the pinning region (the region between the a-axis and the two dot-dashed curves). To better illustrate the significance and the presence of the stable heterogeneous n-periodic stationary solutions of the LDE (1.1) in the pinning region, we include the existence regions for the two-periodic stable stationary solutions (dotted edge), the three-periodic stable stationary solutions (dashed edge) and the four-periodic stable stationary solutions (solid edge).

The bichromatic waves connecting homogeneous and two-periodic solutions were examined in [19]. The tri- and quadrichromatic waves incorporating three- and four-periodic solutions were studied in detail in [20]. Stationary solutions with analogous construction idea, the *oscillatory plateaus* whose limits approach homogeneous steady states and there exists a middle section close to a periodic stationary solution, were analysed in [7].

Motivated by the importance of detailed understanding of the existence of the stationary solutions to the analysis of the advanced structures, the focal point of this paper is the examination of the (a, d)-regions in which particular periodic stationary solutions of the LDE (1.1) exist. Our aim is to derive counting formulas for inequivalent existence regions; the notion of equivalence is rigorously defined in the forthcoming section since it requires certain technical preliminaries. It is useful to have a detailed knowledge of the shape of the regions because of their connection to other phenomena. It has been shown in [19,20] that they are closely related to the travelling regions of the multichromatic waves. As simulations hint (see Figure 1.1), the regions corresponding to the stable stationary solutions seem to inhabit mainly the pinning region. Finally, we emphasize their obvious significance as the condition for emergence of spatial patterns in the LDE (1.1). To reach the goal, we employ the idea from [21] where we have shown a one-to-one correspondence of the LDE (1.1) n-periodic stationary solutions and

stationary solutions of the Nagumo graph differential equation (GDE) on an n-vertex cycle

$$\begin{cases} \mathrm{u}_1'(t) = d\big(\mathrm{u}_n(t) - 2\mathrm{u}_1(t) + \mathrm{u}_2(t)\big) + f\big(\mathrm{u}_1(t); a\big), \\ \mathrm{u}_2'(t) = d\big(\mathrm{u}_1(t) - 2\mathrm{u}_2(t) + \mathrm{u}_3(t)\big) + f\big(\mathrm{u}_2(t); a\big), \\ \qquad \vdots \\ \mathrm{u}_i'(t) = d\big(\mathrm{u}_{i-1}(t) - 2\mathrm{u}_i(t) + \mathrm{u}_{i+1}(t)\big) + f\big(\mathrm{u}_i(t); a\big), \\ \qquad \vdots \\ \mathrm{u}_n'(t) = d\big(\mathrm{u}_{n-1}(t) - 2\mathrm{u}_n(t) + \mathrm{u}_1(t)\big) + f\big(\mathrm{u}_n(t); a\big), \end{cases} \tag{1.6}$$

and, subsequently, with vectors of length n having elements in the three letter alphabet $\mathcal{A}_3 = \{\mathfrak{o}, \mathfrak{a}, \mathfrak{1}\}$, also called the *words*. The words encode the origin of the bifurcation branches for $d = 0$ whose existence can be shown by using the implicit function theorem for $d > 0$ small enough. Moreover, the implicit function theorem also implies that the solutions preserve their stability and the asymptotically stable solutions can be thus identified with words created with the two letter alphabet $\mathcal{A}_2 = \{\mathfrak{o}, \mathfrak{1}\}$. The region in the (a, d)-space belonging to a solution labelled by a word $\mathfrak{w}$ is denoted by $\Omega_{\mathfrak{w}} \subset \mathcal{H} = [0, 1] \times \mathbb{R}^+$. Since the stationary problem for (1.6) is equivalent to the problem of searching for the roots of a 3^n-th order polynomial it is a convoluted task to derive some information about the regions. There are known lower estimates for their upper boundaries, [12], asymptotics near threshold points $a \approx 0$, $a \approx 1$ and numerical results, both [19, 20]. The computations and the numerical simulations can be cumbersome to carry out and thus the exploitation of the equation symmetries is beneficial. The idea is to observe, whether a symmetry present in the equation relates two regions $\Omega_{\mathfrak{w}}$ without any a-priori knowledge of their shapes. For example, the LDE (1.1) is invariant to an index shift and the GDE (1.6) is invariant to the rotation of indices. Consider $n = 3$, then given a parameter tuple $(a, d) \in \mathcal{H}$, if there exists a stationary solution u_1 of the GDE (1.6) emerging from $(0, 0, 1)$ for $d = 0$, then there surely exist solutions $\mathrm{u}_2, \mathrm{u}_3$ emerging from $(0, 1, 0), (1, 0, 0)$, respectively. Moreover, $\mathrm{u}_1, \mathrm{u}_2, \mathrm{u}_3$ have identical values which are just rotated by one element to the left. We can thus say that the regions of existence of the solutions emerging from $(0, 0, 1), (0, 1, 0)$ and $(1, 0, 0)$ are identical, i.e., $\Omega_{\mathfrak{oo1}} = \Omega_{\mathfrak{o1o}} = \Omega_{\mathfrak{1oo}}$.

We show how the symmetries of the LDE (1.1) and the GDE (1.6) correspond and how they propagate to the set of the labelling words $\mathcal{A}_3^n$. Namely, the index rotation $i \mapsto i + 1$, the reflection $i \mapsto n - i + 1$ create word subsets whose respective regions are identical. The value switch $\mathfrak{o} \leftrightarrow \mathfrak{1}$ relates solution types whose respective regions are axially symmetric to each other. To this end, we define groups acting on the set of the words $\mathcal{A}_3^n$ and compute the number of their orbits (the number of the word subsets which are pairwise unreachable by the action of the group) via Burnside's lemma, Theorem 2.6. We next restrict the computations to the words whose primitive period is equal to their length since the periodic extension of the GDE (1.6) stationary solution of a certain type (e.g., $\mathfrak{oaoaoa}$) is identical to a periodic extension of its subword with the length equal to the original word's primitive period ($\mathfrak{oa}$ here). The main tool is Möbius inversion formula in this case, Theorem 2.7. The division of the word set $\mathcal{A}_3^n$ into orbits with respect to the action of a group can be achieved with the cost proportional to the number of the words (3^n in this case), see [9]. Our results do not help with the generation of the representative words directly but enable us to easily determine their number. All results are also provided for asymptotically stable stationary solutions of the LDE (1.1) whose corresponding labelling set is $\mathcal{A}_2^n$.

The paper is organized as follows. In §2 we provide an overview of the properties of

the periodic stationary solutions of the LDE (1.1) including the introduction of the labelling scheme and the statement of our main result, Theorem 2.9. We next include a list of relevant symmetries of the equation and their influence on the regions Ω_w and conclude with presentation of the used group-theoretical tools together with the commentary of the known results. Using the formal definitions from the preceding text, §3 is devoted to the derivation of lemmas needed for the proof of the main statement in §4. The final paragraphs elaborate on possible extensions to other models and we discuss open questions therein.

2 Preliminaries

2.1 Periodic stationary solutions and existence regions

Searching for a general stationary solution of the LDE (1.1) requires solving a countable system of nonlinear analytic equations. The restriction to periodic solutions simplifies the case to a finite-dimensional problem. Indeed, the problem is thus reduced to finding stationary solutions of the GDE (1.6).

Lemma 2.1 ([21, Lemma 1]). *Let $n \geq 3$. The vector $\mathrm{u} = (\mathrm{u}_1, \mathrm{u}_2, \ldots, \mathrm{u}_n)$ is a stationary solution of the GDE (1.6) if and only if its periodic extension u is an n-periodic stationary solution of the LDE (1.1). Moreover, u is an asymptotically stable solution of the GDE (1.6) if and only if u is an asymptotically stable solution of the LDE (1.1) with respect to the ℓ^∞-norm.*

If $\mathrm{u} = (\mathrm{u}_1, \mathrm{u}_2, \ldots, \mathrm{u}_n) \in \mathbb{R}^n$ is a vector then the periodic extension $(u_i)_{i\in\mathbb{Z}} \in \ell^\infty$ of u satisfies $u_i = \mathrm{u}_{1+\mathrm{mod}\,(i,n)}$ for all $i \in \mathbb{Z}$. In the further text, the function $\mathrm{mod}\,(a,b)$ denotes the remainder of the integer division of a/b for $a, b \in \mathbb{N}$.

Let us denote the function on the right-hand side of the GDE (1.6) by $h\colon \mathbb{R}^n \times (0,1) \times \mathbb{R}_0^+ \to \mathbb{R}^n$,

$$h(\mathrm{u}; a, d) = \begin{pmatrix} d(\mathrm{u}_n - 2\mathrm{u}_1 + \mathrm{u}_2) + f(\mathrm{u}_1; a) \\ \vdots \\ d(\mathrm{u}_{i-1} - 2\mathrm{u}_i + \mathrm{u}_{i+1}) + f(\mathrm{u}_i; a) \\ \vdots \\ d(\mathrm{u}_{n-1} - 2\mathrm{u}_n + \mathrm{u}_1) + f(\mathrm{u}_n; a) \end{pmatrix}. \tag{2.1}$$

The problem of finding a stationary solution of the GDE (1.6) can be now reformulated as

$$h(\mathrm{u}; a, d) = 0. \tag{2.2}$$

The problems of type (2.2), i.e., a diagonal nonlinear perturbation of a finite-dimensional linear operator, are being treated with a wide spectrum of methods ranging from variational techniques, topological approaches to monotone operator theory, see [37] and references therein. We derive some information about the system using the perturbation theory. Suppose $d = 0$, then the problem

$$h(\mathrm{u}; a, 0) = 0 \tag{2.3}$$

has precisely 3^n solutions $\mathrm{u} \in \mathbb{R}^n$ which are vectors of length n with the coordinates in the set $\{0, a, 1\}$; the system (2.3) contains n independent equations. There is also an easy way to determine the stability of the roots of (2.3). One can readily calculate that

$$f'(0; a) = -a, \qquad f'(a; a) = a(1-a), \qquad f'(1; a) = a - 1,$$

which gives $f'(s;a) < 0$ for either $s = 0$ or $s = 1$ and $f'(s;a) > 0$ for $s = a$. The derivative of the function h with respect to the first variable, $D_1h(\mathrm{u};a,0)$, is a regular diagonal matrix at each solution of (2.3)

$$D_1h(\mathrm{u};a,0) = \operatorname{diag}\big(f'(\mathrm{u}_1;a), f'(\mathrm{u}_2;a), \dots, f'(\mathrm{u}_n;a)\big).$$

If the solution vector contains the value a then it is an unstable stationary solution of the GDE (1.6) and it is stable otherwise for $d = 0$. Let some $a^* \in (0,1)$ be given. The implicit function theorem now ensures the existence of the solutions of the system (2.2) for $(a,d) \in \mathcal{U} \cap \mathcal{H}$, where $\mathcal{U}$ is some neighbourhood of the point $(a^*,0)$. The parameter dependence is smooth and the sign of the Jacobian is preserved.

The discussion above justifies the introduction of the naming scheme for the roots of (2.2) where each solution is identified with the origin of its bifurcation branch at $d = 0$. It is important to realize that the parameter $a \in (0,1)$ is allowed to vary in our considerations. The identification must be made through the substitute alphabet $\mathcal{A}_3 = \{\mathfrak{o}, \mathfrak{a}, \mathfrak{1}\}$ and we define a function $\mathrm{w}_{|a}\colon \mathcal{A}_3^n \to \{0,a,1\}^n$ for given $a \in [0,1]$ by

$$(\mathrm{w}_{|a})_i = \begin{cases} 0, & \mathrm{w}_i = \mathfrak{o}, \\ a, & \mathrm{w}_i = \mathfrak{a}, \\ 1, & \mathrm{w}_i = \mathfrak{1}. \end{cases}$$

Definition 2.2 ([20, Definition 2.1])**.** Consider a word $\mathrm{w} \in \mathcal{A}_3^n$ together with a triplet

$$(\mathrm{u},a,d) \in [0,1]^n \times (0,1) \times \mathbb{R}_0^+.$$

Then we say that u is an equilibrium of the type w if there exists a C^1-smooth curve

$$[0,1] \ni t \mapsto \big(\mathrm{v}(t), \alpha(t), \delta(t)\big) \in [0,1]^n \times (0,1) \times \mathbb{R}_0^+$$

so that we have

$$(\mathrm{v},\alpha,\delta)(0) = (\mathrm{w}_{|a}, a, 0),$$
$$(\mathrm{v},\alpha,\delta)(1) = (\mathrm{u}, a, d),$$

together with

$$h(\mathrm{v}(t);\alpha(t),\delta(t)) = 0, \qquad \det D_1h(\mathrm{v}(t);\alpha(t),\delta(t)) \neq 0$$

for all $0 \leq t \leq 1$.

We define an open pathwise connected set for each $\mathrm{w} \in \mathcal{A}_3^n$ by

$$\Omega_{\mathrm{w}} = \big\{(a,d) \in \mathcal{H} \mid \text{the system (2.2) admits a solution of the type w}\big\}.$$

Under further considerations, it can be shown that any parameter-dependent solution $u_{\mathrm{w}}(a,d)$ of type w of the system (2.2) is uniquely defined in Ω_{w} and if $(a,d) \in \Omega_{\mathrm{w}_1} \cap \Omega_{\mathrm{w}_2} \neq \emptyset$ for any two given words $\mathrm{w}_1 \neq \mathrm{w}_2$ then $u_{\mathrm{w}_1}(a,d) \neq u_{\mathrm{w}_2}(a,d)$. We recommend the reader to consult [20, §2.1] for a full-length discussion. The notion of solution type can be now passed on to the periodic stationary solutions of the LDE (1.1) via the statement of Lemma 2.1, see Figure 2.1 for illustration.

Remark 2.3. The definition of the naming scheme, Definition 2.2, ensures that a solution u_{w} of a given type $\mathrm{w} \in \mathcal{A}_3^n$ preserves its stability inside Ω_{w} since the determinant of the Jacobian matrix is not allowed to change its sign. Words from $\mathcal{A}_2^n = \{\mathfrak{o}, \mathfrak{1}\}^n$ thus represent asymptotically stable steady states.

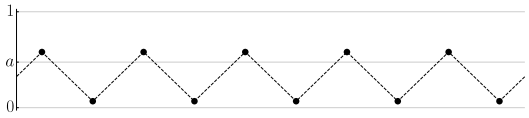

(a) A two-periodic stationary solution of type $\mathfrak{oa}$.

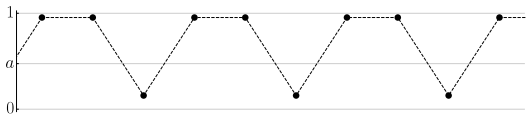

(b) A three-periodic stationary solution of type $\mathfrak{o11}$.

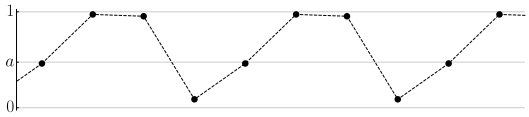

(c) A four-periodic stationary solution of type $\mathfrak{oa11}$.

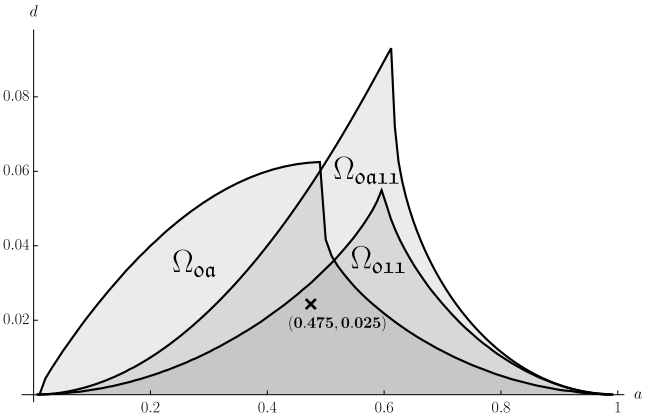

(d) Regions of existence Ω_{w} for solutions of type $\mathfrak{oa}$, $\mathfrak{o11}$, $\mathfrak{oa11}$.

Figure 2.1: Examples of two-, three- and four-periodic stationary solutions of the LDE (1.1) and the regions of existence for solutions of their respective type. The parameters $(a, d) = (0.475, 0.025)$ are set to be identical in all three cases.

2.2 Symmetries of the periodic solutions

We start with a list of symmetries of the system (2.2) which are relevant to the similarities of the regions Ω_{w} and then discuss their general impact on the number of the regions. Note that the results apply to the periodic stationary solutions of the LDE (1.1) via Lemma 2.1.

2.2.1 Rotations

Let the rotation operator $r : \mathcal{A}_3^n \to \mathcal{A}_3^n$ be defined by

$$\big(r(\mathrm{w})\big)_i = \mathrm{w}_{1+\mathrm{mod}\,(i,n)} \tag{2.4}$$

for $i = 1, 2, \ldots, n$ with obvious extension to vectors in $[0,1]^n$. A shift in indexing in (2.2) shows that $\mathrm{u} \in [0,1]^n$ is the system (2.2) solution of type $\mathrm{w} \in \mathcal{A}_3^n$ if and only if $r(\mathrm{u})$ is a solution of type $r(\mathrm{w})$. Note that this is true in general even if u cannot be assigned a type; the claim "u is a solution of the system (2.2)" is invariant with respect to the rotation r. As a direct consequence, we have

$$\Omega_{\mathrm{w}} = \Omega_{r(\mathrm{w})}$$

for all $\mathrm{w} \in \mathcal{A}_3^n$.

The transformation r generates a finite cyclic group of order n which we denote by

$$C_n = \big(\{r^0, r^1, \ldots, r^{n-1}\}, \circ\big).$$

where the group operation $\circ$ is composition of the rotations $r^i \circ r^j = r^{\mathrm{mod}\,(i+j,n)}$. For the sake of consistency with the future notation, we denote the identity element e by r^0 and $r^1 = r$. Let us mention one fact which is implicitly used throughout the paper. If i and n are relatively coprime, then r^i is a generator of the group C_n. For example, let $n = 4$, then the repetitive

composition of r^3 gives the sequence $r^3 \to r^2 \to r^1 \to r^0 \to r^3 \to \dots$ which covers the whole element set of C_4. On the other hand, the composition of r^2 gives $r^2 \to r^0 \to r^2 \to \dots$ which does not span the whole element set of C_4.

2.2.2 Reflections

Let the reflection operator $s : \mathcal{A}_3^n \to \mathcal{A}_3^n$ be defined by

$$\big(s(\mathrm{w})\big)_i = \mathrm{w}_{n-i+1} \tag{2.5}$$

together with its natural extension to vectors in $[0,1]^n$. Similar argumentation as in the previous paragraph shows that $\mathrm{u} \in [0,1]^n$ is a solution of type w of the system (2.2) if and only if $s(\mathrm{u})$ is a solution of type $s(\mathrm{w})$.

Adding the reflection s to the cyclic group C_n results in construction of the dihedral group D_n which is generated by the transformations r and s. Let us denote the composition of the rotation r^i and the reflection s by $sr^i = r^i \circ s$ (i.e., we first reflect and then rotate). For the sake of consistency, we also set $sr^0 = s$. This allows us to define the dihedral group

$$D_n = \big(\{r^0, r^1, \dots, r^{n-1}, sr^0, sr^1, \dots, sr^{n-1}\}, \circ\big)$$

and

$$\Omega_{\mathrm{w}} = \Omega_{g(\mathrm{w})}$$

holds for all $\mathrm{w} \in \mathcal{A}_3^n$ and $g \in D_n$.

2.2.3 Value permutation

The third symmetry exploits a specific property of the cubic nonlinearity

$$f(s;a) = -f(1-s;1-a)$$

with $s, a \in [0,1]$. We therefore have

$$h(\mathrm{u};a,d) = -h(\mathbf{1}-\mathrm{u};1-a,d) \tag{2.6}$$

for any $\mathrm{u} \in [0,1]^n$ and $a \in [0,1]$ where the subtraction $\mathbf{1} - \mathrm{u}$ is element-wise. Let us define the value permutation $\pi : \mathcal{A}_3^n \to \mathcal{A}_3^n$ by

$$\big(\pi(\mathrm{w})\big)_i = \begin{cases} \mathfrak{1}, & \mathrm{w}_i = \mathfrak{0}, \\ \mathfrak{a}, & \mathrm{w}_i = \mathfrak{a}, \\ \mathfrak{0}, & \mathrm{w}_i = \mathfrak{1}. \end{cases} \tag{2.7}$$

The equality (2.6) now shows that u is a solution of type w of the system (2.2) if and only if $\mathbf{1} - \mathrm{u}$ is a solution of type $\pi(\mathrm{w})$ with $a \mapsto 1-a$. As a direct consequence,

$$\Omega_{\mathrm{w}} = \mathcal{T}\big(\Omega_{\pi(\mathrm{w})}\big)$$

holds for all $\mathrm{w} \in \mathcal{A}_3^n$ where $\mathcal{T} \colon \mathcal{H} \to \mathcal{H}$ is

$$\mathcal{T}(a,d) = (1-a,d). \tag{2.8}$$

The transformation $\mathcal{T}$ is a vertical reflection with respect to the line $a = 1/2$.

The operation π generates the two element group

$$\Pi = \big(\{e, \pi\}, \circ\big),$$

where e is the identity element. The group Π can be also restricted to operate on the set of all words made with the two letter alphabet $\mathcal{A}_2$ by

$$\big(\pi(\mathrm{w})\big)_i = \begin{cases} \mathtt{1}, & \mathrm{w}_i = \mathtt{0}, \\ \mathtt{0}, & \mathrm{w}_i = \mathtt{1}. \end{cases}$$

To enlighten the notation, we denote the symbol permutation group by the letter Π regardless of the used alphabet.

In virtue of the previous notation, let us define $\pi r^i = r^i \circ \pi$ and $\pi s r^i = r^i \circ s \circ \pi$ and the group C_n^Π by

$$C_n^\Pi = \big(\{r^0, r^1, \ldots, r^{n-1}, \pi r^0, \pi r^1, \ldots, \pi r^{n-1}\}, \circ\big).$$

Note that the group C_n^Π contains elements from C_n and the elements from C_n composed with the symbol permutation π. Equivalently, we define the group D_n^Π by

$$D_n^\Pi = \left(\left\{ \begin{array}{l} r^0, r^1, \ldots, r^{n-1}, \pi r^0, \pi r^1, \ldots, \pi r^{n-1}, \\ s r^0, s r^1, \ldots, s r^{n-1}, \pi s r^0, \pi s r^1, \ldots, \pi s r^{n-1} \end{array} \right\}, \circ\right).$$

Although our main aim is the examination of the action of the group D_n^Π it is convenient to study the group C_n^Π separately to be able to obtain partial results which are used in the proof of the main theorem. Let us also emphasize that the action of the groups C_n^Π and D_n^Π preserves stability of the corresponding solutions.

2.2.4 Primitive periods

Let us assume that a word w of length n has a primitive period of length $m < n$ (say, $\mathtt{1aa1aa}$), i.e., it consists of n/m-times repeated word w_m of length m ($\mathtt{1aa}$ in this case). Then surely

$$\Omega_{\mathrm{w}} = \Omega_{\mathrm{w}_m};$$

their respective regions are identical. It is not difficult to include this in the counting formulas alone but the interplay with the group operations $(C_n, D_n, C_n^\Pi, D_n^\Pi)$ is more intricate and is treated later via Möbius inversion formula, Theorem 2.7.

2.2.5 Other solution properties

It is clear that regions belonging to the constant solutions of type $\mathtt{00}\ldots\mathtt{0}$, $\mathtt{aa}\ldots\mathtt{a}$ and $\mathtt{11}\ldots\mathtt{1}$ are trivial

$$\Omega_{\mathtt{00}\ldots\mathtt{0}} = \Omega_{\mathtt{aa}\ldots\mathtt{a}} = \Omega_{\mathtt{11}\ldots\mathtt{1}} = \mathcal{H}.$$

Another notable similarity of regions can be illustrated on the words $\mathtt{01}$ and $\mathtt{0011}$. Argumentation in [20, Section 4] shows that the region $\Omega_{\mathtt{0011}}$ has exactly the same shape as twice vertically stretched region $\Omega_{\mathtt{01}}$. Indeed, we can consider $\mathrm{u}_1 = \mathrm{u}_2$ and $\mathrm{u}_3 = \mathrm{u}_4$ for solution of type $\mathtt{0011}$ and the system (2.2) reduces to two equations with halved diffusion coefficient

d. We were however not able to generalize this observation to other types of solutions since, e.g., the natural candidate $\Omega_{\mathtt{oooiii}}$ does not possess this property since $u_1 \neq u_2 \neq u_3$ holds in general.

Motivated by the previous paragraphs, we define the notion of similarity of the sets Ω_w.

Definition 2.4. Two regions $\Omega_{w_1}, \Omega_{w_2} \subset \mathcal{H}$ are called *qualitatively equivalent* if either

$$\Omega_{w_1} = \Omega_{w_2} \quad \text{or} \quad \Omega_{w_1} = \mathcal{T}(\Omega_{w_2}).$$

Two sets are called *qualitatively distinct* if they are not qualitatively equivalent.

2.3 Orbits and equivalence classes

Orbit of a word from $\mathcal{A}_3^n$ is a subset of $\mathcal{A}_3^n$ reachable by the action of some group G. As indicated in the previous section, we are interested in the number of different orbits since each orbit with respect to the group D_n^Π contains words whose respective regions are qualitatively equivalent. In fact, the orbits divide the sets of words $\mathcal{A}_2^n, \mathcal{A}_3^n$ into equivalence classes, i.e., two words w_1, w_2 belong to the same equivalence class (have the same orbit) if there exists a group operation $g \in G$ such that $w_1 = g(w_2)$. Burnside's lemma (Theorem 2.6) and Möbius inversion formula (Theorem 2.7) are the main tools for determining the number of the classes and the classes representing words with a given primitive period, respectively.

Example 2.5. There are 27 words of length $n = 3$ made with the alphabet $\mathcal{A}_3 = \{\mathtt{o}, \mathtt{a}, \mathtt{i}\}$:

$$\begin{aligned} W_{\mathcal{A}_3}(3) = \{&\mathtt{ooo}, \mathtt{ooa}, \mathtt{ooi}, \mathtt{oao}, \mathtt{oaa}, \mathtt{oai}, \mathtt{oio}, \mathtt{oia}, \mathtt{oii},\\ &\mathtt{aoo}, \mathtt{aoa}, \mathtt{aoi}, \mathtt{aao}, \mathtt{aaa}, \mathtt{aai}, \mathtt{aio}, \mathtt{aia}, \mathtt{aii},\\ &\mathtt{ioo}, \mathtt{ioa}, \mathtt{ioi}, \mathtt{iao}, \mathtt{iaa}, \mathtt{iai}, \mathtt{iio}, \mathtt{iia}, \mathtt{iii}\}. \end{aligned}$$

Taking into account the action of the group C_3, there are 11 equivalence classes

$$\begin{aligned} W_{\mathcal{A}_3}^{C_3}(3) = \{&\{\mathtt{ooo}\}, \{\mathtt{aaa}\}, \{\mathtt{iii}\},\\ &\{\mathtt{ooa}, \mathtt{oao}, \mathtt{aoo}\}, \{\mathtt{ooi}, \mathtt{oio}, \mathtt{ioo}\}, \{\mathtt{oaa}, \mathtt{aao}, \mathtt{aoa}\},\\ &\{\mathtt{oai}, \mathtt{aio}, \mathtt{ioa}\}, \{\mathtt{oia}, \mathtt{iao}, \mathtt{aoi}\}, \{\mathtt{oii}, \mathtt{iio}, \mathtt{ioi}\},\\ &\{\mathtt{aai}, \mathtt{aia}, \mathtt{iaa}\}, \{\mathtt{aii}, \mathtt{iia}, \mathtt{iai}\}\}, \end{aligned}$$

while the action of the group D_3 merges two of these classes

$$\begin{aligned} W_{\mathcal{A}_3}^{D_3}(3) = \{&\{\mathtt{ooo}\}, \{\mathtt{aaa}\}, \{\mathtt{iii}\},\\ &\{\mathtt{ooa}, \mathtt{oao}, \mathtt{aoo}\}, \{\mathtt{ooi}, \mathtt{oio}, \mathtt{ioo}\}, \{\mathtt{oaa}, \mathtt{aao}, \mathtt{aoa}\},\\ &\{\mathtt{oai}, \mathtt{aio}, \mathtt{ioa}, \mathtt{iao}, \mathtt{aoi}, \mathtt{oia}\}, \{\mathtt{oii}, \mathtt{iio}, \mathtt{ioi}\},\\ &\{\mathtt{aai}, \mathtt{aia}, \mathtt{iaa}\}, \{\mathtt{aii}, \mathtt{iia}, \mathtt{iai}\}\}. \end{aligned}$$

The action of the groups C_3^Π and D_3^Π divides the set of the words into the same system of 6 equivalence classes

$$\begin{aligned} W_{\mathcal{A}_3}^{C_3^\Pi}(3) = W_{\mathcal{A}_3}^{D_3^\Pi}(3) = \{&\{\mathtt{ooo}, \mathtt{iii}\}, \{\mathtt{aaa}\},\\ &\{\mathtt{ooa}, \mathtt{oao}, \mathtt{aoo}, \mathtt{iia}, \mathtt{iai}, \mathtt{aii}\}, \{\mathtt{ooi}, \mathtt{oio}, \mathtt{ioo},\\ &\mathtt{iio}, \mathtt{ioi}, \mathtt{oii}\}, \{\mathtt{oaa}, \mathtt{aao}, \mathtt{aoa}, \mathtt{iaa}, \mathtt{aai}, \mathtt{aia}\},\\ &\{\mathtt{oai}, \mathtt{aio}, \mathtt{ioa}, \mathtt{iao}, \mathtt{aoi}, \mathtt{oia}\}\}. \end{aligned}$$

See Figure 2.2 for a graphical illustration of the equivalence classes.

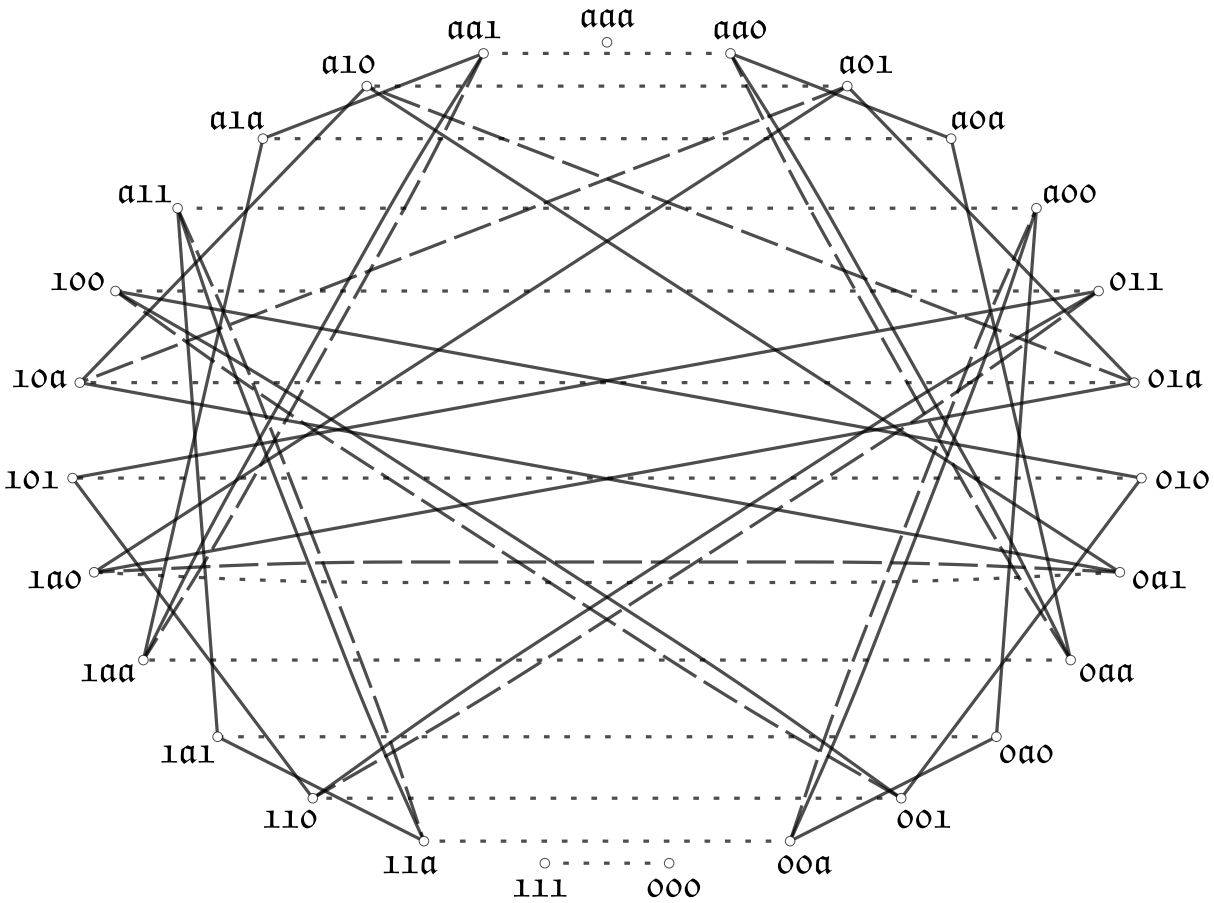

Figure 2.2: A diagram capturing the action of the groups C_3, D_3, C_3^{Π} and D_3^{Π} on the set of three-letter words made with the alphabet $\mathcal{A}_3$. The presence of a line connecting two words indicates the existence of an operation transforming the solutions onto each other. The rotation r is expressed by a solid line, the reflection s is expressed by a dashed line and the symbol permutation π is expressed by a dotted line. Every maximal connected subgraph with appropriate line types represents one equivalence class with respect to the action of a certain group, e.g., the action of C_3^{Π} is depicted by solid and dotted lines.

The crucial question is whether we can determine the number of equivalence classes in a systematic manner. A useful tool for this is Burnside's lemma [8].

Theorem 2.6 (Burnside's lemma)**.** *Let G be a finite group operating on a finite set S. Let $I(g)$ be the number of set elements such that the group operation $g \in G$ leaves them invariant. Then the number of distinct orbits O is given by the formula*

$$O = \frac{1}{|G|} \sum_{g \in G} I(g).$$

The power of Burnside's lemma lies in the fact that one counts fixed points of the group operations instead of the orbits themselves. This can be much simpler in many cases as can be seen in the forthcoming sections.

The number of the orbits induced by the action of the group C_n is usually called the number of the *necklaces* made with n beads in two (the alphabet $\mathcal{A}_2$) or three (the alphabet $\mathcal{A}_3$)

colors. The *bracelets* are induced by the action of the dihedral group D_n. Due to the lack of a common terminology, we call the classes induced by the action of the groups C_n^{Π} and D_n^{Π} the *permuted necklaces* and the *permuted bracelets*, respectively.

Burnside's lemma does not take into account the primitive period of the words. For example, the existence region of the solutions of type `0a1` coincides with the region of `0a10a1` and thus cannot be counted twice. The assumption of the primitive period of a given length together with the action of the cyclic group C_n create classes which are called the *Lyndon necklaces*. The *Lyndon bracelets* are a natural counterpart resulting from the action of the dihedral group D_n together with the assumption of a given primitive period length. The classes representing words with a given primitive period length without specification of the group are called the *Lyndon words*. We emphasize that the terminology is not fully unified in the literature but the one presented here suits our purpose best without rising any unnecessary confusion.

Theorem 2.7 (Möbius inversion formula)**.** *Let $f, g : \mathbb{N} \to \mathbb{R}$ be two arithmetic functions such that*

$$f(n) = \sum_{d|n} g(d),$$

holds for all $n \in \mathbb{N}$. Then the values of the latter function g can be expressed as

$$g(n) = \sum_{d|n} \mu\left(\frac{n}{d}\right) f(d),$$

where μ is the Möbius function.

The Möbius function μ was first introduced in [30] as

$$\mu(n) = \begin{cases} (-1)^{P(n)}, & \text{each prime factor of } n \text{ is present at most once,} \\ 0, & \text{otherwise,} \end{cases}$$

where $P(n)$ number of the prime factors of n. Use of Möbius inversion formula is a straightforward one. Let us assume, that we know the number $f(n)$ of the equivalence classes induced by the action of one of the above defined groups (C_n, D_n, C_n^{Π}, D_n^{Π}) for each $n \in \mathbb{N}$ (note that the group actions preserve the length of the primitive period of each of the words). Then for each n, this number $f(n)$ is given as the sum of the number of equivalence classes representing the words with primitive period of length d dividing n.

In the further text, we extensively exploit two crucial properties of Möbius inversion formula. Firstly, the formula is linear in the sense, that

$$\sum_{i=1}^{m} \alpha_i f_i(n) = \sum_{d|n} g(d)$$

implies

$$g(n) = \sum_{d|n} \mu\left(\frac{n}{d}\right) \sum_{i=1}^{m} \alpha_i f_i(d) = \sum_{i=1}^{m} \alpha_i \sum_{d|n} \mu\left(\frac{n}{d}\right) f_i(d),$$

and thus, each f_i can be treated separately. Secondly, we can freely exchange indices in the following manner

$$g(n) = \sum_{d|n} \mu\left(\frac{n}{d}\right) f(d) = \sum_{d|n} \mu(d)\, f\left(\frac{n}{d}\right)$$

since $n = n/d \cdot d$.

Example 2.8. We complement Example 2.5 with the list of equivalence classes of the of the words with length $n = 4$ made with the alphabet $\mathcal{A}_2 = \{0, 1\}$. There exist words of length 4 with the primitive period 2 and thus the set of the equivalence classes and the set of the Lyndon words will differ not by only the trivial constant words $\{0000\}, \{1111\}$. There are 16 words of length 4

$$\begin{aligned}\mathrm{W}_{\mathcal{A}_2}(4) = \big\{&0000, 0001, 0010, 0011, 0100, 0101, 0110, 0111,\\ &1000, 1001, 1010, 1011, 1100, 1101, 1110, 1111\big\}.\end{aligned}$$

We next include the equivalence classes induced by the action of the groups C_4, D_4, C_4^{Π}, D_4^{Π}. The words with the primitive period of length smaller than 4 are highlighted by a grey color

$$\begin{aligned}\mathrm{W}_{\mathcal{A}_2}^{C_4}(4) = \mathrm{W}_{\mathcal{A}_2}^{D_4}(4) = \big\{&\{0000\}, \{1111\}, \{0101, 1010\}, \{0011, 0110, 1100, 1001\},\\ &\{0001, 0010, 0100, 1000\}, \{0111, 1110, 1101, 1011\}\big\},\\ \mathrm{W}_{\mathcal{A}_2}^{C_4^{\Pi}}(4) = \mathrm{W}_{\mathcal{A}_2}^{D_4^{\Pi}}(4) = \big\{&\{0000, 1111\}, \{0101, 1010\}, \{0011, 0110, 1100, 1001\},\\ &\{0001, 0010, 0100, 1000, 1110, 1101, 1011, 0111\}\big\}.\end{aligned}$$

This introduction allows us to state the main theorem of the paper which gives an upper estimate of qualitatively distinct regions belonging to words of length m which ranges from one up to some given value $n \in \mathbb{N}$. We must combine the action of the dihedral group D_m^{Π} with the assumption of the primitive period equal to the word length (Lyndon bracelets) for each $m \leq n$. It is however upper estimate only, since we cannot be sure whether there exist two qualitatively equivalent regions whose labelling words are not related via any of the above mentioned symmetries. Numerical simulations however indicate that the upper bound may be close to optimal, [20].

Since the expressions in the theorem may look confusing at the first sight we include a short preliminary commentary. The function $BL_k^{\pi}(m)$ denotes the number of the permuted Lyndon bracelets of length m and the formulas are defined by parts since they incorporate the number of the bracelets which cannot be written in a consistent form for even and odd m's. The functions $\#_{\mathcal{A}_k}^{\leq}(n)$ just add the numbers of Lyndon bracelets of length ranging from two to n including the one region $\Omega_0 = \Omega_a = \Omega_1 = \mathcal{H}$ identical for all homogeneous solutions.

Theorem 2.9. *Let $n \geq 2$ be given. There are at most*

$$\#_{\mathcal{A}_3}^{\leq}(n) = 1 + \sum_{m=2}^{n} BL_{\mathcal{A}_3}^{\pi}(m) \tag{2.9}$$

qualitatively distinct regions Ω_{w}, $\mathrm{w} \in \mathcal{A}_3^m$, out of which at most

$$\#_{\mathcal{A}_2}^{\leq}(n) = 1 + \sum_{m=2}^{n} BL_{\mathcal{A}_2}^{\pi}(m) \tag{2.10}$$

regions belong to the asymptotically stable stationary solutions, where

$$BL^{\pi}_{\mathcal{A}_3}(m) = \frac{1}{4m}\left[\sum_{d|m,\, d\,odd} \mu(d)\, 3^{\frac{m}{d}} + X_{NL}(m) + 2m \sum_{d|m} \mu\left(\frac{m}{d}\right) X^{\pi}_{B,3}(d)\right], \tag{2.11}$$

$$BL^{\pi}_{\mathcal{A}_2}(m) = \frac{1}{4m}\left[\sum_{d|m,\, d\,odd} \mu(d)\, 2^{\frac{m}{d}} + 2n \sum_{d|m} \mu\left(\frac{m}{d}\right) X^{\pi}_{B,2}(d)\right], \tag{2.12}$$

$$X_{NL}(m) = \begin{cases} 1, & m = 1, \\ -1, & m = 2^{\alpha},\ \alpha \in \mathbb{N}, \\ 0, & \textit{otherwise} \end{cases}$$

and

$$X^{\pi}_{B,3}(d) = \begin{cases} \frac{4}{3} \cdot 3^{\frac{d}{2}}, & d \textit{ is even}, \\ 2 \cdot 3^{\frac{d-1}{2}}, & d \textit{ is odd}, \end{cases} \qquad X^{\pi}_{B,2}(d) = \begin{cases} 2^{\frac{d}{2}}, & d \textit{ is even}, \\ 2^{\frac{d-1}{2}}, & d \textit{ is odd}. \end{cases} \tag{2.13}$$

The formulas from Theorem 2.9 are enumerated in Table 2.1.

n	3^n	2^n	$\#^{\leq}_{\mathcal{A}_3}(n)$	$BL^{\pi}_{\mathcal{A}_3}(n)$		$\#^{\leq}_{\mathcal{A}_2}(n)$	$BL^{\pi}_{\mathcal{A}_2}(n)$	
2	9	4	3	2	{01, 0a}	2	1	{01}
3	27	8	7	4	{00a, 001, 0a1, 0aa}	3	1	{001}
4	81	16	16	9	{000a, 0001, 00aa, 00a1, 0011, 0a0a, 0aaa, 0aa1, 0a1a}	5	2	{0001, 0011}
5	243	32	36	20	not listed	8	3	{00001, 00011, 00101 }
6	729	64	80	44	not listed	13	5	{000001, 000011, 000101, 000111, 001011}
7	2187	128	184	104	not listed	21	8	not listed
8	6561	256	437	253	not listed	35	14	not listed
9	19683	512	1061	624	not listed	56	21	not listed
10	59049	1024	2689	1628	not listed	95	39	not listed

Table 2.1: Enumerated formulas from Theorem 2.9. The columns for 3^n and 2^n are added for comparison since there are in total 3^n regions Ω_{w} with $\mathrm{w} \in \mathcal{A}_3^n$ and 2^n of them correspond to the asymptotically stable stationary solutions. The unlabelled columns list the lexicographically smallest representatives of the Lyndon bracelets of a given length created with the respective alphabets; further lists are omitted to prevent clutter. Note that $\#^{\leq}_{\mathcal{A}_k}(n+1) = \#^{\leq}_{\mathcal{A}_k}(n) + BL^{\pi}_{\mathcal{A}_k}(n+1)$ holds for $n \geq 2$ and $k = 2, 3$.

2.4 Known results

Here, we summarize known results relevant to the focus of this paper. This summary consists of two parts since our main result, Theorem 2.9, contributes to the knowledge of the periodic stationary solutions of the LDE (1.1) as well as to the theory of combinatorial enumeration.

The number of equivalence classes with respect to the action of the groups C_n and D_n and their connection to the stationary solutions of the GDE (1.6) and the LDE (1.1) were studied in the paper [21]. The results considered all stationary solutions (words from $\mathcal{A}_3^n$) as well as the stable solutions (words from $\mathcal{A}_2^n$). Möbius inversion formula was used therein to determine the numbers of the Lyndon necklaces and the Lyndon bracelets.

A more general case of the group C_n^Π which acted on the set of words created with a given number of symbols not necessarily less or equal to three was considered in [13]. The author also simplified the counting formulas for the permuted necklaces and the permuted Lyndon necklaces for the case of two symbols, i.e., the alphabet $\mathcal{A}_2$, to the form which also appears in this paper, Lemmas 3.3 and 3.10. However, none of the presented results could be directly applied to the case of the transformation π acting on the words from $\mathcal{A}_3^n$. Formally, the studied object was the group product of a cyclic group C_n and a symmetric group S_k (the group of all permutations of k symbols). This coincides with our case only if $k = 2$, i.e., the words are created with a two symbol alphabet $\mathcal{A}_2$. If $k = 3$, then the group C_n^Π is isomorphic to the group product $C_n \times G$ where G is only a specific subgroup of S_3. Let us also mention that the problem was studied from the combinatorial point of view.

The authors in [14] were among other results able to derive a general counting formula for the permuted bracelets and the permuted Lyndon bracelets of words created with an arbitrary number of symbols. As in the case of the necklaces in [13], the results relevant to this paper cover the case of the reduced alphabet $\mathcal{A}_2$ only. The generality of the presented formulas however comes with a cost of their complexity. Taking advantage of our more specific setting, we are able to utilize alternative approach which enables us to further simplify the formulas for the case of the words from $\mathcal{A}_2^n$. Also, the focus of the work lied mainly in clarifying certain combinatorial concepts.

3 Counting of equivalence classes

We continue with listing and deriving auxiliary counting formulas as well as those which are directly used to prove the main result, Theorem 2.9.

In this section, (m, n) denotes the greatest common divisor of $m, n \in \mathbb{N}$.

3.1 Counting of non-Lyndon words

We start with counting of the necklaces of length n made with k symbols.

Lemma 3.1 ([34, p. 162])**.** *Given $n \in \mathbb{N}$, the number of equivalence classes induced by the action of the group C_n on the set of all words of length n made with a k-symbol alphabet is*

$$N_k(n) = \frac{1}{n} \sum_{d|n} \varphi(d) k^{\frac{n}{d}}. \tag{3.1}$$

The function $\varphi(d)$ is the Euler totient function which counts relatively coprime numbers to d, see [2]. Another classical result concerns the number of the bracelets of length n made with k symbols.

Lemma 3.2 ([34, p. 150])**.** *Given $n \in \mathbb{N}$, the number of equivalence classes induced by the action of the group D_n on the set of all words of length n made with a k-symbol alphabet is*

$$B_k(n) = \frac{1}{2}\big[N_k(n) + X_{B,k}(n)\big], \tag{3.2}$$

where

$$X_{B,k}(n) = \begin{cases} \dfrac{k+1}{2}\, k^{\frac{n}{2}}, & n \text{ is even}, \\ k^{\frac{n+1}{2}}, & n \text{ is odd}. \end{cases} \tag{3.3}$$

The formulas for the necklaces and the bracelets can be derived for a general number of symbols k. If we take the symbol permutation π into the account, the formulas regarding the alphabets $\mathcal{A}_2$ and $\mathcal{A}_3$ are slightly different and thus, we treat both cases separately. The main difference is that there are no invariant words with respect to the value permutation π with the alphabet $\mathcal{A}_2$ and n odd. Indeed, the necessary condition for the invariance is that the word has the same number of ɔ's and ɪ's. This can be bypassed by the use of the symbol ɑ from the alphabet $\mathcal{A}_3$.

Lemma 3.3 ([13, p. 300])**.** *Given $n \in \mathbb{N}$, the number of equivalence classes induced by the action of the group C_n^{Π} on the set of all words of length n made with the alphabet $\mathcal{A}_2$ is*

$$N^{\pi}_{\mathcal{A}_2}(n) = \frac{1}{2n}\left[\sum_{d|n,\, d\, odd} \varphi(d)\, 2^{\frac{n}{d}} + 2 \sum_{d|n,\, d\, even} \varphi(d)\, 2^{\frac{n}{d}}\right]. \tag{3.4}$$

A somewhat similar formula can be derived for the necklaces made with the three-letter alphabet $\mathcal{A}_3$.

Lemma 3.4. *Given $n \in \mathbb{N}$, the number of equivalence classes induced by the action of the group C_n^{Π} on the set of all words of length n made with the alphabet $\mathcal{A}_3$ is*

$$N^{\pi}_{\mathcal{A}_3}(n) = \frac{1}{2n}\left[\sum_{d|n,\, d\, odd} \varphi(d)\left(1 + 3^{\frac{n}{d}}\right) + 2 \sum_{d|n,\, d\, even} \varphi(d)\, 3^{\frac{n}{d}}\right]. \tag{3.5}$$

Proof. The group C_n^{Π} contains the pure rotations r_i and the rotations with the symbol permutations $r\pi_i$ totalling $2n$ operations. A direct application of Burnside's lemma (Theorem 2.6) yields

$$N^{\pi}_{\mathcal{A}_3}(n) = \frac{1}{2n}\left[\sum_{l=0}^{n-1} I(r^l) + \sum_{l=0}^{n-1} I(\pi r^l)\right].$$

The expression (3.1) in the context of Lemma 3.1 shows that

$$\sum_{l=0}^{n-1} I(r^l) = \sum_{d|n} \varphi(d) 3^{\frac{n}{d}}.$$

Given $l = 0, 1, \ldots, n-1$, the aim is to express the general form of a word w invariant to the operation πr^l. A rotation by l positions induces a permutation of the word's w letters with (n,l) cycles of length $n/(n,l)$. The word w is then divided into $n/(n,l)$ disjoint subwords of length (n,l). Assume that the first (n,l) letters of the word w are given. A repeated application of the operation πr^l then determines the form of all the remaining subwords of length (n,l). Indeed, the rotation by l positions applied to a word of length n induces a rotation by $l/(n,l)$ positions of the $n/(n,l)$ subwords because $l/(n,l)$ and $n/(n,l)$ are relatively coprime. Here, the parity of the subwords' number $n/(n,l)$ must be considered. If $n/(n,l)$ is odd, then the only possible word invariant to πr^l is constant ɑ's. The even $n/(n,l)$ allows $3^{(n,l)}$ possible words.

Let us pick an arbitrary divisor d of n. Then, surely $d = n/(n,l)$ for some $l \in \{0,1,\dots, n-1\}$. The cyclic group C_d with d elements can be generated by $\varphi(d)$ different values relatively coprime to d.

The argumentation above results in

$$\begin{aligned} N^{\pi}_{\mathcal{A}_3}(n) &= \frac{1}{2n}\left[\sum_{l=0}^{n-1} I(r^l) + \sum_{l=0}^{n-1} I(\pi r^l)\right], \\ &= \frac{1}{2n}\left[\sum_{d|n} \varphi(d)\, 3^{\frac{n}{d}} + \sum_{d|n,\, d\,\text{odd}} \varphi(d) + \sum_{d|n,\, d\,\text{even}} \varphi(d)\, 3^{\frac{n}{d}}\right], \\ &= \frac{1}{2n}\left[\sum_{d|n,\, d\,\text{odd}} \varphi(d)\left(1 + 3^{\frac{n}{d}}\right) + 2\sum_{d|n,\, d\,\text{even}} \varphi(d)\, 3^{\frac{n}{d}}\right]. \end{aligned}$$ □

We now approach to the formulas regarding the group D^{Π}_n; the permuted bracelets. As in the previous text, we treat the cases of the alphabets $\mathcal{A}_2$ and $\mathcal{A}_3$ separately. A general counting formula regarding the alphabet $\mathcal{A}_2$ as a special case was derived in [14]. We present an alternative proof which can be generalized to the case of the alphabet $\mathcal{A}_3$.

Lemma 3.5. *Given $n \in \mathbb{N}$, the number of equivalence classes induced by the action of the group D^{Π}_n on the set of all words of length n made with the alphabet $\mathcal{A}_2$ is*

$$B^{\pi}_{\mathcal{A}_2}(n) = \frac{1}{2}\left[N^{\pi}_{\mathcal{A}_2}(n) + X^{\pi}_{B,2}(n)\right], \tag{3.6}$$

where

$$X^{\pi}_{B,2}(n) = \begin{cases} 2^{\frac{n}{2}}, & n \text{ is even}, \\ 2^{\frac{n-1}{2}}, & n \text{ is odd}. \end{cases} \tag{3.7}$$

Proof. The group D^{Π}_n contains the rotations r^i, the rotations with the reflection sr^i, the rotations with the symbol permutation πr^i and the rotations with the reflection and the symbol permutation $\pi s r^i$. Burnside's lemma (Theorem 2.6) then yields

$$N^{\pi}_{\mathcal{A}_3}(n) = \frac{1}{4n}\left[\sum_{l=0}^{n-1} I(r^l) + \sum_{l=0}^{n-1} I(\pi r^l) + \sum_{l=0}^{n-1} I(sr^l) + \sum_{l=0}^{n-1} I(\pi s r^l)\right].$$

The equivalence classes induced by the transformations r^l and πr^l are enumerated in the expression (3.4) of Lemma 3.3. Each line in formula (3.3) counts the number of orbits with respect to the rotation with reflection sr^l.

First, we clarify certain concepts valid for the operation sr^l and subsequently apply them to the case of $\pi s r^l$. The composition of the rotation and the reflection is not commutative in general, but $sr^l = r^l \circ sr^0 = sr^0 \circ r^{n-l}$ holds for $l = 0,1,\dots,n-1$. This formula and the group associativity yields

$$sr^l \circ sr^l = (r^l \circ sr^0) \circ (sr^0 \circ r^{n-l}) = r^l \circ r^{n-l} = r^0 = e.$$

Thus, the induced permutation of the word's letters has cycles of the length 1 or 2 only.

Given $l = 0,1,\dots,n-1$, then

$$\left(sr^l(\mathrm{w})\right)_i = \mathrm{w}_{n-l-i+1}$$

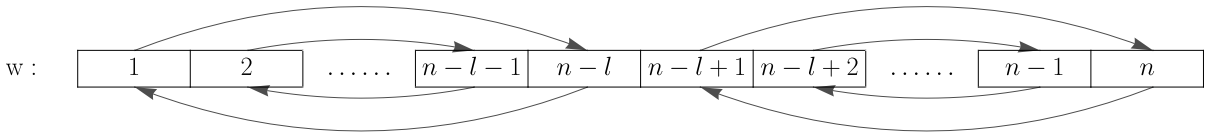

Figure 3.1: Illustration of operation of the group transformation rs_l on the word w of length n. The transformation sr^l divides the word w into two subwords whose elements starting from the edges map to each other.

for $i \leq \lceil l/2 \rceil$. Due to the composition formula, the positions from $n-l+1$ to n transform accordingly. This induces a partition of the word w into two subwords, see Figure 3.1 for illustration. The combined parities of n and l determine the parity of the subwords' length and thus whether there is a middle letter mapped to itself. For any subword of odd length, there is exactly one loop. All possible combinations are

$n \backslash l$	even	odd
even	even, even	odd, odd
odd	odd, even	even, odd

.

Let us now assume the operation πsr^l. If n is odd, then one of the subwords induced by the action of sr^l is always odd and thus there are no words fixed by πsr^l. If n is even the only possibility for the word w to be fixed is when l is also even. There are then $n/2$ cycles of length 2 leading to $n/2 \cdot 2^{n/2}$ words fixed by the operation of the form πsr^i.

The summing of all cases and including (3.3) for $I(sr^l)$ results in

$$\begin{aligned} B^{\pi}_{\mathcal{A}_2}(n)\Big|_{n \text{ even}} &= \frac{1}{4n}\left[2n \cdot N^{\pi}_{\mathcal{A}_2}(n) + \frac{3n}{2} \cdot 2^{\frac{n}{2}} + \frac{n}{2} \cdot 2^{\frac{n}{2}}\right], \\ &= \frac{1}{2}\left[N^{\pi}_{\mathcal{A}_2}(n) + 2^{\frac{n}{2}}\right], \\ B^{\pi}_{\mathcal{A}_2}(n)\Big|_{n \text{ odd}} &= \frac{1}{4n}\left[2n \cdot N^{\pi}_{\mathcal{A}_2}(n) + n \cdot 2^{\frac{n+1}{2}}\right] \\ &= \frac{1}{2}\left[N^{\pi}_{\mathcal{A}_2}(n) + 2^{\frac{n-1}{2}}\right]. \end{aligned}$$

□

A general idea presented in the proof of Lemma 3.5 can be applied to the case of the three letter alphabet $\mathcal{A}_3$.

Lemma 3.6. *Given $n \in \mathbb{N}$, the number of equivalence classes induced by the action of the group D^{Π}_n on the set of all words of length n made with the alphabet $\mathcal{A}_3$ is*

$$B^{\pi}_{\mathcal{A}_3}(n) = \frac{1}{2}\left[N^{\pi}_{\mathcal{A}_3}(n) + X^{\pi}_{B,3}(n)\right], \tag{3.8}$$

where

$$X^{\pi}_{B,3}(n) = \begin{cases} \frac{4}{3} \cdot 3^{\frac{n}{2}}, & n \text{ is even}, \\ 2 \cdot 3^{\frac{n-1}{2}}, & n \text{ is odd}. \end{cases} \tag{3.9}$$

Proof. As in the proof of Lemma 3.5, the only operations to be considered in detail are of the form πsr^i. For the sake of completeness, we note that there are $2n \cdot 3^{n/2}$ (for n even)

and $n \cdot 3^{(n+1)/2}$ (for n odd) words invariant to the action of transformations of the form sr^i, see (3.3).

Let $l = 0, 1, \ldots, n-1$ be given. The operation sr^l induces a letter permutation with cycles of length 1 or 2. In order for the word w to be fixed by the operation πsr^l, positions in the cycle of length 1 can contain the letter $\mathfrak{a}$ only.

If n is odd, then there are $(n-1)/2$ cycles of length 2 leading to $n \cdot 3^{(n-1)/2}$ fixed words. If n is even, then there are two cycles of length 1 only if l is odd. Summing over all $l = 0, \ldots, n-1$ leads to $n/2 \cdot (3^{n/2-1} + 3^{n/2})$.

The summary of the results gives

$$\begin{aligned} B^{\pi}_{\mathcal{A}_3}(n)\Big|_{n \text{ even}} &= \frac{1}{4n}\left[2n \cdot N^{\pi}_{\mathcal{A}_3}(n) + 2n \cdot 3^{\frac{n}{2}} + \frac{n}{2} \cdot (3^{\frac{n}{2}-1} + 3^{\frac{n}{2}})\right], \\ &= \frac{1}{2}\left[N^{\pi}_{\mathcal{A}_3}(n) + \frac{4}{3} \cdot 3^{\frac{n}{2}}\right], \\ B^{\pi}_{\mathcal{A}_3}(n)\Big|_{n \text{ odd}} &= \frac{1}{4n}\left[2n \cdot N^{\pi}_{\mathcal{A}_2}(n) + n \cdot 3^{\frac{n+1}{2}} + n \cdot 3^{\frac{n-1}{2}}\right], \\ &= \frac{1}{2}\left[N^{\pi}_{\mathcal{A}_3}(n) + 2 \cdot 3^{\frac{n-1}{2}}\right]. \end{aligned}$$

□

3.2 Counting of the Lyndon words

To derive the forthcoming formulas, we use a special property of the Möbius function μ and the Euler totient function φ; these functions are multiplicative. An arithmetic function $\psi : \mathbb{N} \to \mathbb{R}$ is multiplicative if and only if $\psi(1) = 1$ and $\psi(ab) = \psi(a)\psi(b)$ provided a and b are relatively coprime. To prove that two multiplicative functions ψ_1, ψ_2 are equal it is enough to show that $\psi_1(p^\alpha) = \psi_2(p^\alpha)$ for all prime p and $\alpha \in \mathbb{N}$. For further information about the multiplicative functions see, e.g., [2].

We start with a technical lemma which is used later.

Lemma 3.7. *The identity*

$$\sum_{d|n} \mu\left(\frac{n}{d}\right) \frac{n}{d}\, \varphi(d) = \mu(n) \tag{3.10}$$

holds for any $n \in \mathbb{N}$. Furthermore, the following identities hold for any n even,

$$\sum_{d|n,\, d \text{ even}} \mu\left(\frac{n}{d}\right) \frac{n}{d}\, \varphi(d) \;\Big|_{n \text{ even}} = -\mu(n), \tag{3.11}$$

$$\sum_{d|n,\, d \text{ odd}} \mu\left(\frac{n}{d}\right) \frac{n}{d}\, \varphi(d) \;\Big|_{n \text{ even}} = 2\mu(n). \tag{3.12}$$

Proof. The expression (3.10) is an equality of two multiplicative functions. It is sufficient to verify the formula for $n = p^\alpha$, where p is a prime and $\alpha \in \mathbb{N}$, [2]. If $\alpha \geq 2$ then $\mu(p^\alpha) = 0$ and

$$\sum_{d|n} \mu\left(\frac{n}{d}\right) \frac{n}{d}\, \varphi(d) = \mu(p)\, p\, \varphi(p^{\alpha-1}) + \mu(1)\, \varphi(p^\alpha) = -p^{\alpha-1}(p-1) + p^{\alpha-1}(p-1) = 0,$$

if $\alpha = 1$, then $\mu(p^\alpha) = -1$ and

$$\sum_{d|n} \mu\left(\frac{n}{d}\right) \frac{n}{d}\, \varphi(d) = \mu(p)\, p\, \varphi(1) + \mu(1)\, \varphi(p) = -p + p - 1 = -1,$$

if $\alpha = 0$, then $\mu(p^\alpha) = 1$ and

$$\sum_{d|n} \mu\left(\frac{n}{d}\right) \frac{n}{d}\, \varphi(d) = \mu(1)\, 1\, \varphi(1) = 1.$$

This proves (3.10).

Let us assume, that the even integer $n \in \mathbb{N}$ has the form $n = 2^\beta P$, where P is a product of odd primes. We can now rewrite (3.12) as

$$\sum_{d|n,\, d\,\text{odd}} \mu\left(\frac{n}{d}\right) \frac{n}{d}\, \varphi(d) = \sum_{d|n/2^\beta} \mu\left(\frac{n}{d}\right) \frac{n}{d}\, \varphi(d).$$

If $\beta \geq 1$, then the fraction n/d always contains a squared prime factor and thus $\mu(n/d) = 0$ which corresponds to $\mu(2^\beta P) = 0$. Suppose $\beta = 1$. We can now use the substitution $m = n/2$ together with the formula (3.10)

$$\begin{aligned}\sum_{d|n/2} \mu\left(\frac{n}{d}\right) \frac{n}{d}\, \varphi(d) &= \sum_{d|m} \mu\left(\frac{2m}{d}\right) \frac{2m}{d}\, \varphi(d) \\ &= -2 \sum_{d|m} \mu\left(\frac{m}{d}\right) \frac{m}{d}\, \varphi(d) = -2\mu(m) = -2\mu\left(\frac{n}{2}\right) = 2\mu(n).\end{aligned}$$

The first sign change is possible due to the fact that the fraction m/d is an odd integer and thus 2 is not part of its prime factorization. The second one utilizes the same idea. This concludes the proof of (3.12).

The identity (3.11) follows from (3.10) and (3.12) since

$$\sum_{d|n} f(d) = \sum_{d|n,\, d\,\text{even}} f(d) + \sum_{d|n,\, d\,\text{odd}} f(d),$$

holds for any $n \in \mathbb{N}$. □

The counting formula for the Lyndon necklaces can be derived by a direct argument as in [15] but we choose more technical approach whose idea is useful in later proofs.

Lemma 3.8. *Given $n \in \mathbb{N}$, the number of the Lyndon necklaces (the group C_n) with period n on the set of all words of length n made with k symbols is*

$$NL_k(n) = \frac{1}{n} \sum_{d|n} \mu\left(\frac{n}{d}\right) k^d. \tag{3.13}$$

Proof. Since

$$L_k(n) = \sum_{d|n} NL_k(n)$$

holds for all $n \in \mathbb{N}$ the use of the Möbius inversion formula (Theorem 2.7) and the subsequent

substitution $d = ml$ yields

$$\begin{aligned} NL_k(n) &= \sum_{m|n} \mu(m)\, L_k\left(\frac{n}{m}\right), \\ &= \sum_{m|n} \mu(m)\, \frac{m}{n} \sum_{l|m/n} \varphi(l)\, k^{\frac{n}{ml}}, \\ &= \frac{1}{n} \sum_{d|n} k^{\frac{n}{d}} \sum_{l|d} \mu\left(\frac{d}{l}\right) \frac{d}{l}\, \varphi(l), \\ &= \frac{1}{n} \sum_{d|n} k^{\frac{n}{d}}\, \mu(d). \end{aligned}$$

The last step uses (3.10). □

The counting formula for the Lyndon bracelets is a direct consequence of Möbius inversion formula (Theorem 2.7) and Lemmas 3.2 and 3.8.

Lemma 3.9. *Given $n \in \mathbb{N}$, the number of the Lyndon bracelets (the group D_n) with period n on the set of all words of length n made with k symbols is*

$$BL_k(n) = \frac{1}{2}\left[NL_k(n) + \sum_{d|n} \mu\left(\frac{n}{d}\right)\, X_{B,k}(d)\right], \tag{3.14}$$

where $X_{B,k}(d)$ is given by (3.3).

We continue with the counting formulas for the permuted Lyndon necklaces.

Lemma 3.10 ([13, p. 301])**.** *Let $n \in \mathbb{N}$ be given. The number of the permuted Lyndon necklaces (the group C_n^{Π}) with period n on the set of all words of length n made with the alphabet $\mathcal{A}_2$ is*

$$NL^{\pi}_{\mathcal{A}_2}(n) = \frac{1}{2n} \sum_{d|n,\, d\ odd} \mu(d)\, 2^{\frac{n}{d}}. \tag{3.15}$$

As previously mentioned, the statement of Lemma 3.10 cannot be generalized to the case of the three-letter alphabet $\mathcal{A}_3$ in a straightforward manner.

Lemma 3.11. *Given $n \in \mathbb{N}$, the number of the permuted Lyndon necklaces (the group C_n^{Π}) with period n on the set of all words of length n made with the alphabet $\mathcal{A}_3$ is*

$$NL^{\pi}_{\mathcal{A}_3}(n) = \frac{1}{2n}\left[\sum_{d|n,\, d\ odd} \mu(d)\, 3^{\frac{n}{d}} + X_{NL}(n)\right], \tag{3.16}$$

where

$$X_{NL}(n) = \begin{cases} 1, & n = 1, \\ -1, & n = 2^{\alpha},\ \alpha \in \mathbb{N}, \\ 0, & \textit{otherwise}. \end{cases}$$

Proof. We directly apply Möbius inversion formula (Theorem 2.7) to (3.5) in an adjusted form

$$N^{\pi}_{\mathcal{A}_3}(n) = \frac{1}{2n}\left[\sum_{d|n} \varphi(d)\, 3^{\frac{n}{d}} + \sum_{d|n,\, d\ \text{even}} \varphi(d)\, 3^{\frac{n}{d}} + \sum_{d|n,\, d\ \text{odd}} \varphi(d)\right].$$

Thanks to the linearity of Möbius inversion formula, we may threat the expression summandwise. For the sake of simplicity, the first summand is readily rewritten in the virtue of Lemma 3.8

$$\begin{aligned} NL^{\pi}_{\mathcal{A}_3}(n) &= \sum_{m|n} \mu(m)\, N^{\pi}_{\mathcal{A}_3}\left(\frac{n}{m}\right), \\ &= \frac{1}{2n} \sum_{d|n} \mu(d)\, 3^{\frac{n}{d}} + \sum_{m|n} \mu(m)\, \frac{m}{2n} \sum_{l|n/m,\, l \text{ even}} \varphi(l)\, 3^{\frac{n}{ml}} + \sum_{d|n} \mu\left(d\right) \frac{d}{2n} \sum_{l|n/d,\, l \text{ odd}} \varphi(l). \end{aligned}$$

We now want to show that

$$\sum_{m|n} \mu(m)\, \frac{m}{2n} \sum_{l|n/m,\, l \text{ even}} \varphi(l)\, 3^{\frac{n}{ml}} = -\frac{1}{2n} \sum_{d|n,\, d \text{ even}} \mu(d)\, 3^{\frac{n}{d}},$$

which proves the first part of (3.16). Indeed, the use of the substitution $d = ml$ in the virtue of the proof of Lemma 3.8 and (3.11) yields

$$\sum_{m|n} \mu(m)\, \frac{m}{2n} \sum_{l|n/m,\, l \text{ even}} \varphi(l)\, 3^{\frac{n}{ml}} = \frac{1}{2n} \sum_{d|n} 3^{\frac{n}{d}} \sum_{l|n/d,\, l \text{ even}} \mu\left(\frac{d}{l}\right) \frac{d}{l}\, \varphi(l) = -\frac{1}{2n} \sum_{d|n,\, d \text{ even}} \mu(d)\, 3^{\frac{n}{d}}.$$

The rest of the proof is concluded by the evaluation of

$$\sum_{d|n} \mu\left(d\right) \frac{d}{2n} \sum_{l|n/d,\, l \text{ odd}} \varphi(l).$$

Any number $m \in \mathbb{N}$ can be expressed as $m = 2^{\alpha} P$, where $\alpha \in \mathbb{N}_0$ and P is a product of odd primes. Then

$$\frac{1}{m} \sum_{d\,/\,m,\, d \text{ odd}} \varphi(d) = \frac{P}{m} = \frac{1}{2^{\alpha}} \tag{3.17}$$

since

$$\sum_{d|m} \varphi(d) = m,$$

holds in general, [2].

Assume now that $n \in \mathbb{N}$ can be expressed as $n = 2^{\beta} Q$, where $\beta \in \mathbb{N}_0$ and Q is a product of odd primes. Let us turn our attention to the equality

$$\frac{1}{n} X_{NL(n)} = \sum_{d|n} \mu\left(d\right) \frac{d}{n} \sum_{l|n/d,\, l \text{ odd}} \varphi(l).$$

Any $d|n$ can be represented as $2^{\gamma} R$, where $0 \leq \gamma \leq \beta$ and R is a product of odd primes. Decomposing the expression by the exponent γ and using (3.17) lead to

$$\frac{1}{n} X_{NL(n)} = \sum_{\gamma=0}^{\beta} \sum_{R|Q} \mu(2^{\gamma} R)\, \frac{1}{2^{\beta-\gamma}} = \sum_{\gamma=0}^{\beta} \frac{1}{2^{\beta-\gamma}} \sum_{R|Q} \mu(2^{\gamma} R). \tag{3.18}$$

Assume that $\beta = 0$ and $Q = 1$. A straightforward computation gives

$$\left.\frac{1}{n} X_{NL(n)}\right|_{n=1} = \mu(1) \cdot 1 = 1.$$

Assume that $\beta > 1$ and $Q = 1$. If we consider $\gamma \geq 2$ in (3.18), then $\mu(2^\gamma R) = 0$. The sum can be now evaluated

$$\frac{1}{n} X_{NL(n)}\Big|_{n=2^\beta} = \mu(1)\,\frac{1}{2^\beta} + \mu(2)\,\frac{1}{2^{\beta-1}} = -\frac{1}{2^\beta} = -\frac{1}{n}.$$

Assume that $Q > 1$. Let us fix γ such that $0 \leq \gamma \leq \beta$. Without loss of generality, we can assume that $\gamma \leq 1$ and each prime factor in R is present at most once. Indeed, $\mu(2^\gamma R) = 0$ otherwise. The sign of the nonzero expression $\mu(2^\gamma R)$ is now dependent on the number of prime factors of R. If there are m prime factors in Q, then R with l factors can be chosen in $\binom{m}{l}$ possible ways. The sign of $\mu(2^\gamma R)$ alternates as l increases and we have

$$\sum_{l=0}^{m} (-1)^l \binom{m}{l} = 0.$$

This results in

$$\frac{1}{n} X_{NL(n)}\Big|_{n=2^\beta Q} = 0. \qquad \square$$

We conclude this section with two lemmas that are direct consequences of Möbius inversion formula (Theorem 2.7), Lemma 3.5 (respectively 3.6) and Lemma 3.8.

Lemma 3.12. *Given $n \in \mathbb{N}$, the number of the permuted Lyndon bracelets (the group D_n^Π) with period n on the set of all words of length n made with the alphabet $\mathcal{A}_2$ is*

$$BL^\pi_{\mathcal{A}_2}(n) = \frac{1}{2}\left[NL^\pi_{\mathcal{A}_2}(n) + \sum_{d|n} \mu\left(\frac{n}{d}\right)\, X^\pi_{B,2}(d)\right], \tag{3.19}$$

where $NL^\pi_{\mathcal{A}_2}(n)$ and $X^\pi_{B,2}(d)$ are given by (3.15) and (3.7), respectively.

Lemma 3.13. *Given $n \in \mathbb{N}$, the number of the permuted Lyndon bracelets (the group D_n^Π) with period n on the set of all words of length n made with the alphabet $\mathcal{A}_3$ is*

$$BL^\pi_{\mathcal{A}_3}(n) = \frac{1}{2}\left[NL^\pi_{\mathcal{A}_3}(n) + \sum_{d|n} \mu\left(\frac{n}{d}\right)\, X^\pi_{B,3}(d)\right], \tag{3.20}$$

where $NL^\pi_{\mathcal{A}_3}(n)$ and $X^\pi_{B,3}(d)$ are given by (3.16) and (3.9), respectively.

4 Conclusion

We start the final part of this paper with the proof of the main result, Theorem 2.9.

Proof of Theorem 2.9. For given $n \geq 2$ the sequence $BL^\pi_{\mathcal{A}_3}(n)$ gives the number of the permuted Lyndon bracelets, i.e., the equivalence classes of words with respect to the rotations r^i, the reflection s, the value permutation π (group D_n^Π), their compositions and with primitive period of length n. As discussed in §2.2, regions Ω_w surely have identical (the rotations r_i, the reflections s) or similar, with respect to the operator $\mathcal{T}$ defined by (2.8), (the value permutation π) shape and are thus qualitatively equivalent (see Definition 2.4). The expression (2.11) is exactly (3.20) with (3.16) substituted and (2.13) corresponds to (3.9). We sum $BL^\pi_{\mathcal{A}_3}(n)$ from $m = 2$ to avoid including trivial existence regions for the constant words $\mathfrak{o}\mathfrak{o}\ldots\mathfrak{o}$, $\mathfrak{a}\mathfrak{a}\ldots\mathfrak{a}$ and $\mathfrak{1}\mathfrak{1}\ldots\mathfrak{1}$

which are represented by the additional 1, this yields (2.9). The formulas are upper estimates only since we cannot eliminate the possibility that there are two qualitatively equivalent regions whose respective words are not related by any of the symmetries. Similar argumentation holds for regions belonging to the stable stationary solutions since the corresponding words are made with the alphabet $\mathcal{A}_2$, Lemma 2.1 and Definition 2.2. The expression (2.12) is equal to (3.19) where $BL^{\pi}_{\mathcal{A}_2}(n)$ is given by (3.15). □

The approach presented here can be used to obtain similar results in other or more general settings. The two main extension directions are the change of a spatial structure and the change of dynamics. The extensions can be combined but we present them separately for the sake of clarity.

4.1 Change of spatial structure

4.1.1 Graphs with nontrivial automorphism

The main objects of interests were the LDE (1.1) and the GDE (1.6) in this paper. In general, given a graph $\mathcal{G} = (V, E)$, the Nagumo graph differential equation can be written as

$$\mathrm{u}_i'(t) = d \sum_{j \in \mathcal{N}(i)} \big(\mathrm{u}_j(t) - \mathrm{u}_i(t)\big) + f\big(\mathrm{u}_i(t); a\big),$$

where $i \in V$ and $\mathcal{N}(i)$ is the set of all neighbours of the vertex i, i.e., $j \in \mathcal{N}(i)$ if and only if $(i, j) \in E$. Provided the graph $\mathcal{G}$ has a nontrivial automorphism (a nontrivial self-map which preserves the edge-vertex connectivity) the approach used here can be extended. Indeed, the group D_n is the automorphism group of the cycle graph with n vertices and all computations can be carried out by replacing the dihedral group D_n with the automorphism group of the graph $\mathcal{G}$.

4.1.2 Multi-dimensional square lattices

The underlying spatial structure of the LDE (1.1) is a one-dimensional lattice, an infinite path graph. Examination of bistable reaction-diffusion systems on multi-dimensional square lattices has been carried out, see e.g., [11, 18, 22]. For example, let us have a bistable reaction-diffusion system on the two-dimensional square lattice

$$u_{i,j}'(t) = d\big(u_{i-1,j}(t) + u_{i+1,j}(t) + u_{i,j-1}(t) + u_{i,j+1}(t) - 4u_{i,j}(t)\big) + f\big(u_{i,j}(t); a\big), \tag{4.1}$$

for $i, j \in \mathbb{Z}$. A reproduction of the proof of Lemma 2.1 together with the comparison principle [16, Proposition 3.1] show that the stationary solutions of the LDE (4.1) in the form of a repeated 2×2 pattern are equivalent to the stationary solutions of the GDE (1.6) on four vertices with the doubled diffusion rate d, see Figure 4.1 for illustration.

4.2 Change of dynamics

Various changes in the nonlinear part of (1.1) are discussed here. The proof of Lemma 2.1 in [21, Lemma 1] is actually independent of the nonlinear term with one exception. Indeed, the only part of the proof dependent on the specific nonlinear term is the comparison principle from [11, Lemma 1] and the only assumption is the existence of two ordered steady states of the equation, constant 0 and constant 1 in our case. This is satisfied for bistable and multistable reaction terms presented here.

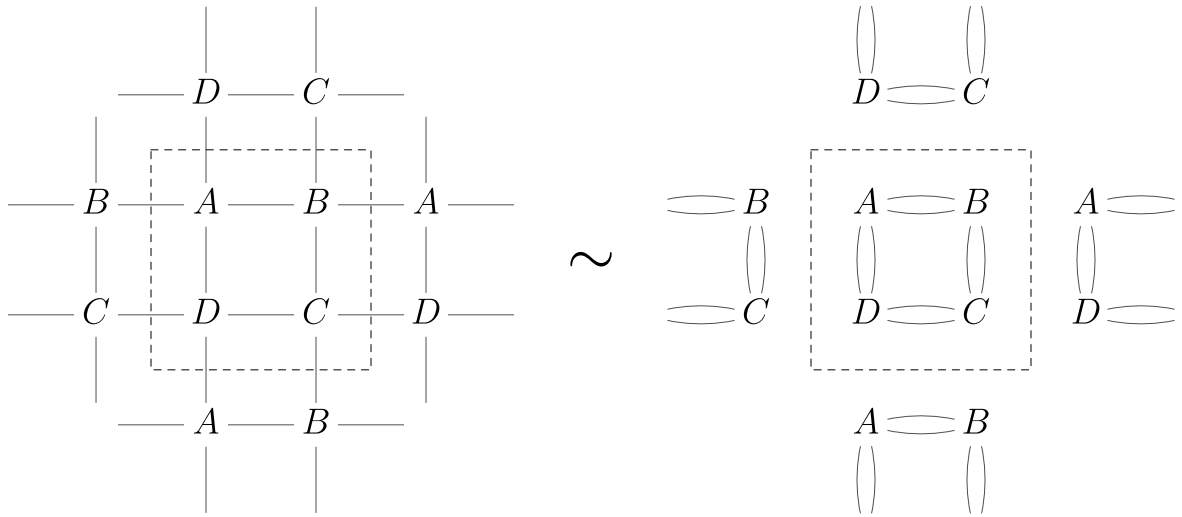

Figure 4.1: Illustration of a possible Lemma 2.1 extension for patterns on two-dimensional lattices. A general idea is that the edges crossing the dashed line are wrapped back inside from the opposite sides.

4.2.1 Scaled cubic nonlinearity

The cubic bistable nonlinear term (1.2) is dependent on one parameter only and moreover, the value of the parameter is actually one of its roots. Let us assume the function

$$f_{\mathrm{cub}}(s,\mathrm{p}) = s\big(s-\nu_-(\mathrm{p})\big)\big(\nu_+(\mathrm{p})-s\big), \tag{4.2}$$

where $\mathrm{p}\in\Theta\subset\mathbb{R}^m$ is a detuning vector, Θ is an open set and we assume that $\nu_-,\nu_+\colon\Theta\to\mathbb{R}^+$ and $0<\nu_-(\mathrm{p})<\nu_+(\mathrm{p})$ for all $\mathrm{p}\in\Theta$. The term f_{cub} has two bounding roots 0 and $\nu_+(\mathrm{p})$ for any given $\mathrm{p}\in\Theta$. The LDE (1.1) with f_{cub} thus admits the comparison principle and its n-periodic stationary solutions correspond to the stationary solutions of its respective GDE on a cycle graph with n vertices.

The stationary problem for the GDE can be written in the form

$$\widetilde{h}(\mathrm{u};\mathrm{p},d)=0, \tag{4.3}$$

where

$$\widetilde{h}_i(\mathrm{u};\mathrm{p},d) = d(\mathrm{u}_{i-1}-2\mathrm{u}_i+\mathrm{u}_{i+1})+f_{\mathrm{cub}}(\mathrm{u}_i,\mathrm{p}).$$

We omitted the modulo wrapping at vertices 1 and n as in (2.2) to enlighten the notation. A direct computation yields

$$\widetilde{h}(\mathrm{u};\mathrm{p},d) = \nu_+^3(\mathrm{p})\,h\left(\frac{\mathrm{u}}{\nu_+(\mathrm{p})};\frac{\nu_-(\mathrm{p})}{\nu_+(\mathrm{p})},\frac{d}{\nu_+^2(\mathrm{p})}\right).$$

This enables us to define solution types for (4.3) via Definition 2.2 (the sign of the first derivative's determinant agrees) and to obtain corresponding existence regions $\widetilde{\Omega}_{\mathrm{w}}$ through the implicit transformation

$$\widetilde{\Omega}_{\mathrm{w}} = \left\{(\mathrm{p},d)\in\Theta\times\mathbb{R}_0^+ \;\middle|\; \left(\frac{\nu_-(\mathrm{p})}{\nu_+(\mathrm{p})},\frac{d}{\nu_+^2(\mathrm{p})}\right)\in\Omega_{\mathrm{w}}\right\}. \tag{4.4}$$

An example of system leading to (4.3) is the reduced version of the model decribing potential propagation in myelinated axon with recovery [4]

$$\begin{aligned} u_i'(t) &= d\big(u_{i-1}(t) - 2u_i(t) + u_{i+1}(t)\big) + f_{\text{Bell}}\big(u_i(t); a, b\big) - v_i(t), \\ v_i'(t) &= \sigma\, u_i(t) - \gamma\, v_i(t) \end{aligned} \tag{4.5}$$

such that

$$f_{\text{Bell}}\big(s; a, b\big) = s(s-a)(b-s).$$

Via approach similar to [4], we assume, that the change of the recovery value v_i is faster than the change in u_i and thus the second equation in (4.5) resides at its steady state. The problem can be then expressed as

$$u_i'(t) = d\big(u_{i-1}(t) - 2u_i(t) + u_{i+1}(t)\big) + f_{\text{Bell}}\big(u_i(t); a, b\big) - \beta\, u_i(t)$$

with $\beta = \sigma/\gamma$ possibly small and the generalization of Lemma 2.1 ensures the equivalence of the periodic steady states of (4.5) and the system (4.3) solutions. We can directly determine

$$\mathbf{p} = (a, b, \beta), \quad \Theta = \left((a, b, \beta) \in \mathbb{R}^3 \,\middle|\, a, b, \beta > 0,\ b > a,\ \beta < \frac{(a-b)^2}{4} \right), \tag{4.6}$$

$$\nu_\pm(a, b, \beta) = \frac{1}{2}\Big(a + b \pm \sqrt{(a-b)^2 - 4\beta}\Big). \tag{4.7}$$

The inequality $b > a$ preserves the bistable behaviour in the original equation. See Figure 4.2 for illustration.

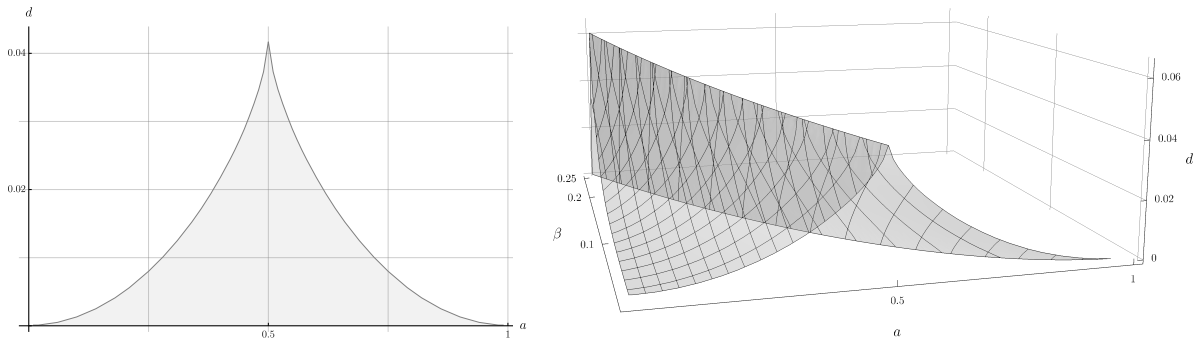

Figure 4.2: The left panel depicts the region $\Omega_{\mathfrak{o}1}$ for the equation (1.1) and its comparison to the same region for (4.5) obtained via the transformation in (4.4). The parameter $b = 1$ was set.

4.2.2 Polynomial nonlinearity of higher order

This paper focused on the model (1.1) with the cubic bistable nonlinearity

$$f(s; a) = s(1-s)(s-a).$$

The idea presented in §2.1 can be extended to a general polynomial nonlinearity provided it allows a spatially nonhomogeneous steady state of the LDE (1.1) or the GDE (1.6)

$$f_{\text{ext}}(s; a_1, \ldots, a_q) = s(1-s)\prod_{i=1}^{q}(s - a_i)$$

for $q \geq 3$ odd, $a_i \in (0,1)$ and $a_i \neq a_j$ for all $i, j \in \{1, \ldots, q\}$ such that $i \neq j$. Note that

$$f_{\mathrm{ext}}(s; a_1, \ldots, a_q) = -f_{\mathrm{ext}}(1-s; 1-a_1, \ldots, 1-a_q)$$

holds and the value permutation π can be thus redefined as

$$\big(\pi(\mathtt{w})\big)_i = \begin{cases} \mathtt{1}, & \mathtt{w}_i = \mathtt{0}, \\ \mathtt{a}_{q-i+1}, & \mathtt{w}_i = \mathtt{a}_i,\ i = 1, \ldots, q, \\ \mathtt{0}, & \mathtt{w}_i = \mathtt{1}. \end{cases}$$

The counting formulas for the necklaces (3.1), the bracelets (3.2) and the Lyndon words (3.13), (3.14) can be then straightforwardly applied with $k = q + 2$ for all solutions and $k = 2 + (q-1)/2$ for asymptotically stable solutions.

The cubic-quintic nonlinearity, [5],

$$f_{\mathrm{cq}}(s, \mu) = \mu s + 2s^3 - s^5$$

has five distinct roots

$$\Big\{0, \pm\sqrt{1 \pm \sqrt{1-\mu}}\Big\}.$$

for $\mu \in (0,1)$. The LDE with f_{cq} can be rescaled for the stationary solutions to fit the interval $[0,1]$ and the approach described in the previous paragraph can be used. Note that sequence of $1/2$'s is then always a stationary solution regardless of μ and all the counting formulas would count not only shape-distinct regions $\Omega_{\mathtt{w}}$ but distinct periodic stationary solutions. This is true for (1.1) only if $a = 1/2$.

4.2.3 General bistable nonlinearity

A system with a general bistable nonlinearity f_{gen} as considered in [24]

1. $f_{\mathrm{gen}}(0) = f_{\mathrm{gen}}(a) = f_{\mathrm{gen}}(1) = 0$, $0 < a < 1$ and $f_{\mathrm{gen}}(x) \neq 0$ for $x \neq 0, a, 1$,
2. $f_{\mathrm{gen}}(x) < 0$ for $0 < x < a$ and $f_{\mathrm{gen}}(x) > 0$ for $a < x < 1$,
3. $f'_{\mathrm{gen}}(x_0) = f'_{\mathrm{gen}}(x_1) = 0$, $0 < x_0 < a < x_1 < 1$ and $f'_{\mathrm{gen}}(x) \neq 0$ for $x \neq x_0, x_1$,

can be only partially treated by the methods presented here. The conditions above allow the application of the implicit function theorem. It is however possible for a general bistable nonlinearity to exhibit the "blue sky" bifurcation before any of the determinants in Definition 2.2 reaches zero, see [31, §1.2.2]. Moreover, the action of the value permutation group Π can be included only if f_{gen} can be expressed in a form such that

$$f_{\mathrm{gen}}(x; a) = -f_{\mathrm{gen}}(1-x; 1-a)$$

holds.

4.2.4 Multi-dimensional local dynamics

The local dynamics at an isolated vertex of models (1.1) and (1.6) are one-dimensional since the behaviour at a single vertex can be described by a single equation. This is not always the case in many reaction-diffusion models. For example, the Lotka–Volterra competition model on a graph as in [35]

$$\begin{aligned} u_i'(t) &= d_u \sum_{j\in N(i)} \big(u_j(t) - u_i(t)\big) + \rho_u u_i(t)\big(1 - u_i(t) - \alpha v_i(t)\big), \\ v_i'(t) &= d_v \sum_{j\in N(i)} \big(v_j(t) - v_i(t)\big) + \rho_v v_i(t)\big(1 - \beta u_i(t) - v_i(t)\big), \end{aligned} \tag{4.8}$$

where $N(i)$ is the set of all neighbours of the vertex i, locally possesses two asymptotically stable stationary solutions (originating from the points $(0,1)$ and $(1,0)$ which can be denoted by $\mathfrak{o},\mathfrak{i}$) and one unstable nontrivial stationary solution (originating from the point $((1-\alpha)/(1-\alpha\beta),(1-\beta)/(1-\alpha\beta))$ here denoted by $\mathfrak{a}$) at each separated vertex provided $\alpha,\beta > 1$. The solutions containing elements originating from $(0,0)$ are not considered since their immediate continuation is directed outside the positive quadrant. The implicit function theorem assures that the naming scheme from Definition 2.2 can be employed. A proper scaling results in $\rho_u = \rho_v = 1$ and the regions of existence are pathwise connected sets of points $(d_u, d_v, \alpha, \beta) \in \mathbb{R}_0^+ \times \mathbb{R}_0^+ \times (1,\infty) \times (1,\infty)$. As in [35], it is convenient to fix the ratio $\eta := d_u/d_v$ and consider the regions Ω_w in a three-dimensional space only. The stationary problem for (4.8) is now invariant with respect to the transformation $u_i \leftrightarrow v_i$, $\alpha \leftrightarrow \beta$ and all counting results can be thus applied provided the underlying graph has a nontrivial automorphism.

4.3 Open questions

The idea of Lemma 2.1 is such that the restriction to the periodic stationary solutions of the LDE (1.1) allows us to formally divide the lattice into a countable number of identical finite graphs. Similar approach was used in §4.1. General equivalence claim which helps to reduce the search for an arbitrary periodic patterns in sufficiently regular infinite graphs (e.g., triangular lattice, hexagonal lattice) into a finite-dimensional problem is still missing.

Acknowledgements

Author acknowledges the support of the project LO1506 of the Czech Ministry of Education, Youth and Sports under the program NPU I and the support of Grant Agency of the Czech Republic, project no. 18-03253S. The author is grateful to Petr Stehlík and Jonáš Volek for their valuable comments and patience. The author would also like to express his gratitude to the anonymous referee.

References

[1] L. J. S. Allen, Persistence, extinction, and critical patch number for island populations, *J. Math. Biol.* **24**(1987), No. 6, 617–625. https://doi.org/10.1007/bf00275506; MR0880448; Zbl 0603.92019

[2] T. M. Apostol, *Introduction to analytic number theory*, Springer-Verlag, New York, 1976. https://doi.org/10.1007/978-1-4757-5579-4; MR0434929; Zbl 0335.10001

[3] G. W. Beeler, H. Reuter, Reconstruction of the action potential of ventricular myocardial fibres, *J. Physiol.* **268**(1977), No. 1, 177–210. https://doi.org/10.1113/jphysiol.1977.sp011853

[4] J. Bell, Some threshold results for models of myelinated nerves, *Math. Biosci.* **54**(1981), No. 3–4, 181–190. https://doi.org/10.1016/0025-5564(81)90085-7; MR0630848; Zbl 0454.92009

[5] G. Boudebs, S. Cherukulappurath, H. Leblond, J. Troles, F. Smektala, F. Sanchez, Experimental and theoretical study of higher-order nonlinearities in chalcogenide glasses, *Opt. Commun.* **219**(2003), No. 1–6, 427–433. https://doi.org/10.1016/s0030-4018(03)01341-5

[6] J. J. Bramburger, Rotating wave solutions to lattice synamical systems I: The anti-continuum limit, *J. Dynam. Differential Equations* **31**(2019), No. 1, 469–498. https://doi.org/10.1007/s10884-018-9678-7; MR3935152; Zbl 07047675

[7] J. J. Bramburger, B. Sandstede, Spatially localized structures in lattice dynamical systems, *J. Nonlinear Sci.* **30**(2020), No. 2, 603–644. https://doi.org/10.1007/s00332-019-09584-x; MR4081151; Zbl 1440.37072

[8] W. Burnside, *Theory of groups of finite order*, Cambridge University Press, 1911.

[9] G. Butler, Fundamental algorithms for permutation groups, Springer Berlin Heidelberg, 1991. MR1225579; Zbl 0785.20001

[10] J. W. Cahn, J. Mallet-Paret, E. S. Van Vleck, Traveling wave solutions for systems of ODEs on a two-dimensional spatial lattice, *SIAM J. Appl. Math.* **59**(1999), No. 2, 455–493. https://doi.org/10.1137/s0036139996312703; MR1654427; Zbl 0917.34052

[11] X. Chen, J.-S. Guo, C.-C. Wu., Traveling waves in discrete periodic media for bistable dynamics, *Arch. Ration. Mech. An.* **189**(2008), 189–236. https://doi.org/10.1007/s00205-007-0103-3; MR2413095; Zbl 1152.37033

[12] C.-Y. Cheng, C.-W. Shih, Pattern formations and spatial entropy for spatially discrete diffusion equations, *Phys. D* **204**(2005), No. 3–4, 135–160. https://doi.org/10.1016/j.physd.2005.04.007; MR2148376; Zbl 1081.37052

[13] N. J. Fine, Classes of periodic sequences, *Illinois J. Math.* **2**(1958), No. 2, 285–302. https://doi.org/10.1215/ijm/1255381350

[14] E. N. Gilbert, J. Riordan, Symmetry types of periodic sequences, *Illinois J. Math.* **5**(1961), No. 4, 657–665. https://doi.org/10.1215/ijm/1255631587

[15] S. W. Golomb, B. Gordon, L. R. Welch, Comma-free codes, *Canadian J. Math.* **10**(1993), 202–209. https://doi.org/10.4153/cjm-1958-023-9; MR0095091; Zbl 0081.14601

[16] A. Hoffman, H. Hupkes, E. V. Vleck, Entire solutions for bistable lattice differential equations with obstacles, *Mem. Am. Math. Soc.* **250**(2017), No. 1188. https://doi.org/10.1090/memo/1188; MR3709723; Zbl 1406.34003

[17] R. Hošek, J. Volek, Discrete advection-diffusion equations on graphs: maximum principle and finite volumes, *Appl. Math. Comput.* **361**(2019), 630–644. https://doi.org/10.1016/j.amc.2019.06.014; MR3973160 ; Zbl 1429.65212

[18] H. J. Hupkes, L.Morelli, Travelling corners for spatially discrete reaction-diffusion systems, *Commun. Pure Appl. Anal.* **19**(2020), No. 3, 1609–1667. https://doi.org/10.3934/cpaa.2020058; MR4064047; Zbl 1436.34009

[19] H. J. Hupkes, L. Morelli, P. Stehlík, Bichromatic travelling waves for lattice Nagumo equations, *SIAM J. Appl. Dyn. Syst.* **18**(2019), No. 2, 973–1014. https://doi.org/10.1137/18m1189221; MR3952666; Zbl 1428.34029

[20] H. J. Hupkes, L. Morelli, P. Stehlík, V. Švígler, Multichromatic travelling waves for lattice Nagumo equations, *Appl. Math. Comput.* **361**(2019), 430–452. https://doi.org/10.1016/j.amc.2019.05.036; MR3961829; Zbl 1428.34030

[21] H. J. Hupkes, L. Morelli, P. Stehlík, V. Švígler, Counting and ordering periodic stationary solutions of lattice Nagumo equations, *Appl. Math. Lett.* **98**(2019), 398–405. https://doi.org/10.1016/j.aml.2019.06.038; MR3980231; Zbl 1423.92258

[22] H. J. Hupkes, E. S. Van Vleck, Negative diffusion and traveling waves in high dimensional lattice systems, *SIAM J. Math. Anal.* **45**(2013), No. 3, 1068–1135. https://doi.org/10.1137/120880628; MR3049651; Zbl 1301.34098

[23] H. J. Hupkes, E. S. Van Vleck, Travelling waves for complete discretizations of reaction diffusion systems, *J. Dynam Differential Equations* **28**(2016), No. 3–4, 955–1006. https://doi.org/10.1007/s10884-014-9423-9; MR3537361; Zbl 1353.34094

[24] J. P. Keener, Propagation and its failure in coupled systems of discrete excitable cells, *SIAM J. Appl. Math.* **47**(1987), No. 3, 556–572. https://doi.org/10.1137/0147038; MR0889639; Zbl 0649.34019

[25] P. G. Kevrekidis, The discrete nonlinear Schrödinger equation, Springer, 2009. https://doi.org/10.1007/978-3-540-89199-4

[26] I. Z. Kiss, J. C. Miller, P. L. Simon, *Mathematics of epidemics on networks. From exact to approximate models*, Springer, 2017. https://doi.org/10.1007/978-3-319-50806-1; MR3644065; Zbl 1373.92001

[27] J. Laplante, T. Erneux., Propagation failure and multiple steady states in an array of diffusion coupled flow reactors, *Phys. A* **188**(1992), No. 1–3, 89–98. https://doi.org/10.1016/0378-4371(92)90256-P

[28] S. A. Levin, Dispersion and population interactions, *Am. Nat.* **108**(1974), No. 960, 207–228. https://doi.org/10.1086/282900

[29] T. Lindeberg, Scale-space for discrete dignals, *IEEE T. Pattern Anal.* **12**(1990), No. 3, 234–254. https://doi.org/10.1109/34.49051

[30] A. F. Möbius, Über eine besondere Art von Umkehrung der Reihen (in German) [About a special kind of reversal of the series], *J. Reine Angew. Math* **9**(1832), 105–123. https://doi.org/10.1515/crll.1832.9.105; MR1577896

[31] L. Morelli, *Travelling patterns on discrete media*, PhD Thesis, Leiden University, 2019.

[32] J. Nagumo, S. Arimoto, S. Yoshizawa, An active pulse transmission line simulating nerve axon, *Proc. IRE* **50**(1962), No. 10, 2061–2070. https://doi.org/10.1109/jrproc.1962.288235

[33] J. Nagumo, S. Yoshizawa, S. Arimoto, Bistable transmission lines, *IEEE T. Circuit Th.* **12**(1965), No. 3, 400–412. https://doi.org/10.1109/tct.1965.1082476

[34] J. Riordan, An introduction to combinatorial analysis, John Wiley & Sons, Inc., 1958.

[35] A. Slavík, Lotka–Volterra competition model on graphs, *SIAM J. Appl. Dyn. Syst.* **19**(2020), No. 2, 725–762. https://doi.org/10.1137/19m1276285; MR4081801; Zbl 1437.92103

[36] P. Stehlík, Exponential number of stationary solutions for Nagumo equations on graphs, *J. Math. Anal. Appl.* **455**(2017), No. 2, 1749–1764. https://doi.org/10.1016/j.jmaa.2017.06.075; MR3671252; Zbl 1432.35214

[37] J. Volek, Landesman–Lazer conditions for difference equations involving sublinear perturbations, *J. Difference Equ. Appl.* **22**(2016), No. 11, 1698–1719. https://doi.org/10.1080/10236198.2016.1234617; MR3590409; Zbl 1361.39003

[38] B. Zinner, Existence of traveling wavefront solutions for the discrete Nagumo equation, *J. Differential Equations* **96**(1992), No. 1, 1–27. https://doi.org/10.1016/0022-0396(92)90142-a; MR1153307; Zbl 0752.34007